FUNDACIÓN AQUAE

TESIS

Evaluation of the performance and sustainability of algal-bacterial processes during wastewater treatment using a mass balance approach

Cynthia Alcántara Pollo

Valladolid 2017

Departamento de Ingeniería Química y Tecnología del Medio Ambiente de la Universitad de Valladolid

AQUAE FUNDACIÓN

Evaluation of the performance and sustainability of algal-bacterial processes during wastewater treatment using a mass balance approach

Cynthia Alcántara Pollo

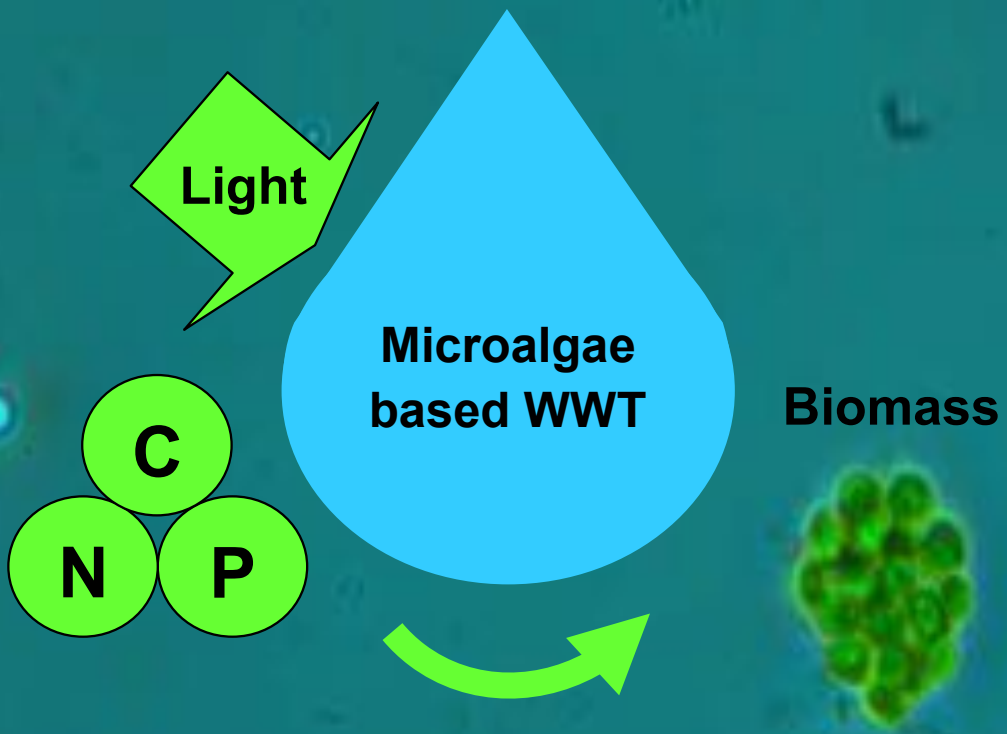

UVa

Universidad de Valladolid

ESCUELA DE INGENIERÍAS INDUSTRIALES

DEPARTAMENTO DE INGENIERÍA QUÍMICA Y TECNOLOGÍA DEL MEDIO AMBIENTE

TESIS DOCTORAL:

Evaluation of the performance and sustainability of algal-bacterial processes during wastewater treatment using a mass balance approach

Presentada por Cynthia Alcántara Pollo para optar al grado de doctora por la Universidad de Valladolid

Dirigida por:

Raúl Muñoz Torre
Pedro A. García-Encina

Universidad de Valladolid

ESCUELA DE INGENIERÍAS INDUSTRIALES

DEPARTAMENTO DE INGENIERÍA QUÍMICA Y TECNOLOGÍA DEL MEDIO AMBIENTE

TESIS DOCTORAL:

Evaluación del rendimiento y sostenibilidad de los procesos alga-bacteria durante el tratamiento de aguas residuales mediante balances de materia

Presentada por Cynthia Alcántara Pollo para optar al grado de doctora por la Universidad de Valladolid

Dirigida por:

Raúl Muñoz Torre
Pedro A. García-Encina

Memoria para optar al grado de Doctor, con

Mención Doctor Internacional, presentada

por la Ingeniera Química:

Cynthia Alcántara Pollo

Siendo tutores en la **Universidad de Valladolid:**

Raúl Muñoz Torre

Pedro A. García-Encina

Y en **Massey University** (Nueva Zelanda):

Prof. Benoit Guieysse

Valladolid, _____ de _____ 2015

UNIVERSIDAD DE VALLADOLID

ESCUELA DE INGENIERÍAS INDUSTRIALES

Secretaría

La presente tesis doctoral queda registrada en el folio número_____ del correspondiente libro de registro número _____

Valladolid, _____ de _____ 2015

Fdo. El encargado del registro

Raúl Muñoz Torre
Profesor Contratado Doctor Permanente
Departamento de Ingeniería Química y Tecnología del Medio Ambiente Universidad de Valladolid
y
Pedro A. García-Encina
Catedrático de Universidad
Departamento de Ingeniería Química y Tecnología del Medio Ambiente Universidad de Valladolid

Certifican que:

CYNTHIA ALCÁNTARA POLLO ha realizado bajo su dirección el trabajo "*Evaluation of the performance and sustainability of algal-bacterial processes during wastewater treatment using a mass balance approach*", en el Departamento de Ingeniería Química y Tecnología del Medio Ambiente de la Escuela de Ingenierías Industriales de la Universidad de Valladolid. Considerando que dicho trabajo reúne los requisitos para ser presentado como Tesis Doctoral expresan su conformidad con dicha presentación.

Valladolid, a _____ de_____ de 2015

Fdo. Raúl Muñoz Torre Fdo. Pedro A. García-Encina

Reunido el tribunal que ha juzgado la Tesis Doctoral titulada "*Evaluation of the performance and sustainability of algal-bacterial processes during wastewater treatment using a mass balance approach*" presentada por la Ingeniera Química Cynthia Alcántara Pollo y en cumplimiento con lo establecido por el Real Decreto 99/2011 de 28 de enero de 2011 acuerda conceder por_____ la calificación de _____.

Valladolid, a _____ de_____ de 2015

PRESIDENTE SECRETARIO

1er Vocal 2º Vocal 3er Vocal

Agradecimientos / Acknowledgements

A Raúl, por su paciencia e incansable dedicación desde el primer día en el que me embarqué en este reto. Por haberme demostrado con su exigencia, perseverancia y conocimientos que nada es imposible si se da lo mejor de uno mismo. Por haber sabido alentar mi motivación como investigadora. Por su gran corazón.

A Pedro, por compartir conmigo su experiencia y conocimiento. Por su capacidad de "quitar hierro al asunto" en situaciones de estrés.

A Esther, por su altruismo, transparencia y bondad en peligro de extinción. Por su capacidad de esfuerzo siempre con una sonrisa. Gracias por tu energía "*Super Alga*".

A Jose Estrada, Raquel, Marta Alzate y Araceli, por su ayuda desinteresada cuando la he necesitado.

A los compañeros con los que he tenido el placer de coincidir durante estos cuatro años: Andreita, Carol Bellido, Cris Toquero, Ieva, Juanki, Carol Fernández, Cano, Jaime, Roberto, Roxana, Jesús, Mayara, Osvaldo, Dimas, Sari…Gracias por hacer divertidas las horas de laboratorio.

A todo el Departamento de Ingeniería Química y Tecnología del Medio Ambiente de la UVa por formarme como profesional. Con especial cariño a Polanco y Fidel con sus frases míticas "*El ingeniero es el que se las ingenia*" y "*El que corta su propia leña se calienta dos veces*".

Al "*Aquelarre*": Anita, Begoña, Ivonne, Rebeca, Laura, Miri y especialmente a Sheila, Lari y Flor por tantas risas y conversaciones, por su amistad.

To Benoit Guieysse for give me the opportunity to join his lab at Massey University and live an unforgettable experience in New Zealand, an amazing country. For all the things I have learnt from him and his experience. Thanks to him and Mahalee for make me feel at home. Quentin, John Edwards, Edouard, Julia, Anne-Marie, Chris, John Sykes, thanks for your help and the funny moments we shared.

A Armando González por ofrecerme la oportunidad de unirme a su equipo en el Instituto de Ingeniería de la UNAM en México D.F. Por su sencillez y humildad. A Mariana, Cristy, Claudia, Kenia y Margarita, por acogerme desde el primer día como una más en el grupo, por tantos buenos momentos dentro y fuera del instituto.

A mi amiga Marta Pérez por ser un gran apoyo a pesar de los momentos tan duros que le ha tocado vivir. Es un orgullo tenerte como amiga.

A mi familia. A mi madre por ser siempre la luz en mi camino. A mi hermana, por ayudarme a recuperar la perspectiva cuando los árboles no me dejaban ver el bosque. A mi abuela, por su bondad y ayuda desinteresada. No habría llegado hasta aquí sin vosotras. Gracias por vuestro amor incondicional.

A Clemente, por estar siempre a mi lado, estuviera equivocada o no. Por hacer que la distancia solo sea eso, distancia. Por haber vivido esta experiencia como suya. Gracias por ser mi compañero de camino.

Gracias. Thank you.




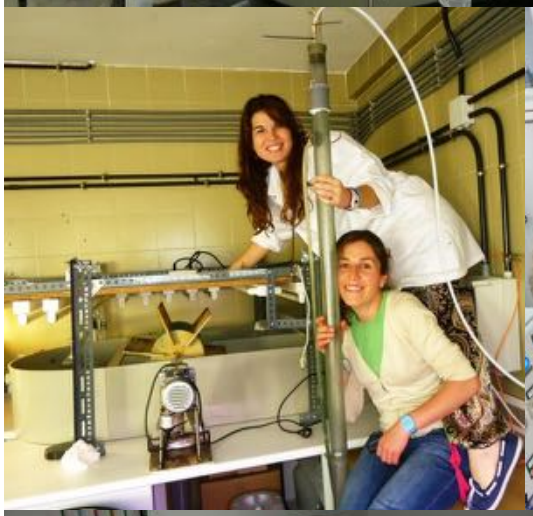
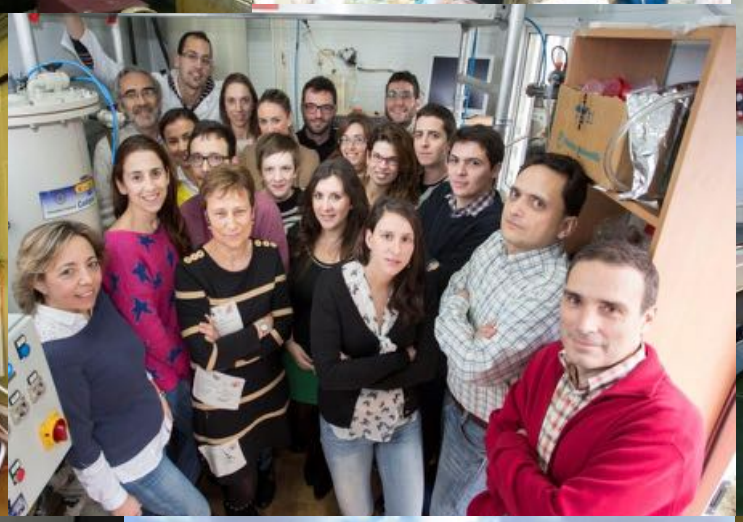

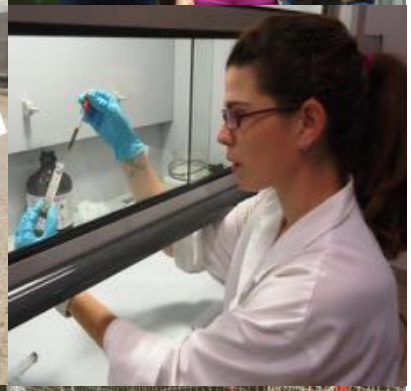


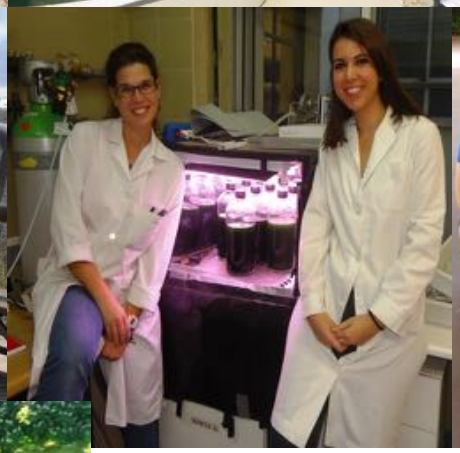

PhD experiences… **May 2011- July 2015**

Índice de contenidos

Resumen I
Abstract V
Relación de Artículos pertenecientes a la tesis IX
Contribución a los artículos incluidos en la tesis X
1. Introducción 1
1.1. Breve introducción del desempeño y sostenibilidad de los procesos alga-bacteria para el control de la contaminación 3
1.1.1. Tratamiento de aguas residuales con microalgas: Potencial de la simbiosis alga-bacteria 5
1.1.1.1. Eliminación de carbono en sistemas alga-bacteria 6
1.1.1.2. Eliminación de nutrientes en sistemas alga-bacteria 8
1.1.1.2.1. Eliminación de nutrientes por asimilación 8
1.1.1.2.2. Eliminación de nutrientes abiótica 11
1.1.1.2.3. Eliminación de nutrientes desasimilatoria 12
1.1.1.3. Mejora de la eliminación de nutrientes mediante el suministro adicional de CO_2 13
1.1.1.3.1. CO_2 procedente del biogás 15
1.1.1.3.2. CO_2 procedente de gases de combustión 17
1.1.1.4. Eliminación de metales pesados en sistemas alga-bacteria 18
1.1.1.5. Eliminación de patógenos en sistemas alga-bacteria 18
1.1.2. Tecnología de fotobiorreactores en el tratamiento de aguas residuales 19
1.1.2.1. Fotobiorreactores abiertos con biomasa en suspensión 20
1.1.2.2. Fotobiorreactores cerrados con biomasa en suspensión 20
1.2. Valorización de la biomasa microalgal 22
1.2.1. Biomasa microalgal como biofertilizante 22
1.2.2. Producción de biogás 23
1.2.3. Producción de biodiesel 26
1.2.4. Producción de bioetanol 27
1.2.5. Producción de biohidrógeno 27
1.3. Consideraciones energéticas en las tecnologías de tratamiento de aguas residuales con algas y bacterias 29
1.4. Consideraciones ambientales en las tecnologías de tratamiento de aguas residuales con algas y bacterias 34
1.4.1. Emisiones de N_2O y su huella de CO_2 asociada 36
1.4.2. Huella hídrica 38
1.5 Referencias 39
2. Objetivos y alcance de la tesis 45
2.1 Justificación de la tesis 47
2.2 Objetivos 48
2.3 Desarrollo de la tesis 49
3. Mixotrophic metabolism of *Chlorella sorokiniana* and algal-bacterial consortia under extended dark-light periods and nutrient starvation 51
4. Evaluation of wastewater treatment in a novel anoxic-aerobic algal-bacterial photobioreactor with biomass recycling through carbon and nitrogen mass balances 69
5. Evaluation of the simultaneous biogas upgrading and treatment of centrates in a HRAP through C, N and P mass balances 85
6. Evaluation of mass and energy balances in the integrated microalgae growth-anaerobic digestion process 95
7. Nitrous oxide emissions from high rate algal ponds treating domestic wastewater 107
8. Conclusiones y trabajo futuro 129
9. Sobre el autor 135

Table of contents

Resumen I
Abstract V
List of publications IX
Contribution to the papers included in the thesis X
1. Introduction 1
1.1. A brief introduction to the performance and sustainability of algal-bacterial processes for pollution control 3
1.1.1. Microalgae based wastewater treatment (WWT): The potential of algal-bacterial symbiosis 5
1.1.1.1. Carbon removal in algal-bacterial systems 6
1.1.1.2. Nutrient removal in algal-bacterial systems 8
1.1.1.2.1. Assimilatory nutrient removal 8
1.1.1.2.2. Abiotic nutrient removal 11
1.1.1.2.3. Dissimilatory nutrient removal 12
1.1.1.3. Enhanced nutrient removal based on the additional supply of CO_2 13
1.1.1.3.1. CO_2 from biogas 15
1.1.1.3.2. CO_2 from flue gas 17
1.1.1.4. Heavy metal removal in algal-bacterial systems 18
1.1.1.5. Pathogen removal in algal-bacterial systems 18
1.1.2. Photobioreactor technology in WWT 19
1.1.2.1. Open suspended growth photobioreactors 20
1.1.2.2. Enclosed suspended growth photobioreactors 20
1.2. Microalgal biomass valorization 22
1.2.1. Microalgae biomass as biofertilizer 22
1.2.2. Biogas production 23
1.2.3. Biodiesel production 26
1.2.4. Bioethanol production 27
1.2.5. Biohydrogen production 27
1.3. Energy considerations in algal-bacterial WWT technologies 29
1.4. Environmental considerations in algal-bacterial WWT technologies 34
1.4.1. N_2O emissions and their associated CO_2 footprint 36
1.4.2. Water footprint 38
1.5 References 39
2. Aims and scope 45
2.1 Justification of the thesis 47
2.2 Main objectives 48
2.3 Development of the thesis 49
3. Mixotrophic metabolism of *Chlorella sorokiniana* and algal-bacterial consortia under extended dark-light periods and nutrient starvation 51
4. Evaluation of wastewater treatment in a novel anoxic-aerobic algal-bacterial photobioreactor with biomass recycling through carbon and nitrogen mass balances 69
5. Evaluation of the simultaneous biogas upgrading and treatment of centrates in a HRAP through C, N and P mass balances 85
6. Evaluation of mass and energy balances in the integrated microalgae growth-anaerobic digestion process 95
7. Nitrous oxide emissions from high rate algal ponds treating domestic wastewater 107
8. Conclusions and future work 129
9. About the author 135

Resumen

En la actualidad, el rápido crecimiento de la población humana sumado al uso masivo de combustibles fósiles está provocando la emisión descontrolada de grandes cantidades de aguas residuales y gases de efecto invernadero que amenazan la sostenibilidad ambiental del planeta. Esta situación está motivando un incremento en la investigación en procesos de bajo coste y ambientalmente sostenibles para el control eficiente de la contaminación. En este contexto, las aguas residuales domésticas o los efluentes procedentes de la digestión anaerobia de residuos, se caracterizan por su alta carga en nitrógeno (N) y fósforo (P), los cuales deben ser retirados del agua residual antes de su descarga para evitar la contaminación y eutrofización de las aguas naturales. A día de hoy, se dispone de una amplia gama de tecnologías destinadas a la eliminación de nutrientes en las estaciones depuradoras de aguas residuales (EDARs) basadas en procesos físico-químicos y biológicos. Sin embargo, el tratamiento de aguas residuales (TAR) a menudo implica altos costes tanto de inversión como de operación, lo que limita la completa recuperación de los nutrientes contenidos en el agua residual. En este escenario, los procesos biológicos alga-bacteria se han establecido como una tecnología de TAR económica y sostenible, basada en la simbiosis entre ambos microorganismos. La capacidad de las microalgas para eliminar de forma simultánea carbono (C) (orgánico (CO) e inorgánico (CI)), N y P vía asimilación mixotrófica, sumado a la oxigenación fotosintética capaz de soportar la oxidación biológica de la materia orgánica y NH_4^+, representan ventajas clave en comparación con las tecnologías de TAR convencionales. No obstante, aún existen limitaciones técnicas y microbiológicas que limitan la aplicación generalizada del TAR con algas y bacterias. La identificación de estas limitaciones y el desarrollo de soluciones para superar las mismas serán decisivos a la hora de consolidar esta biotecnología sostenible para el TAR.

En esta tesis, el potencial de la simbiosis entre algas y bacterias durante el TAR en términos de eficiencia y sostenibilidad ambiental durante el tratamiento de la contaminación, se ha evaluado mediante balances de materia al C, N y P con el objetivo de desarrollar nuevas estrategias de operación y configuraciones de fotobiorreactores que puedan contribuir a superar las principales limitaciones de esta biotecnología.

En el **Capítulo 3**, se lleva a cabo un estudio fundamental del metabolismo mixotrófico bajo condiciones de estrés (crecimiento bajo largos periodos de luz (aerobios)-oscuridad (anaerobios) y en ausencia de nutrientes) de un cultivo axénico de *Chlorella sorokiniana* y un consorcio alga-bacteria mediante balances de materia al C, N y P. La hidrólisis de la glucosa a ácidos grasos volátiles durante el periodo de oscuridad, solamente tuvo lugar en los consorcios alga-bacteria, lo cual supuso una mayor eliminación de CO, $N\text{-}NH_4^+$ y $P\text{-}PO_4^{-3}$ durante las subsiguientes etapas de luz en comparación con los cultivos axénicos de *C. sorokiniana*, poniendo de manifiesto la función simbiótica del metabolismo bacteriano durante el TAR. Por otra parte, la ausencia de N y P promovió la asimilación de C-acetato y C-glucosa, lo que supuso un aumento considerable tanto en la productividad de la biomasa como en el contenido de carbohidratos en *C. sorokiniana* y en los consorcios alga-bacteria, al tiempo que demostró la versatilidad metabólica de los consorcios alga-bacteria bajo distintas condiciones de estrés. Estos resultados confirmaron el potencial de la simbiosis entre algas y bacterias indígenas como plataforma tecnológica para consolidar el TAR unido a la producción de energía basado en el uso de microalgas a escala industrial.

Algunas de las limitaciones técnicas que todavía dificultan la implementación del TAR con algas y bacterias a gran escala, están relacionadas con su limitada capacidad para eliminar de forma completa los nutrientes presentes en aguas residuales con bajos ratios C/N, o con la baja capacidad de sedimentación de algunas especies de microalgas, lo que conlleva a una concentración de sólidos suspendidos totales (SST) en los efluentes de estos procesos mayor que la permitida por la ley Europea de vertidos. En el **Capítulo 4** se evalúa, mediante balances de materia al C y N, tanto la eficiencia de eliminación de C y N, como la capacidad de sedimentación de la biomasa de un novedoso fotobiorreactor anóxico-aerobio de algas y bacterias con recirculación de biomasa. En estas condiciones, la simbiosis entre algas y bacterias, implementada en esta innovadora configuración de fotobiorreactor permitió obtener unas altas eficiencias de eliminación de CO (86-90%), CI (57-98%) y N total (68-79%) con un tiempo de residencia hidráulico de 2 días y un tiempo de residencia del fango de 20 días. La intensidad y el régimen de luz, junto con la concentración de oxígeno disuelto en el medio, controlaron el alcance de los mecanismos de eliminación asimilatorios o

desasimilatorios del N. La producción de $N\text{-}NO_3^-$ fue despreciable a pesar de las altas concentraciones de O_2, lo que dio como resultado una desnitrificación únicamente basada en la reducción de NO_2^-. La recirculación de biomasa dio lugar a una rápida sedimentación de los flóculos de biomasa algal y por tanto a una concentración de SST en el efluente por debajo de la máxima exigida por la ley Europea de vertidos.

El suministro externo de CO_2 en cultivos alga-bacteria puede aportar el C adicional requerido para mejorar la eliminación de los nutrientes por asimilación durante el TAR con bajos ratios C/N. En este escenario, el biogás obtenido a través de la digestión anaerobia de la biomasa algal, puede ser depurado mediante la fijación fotosintética del CO_2 contenido en el mismo. El **Capítulo 5** se centra en el estudio, mediante balances de materia al C, N y P, de los mecanismos de eliminación involucrados en la captura simultánea de CO_2 del biogás, y la eliminación de C y nutrientes de digestatos diluidos en un High Rate Algal Pond (HRAP) de 180 L interconectado con una columna de absorción. En este estudio, la baja intensidad lumínica aportada al sistema, junto con la baja velocidad de recirculación de líquido desde el HRAP a la columna de absorción, conllevó una baja absorción de $C\text{-}CO_2$ (55%) y una baja productividad de biomasa de 2.2 $g/m^2 \cdot d$. A pesar de la baja intensidad de luz, esta eliminación de $C\text{-}CO_2$ del biogás supuso un aumento en el contenido energético del mismo del 19%, lo que demuestra el potencial de este proceso combinado de TAR con depuración del biogás. De la misma forma el CI disponible en el caldo de cultivo controló de forma directa la cantidad de nutrientes eliminados por asimilación. En este contexto, la baja intensidad lumínica representó una ventaja competitiva para las bacterias nitrificantes (solo un 14% del N de entrada fue transformado en $N_{biomasa}$), siendo la nitrificación el principal mecanismo de eliminación de NH_4^+, con un 47% del $N\text{-}NH_4^+$ a la entrada transformado en $N\text{-}NO_3^-$. Del mismo modo, se planteó como hipótesis una acumulación de P por encima de los requerimientos estructurales como consecuencia de la limitación de luz y del elevado contenido en P estructural (2.5%), lo que resultó en una eliminación de $P\text{-}PO_4^{-3}$ como biomasa del 77%. Por lo tanto, la intensidad lumínica y el tiempo de residencia del biogás en la columna de absorción se identificaron como parámetros clave de operación durante el proceso simultáneo de TAR y depuración de biogás con microalgas.

Además, la sostenibilidad del TAR basado en microalgas, puede ser mejorada en términos energéticos mediante la digestión anaerobia de la biomasa cosechada durante el proceso de tratamiento. En el **Capítulo 6** se lleva a cabo un estudio del sistema integrado crecimiento-digestión anaerobia de biomasa algal utilizando balances de materia y energía. La biomasa algal fue previamente cultivada bajo condiciones fotoautotróficas o mixotróficas. Los resultados mostraron que ≈ 50% del C inicial en forma de biomasa fue hidrolizado y transformado mayoritariamente en biogás (90% del C hidrolizado), con una composición del 30% (v/v) de CO_2 y del 70% (v/v) de CH_4. El 10% restante del C hidrolizado aparece como CO y CI disuelto tras la digestión anaerobia de la biomasa cultivada de forma fotoautotrófica y mixotrófica. El CH_4 contenido en el biogás representó más del 50% de la energía química fijada como biomasa durante la etapa de cultivo microalgal. Estos resultados sugieren que tanto el grado de la hidrólisis de biomasa, como la composición del biogás, no estuvieron influenciados por las condiciones de cultivo de la microalga digerida, poniendo de manifiesto el potencial de la digestión anaerobia como una de las alternativas más económicas y eficientes en la valorización energética de las microalgas.

Finalmente, la capacidad de las microalgas y las bacterias asociadas para sintetizar N_2O durante el TAR pueden comprometer la sostenibilidad ambiental de esta biotecnología. Por tanto, con el objetivo de evaluar el impacto de la producción de N_2O en la huella de C en los procesos de TAR con algas y bacterias, se cuantificaron las emisiones de N_2O en dos sistemas: un HRAP (**Capítulo 7**) y un fotobiorreactor anóxico-aerobio (**Capítulo 4**). El HRAP mostró un factor de emisión durante 24 horas de 4.7×10^{-5} g N-N_2O/g N-entrada con una carga típica de 7.1 g N/$m^3_{reactor}$·d. De la misma forma, las emisiones durante el TAR en el fotobiorreactor anóxico-aerobio presentaron un valor de 5.2×10^{-6} g N-N_2O/g N-entrada con una carga de 50 g N/$m^3_{reactor}$·d. Los factores de emisión de N_2O obtenidos en ambos estudios fueron significativamente menores que los reportados típicamente en EDARs convencionales (IPCC), lo que confirmó que las emisiones de N_2O en sistemas alga-bacteria no comprometen la sostenibilidad ambiental de los TAR en lo que respecta a su contribución en el calentamiento global del planeta.

Abstract

The uncontrolled discharge of large amounts of wastewaters and greenhouse gases mediated by the rapid increase in human population and the massive use of fossil fuel resources are strongly threatening today's global environmental sustainability. These environmental challenges are motivating research on low cost, environmentally friendly and resource efficient pollution control technologies. In this context, domestic wastewaters or anaerobic digestion effluents are characterized by their high loads of nitrogen (N) and phosphorus (P), which must be treated before discharge to avoid water pollution and eutrophication of natural water bodies. A wide range of technologies is nowadays available for nutrient removal in wastewater treatment plants (WWTPs) based on both physical-chemical and biological processes. However, conventional wastewater treatment (WWT) often entails high investment and operational costs, which do not allow for a complete recovery of the nutrients contained in the wastewater. In this regard, algal-bacterial processes have emerged as a cost-effective and sustainable WWT technology based on the synergistic relationships established between microalgae and bacteria. The capacity of microalgae to simultaneously remove carbon (C) (organic (OC) and inorganic (IC)), N and P via mixotrophic assimilation, together with the *in-situ* photosynthetic oxygenation capable of supporting the biological oxidation of organic matter and NH_4^+, represent key advantages in comparison with conventional WWT technologies. Nevertheless, there are still several technical and microbiological limitations that hinder the widespread implementation of algal-bacterial-based WWT. The identification of those limitations and the development of solutions to overcome them will be of key relevance in the consolidation of this sustainable water pollution control biotechnology.

In the present thesis, the potential of the symbiosis between microalgae and bacteria during WWT in terms of pollution treatment efficiency and environmental sustainability was assessed using a C, N and P mass balance approach in order to develop innovative operational strategies and photobioreactor configurations that could eventually overcome the main limitations of microalgae-based WWT.

In the **Chapter 3**, a fundamental study of the mixotrophic metabolism under stress conditions (growth under extended light (aerobic)-dark (anaerobic) cycles and nutrient deprivation) of an axenic culture of *Chlorella sorokiniana* and a microalgal-bacterial consortium was carried out and assessed using C, N and P mass balances. The hydrolysis of glucose into volatile fatty acids during the dark periods occurred only in microalgal-bacterial cultures and resulted in OC, N-NH_4^+ and P-PO_4^{-3} removals in the subsequent illuminated periods higher than in *C. sorokiniana* cultures, which highlighted the symbiotic role of bacterial metabolism during WWT. On the other hand, N and P deprivation boosted both C-acetate and C-glucose assimilation and resulted in unexpectedly high biomass productivities and carbohydrate contents in both *C. sorokiniana* and the microalgal-bacterial cultures, which demonstrated the high metabolic flexibility of algal-bacterial consortia under different stress conditions. These results confirmed the potential of indigenous microalgae-bacteria symbiotic consortia as a platform technology to consolidate an industrial scale microalgae-to-bioenergy technology based on WWT.

Some of the main technical limitations that hinder the full-scale implementation of algal-bacterial WWT technologies derive from their limited performance to completely remove all nutrients present in wastewaters with a low C/N ratio or from the poor sedimentation capability of some microalgae species that results in effluent total suspended solid (TSS) concentrations above the maximum EU discharge limits. In **Chapter 4**, the C and N removal efficiency and biomass sedimentation capability of a novel anoxic-aerobic algal-bacterial photobioreactor with biomass recycling were evaluated using C and N mass balances. In this context, algal-bacterial symbiosis, implemented in this innovative nitrification-denitrification photobioreactor configuration supported efficient OC (86-90%), IC (57-98%) and total N (68-79%) removals at a hydraulic residence time of 2 days and a sludge retention time of 20 days. The intensity and regime of light supply along with the dissolved oxygen concentration governed the extent of the assimilatory and dissimilatory N removal mechanisms. Unexpectedly, N-NO_3^- production was negligible despite the high dissolved O_2 concentrations, denitrification being only based on NO_2^- reduction.

Biomass recycling resulted in rapidly settling algal flocs and TSS concentrations below the EU maximum discharge limits.

An external CO_2 addition into the algal-bacterial cultivation broth can provide the additional C source required to boost nutrient removal by assimilation during the treatment of wastewaters with a low C/N ratio. In this regard, the biogas obtained from the anaerobic digestion of the algal-bacterial biomass could be upgraded by capturing the CO_2 contained in the biogas via photosynthesis. **Chapter 5** was focused on the evaluation of the removal mechanisms involved in the simultaneous capture of CO_2 from a simulated biogas and removal of C and nutrients from diluted centrates in an indoor 180-L High Rate Algal Pond (HRAP) interconnected to an absorption column using also a C, N and P mass balance approach. In this study, the low impinging irradiation used in the HRAP together with the low liquid recirculation rate from the HRAP to the absorption column resulted in a low C-CO_2 absorption (55%) and consequently in a low biomass productivity of 2.2 $g/m^2 \cdot d$. Despite the low light intensity, this C-CO_2 removal from biogas entailed an increase of 19% in the biogas energy content, which highlighted the potential of this combined WWT-biogas upgrading process. Likewise, IC availability in the culture broth directly controlled the extent of nutrient removal via assimilation. In this context, the low irradiation provided a competitive advantage to nitrifying bacteria over microalgae (only 14% of the N input was converted to $N_{biomass}$), nitrification being the main NH_4^+ removal mechanism with a 47% of the N-NH_4^+ input transformed into N-NO_3^-. Similarly, a luxury uptake of P mediated by light limitation was hypothesized based on the high P biomass content (2.5%), which resulted in a P-PO_4^{-3} removal as biomass of 77%. Therefore, the light intensity in the HRAP and biogas residence time in the absorption column were identified as key operational parameters during the simultaneous microalgae-based biogas upgrading and WWT.

In addition, the sustainability of microalgae-based WWT can be improved in terms of energy recovery via anaerobic digestion of the biomass harvested during WWT. In this context, an evaluation using mass and energy balances of the integrated microalgae growth-anaerobic digestion process was performed in **Chapter 6**. The microalgae were

previously cultivated under photoautotrophic and mixotrophic conditions. The results showed that ≈ 50% of the initial C as biomass was hydrolyzed and mainly found as biogas (90 % of the hydrolyzed C) containing 30% (v/v) of CO_2 and 70% (v/v) of CH_4, while the dissolved OC and IC only represented 10% of total final C after anaerobic digestion of both photoautrophically and mixotrophically-grown microalgae. The CH_4 contained in the biogas accounted for an energy recovery of up to 50% from the chemical energy fixed as biomass during microalgae cultivation. These results suggested that the extent of biomass hydrolysis and biogas composition were not influenced by microalgae cultivation mode and demonstrated the potential of anaerobic digestion as one of the most cost-effective routes for the energy valorization of microalgae.

Finally, the benefits brought about by the use of wastewater as a source of nutrients and water might be compromised by the ability of microalgae and associated bacteria to synthesize N_2O, which can jeopardize the environmental sustainability of microalgal-bacterial WWT biotechnologies. Thus, in order to assess the impact of N_2O production on a net greenhouse gas mass balance, N_2O emissions were quantified in two different algal-bacterial WWT systems: a HRAP (**Chapter 7**) and an anoxic-aerobic photobioreactor (**Chapter 4**). A 24-hr average emission factor of 4.7×10^{-5} g N-N_2O/g N-input was recorded from HRAP cultures sampled under a typical N-loading of 7.1 g $N/m^3_{reactor}$·d. Likewise, the quantification of the N_2O emissions from the algal-bacterial nitrification-denitrification photobioreactor revealed that this system only generated significant N_2O emissions in the photobioreactor, which resulted in average N_2O emission factor of 5.2×10^{-6} g N-N_2O/g N-input under a N-loading of 50 g $N/m^3_{reactor}$·d. Therefore, the N_2O emission factors obtained in both studies were significantly lower than the IPCC emission factors reported for conventional WWTPs, which confirmed that N_2O emissions from these algal-bacterial photobioreactors should not compromise the environmental sustainability of WWT in terms of global warming impact.

List of publications

The following publications are presented as part of the present thesis. ~~Four~~ of them are published in international journals indexed in Journal Citation Report (JCR) (Papers I, III, IV and V). Paper II has been submitted for publication.

Paper I. Alcántara, C., Fernández, C., García-Encina, P.A., Muñoz, R., 2015. *Mixotrophic metabolism of Chlorella sorokiniana and algal-bacteria consortia under extended dark-light periods and nutrient starvation*. Applied Microbiology and Biotechnology. 99(5), 2393-2404.

Paper II. Alcántara, C., Domínguez, J.M., García, D., Blanco, S., Pérez, R., García-Encina, P.A., Muñoz, R., 2015. *Evaluation of wastewater treatment in a novel anoxic-aerobic algal-bacterial photobioreactor with biomass recycling through carbon and nitrogen mass balances* (Bioresource Technology. 191, 173-186).

Paper III. Alcántara, C., García-Encina, P.A., Muñoz, R., 2015. *Evaluation of the simultaneous biogas upgrading and treatment of centrates in a HRAP through C, N and P mass balances* (Water Science and Technology Journal, doi: 10.2166/wst.2015.198).

Paper IV. Alcántara, C., García-Encina, P.A., Muñoz, R., 2013. *Evaluation of mass and energy balances in the integrated microalgae growth-anaerobic digestion process*. Chemical Engineering Journal. 221, 238–246.

Paper V. Alcántara, C., Muñoz, R., Norvill, Z., Plouviez, M., Guieysse, B., 2015. *Nitrous oxide emissions from high rate algal ponds treating domestic wastewater*. Bioresource Technology. 177, 110-117.

Contribution to the papers included in the thesis

Paper I. In this work I was responsible of the design, start-up and operation of the experimentation in collaboration with Carolina Fernández. I performed the mass balance calculations, results evaluation and manuscript writing under the supervision of Dr. Raúl Muñoz and Dr. Pedro A. García-Encina.

Paper II. I was responsible of the design, start-up and operation of the experimental set-up in collaboration with Jesús M. Domínguez and Dimas García. I performed the mass balance calculations, results evaluation and manuscript writing under the supervision of Dr. Raúl Muñoz and Dr. Pedro A. García-Encina. Dr. Saúl Blanco and Dr. Rebeca Pérez were responsible of the characterization of the microalgal and bacterial populations, respectively, where I contributed in the data analysis and discussion.

Paper III. In this work I was responsible for the design, start-up and operation of the experimental set-up, the mass balance calculations, results evaluation and manuscript writing under the supervision of Dr. Raúl Muñoz and Dr. Pedro A. García-Encina.

Paper IV. During this research I was in charge of the design, start-up and operation of the experimental set-up, the mass and energy balance calculations, results evaluation and manuscript writing under the supervision of Dr. Raúl Muñoz and Dr. Pedro A. García-Encina.

Paper V. In this work I was in charge of the design, start-up and operation of the experimental set-up in collaboration with Zane Norvill. I performed the mass balance calculations, results evaluation and manuscript writing under the supervision of Dr. Benoit Guieysse and Dr. Raúl Muñoz. Maxence Plouviez was responsible of the characterization of the bacterial populations, where I contributed in the data analysis and discussion. This work was carried out in the School of Engineering and Advanced Technology, Massey University, Palmerston North (New Zealand).

Introduction

Chapter 1

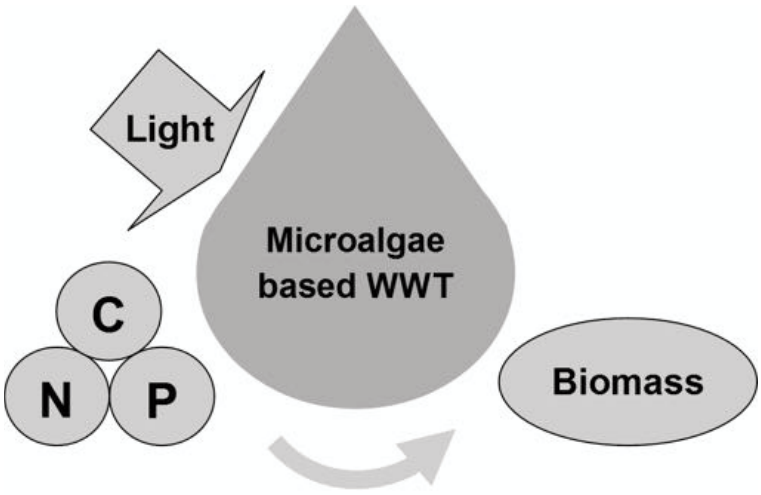

1.1. A brief introduction to the performance and sustainability of algal-bacterial processes for pollution control

The current scenario of rapid increase in urban population worldwide is generating very large amounts of domestic wastewater and greenhouse gases such as carbon dioxide (CO_2) or nitrous oxide (N_2O), which represent two of the major challenges to the global environmental sustainability nowadays. Domestic wastewaters or anaerobic digestion effluents are characterized by their high loads of nitrogen (N) and phosphorus (P), which must be treated before discharge to avoid water pollution and eutrophication of rivers and lakes. A wide range of techniques is nowadays available for nutrient removal in wastewater treatment plants (WWTPs), which are based on both physical-chemical mechanisms and biological processes involving different combinations of anaerobic, aerobic and anoxic stages. Unfortunately, these techniques often entail high investment and operational costs and do not allow frequently for a recovery of nutrients (Ruiz-Martínez et al., 2012). In this context, the main limitation of conventional biological nutrient removal technologies in WWTPs is the lack of enough C to completely remove by assimilation the N or P present in the wastewater (Arbib et al., 2014; Domínguez et al., 2013). Algal-bacterial symbiosis can support a cost-effective and sustainable wastewater treatment (WWT) due to the capacity of microalgae to simultaneously remove C (organic and inorganic), N and P via mixotrophic assimilation (**Chapter 3**), which coupled with microalgae luxury P uptake, results in high C, N, and P removals at relatively short hydraulic retention times (HRTs) (Arbib et al., 2014, Powell et al., 2008). In addition, the *in-situ* photosynthetic oxygenation provided by microalgae can support the microbial oxidation of recalcitrant and toxic organic contaminants and reduce the costs and environmental impacts associated with conventional mechanical aeration in activated sludge systems (Chae and Kang, 2013; Muñoz and Guieysse, 2006). The high pH and dissolved O_2 concentrations induced by microalgal photosynthesis can also enhance heavy metal removal and trigger pathogen deactivation (Heubeck et al., 2007; Muñoz and Guieysse, 2006). Microalgae-based WWT systems must be designed and operated to optimize light and inorganic carbon (IC) supply, while minimizing construction and operation costs (Muñoz and Guieysse,

2006; Tredici, 2004), High Rate Algal Ponds (HRAPs) being so far the most cost-effective microalgae-based WWT photobioreactor configuration (Lehr and Posten, 2009; Park et al., 2011a).

On the other hand, the exhaustion of fossil fuel resources and CO_2 accumulation in the atmosphere as a result of industrial anthropogenic activities are strongly motivating research on innovative renewable energy sources and CO_2 mitigation strategies (Wilbanks and Fernandez, 2014). In this context, microalgae have the ability to mitigate greenhouse emissions by photosynthetically fixing 1.8 kg of CO_2 per kg of biomass photosynthesized. Photoautotrophic microalgae growth can support both the mitigation of greenhouse emissions by capturing CO_2 from industrial gas emission and the removal of nutrients from wastewaters with a low C/nutrient ratio such as livestock and anaerobic effluents (De Godos et al., 2010; Park and Craggs, 2010; Singh et al., 2011). In this context, the supply of biogas (**Chapter 5**) or flue gas to HRAPs could eventually provide the additional C source (as CO_2) required for nutrient removal by assimilation, which results in a significant production of biomass. The microalgal biomass generated during WWT could be further used as slow nutrient release fertilizer (Mulbry et al., 2005) or transformed into biofuels following lipid trans-esterification (biodiesel), fermentation (bioethanol or biohydrogen) or anaerobic digestion (biomethane) (**Chapter 6**), thus increasing the economic and environmental sustainability of this platform WWT biotechnology via recovery of nutrients and/or energy. In this regard, anaerobic digestion (AD) appears as one of the less energy intensive and most environmentally friendly alternatives for biofuel production based on its low nutrient and water footprint (Ehimen et al., 2011; Sialve et al., 2009).

However, despite the above mentioned advantages, microalgae-based wastewater treatment processes still present severe technical limitations that hinder their full-scale implementation such as i) the lack of systematic empirical studies quantitatively evaluating the metabolism of microalgae and microalgae-bacteria consortia under different stress conditions (**Chapter 3**) ii) the limited performance to completely remove all nutrients in wastewaters with a low C/N ratio (**Chapter 4 and 5**), iii) the poor sedimentation ability of some microalgae species that results in effluent total

suspended solid concentrations above the maximum EU discharge limits (**Chapter 4**), iv) the limited knowledge on the nutrient and energy recovery during the anaerobic digestion of the microalgae produced from WWT (**Chapter 6**), or v) the ability of microalgal-bacterial cultures to synthesis N_2O, which could eventually jeopardize the environmental sustainability of these processes (**Chapter 4** and **Chapter 7**). In this thesis, the performance of microalgae-based WWT in terms of C, N and P removal was assessed under different operational strategies and photobioreactor configurations using a C, N and P mass balance approach. In addition, the environmental sustainability of these configurations was also studied by quantifying and comparing the N_2O emissions and their associated CO_2 footprint with other WWT technologies. Finally, the potential of microalgal biomass AD for energy production as CH_4 and nutrient recovery was also assessed.

1.1.1. Microalgae-based wastewater treatment (WWT): The potential of algal-bacterial symbiosis

Wastewater constitutes a free water and nutrients source for microalgae cultivation capable of supporting microalgae productivities as high as conventional fertilized-based media. Both domestic (Posadas et al., 2015), livestock (De Godos et al., 2009a), agro-industrial (De Godos et al., 2010) and industrial wastewaters (Tarlan et al., 2002) have been shown to support microalgae growth. In this context, the synergistic relationship between microalgae (including cyanobacteria) and bacteria can support an efficient and sustainable carbon and nutrient removal from wastewater based on the symbiosis established between microalgae and bacteria. In addition, **Chapter 3** demonstrated that algal-bacterial consortia presented a higher resilience under culture stress conditions than axenic microalgae cultures, which highlighted the potential of indigenous microalgae-bacteria symbiotic consortia as a platform technology to avoid the high cost and technical limitations associated with the axenic cultivation of microalgae in order to consolidate an industrial scale microalgae-to-biofuel technology based on WWT. The potential and implications of metabolic pathways involved in C, N and P removal in algal-bacterial based WWT are discussed below:

1.1.1.1. Carbon removal in algal-bacterial systems

Eukaryotic microalgae and prokaryotic cyanobacteria (both commonly referred to as microalgae) are capable of bioconverting CO_2 into microalgae biomass using the electrons released during the light-dependent water photolysis as showed in equation [1] (Masojídek et al., 2004):

$$CO_2 + H_2O + photons + nutrients \rightarrow O_2 + CH_{1.63}N_{0.14}O_{0.43}P_{0.006}S_{0.005} + waste\ heat \quad [1]$$

In this context, microalgal biomass contains approximately 43-56% of carbon (Arbib et al., 2014; Sydney et al., 2010), 1.8 kg of CO_2 being approx. required per kg of microalgae produced (**Chapter 6**; Chisti, 2007; Lardon et al., 2009). Despite the inhibitory CO_2 concentration thresholds in microalgae are strain specific, tolerances to CO_2 concentrations of up to 50% have been reported in *Scenedesmus Obliquus* strains (Arbib et al., 2014; Lam et al., 2012). The high tolerance of some microalgae species to CO_2, together with their year-round production, result in a CO_2 conversion efficiency ≈ 10-50 times higher than terrestrial plants (Li et al., 2008). Moreover, some microalgae are able to obtain the carbon and energy required for growth from organic substrates in the absence of photosynthesis. Thus, the varied spectrum of microalgae nutritional strategies allows both mixotrophic (simultaneous assimilation of organic and inorganic carbon during the photosynthetic process) and heterotrophic growth (use of organic carbon as carbon and energy source to synthesize new cellular material) (Barsanti and Gualteri, 2006). Thus, the complex interactions between microalgae and bacteria during WWT (Figure 1) can support an efficient removal of organic and inorganic carbon, nutrients, heavy metals, recalcitrant compounds and pathogens (Muñoz and Guieysse, 2006).

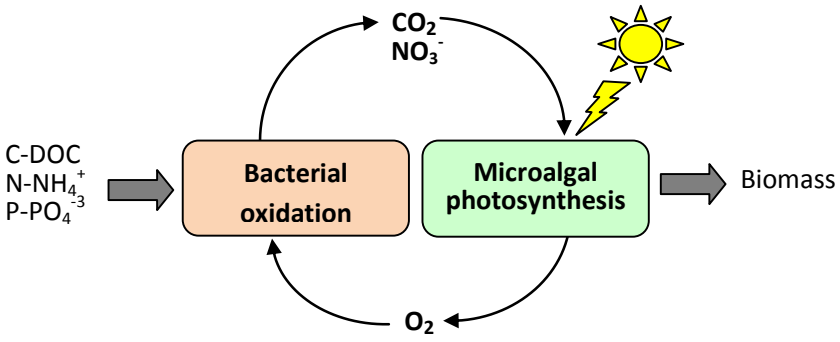

Figure 1. Principle of photosynthetic oxygenation (C-DOC = dissolved organic carbon).

During wastewater treatment, photosynthetic oxygenation, together with microalgal heterotrophic metabolism, can boost the oxidation of the organic matter (O.M.) and ammonium present in the wastewater. This is especially relevant during industrial WWT due to the fact that many recalcitrant and toxic contaminants are much easier to degrade aerobically than anaerobically (Muñoz et al., 2004). In addition, the capacity of microalgae to simultaneously remove C (organic and inorganic) via mixotrophic assimilation entails a high nutrient assimilation potential mediated by the high microalgae productivities (as a result of the assimilation of both wastewater alkalinity and the CO_2 released from O.M. oxidation) (Muñoz and Guieysse, 2006). Moreover, the in-situ generation of dissolved oxygen in the cultivation broth can reduce WWT operation costs (up to 50% of the total operation cost in activated sludge WWTPs is associated with mechanical O_2 supply) and minimize the stripping of hazardous pollutants associated with mechanical aeration (Chae and Kang, 2013). Photosynthetic oxygenation, which depends on the illuminated area, microalgae concentration, temperature and solar irradiation, constitutes a key design parameter determining the minimum HRT required for consistent carbon removal from wastewater (Figure 2).

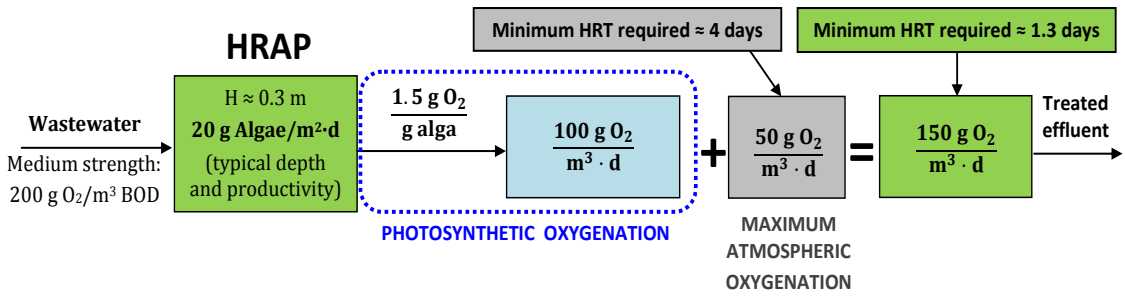

Figure 2. HRT required for the stabilization of the O.M of a medium strength domestic wastewater with and without photosynthetic oxygenation.

HRAPs constitute the most common photobioreactor configuration used for wastewater treatment due to their ease of construction and operation, low operation costs and consistent O.M. removal (Biochemical Oxygen Demand (BOD) and Chemical Oxygen Demand (COD) removals of 95-98% and 80-85%, respectively) (Buelna et al., 1990, Posadas et al., 2015). Hence, the minimum HRT theoretically required for stabilizing 200 g BOD/m^3 in a HRAP with a typical depth of 0.3 m would be

approximately 4 days (i.e. a surface loading of 0.075 m^3 wastewater/m^2 land·d) when process oxygenation was only provided by O_2 diffusion from the atmosphere. However, this HRT decreases to 1.3 days (0.23 m^3 wastewater/m^2 land·d) when active photosynthetic oxygenation supplies the oxygen demand (typically 1.5 g of O_2 per g alga cultivated when ammonium is the only N source) assuming a microalgae productivity of 20 g algae/m^2·d (Figure 2).

1.1.1.2. Nutrient removal in algal-bacterial systems

Three mechanisms have been identified as the main responsible for nutrient removal in algal-bacterial photobioreactors:

1.1.1.2.1. Assimilatory nutrient removal

Microalgae use solar energy to assimilate simultaneously C-CO_2, N and P in the form of new algae biomass during both secondary and tertiary treatment, resulting in a nutrient-free effluent with a high dissolved oxygen concentration. The content of N and P in microalgae ranges from 6.6 to 9.3% (Chisti, 2007; Oswald, 1988) and from 0.2 to 3.9 (Powell et al., 2009), respectively. The large variability in P content is likely due to the occurrence of a luxury phosphorus uptake in some microalgae species. Indeed, the content of P in microalgae is the result of the intracellular P stored as polyphosphate (luxury uptake) and the P assimilated for direct cell growth (structural P) (Powell et al., 2008, 2009). During luxury uptake, P is accumulated over structural P requirements in the form of energy storing polyphosphates, similarly to Polyphosphate Accumulating Organisms (PAOs) during enhanced biological phosphorus removal (EBPR). During EBPR, PAOs are first exposed to an anaerobic environment that promotes the intracellular organic carbon storage as polyhydroxybutyrate (PHB). The hydrolysis of intracellular polyphosphate reserves generates the energy required for anaerobic carbon uptake and intracellular PHB synthesis. Phosphorus removal from the cultivation broth occurs aerobically when the PAOs (using PHB reserves also for energy production, growth and cellular maintenance) take back both the excess of P released anaerobically and the P initially present in the wastewater (Coats et al., 2011). Microalgae luxury P uptake depends on the dissolved P-PO_4^{-3} concentration, the light intensity and the temperature during microalgae cultivation (Powell et al, 2008, 2009).

In this context, the study performed in **Chapter 3** showed different metabolisms when axenic *Chlorella vulgaris* and microalgal-bacterial cultures were exposed to prolonged dark (anaerobic)-light (aerobic) cycles. Indeed, the release of P-PO_4^{-3} by *C. sorokiniana* during the dark stages, together with the decrease in P-PO_4^{-3} assimilation during the subsequent light periods, induced a progressive decline in microalgal $P_{biomass}$ (from 1.5 % to 0.6 %). These results confirmed that microalgae, similarly to PAOs, can release P under anaerobic conditions in the absence of light, but P assimilation in the subsequent illuminated stages did not occur in a similar extent. In contrast, microalgae-bacteria consortia did not release P to the cultivation medium during dark periods and exhibited steady P-PO_4^{-3} removal rates during the illuminated stages, which explained the constant $P_{biomass}$ content in the algal-bacterial biomass (≈ 1%). Despite microalgae-bacteria consortia showed a higher resilience than *C. sorokiniana* to the absence of energy supply during the extended dark stages, cultivation under extended dark-light periods did not boost PHB accumulation neither in *C. sorokiniana* nor in the algal bacterial consortium.

However, based on the fact that the operational control of EBPR processes is complex and microalgae P luxury uptake as P removal technology is still in an embryonic phase, the addition of chemical reagents such as aluminum and ferric salts for phosphorus precipitation is often used in WWTPs (Beltrán et al., 2009). Phosphorus precipitation occurs when aluminum or ferric salts are added to the wastewater to form insoluble precipitates that will be further removed by sedimentation or filtration. In this context, aluminum (Al^{3+}) or ferric (Fe^{3+}) cations react with the soluble phosphorus present in the wastewater as orthophosphate (PO_4^{3-}) to form the corresponding insoluble orthophosphate salt as showed in equations [2] and [3]:

$$Al^{+3} + 3OH^{-} \rightarrow Al(OH)_3 \quad [2]$$

$$Fe^{+3} + 3OH^{-} \rightarrow Fe(OH)_3 \quad [3]$$

P removal by chemical precipitation is faster and easier to control and operate than EPBR technology. However, chemical P precipitation can remove part of the COD present in the wastewater, limiting nutrient removal by assimilation or nitrification-denitrification, which may require the external supply of synthetic O.M. such as

methanol (Beltrán et al., 2009). In addition, when ferric salts are added directly into the biological reactor to avoid additional treatment units (1-3 mol Fe per mol P_{inlet}), the use of the precipitation agent is limited as P removal only occurs at high pH (pH ≈ 9). Finally, salt addition unavoidably increases sludge generation, which must be treated in order to separate the chemical agents if the sludge is to be applied for soil recovery, which represents an environmental and economic disadvantage in comparison with biological P removal technologies.

Assuming a nitrogen and phosphorous content in microalgae of 9% and 1%, respectively, a HRT of 7-7.5 days would be required to completely remove via assimilation the concentrations of N and P typically encountered in medium strength domestic wastewater based on a microalgae productivity of 20 g algae/m²·d (Figure 3).

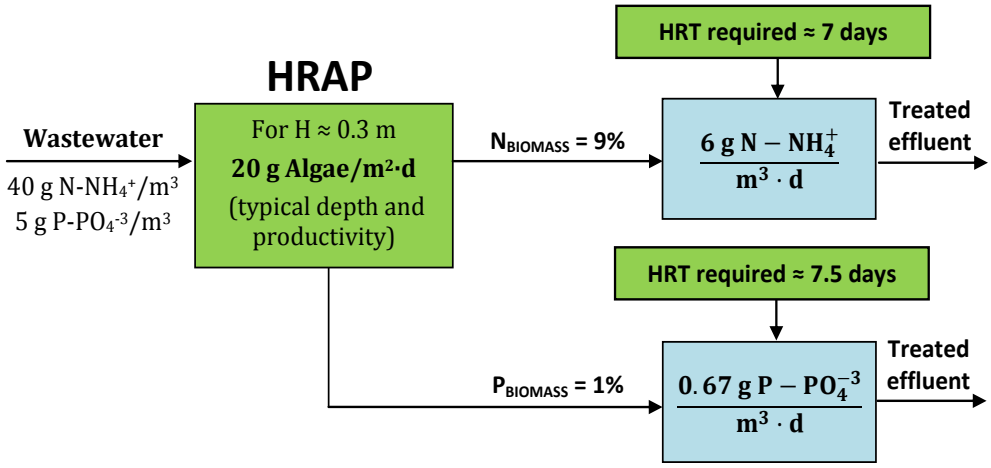

Figure 3. Estimated minimum HRTs required for the treatment of N and P concentrations in a medium strength domestic wastewater based on nutrient assimilation into microalgal biomass.

Therefore, the use of microalgae and bacteria during microalgae-based wastewater treatment in HRAPs allows for a simultaneous C, N and P removal at relatively short HRTs (3-10 days) (Posadas et al., 2015), which entails a considerable reduction in HRT/land use compared to conventional stabilization ponds (≈ 15-30 days) (Kivaisi, 2001). Despite the HRTs during biological nutrient removal in activated sludge processes are lower than those applied in HRAPs (≈ 12 hours) (Coats et al., 2011), the energy required during these conventional mechanically aerated processes is significantly higher than in microalgae-based WWT processes (section 1.3.).

1.1.1.2.2. Abiotic nutrient removal

Microalgal photosynthesis brings along an increase in the pH of the cultivation broth as a result of CO_2 removal. This increase shifts the equilibrium of IC species towards CO_3^{-2} (not available for many microalgae species) if the medium is not properly buffered (equation [4]). N-NH_3 stripping occurs in open reactors operated at high pH (Figure 4a) concomitantly with P-PO_4^{-3} precipitation in the presence of Ca^{+2} cations (which is removed from the wastewater in the form of $Ca_5(OH)(PO_4)_3$) (Ruiz-Martínez et al., 2012) (Figure 4b). The equilibria and reactions associated to the mechanisms of abiotic N (equation [5]) and P (equation [6]) removal are defined as follows:

$$CO_2\ (l) + H_2O\ (l) \leftrightarrow H_2CO_3 \leftrightarrow HCO_3^- + H^+ \leftrightarrow CO_3^{2-} + 2H^+ \quad [4]$$

$$NH_4^+ \leftrightarrow NH_3\ (l) + H^+ \leftrightarrow NH_3\ (gas) \quad [5]$$

$$3\ HPO_4^{2-} + 5Ca^{2+} + 4OH^- \rightarrow Ca_5(OH)(PO_4)_3 + 3H_2O \quad [6]$$

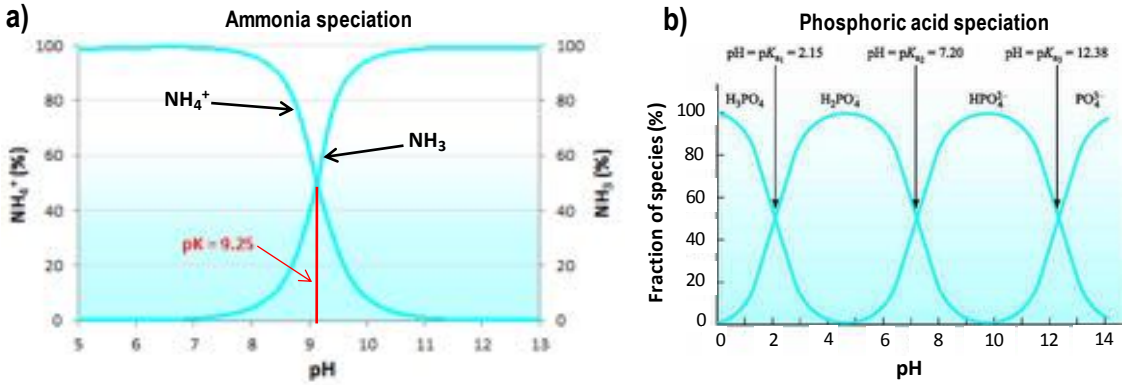

Figure 4. NH_3 (a) and PO_4^{-3} (b) speciation as a function of pH.

Thus, the control of pH during microalgae cultivation at ≈ 7 maximizes C, N and P removals by photosynthetic assimilation. At a neutral pH, inorganic C is mainly present in the form of dissolved CO_2 and HCO_3^- (assimilable carbon forms) while N is retained in the aqueous phase as N-NH_4^+, which prevents N-NH_3 emissions to the atmosphere and favors its assimilation as structural N. Likewise P is incorporated into the cell in the form of orthophosphate as structural P or stored as polyphosphates (Powell et al., 2008, 2009). These assimilatory and abiotic mechanisms support N and P removals in pilot-scale HRAPs of 90-99% and 95-99%, respectively, which highlights the bioremediation potential of this low-cost algal-bacterial biotechnology (Arbib et al., 2013a; De Godos et al., 2010; Posadas et al., 2015).

1.1.1.2.3. Dissimilatory nutrient removal

The removal of nitrogen in conventional activated sludge systems is often carried out by sequential nitrification-denitrification processes. Nitrification is the oxidation of N-NH_4^+ into N-NO_2^- and N-NO_3^-, which is conducted by chemolithotrophic aerobic bacteria. This oxidation takes place in two consecutive stages: N-NH_4^+ is initially oxidized by *Nitrosomonas* and *Nitrosococcus* bacteria into N-NO_2^- (equation [7]), which is further oxidized into N-NO_3^- by *Nitrobacter* bacteria (equation [8]) (Rittmann and McCarty, 2001).

$$NH_4^+ + 1.5\ O_2 \rightarrow NO_2^- + H_2O + 2H^+ \quad [7]$$

$$NO_2^- + 0.5\ O_2 \rightarrow NO_3^- \quad [8]$$

N-NO_2^- and N-NO_3^- can be reduced to N_2 by heterotrophic bacteria under anoxic conditions during denitrification using the O.M. present in the wastewater as electron donor as showed in equation [9] (Rittmann and McCarty, 2001).

$$8NO_3^- + 5CH_3COOH \rightarrow 8HCO_3^- + 6H_2O + 2CO_2 + 4N_2 \quad [9]$$

In microalgal-bacterial photobioreactors, this sequential process can occur simultaneously due to the occurrence of diffusional gradients between the inner part of the algal-bacterial flocs or biofilms and the culture broth. In this context, De Godos et al., 2009b reported a total nitrogen removal efficiency of 94% in a 7.5-L enclosed tubular biofilm photobioreactor fed with undiluted swine slurry at the highest swine slurry loading rate tested (80 g TOC/m^3_r·day and 89 g N–NH_4^+/m^3_r·day) and 7 days of HRT. This high and consistent N removal was likely mediated by the particular mass transport mechanisms established in the biofilm structure (photosynthetic O_2 and TOC/NH_4^+ diffusing from opposite sides of the biofilm), which allowed both the occurrence of a simultaneous denitrification-nitrification process (DO concentrations ≈ 0.2 mg O_2/L and 1 mg N-NO_3^-/L) and the protection of microalgae at the photobioreactor wall from any potential NH_3-mediated inhibitory effect at the high pH and high NH_3 loading rates applied.

On the other hand, a recent study carried out in our laboratory (**Chapter 4**) successfully implemented a denitrification-nitrification process in a novel anoxic-aerobic algal-

bacterial photobioreactor with biomass recycling (Figure 5), which enabled an efficient removal of TOC (88%), IC (82%) and total nitrogen (TN) (75%) during synthetic wastewater treatment at a HRT of 2 days based on a photosynthetically oxygenated nitrification.

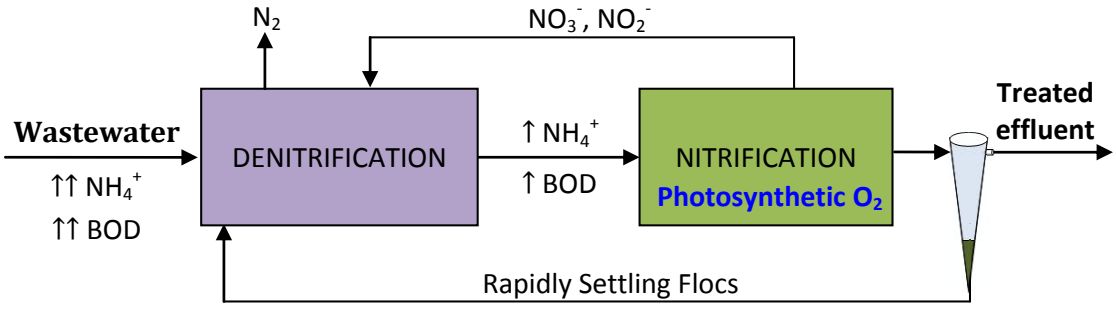

Figure 5. Schematic of a nitrification-denitrification process implemented in algal-bacterial photobioreactors

The availability of IC, governed by IC supply and microalgae activity, and the dissolved oxygen concentration in the photobioreactor directly controlled the extent of N removal by biomass assimilation or nitrification-denitrification dissimilatory mechanisms. In addition, the biomass recycling from the bottom of the settler into the anoxic tank resulted in the enrichment of rapidly settling algal flocs and low effluent total suspended solid (TSS) concentrations.

1.1.1.3. Enhanced nutrient removal based on the additional supply of CO_2

Nowadays, CO_2 emissions contribute approximately with 52% of the total global warming potential (Wilbanks and Fernández, 2014). CO_2 is readily available in the atmosphere in concentrations of 0.03–0.06% (v/v). In this context, microalgae are photoautotrophic microorganisms highly efficient to fix CO_2 into microalgae biomass using solar energy, which can bring along two environmental benefits: i) the mitigation of greenhouse emissions such as biogas from anaerobic digestion or flue gas from fossil fuel combustion by capturing via photosynthesis the CO_2 released in these industrial processes (0.191 kg CO_2 emitted per kWh of electricity produced, WWF Spain, January 2015), and ii) the removal of nutrients from wastewaters with a low C/N/P ratio, which represents an important advantage in comparison with aerobic activated sludge or AD technologies in terms of enhanced nutrient recovery and entails an added

environmental benefit to the process in term of biomitigation of the eutrophication potential of these type of wastewaters (Arbib et al., 2014; De Godos et al., 2010). In this context, the low C/N/P ratio in most wastewaters (typically domestic wastewater or raw centrates) (Table 1), compared to the algal-bacterial biomass composition ratio (100/18/2), often limits the efficiency of nutrient removal in microalgae-based wastewater treatment processes due to a carbon deficiency (Benemann, 2003; Posadas et al., 2013).

Table 1. Carbon, nitrogen and phosphorus composition of different wastewaters.

Type of WW	COD (mg/L)	TOC (mg/L)	IC (mg/L)	TN (mg/L)	TP (mg/L)	C:N:P[1]	Reference
Domestic WW							
Low strenght	250	80	6	20	4	100:23:5	Rawat et al. (2011)
Medium strenght	500	160	12	40	8	100:23:5	Rawat et al. (2011)
	507	181	100	91	7	100:32:3	Posadas et al. (2013)
	412	155	100	92	11	100:36:4	Posadas et al. (2014)
High strenght	1000	290	24	85	15	100:27:5	Rawat et al. (2011)
Animal WW							
Fish farm WW	678	161	65	31	19	100:14:6	Posadas et al. (2014)
Piggery WW[2]	9490	3390	-	1000	310	100:30:9	De Godos et al. (2009a)
Raw centrates[3]	-	76	717	666	101	100:84:13	Posadas et al. (2013)
	-	88	760	736	71	100:86:8	**Chapter 5**

[1]Ratio calculated from the TC (TOC+IC), TN and total phosphorus (TP) concentrations.
[2]Recommended dilution in microalgae-based WW treatment of 20 fold.
[3]Recommended dilution in microalgae-based WW treatment of 8-10 fold.

In this regard, an external CO_2 addition into the mixed liquor can provide the additional C source required to boost nutrient removal by assimilation and result in a significant generation of biomass that could be further used as a feedstock for energy production (**Chapter 6**, section 1.2) or high-added-value products (**Chapter 3**; Chisti, 2013). Moreover, CO_2 addition would also prevent the rise in pH in the culture broth mediated by photosynthetic activity, and therefore mitigate nitrogen losses by $N\text{-}NH_3$ stripping and phosphorus precipitation.

1.1.1.3.1. CO_2 from biogas

Biogas is produced during the AD of O.M. and is mainly composed by CH_4 (55–75%) and CO_2 (25–45%), H_2S (0.005−2%), and N_2, O_2, or H_2 at trace level concentrations (Serejo et al., 2015). Biogas must be upgraded in order to be transformed into biomethane and achieve a composition similar to natural gas. Biomethane consists typically of 95-99% methane and 1-3% CO_2, its final required concentration depending on its intended use and the legislation of the country. In this context, biomethane specifications for injection into natural gas grids in most EU countries require a CO_2 content of less than 3%, whereas vehicle fuel specifications require a combined CO_2-N_2 content of 1.5-4.5% (Ryckebosch et al., 2011). Nowadays, there exist both physical-chemical and biological methane enrichment technologies available to achieve the biomethane required composition. In this context, photosynthetic biogas upgrading allows the valorization of this CO_2 in the form of a valuable algal biomass by photoautotrophically fixing the CO_2 contained in the biogas, with the concomitant production of O_2 (**Chapter 5**). Thus, microalgae-based digestate treatment in HRAPs represents an opportunity to simultaneously remove the CO_2 present in biogas and the residual carbon and nutrients present in the digestates at low energy costs and environmental impacts (Park and Craggs, 2010). Likewise, microalgae-based CO_2 removal during biogas upgrading will result in lower transportation costs and a higher biogas energy content (**Chapter 5**; Serejo et al., 2015). Provided a sufficient CO_2 mass transport from the biogas to the microalgal cultivation broth, the rate of CO_2 fixation, which itself determines the maximum biogas loading rate to be applied to the upgrading unit, is governed by environmental and microbiological factors such as light availability, temperature, pH and dissolved O_2 and biomass concentration in the cultivation broth. Thus, the photosynthetic CO_2 fixation rate linearly increases when increasing light intensity up to a critical species-dependent saturation irradiance (200-400 $\mu E/m^2 \cdot s$), remaining constant afterwards up to a critical photoinhibition value and deteriorating subsequently as a result of the damage in the microalgal photosystem II at high light intensities (Tredici, 2009). Biogas upgrading in algal-bacterial systems has been implemented in tubular photobioreactors (Figure 6a), and HRAPs constructed with additional biogas scrubbing units (Figure 6b), which were capable of removing

CO_2 with efficiencies higher than 80 %, providing a biomethane with CH_4 concentrations of ≈ 90% at 1.5 L biogas/m^2·h and a L/G ratio of 10 (Muñoz et al., 2015; Serejo et al., 2015).

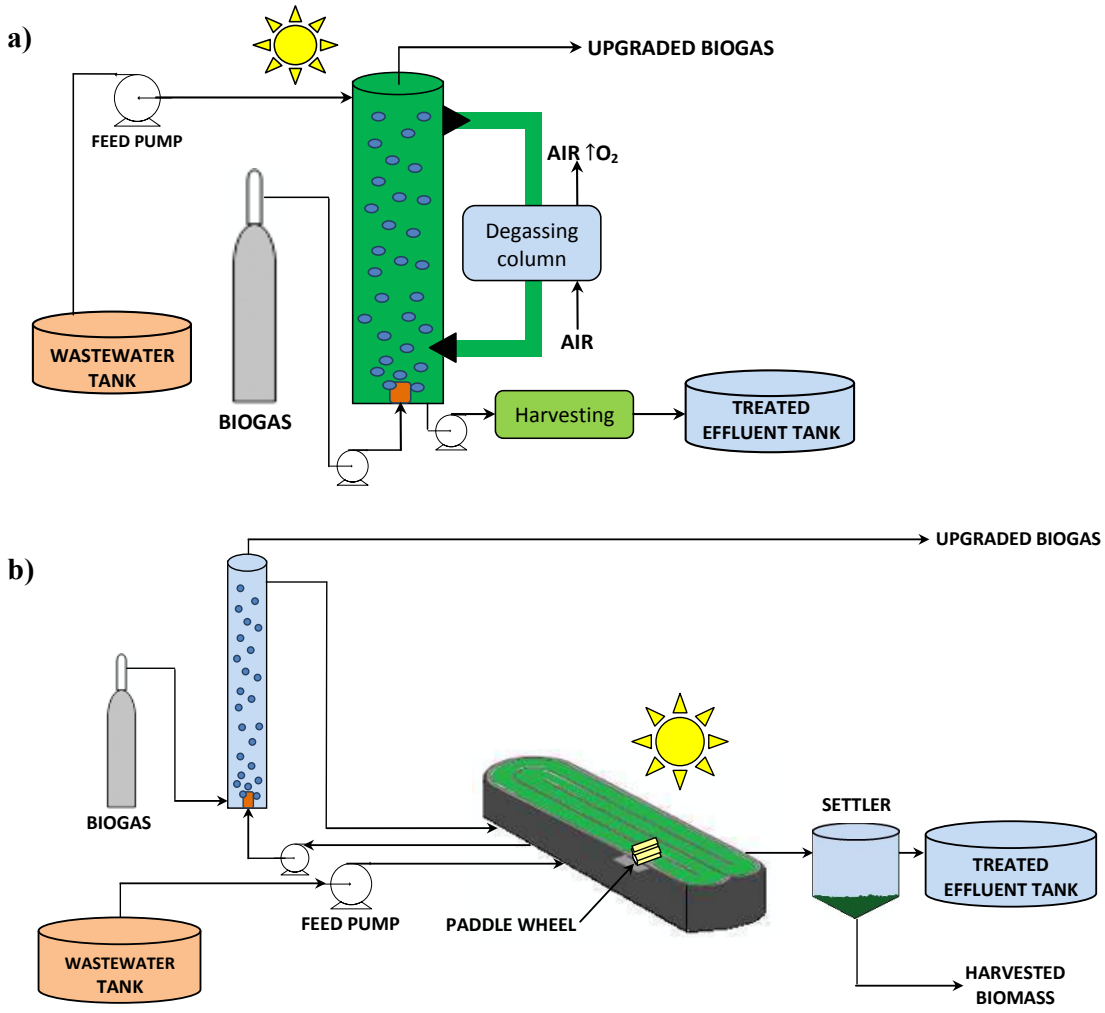

Figure 6. Schematic of algal-bacterial-based biogas upgrading in tubular photobioreactors (a) and HRAPs equipped with an absorption column (b).

In this regard, HRAPs are characterized by a simpler construction and operation and less biofouling problems (Tables 2 and 3) than enclosed photobioreactors (Acién et al., 2012; Craggs et al, 2012). However, HRAPs entail a poor light utilization efficiency (≈ 2 %) (Muñoz et al, 2015), a high water footprint by evaporation (≈ 6 L/m^2·d) (Posadas et al., 2015) and large land requirements (≈ 7 m^2/capita·d) (Alcántara et al., 2015) (Tables 2 and 3). Photobioreactor irradiance and biogas residence time in the absorption column are key parameters during microalgae-based biogas upgrading in order to boost CO_2 sequestration (**Chapter 5**). A direct biogas scrubbing in the photobioreactor (Figure 6a) or a high biogas residence time in the absorption unit (Figure 6b) entails high O_2

concentrations in the upgraded biomethane (5-25 %), which constitutes one of the main limitations of this novel biotechnology (Muñoz et al., 2015). In this context, the injection of biogas in the gas grid is only allowed when the concentration of oxygen in the biogas is below 0.3% (v/v) due to its associated explosion hazards according to the Ministry of Industry, Energy and Tourism of Spain (BOE-A-2013-185). N_2 stripping from the cultivation broth would also result in N_2 concentrations of 6-9% in the upgraded biomethane, which does represent another technical limitation of the process as biomethane regulations in some European countries such as Sweden, Spain or Austria require CH_4 contents over 95 % (Huguen and Le Saux, 2010; Persson et al, 2006; Serejo et al, 2015). Research on biogas upgrading in algal-bacterial processes is currently focused on the minimization of both O_2 and N_2 stripping from the microalgae cultivation broth to the upgraded biomethane. In this context, the in situ generated O_2 could be subsequently used by sulfur oxidizing bacteria to oxidize the H_2S present in the biogas to sulfate, thus allowing for an integral biogas upgrading. In this scenario, Bahr et al. (2014) reported biogas O_2 concentrations of ≈ 0.3 % at a low L/G ratio of 1 and a pH in the cultivation broth of 9-10. Therefore, further research is needed based on the potential of this biotechnology as a platform of biogas upgrading technology during microalgae-based WWT.

1.1.1.3.2. CO_2 from flue gas

Another free source of CO_2 is flue gas, which contains 6–15% (v/v) of CO_2 (Rahaman et al., 2011). Typically, flue gas is composed by 10% CO_2, 10.5 H_2O, 4.5% O_2 and 75% N_2 (Xu et al., 2003). Flue gas could be sparged in HRAPs in order to supply the extra CO_2 to remove wastewater nutrients via biomass assimilation. In this context, Posadas et al. (2015) reported TOC removals of 84% and TN removals of 66%, corresponding with biomass productivities of 13 $g/m^2 \cdot d$, during secondary domestic wastewater treatment in an outdoors 800-L HRAP constructed with a sump (width 0.36 m, depth 1 m) provided with flue gas and operating at a HRT of 2.8 d under a light irradiance of 2125 $\mu E/m^2 \cdot s$ (9.3 h/day). Similarly, Arbib et al. (2013a) operated an outdoors 530-L HRAP constructed with a carbonation sump station (width 0.3 m, depth 1 m) for the treatment of urban wastewater containing 81 mg O_2/L of COD, 24.7 mg N/L and 2.1 mg P/L

under a light irradiance of 2000 μE/m²·s. The biomass productivity and N and P removal efficiencies in the HRAP increased from 10 g TSS/m²·day to 20 g TSS/m²·day, 63% to 95% and 81% to 95%, respectively, when increasing the inorganic carbon concentration in the cultivation broth via flue gas supply (from 0 mL/min to 20 mL/min of < 5% CO_2 flue gas).

In addition, flue gas can support the degassing of the excess of photosynthetic O_2 accumulated in the cultivation broth, especially in enclosed photobioreactors. In this context, flue gas sparging represents an advantage in comparison with conventional air degassing in tubular photobioreactors (Figure 6a) as its lower O_2 concentration (4-5%) compared to air (21%) improves O_2 stripping from the microalgal cultivation broth.

1.1.1.4. Heavy metal removal in algal-bacterial systems

Heavy metals such as cadmium, mercury, zinc, copper, aluminum, chromium, or nickel are among the most hazardous and persistent pollutants in wastewaters, posing a severe threat to both natural ecosystems and human health. Physical/chemical removal technologies such as resin-based adsorption, reverse osmosis or chemical precipitation exhibit high operating costs and often generate hazardous by-products (Gavrilescu, 2004). Interestingly, several studies have consistently shown the superior performance of microalgae biomass for the removal of these persistent inorganic pollutants (Muñoz et al., 2006). In this context, heavy metal removal in microalgae is mediated by a combination of active (excretion of metal-chelating exopolysaccharides or bioaccumulation) (Pereira et al., 2013) and passive (biosorption or heavy metal precipitation by the increase in pH during photosynthesis) (Chojnacka et al., 2005) mechanisms, resulting in removal efficiencies of up to 99 % under continuous flow operation (Cañizares-Villanueva, 2000).

1.1.1.5. Pathogen removal in algal-bacterial systems

Bacteria such as coliforms (mainly *E. coli*) and *Salmonella*, viruses and protozoa constitute the main pathogenic microorganisms identified in wastewaters. Chlorine addition and ozonation represent nowadays the most applied methods for pathogen removal. However, the increasing price of chlorine together with its toxicity for aquatic fauna, and the high cost of ozone production require the development of cost-effective

pathogen removal treatments (Abdel-Raouf et al., 2012). In this context, algal-bacterial systems can support a low-cost and efficient deactivation of pathogens by increasing the pH, temperature, sunlight irradiation and dissolved oxygen concentration in the photobioreactor broth as a result of the photosynthetic activity, reaching removal efficiencies of ≈ 95% at a pH of 9.5 and dissolved oxygen concentrations of ≈ 20 mg O_2/L (El Hamouri et al., 1994; Heubeck et al., 2007; Muñoz and Guieysse, 2006).

1.1.2. Photobioreactor technology in WWT

Photobioreactors devoted to wastewater treatment entail the same basic design and operation criteria than conventional photobioreactors for mass cultivation: high surface/volume ratio to maximize light utilization efficiency (and therefore oxygen production), adequate mixing and degassing, good scalability, low hydrodynamic stress on the algal-bacterial flocs, control over the environmental conditions and low construction and operation costs (Muñoz and Guieysse, 2006; Tredici, 2004). Photobioreactors for wastewater treatment can be classified into open and enclosed systems (Figure 7). Nowadays, the 99% of the about 15,000 tons per year of produced microalgae are cultivated in open ponds (Benemann, 2013).

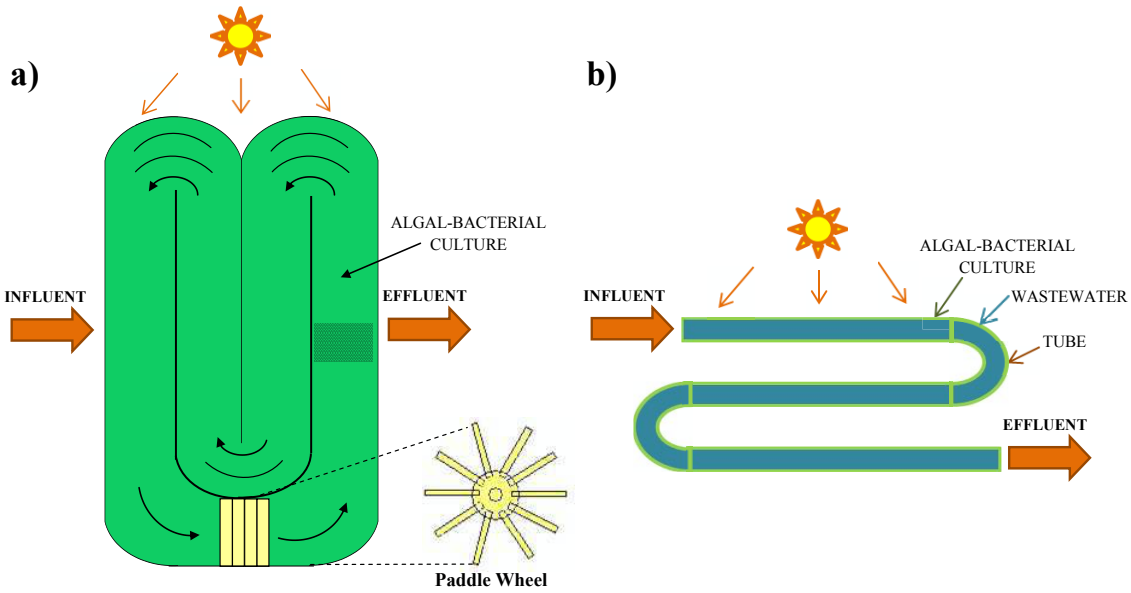

Figure 7. Schematic of a a) high rate algal pond photobioreactor and b) enclosed tubular algal-bacterial photobioreactor.

1.1.2.1. Open suspended growth photobioreactors

Open photobioreactors are extensive systems, easy to construct and operate but poorly controlled in terms of environmental growth conditions, which results in low cost facilities. The control of microalgae concentration and population structure in the cultivation broth are low as a result of its direct contact with the environment, which renders this cultivation technology only recommended for highly resistant (extremophile) microalgae species. The use of open ponds as a platform technology for wastewater treatment started in the early 1950s (Oswald et al., 1957). Open raceways or HRAPs consist of shallow ponds (0.1–0.4 m deep) divided into two or four water channels continuously mixed by paddlewheel mechanical agitation in order to support water circulation and promote the access of microalgae to light and nutrients (Mendoza et al., 2013). HRAPs fed with wastewater (Figure 7a) arguably provide one of the most cost and resource efficient photobioreactor configurations to produce microalgae biomass for biofuel generation, despite their lower algal biomass productivities when compared to enclosed photobioreactors (Acién et al., 2012). The main design and operational characteristic of HRAPs are shown in Table 2.

Table 2. Key design and operation parameters of HRAPs

Parameter	Typical range	References
Investment costs	2-20 €/m^2	Oswald (1988)
Optimal size	1500-5000 m^2	Oswald (1988)
Depth	10-40 cm	Borowitzka (2005)
Length-width ratio (L:W)	40:1	Borowitzka (2005)
Recirculation rate	15-30 cm/s	Borowitzka (2005)
Engine rotation rate	5-20 cm/s	Borowitzka (2005)
Photosynthetic efficiency	2 %	Muñoz et al. (2015)
Productivity	10-25 g/m^2·d	Molina-Grima (1999) Jorquera et al. (2010)
Power consumption	0.1-10 W/m^3	Borowitzka (2005)

1.1.2.2. Enclosed suspended growth photobioreactors

Enclosed photobioreactors (Figure 7b) maintain microalgae cultivation broth protected from the environment, which allows the maintenance of monoalgal and even axenic cultures. The end use of this biomass is usually focused on extraction of high-value products or human nutrition, which counterbalance the high investment and operation

costs of this technology (Leite et al., 2013). The higher photosynthetic efficiency of enclosed photobioreactors (4-6%), supported by their higher illuminated surface-volume ratio and turbulence, results in a microalgae productivity range of 15-45 $g/m^2 \cdot d$, but at the expenses of significantly higher energy consumptions and investment costs (Acién et al, 2012) (Tables 2 and 3). Tubular photobioreactors (TPBR) constitutes the most commonly implemented enclosed microalgae culture technology (Table 3).

Table 3. Key design and operation parameters of tubular photobioreactors

Parameter	Typical range	References
Investment costs	500-3000 €/m^2	Acién et al. (2012)
Tube length	10-200 m	Arbib et al. (2013b)
Tube diameter	2-12 cm	Acién et al. (2012)
Frequency of light/dark cycles	>1 s^{-1}	Molina-Grima et al. (2001)
Culture velocity	1 m/s	Janssen et al. (2003)
Photosynthetic efficiency	4-6 %	Muñoz et al. (2015)
Productivity	15-45 $g/m^2 \cdot d$	Acién et al. (2012) Arbib et al. (2013a)
Power consumption	50-1000 $W/m^3_{reactor}$	Acién et al. (2012)

The efficient control of the operational conditions and the higher ratio of illuminated surface/volume in these photobioreactors compared to open photobioreactors also allow operating with a high biomass concentration and a defined and consistent composition, using microalgae species that are sensitive to pollution (Arbib et al., 2013b). Biofouling constitute the main disadvantage of enclosed photobioreactors, leading to biofilm formation and preventing light penetration into the culture medium. In this context, a recent work published by Arbib et al. 2013b reported biomass productivities of 35 g $TSS/m^2 \cdot day$ and 13 g $TSS/m^2 \cdot day$ in a pilot-scale TPBR (380 L) and HRAP (530 L), respectively, treating a urban wastewater containing 81 mg O_2/L of COD, 24.7 mg N/L and 2.1 mg P/L. However, the TPBR presented a severe performance deterioration as a consequence of the low irradiation caused by biofouling after 30 days of operation, which resulted in a decrease of N and P removals from 98% to 51% and 98% to 75%, respectively. Unlike in the TPBR, N and P removals in the HRAP increased from 63% to 95% and 81% to 95%, respectively, when increasing the inorganic carbon concentration in the culture broth via flue gas supply.

1.2. Microalgal biomass valorization

Microalgal biomass production during WWT can increase the sustainability of this process due to its potential use as biofertilizer or feedstock for biofuel production following anaerobic digestion (biomethane), lipid trans-esterification (biodiesel) or fermentation (bioethanol or biohydrogen) (Figure 8).

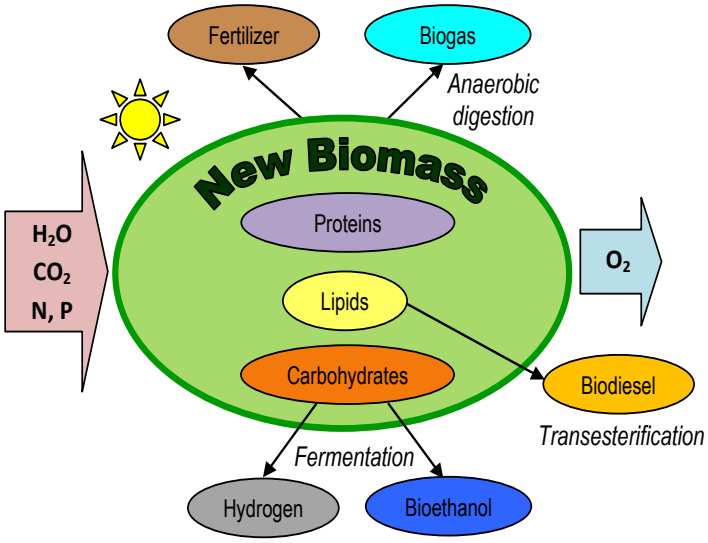

Figure 8. Potential applications of microalgae biomass produced from WWT.

1.2.1. Microalgae biomass as biofertilizer

The highly efficient and simultaneous N and P assimilation during microalgae-based WWT allows for a cost-effective nutrient recycling from wastewaters when microalgal biomass is further used as fertilizer since the production of conventional N and P fertilizers is energy intensive (60 kJ/g N and 15 kJ/g P) (Menger-Krug et al., 2012; Mulbry et al., 2005). For instance, the price of N and P microalgae fertilizers has been estimated to 1.4 €/Kg N and 1.2 €/Kg P, respectively (Chisti, 2013). In this context, microalgae luxury P uptake could support a simultaneous microalgae-based enhanced biological P removal (EBPR) and a nutrient recycling via fertilization with the microalgae biomass harvested (Shilton et al., 2012). In this regard, Mulbry et al. (2005) observed a comparable seedling growth using dried algal biomass and a commercial fertilizer, which demonstrated the potential of microalgae as a fertilizer. In addition, microalgae biomass has an advantage as a slow release fertilizer since only about 3% of the N as biomass would be available as mineral N at the time of application. Thus, the

supply of dried algal biomass to soils would not result in the NH_3 volatilization typically encountered during manure application (Thompson and Meisinger, 2002), while algal biomass may not have to be tilled into soil. This benefit may allow algal biomass to be side-dressed into growing crops. Longer term field studies are needed to assess microalgae harvesting, transportation, stability and the proportion of N and P availability to crops for this biomass to replace traditional fertilizers (Mulbry et al., 2005).

Despite the use of microalgae biomass as fertilizer is still in an embryonic stage, all these merits, along with the low energy consumption of this technology when implemented in HRAPs, represent an important advantage in comparison with aerobic activated sludge or AD technologies in terms of enhanced nutrient recovery (Arbib et al., 2014).

1.2.2. Biogas production

The O.M fraction of almost any form of biomass, including sewage sludge, animal wastes and industrial effluents, can be transformed through AD into biogas, a mixture mainly composed by CH_4 (55–75%) and CO_2 (25–45%), as shown in equation [10] (Ehimen et al., 2011; Ramaraj and Dussadee, 2015):

$$0.\mathrm{M} + \mathrm{H_2O} \rightarrow \mathrm{CH_4} + \mathrm{CO_2} + \mathrm{NH_3} \qquad [10]$$

Overall, the use of crop plant biomass for energy generation today is problematic because of the competition with food or feed production. In this context, AD of microalgal biomass appears as a promising alternative for the production of CH_4, which can be used for gas biofuel generation or directly combusted to generate electricity (Bidart et al., 2014). The productivity and composition of biogas mainly depends on the macroscopic biomass composition (carbohydrates, lipids, proteins and cellulose as main components) (Table 4), the temperature, organic loading rate and HRT during the AD process.

Table 4. Gross composition of several microalgae species and theoretical methane potential during AD (adapted from Sialve et al., 2009).

Strain of microalgae	Proteins (%)	Lipids (%)	Carbohydrates (%)	CH_4 (m^3/Kg VS)

Euglena gracilis	39-61	14-20	14-18	0.5-0.8
Chlamydomonas reinhardtii	48	21	17	0.7
Chlorella pyrenoidosa	57	2	26	0.8
Chlorella vulgaris	51-58	14-22	12-17	0.6-0.8
Dunaliella salina	57	6	32	0.7
Spirulina maxima	60-71	6-7	13-16	0.6-0.7
Spirulina platensis	46-63	4-9	8-14	0.5-0.7
Scenedesmus obliquus	50-56	12-14	10-17	0.6-0.7

In terms of theoretical CH_4 potential, the higher the lipid content of the cell, the higher the potential CH_4 yield. In addition, mesophilic temperatures (35-40 °C) appear to be optimal conditions to maximize CH_4 productivity, while HRTs between 20-30 days are typically applied to maintain methanogenic activity and a complete hydrolysis, the latter often being the limiting-step of the overall conversion of complex substrates to CH_4 (Sialve et al., 2009). In this context, a study on the influence of microalgae cultivation mode (photoautotrophic *vs*. mixotrophic conditions) on biogas composition (**Chapter 6**) revealed that ≈ 50% of the initial C as biomass was hydrolyzed and mainly found as a biogas (90 % of the hydrolyzed C) containing 30% (v/v) of CO_2 and 70% (v/v) of CH_4. Dissolved organic and inorganic C only represented 10% of C hydrolyzed during the AD of both photoautrophically and mixotrophically-grown microalgae. These results suggested that neither the extent of biomass hydrolysis nor biogas composition/productivity were influenced by microalgae cultivation mode. The CH_4 contained in the biogas can represent an energy recovery of up to 50% of the chemical energy fixed as biomass during microalgae cultivation (**Chapter 6**), which converts AD as one of the most cost-effective route for an energy valorization of microalgae. For instance, Harun et al. (2011) demonstrated that more energy could be generated from the production of methane from microalgae (14 MJ/kg_{alga}) compared to biodiesel (6.6 MJ/kg_{alga}) or ethanol (1.8 MJ/kg_{alga}). The energy content of the biogas produced by AD ranges from 16.2 to 30.6 MJ/m^3, with biogas yields typically varying from 0.15 to 0.65 m^3/Kg of dry biomass (Alzate et al., 2012; **Chapter 6**). In this context, algal biogas can be used for electricity generation via on-site combustion (kWh_e, electric KWh) or as a bio-substitute of natural gas (Bio-SNG) (KWh_{th}, thermal KWh) following a strict upgrading for injection into natural gas grids. According to the Spanish legislation Royal Decree 661/2007 the revenue obtained per KWh produced can be calculated

depending on the type of facility (technology and energy source) and the electric power produced. Based on these factors, legislation fixes a regulated price or a market price supplemented by a bonus (within minimum and maximum reference values) for each kWh generated (Table 5). Recently, this Royal Decree (RD) was replaced by RD 413/2014, in which facilities are not rewarded based on the electricity production but on other factors as the initial investment costs, operation costs or plant energy production yield during cogeneration.

Table 5. Biogas generated from digesters[1] (RD 661/2007).

Electric Power (KW)	Regulated price (ct €/kWh)	Upper limit (free market) (ct €/kWh)	Lower limit (free market) (ct €/kWh)
P ≤ 500	14.11	16.55	13.33
P ≥ 500	10.45	11.91	10.31

[1]Plants that use biomass from manures, biofuels and biogas as their main fuel.

In addition, biomass hydrolysis during AD allowed for the recovery of 65 % of N and 80 % of P provided in the microalgae growth stage (**Chapter 6**), which can offset up to 45% of the overall energy required for biofuel production (Oliveira et al., 2012). In this context, Chisti (2013) estimated that if 60% of both the N and P present in the microalgal biomass cultivated in a HRAP are recovered in the effluent of the residual biomass digester and readily available for use in crop production, the monetary value per ton of the recovered HRAP-algal biomass used as substrate for AD would be 63.5 € based on the value of N and P as fertilizer (assuming a HRAP biomass productivity of 25 $g/m^2 \cdot d$ and a N and P content of 6.6% and 1.3%, respectively).

The above rationales suggest that the production of methane via AD is the most feasible and cost-effective route for an energy valorization of microalgae (Park et al., 2011b). Despite AD of microalgae as a feedstock for biogas production has been studied since the early fifties, this technology still requires further investigation before being cost-effectively implemented at large scale. Therefore, future work on the influence of the hydraulic retention time, organic loading rate, temperature, substrate carbon to nitrogen ratio and pretreatments (thermal hydrolysis, ultrasound and biological treatment) is required in order to maximize microalgae biodegradability and their methane conversion yield (Alzate et al., 2012; Ehimen et al., 2011; Passos et al., 2014).

1.2.3. Biodiesel production

Microalgae are regarded as a promising feedstock for sustainable biodiesel production because of their potential accumulation of high oil contents (up to 50-70 % of their dry cell weight), which can be higher than those of conventional energy crops such as soybean, oil palm, jatropha, canola, etc. (Table 6) (Chisti, 2007; Ndimba et al., 2013).

Table 6. Comparison of some biodiesel sources (adapted from Chisti, 2007).

Crop	Oil yield (L/ha)	Land area needed (Mha)[a]
Soybean	446	594
Canola	1190	223
Jatropha	1892	140
Coconut	2689	99
Oil palm	5950	45
Microalgae[b]	136,900	2
Microalgae[c]	58,700	4.5

[a]For meeting 50 % of all transport fuel needs of the United States in 2007.
[b]70 % oil (by wt) in biomass.
[c]30 % oil (by wt) in biomass.

Microalgal lipid consists mainly of triglycerides that can be converted to biodiesel as fatty acid methyl esters (FAME) through transesterification (Figure 9) (Chisti, 2007).

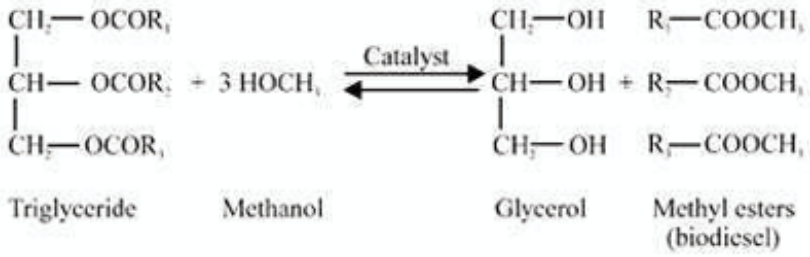

Figure 9. Transesterification of oil to biodiesel. R_{1-3} are hydrocarbon groups.

The lipid content of microalgae can be increased by environmental stress factors such as a limitation in essential nutrients like nitrogen (Simionato et al., 2013), phosphorus (Chu et al. 2013) and trace elements (Concas et al., 2014). Nitrogen depletion in the cultivation broth changes the cellular carbon flux from protein synthesis to lipid synthesis. For instance, the lipid content of *Chlorella vulgaris* can increase from 20% to up to 40% under nitrogen deprivation (Illman et al., 2000). Therefore, understanding carbon distribution into lipids in microalgae will be crucial for designing cultivation strategies in order to increase the competitiveness of microalgal biodiesel in the future biofuel market.

1.2.4. Bioethanol production

Recent attempts to produce bioethanol have focused on carbohydrate-rich microalgae as a feedstock for fermentation due to their high ethanol areal yields in comparison with those of conventional sugar-rich feedstocks (Table 7).

Table 7. Ethanol yield from different sources (adapted from Mussato et al., 2010)

Source	Ethanol yield (L/ha·year)
Corn	3,460-4,020
Wheat	2,590
Cassava	3,310
Sugarcane	6,190-7,500
Sugar beet	5,010-6,680
Microalgae	46,760-140,290

Several species of microalgae have the ability of accumulating high levels of carbohydrates instead of lipids as reserve polymers that can be extracted to produce fermentable sugars to finally produce ethanol as shown in equation [11]:

$$C_6H_{12}O_6 \rightarrow 2CH_3CH_2OH + 2CO_2 \quad [11]$$

Microalgae can accumulate carbohydrates under stress conditions. In this regard, while nitrogen starvation can induce an increase in biomass lipid content (Simionato et al. 2013), the presence of phosphorus plays a key role on lipid productivity under nitrogen deficient conditions in both microalgae (**Chapter 3**; Chu et al. 2013,) and bacteria (**Chapter 3**; Kulaev et al. 1999). Indeed, the absence of phosphorous under nitrogen starvation can turn into a suppression factor for lipid accumulation and promote instead carbohydrate accumulation (**Chapter 3**). Despite the preliminary feasibility test reported, the technology for the commercial production of bioethanol from microalgae, including biomass pre-treatment (Hernández et al., 2014) and continuous fermentation (Mussato et al., 2014), is still in an embryonic stage.

1.2.5. Biohydrogen production

Hydrogen gas (H_2) is assumed to be an optimal energy carrier since it produces only water during its combustion with oxygen. Despite hydrogen is currently produced from non-renewable sources (fossil fuels), it can be generated by microalgae, cyanobacteria and bacteria through biophotolysis or dark fermentation. **Biophotolysis**

is based on the capability of microalgae and cyanobacteria to use the light energy to produce hydrogen, which can occur via two metabolic pathways: direct photolysis and indirect photolysis (Show and Lee, 2013). During direct photolysis two electrons are obtained from the water-splitting reaction and transferred through a light-dependent electron-transport chain located in the thylakoid membrane to ferredoxin, resulting in H_2 production via Fe-hydrogenase pathway under anaerobic conditions as shown in equations [12] and [13]:

$$2H_2O \xrightarrow{\text{Light energy}} 4H^+ + 4e^- + O_2 \quad [12]$$

$$2H^+ + 2e^- \xrightarrow{\text{Fe-Hydrogenase}} H_2 \quad [13]$$

Indirect photolysis is conducted by cyanobacteria that can also synthesize and evolve H_2 through photosynthesis (Levin et al., 2004) as shown in equations [14] and [15]:

$$12H_2O + 6CO_2 \xrightarrow{\text{Light energy}} C_6H_{12}O_6 + 6O_2 \quad [14]$$

$$C_6H_{12}O_6 + 12H_2O \xrightarrow{\text{Light energy}} 12H_2 + 6CO_2 \quad [15]$$

A major technical challenge in H_2 production through biophotolysis is the need for a spatial and/or temporal separation of the photosynthetic H_2 and O_2 production since Fe-hydrogenase is extremely sensitive to O_2 (Show and Lee, 2013). In addition, the low microalgae-based H_2 productivity compared with bacterial dark fermentation is also likely to hinder its full-scale implementation (Table 8).

During **dark or heterotrophic fermentation**, hydrogen can be produced by anaerobic bacteria using carbohydrate-rich microalgae as a substrate without the need of a light energy input as shown in equation [16] (Levin et al., 2004):

$$C_6H_{12}O_6 + 2H_2O \xrightarrow{\text{Dark}} 2CH_3COOH + 4H_2 + 2CO_2 \quad [16]$$

Table 8. Comparison of biological H_2 production processes (Adapted from Levin et al., 2004).

BioH_2 pathway	**Microorganisms**	**H_2 production rate (mmol H_2/L·h)**
Direct photolysis	*Chlamydomonas reinhardtii*	0.07
Indirect photolysis	*Anabaena variabilis*	0.36
Dark fermentation	*Clostridium sp.* strain No 2	64.5

1.3. Energy considerations in algal-bacterial based WWT technologies

Typical WWTPs designed exclusively with secondary treatment are able to satisfactorily meet the discharge levels for organic carbon (quantified as BOD), but fail to comply with N and P discharge levels. Secondary WWTPs effluents commonly exhibit 20–70 mg N/L and 4–12 mg P/L, which only account for a removal of 40% and 12% of the inlet total nitrogen and total phosphorous, respectively (Dominguez et al., 2013). However, the European Directive 98/15/EC establishes a threshold of 10 and 1 mg/L for total N and P, respectively, for water discharges from urban WWTPs in communities with more than 10,000 equivalent inhabitants. Therefore, a further tertiary treatment, and consequently, additional costs are required in order to meet EU discharge limits (Dominguez et al., 2013). Biological Nutrient Removal (BNR) incorporated in activated sludge processes is one of the preferred options for tertiary treatment of urban wastewaters, where ammoniacal nitrogen ($N\text{-}NH_3$) is converted to nitrogen gas (nitrification-denitrification) and phosphorus is removed by an enhanced accumulation in a specialized biomass (Polyphosphate-Accumulating Organisms, PAOs) (Figure 10a). However, conventional BNR processes or P precipitation (when EBPR is not implemented) contribute to the loss of these valuable nutrients via nitrogen denitrification or P precipitation (De Godos et al., 2009a) and are highly energy intensive, accounting for 60-80% of the total energy requirements for wastewater treatment (1.5 kWh/Kg N when O_2 is supplied in the nitrification stage through fine bubble diffusers and 4.6 kWh/Kg N when supplied by superficial aeration) (Dominguez et al., 2013; Méndez et al., 2010; Selvaratnam et al., 2014). In this context, the energy required during activated sludge-based WWT using nitrification-denitrification (AS + ND) as a N removal mechanism (Figure 10a) was estimated and compared with the energy consumed during microalgae-based WWT in HRAPs (Figure 10b) considering the reference scenario shown in Table 9 and 10 for a 20,000 inhabitants city:

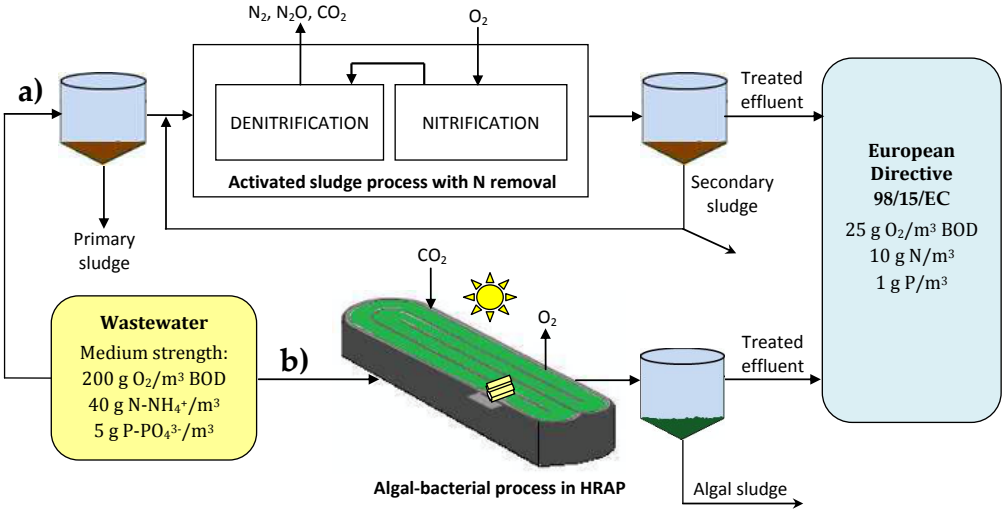

Figure 10. WWT in an AS + ND process (a) and a HRAP (b).

Table 9. Input data for Figure 10a case study (Wildschut, 2010).

Energy required[1]	KWh/capita·d	KWh/m³ww	TER (%)
Pretreatment	0.010	0.05	5.4
Pumping	0.006	0.03	3.4
Grit removal	0.005	0.03	2.6
Primary treatment	0.000	0	0
Secondary treatment	0.158	0.79	88.6
Total energy required (TER)	0.180	**0.90**	100

[1]WWTP for 20,000 inhabitants and a wastewater generation rate of 0.2 m³/capita·d

Table 10. Input data for Figure 10b case study

Input data		
Parameter	**Value**	**References**
Inhabitants (I)	20,000	Metcalf and Eddy (2003)
Flow rate (F) (m³/capita·d)	0.2	Metcalf and Eddy (2003)
HRT (days)	7	Alcántara et al. (2015)
HRAP power consumption (W/$m^3_{Reactor}$)	2[1]	Borowitzka (2005)
Results		
Feeding flow (Q) (m³/d)	4,000	
Reactor volume required (V_R) (m³)	28,000	
Daily energy required (DER) (KWh/d)	1,344	
Total energy required (TER) (KWh/m³ww)	**0.34**	

[1]V_R= 28,000 m³, depth = 0.3 m, flow velocity = 20 cm/s and paddle wheel efficiency = 0.17.

$$Q = I \times F = 20{,}000 \text{ inhabitants} \times 0.2 \frac{m^3_{ww}}{\text{inhabitant}\cdot\text{d}} = 4{,}000 \frac{m^3_{ww}}{\text{d}}$$

$$V_R = Q \times HRT = 4{,}000 \frac{m^3_{ww}}{\text{d}} \times 7\text{d} = 28{,}000\ m^3_R$$

$$DER = 28{,}000\ m^3_R \times 2 \frac{\text{J}}{\text{s}\cdot m^3_R} \times \frac{3600\ \text{s}}{1\ \text{h}} \times \frac{24\ \text{h}}{1\ \text{d}} \times \frac{1\ \text{KWh}}{3600000\ \text{J}} = 1{,}344 \frac{\text{KWh}}{\text{d}}$$

$$\text{TER} = 1344\,\frac{\text{KWh}}{\text{d}} \times \frac{1\ \text{d}}{4000\ \text{m}^3_{\text{ww}}} = \mathbf{0.34}\,\frac{\text{KWh}}{\text{m}^3_{\text{ww treated}}}$$

These simple estimations clearly showed that the energy required during WWT in HRAPs (0.34 KWh/m^3_{WW}) is significantly lower than the energy required in AS + ND activated sludge processes (0.9 KWh/m^3_{WW}). Hence, despite HRAPs are typically operated at high HRTs (3-10 days) compared to activated sludge processes (10-12 h) (Metcalf and Eddy, 2003; Posadas et al., 2015), photosynthetic oxygenation significantly lowers the energy demand for C and N oxidation, which represents an economic and environmental advantage compared with mechanical aeration-based technologies (where up to 50 % of the total energy consumption is associated with mechanical O_2 supply) (Chae and Kang, 2013; Méndez et al., 2010). Thus, microalgae-based WWT in HRAPs offers a low cost and more efficient alternative to conventional tertiary treatment.

On the other hand, activated sludge productivity during urban WW treatment in activated sludge processes (Figure 10a) ranges between 80 and 170 g TSS/m^3ww (Table 11). In this context, the disposal of the waste activated sludge produced can represent up to 50% of the operating cost in WWTPs (Selvaratnam et al., 2014).

Table 11. Sludge productivity during urban WW treatment in activated sludge process

g TSS/m^3ww	References
86[1]	Selvaratnam et al. (2014)
107[2]	Metcalf and Eddy (2003)
91[3]	Metcalf and Eddy (2003)
166[4]	Metcalf and Eddy (2003)
146[5,6]	Escaler et al. (2010)

[1]Activated sludge process only for BOD removal (045 g TSS formed/g BOD removed)
[2]Activated sludge process only for BOD removal. Inlet flow of 22,464 m^3/d.
[3]Activated sludge process for BOD removal and nitrification. Inlet flow of 22,464 m^3/d.
[4]Input COD concentration of 333 g/m^3, 0.4 g VSS/g $COD_{removed}$ and 0.8 g VSS/g TSS.
[5]Input BOD concentration of 200 g/m^3 and BOD removal of 95%.
[6]Prat de LLobregat WWTP (Barcelona) designed for 2,275,000 inhabitants and an average inlet flow of 420,000 m^3/d in 2007.

However, assuming a typical domestic WW composition of 200 g TOC/m^3ww and 100 g IC/m^3ww, the microalgal-bacterial biomass produced can be up to 2.8 times higher than the bacterial biomass productivity due to the additional photosynthetic C

assimilation from the CO_2 released during bacterial respiration and WW alkalinity ($CaCO_3$) (Muñoz and Guieysse, 2006; Selvaratnam et al., 2014). This higher biomass productivity per cubic meter of WW treated in algal-bacterial systems could be regarded as an operation handicap in terms of sludge management in comparison with activated sludge processes. However, the production of this extra algal-bacterial sludge can increase the energy recovery through AD of primary and secondary produced sludge in conventional WWTPs, which represents an advantage in terms of net energy expenditures (Bidart et al., 2014; Selvaratnam et al., 2014). Hence, a model microalgae-based WWTP was proposed (Figure 11) considering the low energy requirements in HRAP-based WWT (Table 12), the nutrient removal and production of a valuable biomass by the fixation of CO_2 from flue gas and the potential energy generation through the AD of this biomass (Table 12). In this context, the energy consumed in the HRAP represented 55% of the electrical energy obtained from CH_4 combustion obtained only of the AD of algal-bacterial biomass.

Table 12. Energy production from the biomass generated in the HRAP in Figure 11 (dashed lines are not considered in this balance)

Parameter	Value	References
CH_4 productivity	0.4 L CH_4/g TSS harvested	**Chapter 6**
Biomass productivity (P)	20 g/m^2_R·d	Alcántara et al. (2015)
Biogas CH_4 content	70%	**Chapter 6**
Biogas energy content	6.5 KWh/m^3	Menger-Krug et al. (2012)
Electricity conversion efficiency (ECE)	35%	Menger-Krug et al. (2012)
HRAP power consumption	2[1] W/m^3_R	Borowitzka (2005)
HRAP energy consumption (EC)	0.014 KWh/m^2_R·d[1]	Borowitzka (2005)
Energy produced (EP)	**0.026 KWh/m^2_R·d**	-

[1]V_R= 28,000 m^3, depth = 0.3 m, flow velocity = 20 cm/s and paddle wheel efficiency = 0.17.

In this scenario, the AD of the algal-bacterial biomass generated in outdoors HRAPs during the combined wastewater treatment-CO_2 capture process can significantly enhance the economic and environmental sustainability of WWT processes in terms of energy production and recovery of CO_2 and nutrients, highlighting the potential of the integration of microalgae-based WWT technology in WWTPs as a net energy-producing platform (Figure 11).

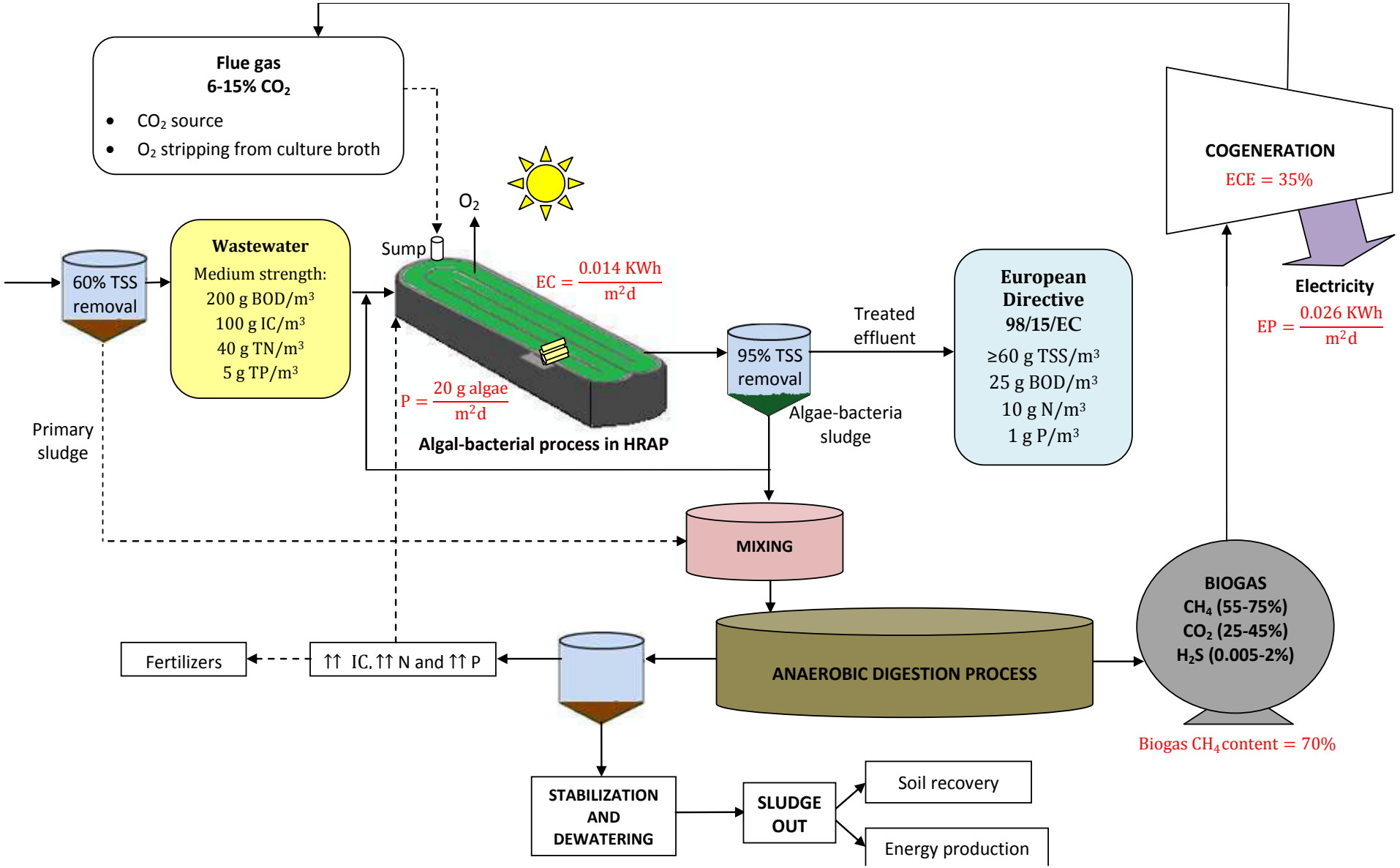

Figure 11. Microalgae-based WWT in a HRAP integrated with AD and recovery of nutrients and CO_2 from gas turbines.

1.4. Environmental considerations of algal-bacterial based WWT technologies

Conventional WWT based on activated sludge processes involve higher energy requirements and therefore a higher CO_2 footprint than HRAP-based WWT (Table 13). In addition, photosynthetic CO_2 fixation during HRAP-based WWT entails a beneficial effect in terms of global warming mitigation. However, the environmental sustainability of microalgae-based WWT has been recently challenged due to the ability of microalgae or associated bacteria to synthesize N_2O, a greenhouse gas with a global warming potential 298 times higher than CO_2, which could jeopardize the benefits associated to photosynthetic CO_2 capture in a net greenhouse gas mass balance (**Chapter 4**; **Chapter 7**; Fagerstone et al., 2011).

Table 13. Comparison of the energy required and associated CO_2 footprint in different WWT technologies.

	Energy required ($KWh/Kg\ BOD_{removed}$)	**Energy required[2] ($KWh/m^3\ WW_{treated}$)**	**Associated CO_2 footprint[3] ($g\ CO_2/\ m^3\ WW_{treated}$)**	**References**
HRAPs	0-0.57	0-0.11	0-21	Mahdy et al. (2015)
Mechanically aerated Ponds	0.8-6.4	0.15-1.22	29-232	Mahdy et al. (2015)
Activated sludge process	1.5-1.97	0.29-0.37	54-72	Oswald (2003); Selvaratnam et al. (2014); Hernández et al. (2010)
Activated sludge + N removal	2.6-6	0.49-1.14	94-218	Hernández et al. (2010)
Anaerobic digestion	-(1-1.5)[1]	0.19	36	Oswald (2003); Van Lier (2008)

[1]Electric power produced from the biogas obtained after anaerobic digestion assuming a 40% of electric conversion efficiency. This value depends on local circumstances (such as the fuel used by the regional power plants).

[2]According to typical energy consumptions in $KWh/Kg\ BOD_{removed}$ and assuming an input BOD concentration of 200 g/m^3 and s BOD removal of 95%.

[3]Assuming a CO_2 emission factor of 0.191Kg CO_2 per KWh consumed (WWF Spain, January 2015).

1.4.1. N_2O emissions and their associated CO_2 footprint

N_2O can be biologically generated by nitrifying bacteria, denitrifying bacteria, nitrifying-denitrifying bacteria, ammonium oxidizing archaea and microalgae (Figure 12). The potential occurrence and significance of these pathways in wastewater treatment HRAPs is discussed below.

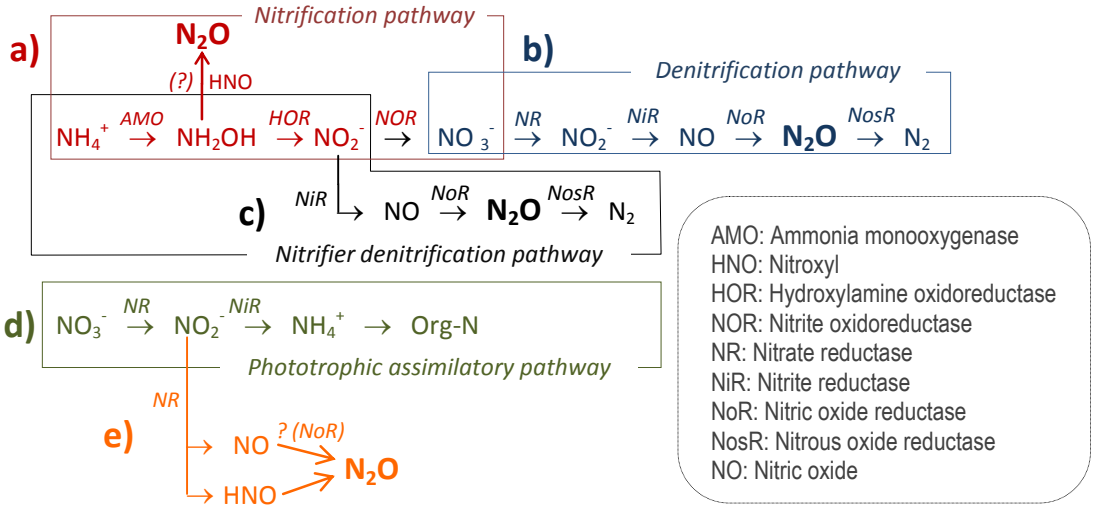

Figure 12. Potential N_2O production metabolic pathways occurring in HRAPs ((?) = unclear pathway and/or putative enzyme type).

During nitrification (Figure 12a), NH_4^+ is first converted to hydroxylamine (NH_2OH) to be further transformed into NO_2^-. N_2O can be produced from NH_2OH by either chemical decomposition or chemical oxidation. Chemical oxidation occurs with NO_2^- as electron acceptor under O_2 limiting conditions (0.1-0.5 mg/L) (Kampschreur et al., 2009; Law et al., 2015). However, N_2O production via NH_2OH aerobic oxidation in ammonia-oxidizing bacteria culture was also observed by Wunderlin et al. (2012) under NO_2^- limiting conditions in the excess of ammonium. Thus, the accumulation of ammonium in HRAPs could result in N_2O production via NH_2OH oxidation based on the high dissolved oxygen concentration (DOC) typically encountered in microalgae culture broths. In contrast, N_2O production via the denitrification or nitrification-denitrification pathways (Figure 12 b, c) during microalgae-based WWT is likely to be less frequent (even at night) as active denitrification occurs below O_2 concentrations of 0.5 mg/L, while the constant O_2 diffusion from the atmosphere can offset the high O_2 consumption mediated by microbial respiration rate at night, anoxic conditions being

prevented in the cultivation broth (Wang et al., 2008). Guieysse et al. (2013a) challenged the significance of N_2O production in well-mixed photobioreactors and demonstrated that axenic *Chlorella vulgaris* could indeed synthesize N_2O, possibly via a Nitrate Reductase (NR)-mediated nitrite reduction into either nitrous oxide (NO) or nitroxyl (HNO) (Figure 12e). In this context, the study performed in **Chapter 7** to assess the potential significance of N_2O emissions from two identical 7-L HRAPs treating synthetic wastewater at 7 days of HRT confirmed that despite HRAPs microcosms demonstrated the ability to generate algal-mediated N_2O when nitrite was externally supplied in the dark, negligible N_2O emissions rates were consistently recorded in the absence of nitrite during a 3.5-month monitoring. Therefore, avoid the accumulation of NO_2^- during the night in HRAPs operated at high loading rates represent an operational factor to prevent N_2O generation given the ability of the algal-bacterial biomass present in the HRAPs to generate N_2O in the presence of exogenous NO_2^- in the dark (Figure 12 a, d, e) (**Chapter 7**).

N_2O emissions lower than 2 nmol N_2O/g TSS·h were consistently recorded from HRAP cultures sampled under a typical N-loading of 7.1 g $N/m^3_{reactor}$·d. A 24-hr average emission rate of 1 nmol N_2O/g TSS·h would thus result in an emission factor of 4.7×10^{-5} g $N\text{-}N_2O$/g N-input and an associated CO_2 footprint of 1.1 g of CO_2/m^3_{WW} in a conventional HRAP. The study performed in **Chapter 4** also evaluated the N_2O production during algal-bacterial nitrification-denitrification in a novel anoxic-aerobic photobioreactor. This system only generated relevant N_2O emissions in the aerobic reactor, which resulted in average N_2O emission factors of 5.2×10^{-6} g $N\text{-}N_2O$/g N-input, corresponding with an associated CO_2 footprint of 0.3 g CO_2/m^3_{WW}. The N_2O emission factors obtained in both microalgae-based wastewater treatment photobioreactor configurations (**Chapter 4** and **Chapter 7**) were significantly lower than the N_2O emission factor typically recorded in WWTPs ($5\text{-}6\cdot10^{-3}$ g $N\text{-}N_2O$/g N-input) (Gustavsson and La Cour Jansen, 2011; IPCC, 2006). In addition, the CO_2 footprint associated with the N_2O emissions recorded in both systems (1.1 and 0.3 g CO_2/m^3_{WW}), compared favorably against the indirect CO_2 footprint from electricity use for aeration and mixing in activated sludge processes (119-378 g CO_2/m^3_{WW}) and even for mixing in HRAPs (3-14 g CO_2/m^3_{WW}). These preliminary estimations suggest that

N_2O emissions in these algal-bacterial photobioreactors should not compromise the environmental sustainability of wastewater treatment in terms of global warming impact.

1.4.2. Water footprint

Although microalgae-based WWT improves water quality, significant amounts of water may be lost from the photobioreactors due to evaporation. Guieysse et al. (2013b) predicted evaporation rates of up to 2.275 $m^3/m^2.yr$ (0.0062 $m^3/m^2 \cdot d$)) in Arizona in 0.25 m algae raceway ponds, which represented 15% of the amount of water treated. Although these water losses may sound 'affordable', the ecological and economical value of water depends on local conditions. In Arizona, an evaporation rate of 2.275 $m^3/m^2.yr$ represents more than 40 years of rainfall equivalent. In addition, water losses entail an overconcentration of the WW contaminants, which itself is a function of HRT. In this context, the HRT (typically imposed by the organic and nutrient load to be treated) influences directly the ratio WW evaporated to WW treated. Based on a 0.0062 $m^3/m^2 \cdot d$ evaporation rate (worst scenario) and a typical deep pond of 0.3 m, the higher the HRT the higher the ratio m^3_{ww} evaporated/m^3_{ww} treated (Figure 13). Therefore, a careful evaluation of water evaporation losses and its associated deterioration of the quality of the treated effluent must be conducted prior to the implementation of HRAPs in water-stressed areas.

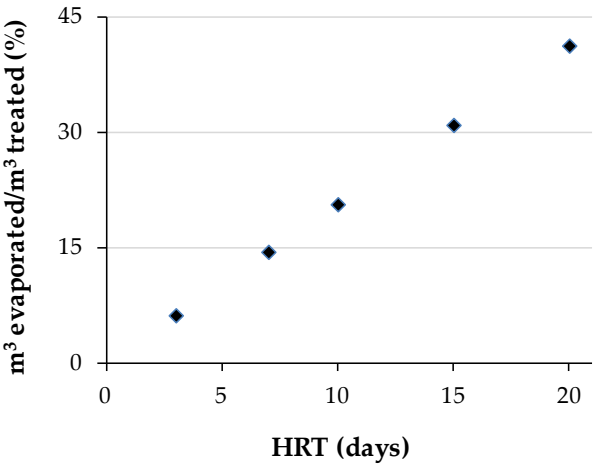

Figure 13. Influence of HRT on the ratio m^3_{ww} evaporated/m^3_{ww} treated.

1.5. References

1. Abdel-Raouf, N., Al-Homaidan, A.A., Ibraheem, I. B. M., 2012. Microalgae and wastewater treatment. Saudi Journal of Biological Sciences 19, 257–275.
2. Acién, F.G., Fernandez, J.M., Magán, J.J., Molina, E., 2012. Production cost of a real microalgae production plant and strategies to reduce it. Biotechnology Advances. 30(6), 1344-1353.
3. Alcántara, C., Posadas, E., Guieysse, B., Muñoz, R., 2015. Microalgae-based wastewater treatment. In: Handbook of Microalgae: Biotechnology Advances. Edited by Se-Kwon K, Elsevier, (in press).
4. Alzate, M.E., Muñoz, R., Rogalla, F., Fdz-Polanco, F., Pérez-Elvira, S.I., 2012. Biochemical methane potential of microalgae: Influence of substrate to inoculum ratio, biomass concentration and pretreatment. Bioresource Technology. 123, 488–494.
5. Arbib, Z., Ruiz, J., Álvarez-Díaz, P., Garrido-Pérez, C., Barragan, J., Perales, J.A., 2013a. Effect of pH control by means of flue gas addition on three different photo-bioreactors treating urban wastewater in long-term Operation. Ecological Engineering. 57, 226– 235.
6. Arbib, Z., Ruiz, J., Álvarez-Díaz, P., Garrido-Pérez, C., Barragan, J., Perales, J.A., 2013b. Long term outdoor operation of a tubular airlift pilot photobioreactor and a high rate algal pond as tertiary treatment of urban wastewater. Ecological Engineering. 52, 143-153.
7. Arbib, Z., Ruiz, J., Álvarez-Díaz, P., Garrido-Pérez, C., Perales, J.A., 2014. Capability of different microalgae species for phytoremediation processes: Wastewater tertiary treatment, CO_2 bio-fixation and low cost biofuels production. Water Research. 49, 465–474.
8. Bahr, M., Díaz, I., Domínguez, A., Sánchez-González, A., Muñoz, R., 2014. Microalgal-biotechnology as a platform for an integral biogas upgrading and nutrient removal from anaerobic effluents. Environmental Science and Technology. 48(1), 573-581.
9. Barsanti, L. and Gualteri, P., 2006. Algae: Anatomy, Biochemistry and Biotechnology. In: General overview (Chapter 1, 1-6); Photosynthesis (Chapter 3, 135-150) and Algal culturing (Chapter 6, 209-228).Taylor and Francis group, Boca Ratón (USA).
10. Beltrán, S., Alferes, J., Corominas, L., Flores, X., Donoso, A., Ayesa, E., 2009. Análisis técnico económico de la implantación de controladores automáticos en las EDAR. In: Hernández Sancho, F., and Fdez.-Polanco, F., El reto de la eficiencia económica en EDAR. Integrando la economía en la concepción, rediseño y gestión de EDAR. Chapter 3, 71-110.
11. Benemann, J.R., 2003. Biofixation of CO_2 and greenhouse gas abatement with microalgae—technology roadmap. Report no. 7010000926 prepared for the U.S. Department of Energy National Energy Technology Laboratory.
12. Benemann, J., 2013. Microalgae for Biofuels and Animal Feeds. Energies. 6, 5869-5886.
13. Bidart, B., Fröhling, M., Schultmann, F., 2014. Electricity and substitute natural gas generation from the conversion of wastewater treatment plant sludge. Applied Energy 113, 404–413.
14. BOE-A-2013-185 (http://www.boe.es/boe/dias/2013/01/07/pdfs/BOE-A-2013-185.pdf. Last visited: 28 Feb 2015).
15. Borowitzka, M.A., 2005. Culturing microalgae in outdoor ponds. In: Andersen, I.R.A. (Ed.), Algal Culturing Techniques. Elsevier, Academic Press, New York, 205–218.
16. Buelna, G., Bhattarai, K.K., de la Noüe, J., Taiganides, E.P., 1990. Evaluation of various flocculants for the recovery of algal biomass grown on pig-waste. Biological Wastes. 31, 211–222.
17. Cañizares-Villanueva, R.O., 2000. Biosorción de metales pesados mediante el uso de biomasa microbiana. Revista Latinoamericana de Microbiología. 42, 131-143.
18. Chae, K.Y and Kang, J., 2013. Estimating the energy independence of a municipal wastewater treatment plant incorporating green energy resources. Energy Conversion and Management. 72, 664-672.
19. Chisti, Y., 2007. Biodiesel from microalgae, Biotechnology Advances. 25, 294–306.
20. Chisti, Y., 2013. Microalgal Biotechnology: Potential and Production. In: De Gruyter bookshelf, ed. by Posten, C. and Walter, C., Berlin, Boston, 97–115. ISBN: 9783110225013.
21. Chojnacka, K., Chojnacki, A., and Gorecka, H., 2005. Biosorption of Cr^{3+}, Cd^{2+} and Cu^{2+} ions by blue-green algae Spirulina sp.: kinetics, equilibrium and the mechanism of the process. Chemosphere 59, 75-84.
22. Chu, F.F., Chu, P.N., Cai, P.J., Li,W.W., Lam, P.K.S., Zeng, R.J., 2013. Phosphorus plays an important role in enhancing biodiesel productivity of *Chlorella vulgaris* under nitrogen deficiency. Bioresource Technology. 134, 341–346.
23. Coats, E.R., Watkins, D.L., Brinkman, C.K., Loge, F.J., 2011. Effect of Anaerobic HRT on Biological Phosphorus Removal and the Enrichment of Phosphorus Accumulating Organisms. Water Environment Research. 83(5), 461-9.

24. Concas, A., Steriti, A., Pisu, M., Cao, G., 2014. Comprehensive modeling and investigation of the effect of iron on the growth rate and lipid accumulation of *Chlorella vulgaris* cultured in batch photobioreactors. Bioresource Technology. 153, 340-350.
25. Craggs, R., Sutherland, D., Campbell, H., 2012. Hectare-scale demonstration of high rate algal ponds for enhanced wastewater treatment and biofuel production. Journal of Applied Phycology. 24, 329-337.
26. De Godos, I., Blanco, S., García-Encina, P., Becares, E., Muñoz, R., 2009a. Long Term operation of High Rate Algae Ponds for the Bioremediation of Piggery Wastewaters at High Loading Rates. Bioresource Technology. 100(19), 4332-4339.
27. De Godos, I., González, C., Becares, E., García-Encina, P.A., Muñoz, R., 2009b. Simultaneous nutrients and carbon removal during pretreated swine slurry degradation in a tubular biofilm photobioreactor. Applied Microbiology and Biotechnology. 82, 187–194.
28. De Godos, I., Blanco, S., García-Encina, P. A., Becares, E. and Muñoz, R., 2010. Influence of flue gas sparging on the performance of high rate algae ponds treating agro-industrial wastewaters. Journal of Hazardous Materials. 179(1-3), 1049–1054.
29. Dominguez Cabanelas, I.T., Arbib, Z., Chinalia, F.A., Souza, C.O., Perales, J.A., Almeida, P.F., Druzian, J.I., Andrade Nascimento, I., 2013. From waste to energy: Microalgae production in wastewater and glicerol. Applied Energy 109, 283–290
30. Ehimen, E.A., Sun, Z.F., Carrington, C.G., Birch, E.J., Eaton-Rye, J.J., 2011. Anaerobic digestion of microalgae residues resulting from the biodiesel production process. Applied Energy 88, 3454–3463.
31. El Hamouri, B., Khallayoune, K., Bouzoubaa, K., Rhallabi, N., and Chalabi, M., 1994. High-rate algal pond performances in faecal coliformes and helminth egg removals. Water Research. 28(1), 171-174.
32. Escaler, I., Massagué, A., Romero, A., Gullón, M., 2010. Resultados de la medida y evaluación del impacto de las emisiones de GEI en EDAR en Cataluña. In: Mata, J and Fdez.-Polanco, F., Ecoeficiencia en la EDAR del Siglo XXI. Aspectos Ambientales y Energéticos.Chapter 2, 26-38.
33. European Directive 98/15/CEE. <http://www.boe.es/doue/1998/067/L00029-00030.pdf>, 1998 (accessed 08.02.15).
34. Fagerstone, K.D., Quinn, J.C., Bradley, T.H., De Long, S.K., Marchese, A.J., 2011. Quantitative measurement of direct nitrous oxide emissions from microalgae cultivation. Environmental Science and Technology. 45, 9449–9456.
35. Gavrilescu, M., 2004. Removal of Heavy Metals from the Environment by Biosorption. Engineering in life Sciences. 4, 219-232.
36. Guieysse, B., Plouviez, M., Coilhac, M., Cazali, L., 2013a. Nitrous oxide (N_2O) production in axenic *Chlorella vulgaris* microalgae cultures: evidence, putative pathways, and potential environmental impacts. Biogeosciences 10, 6737–6746.
37. Guieysse, B., Béchet, Q., Shilton, A., 2013b. Variability and uncertainty in water demand and water footprint assessments of fresh algae cultivation based on case studies from five climatic regions. Bioresource Technology. 128, 317–323.
38. Gustavsson, D.J.I. and la Cour Jansen, J., 2011. Dynamics of nitrogen oxides emission from a full-scale sludge liquor treatment plant with nitritation. Water Science and Technology. 63(12), 2838-2845.
39. Harun, R., Davidson, M., Doyle, M., Gopiraj, R., Danquah, M., Forde, G., 2011. Technoeconomic analysis of an integrated microalgae photobioreactor, biodiesel and biogas production facility. Biomass Bioenergy. 35, 741–747.
40. Hernández, F., Molinos, M., Sala, R., 2010. Aspectos económicos de la gestión energética. In: Mata, J and Fdez.-Polanco, F., Ecoeficiencia en la EDAR del Siglo XXI. Aspectos Ambientales y Energéticos.Chapter 8, 155-172.
41. Hernández, D., Riaño, B., Coca, M., García-González, M.C., 2014. Saccharification of carbohydrates in microalgal biomass by physical, chemical and enzymatic pre-treatments as a previous step for bioethanol production. Chemical Engineering Journal. 262, 939–945.
42. Heubeck, S., Craggs, R.J., Shilton, A., 2007. Influence of CO_2 scrubbing from biogas on the treatment performance of a high rate algal pond. Water Science and Technology. 55(11), 193-200.
43. Huguen, P. and Le Saux, G., 2010. Perspectives for a european standard on biomethane: a Biogasmax proposal. European Biogasmax project http://www.biogasmax.eu/media/d3_8_new_lmcu_bgx _eu_standard_14dec10_vf__077238500_0948_26012011.pdf. Accessed 10 December 2014
44. Illman, A.M., Scragg,A.H., Shales,S.W., 2000. Increase in *Chlorella* strains calorific values when grown in low nitrogen medium, Enzyme and Microbial Technology. 27, 631–635.
45. IPCC, 2006. 2006 IPCC Guidelines for National Greenhouse Gas Inventories. In: Eggleston, H.S., Buendia, L., Miwa, K., Ngara, T., Tanabe, K. (Eds.). IGES, Japan, 6.24–26.26.

46. Janssen, M., Tramper, J., Mur, L.R., Wijffels, R.H., 2003. Enclosed Outdoor Photobioreactors: Light Regime, Photosynthetic Efficiency, Scale-up, and Future Prospects. Biotecnology and Bioengineering. 81, 193-210.
47. Jorquera, O., Kiperstok, A., Sales, E.A., Embiruçu, M., Ghirardi, M.L., 2010. Comparative energy life-cycle analyses of microalgal biomass production in open ponds and photobioreactors. Bioresource Technology 101, 1406–1413.
48. Kampschreur, M.J., Temmink, H., Kleerebezem,R., Jetten, M.S.M., van Loosdrecht, M.C.M., 2009. Nitrous oxide emission during wastewater treatment. Water Research. 43, 4093–4103.
49. Kivaisi, A.K., 2001. The potential for constructed wetlands for wastewater treatment and reuse in developing countries: a review. Ecological Engineerong. 16, 545–560.
50. Kulaev, I., Vagabov, V., Kulakovskaya, T.,1999. New aspects of inorganic polyphosphate metabolism and function. Journal of Bioscience and Bioengineering. 88(2), 111-129.
51. Lam, M.K., Lee, K.T., Mohamed, A.R., 2012. Current status and challenges on microalgae-based carbon capture. Int. J. Greenhouse Gas Control. 10, 456–469.
52. Lardon, L., Hélias, A., Sialve, B., Steyer, J.P., Bernard, O., 2009. Life-cycle assessment of biodiesel production from microalgae. Environmental Science and Technology. 43(17), 6475–6481.
53. Law, Y., Ye, L., Pan, Y., Yuan, Z., 2015. Nitrous oxide emissions from wastewater treatment processes. Philosophical Transactions of the Royal Society B. 367, 1265–1277.
54. Lehr, F. and Posten, C., 2009. Closed photo-bioreactors as tools for biofuel production. Current Opinion in Biotechnology. 20, 280–285.
55. Leite, G.B., Abdelaziz, A.E., Hallenbeck, P.C., 2013. Algal biofuels: Challenges and opportunities. Bioresource Technology 145, 134–141.
56. Levin, D.B., Pitt, L., Love, M., 2004. Biohydrogen production: prospects and limitations to practical application, International Journal of Hydrogen Energy. 29, 173–185.
57. Li, Y., Horsman, M., Wu, N., Lan, C.Q., Dubois-Calero, N., 2008. Biofuels from microalgae. Biotechnology Progress. 24, 815-820.
58. Mahdy, A., Mendez, L., Ballesteros, M., González-Fernández, C., 2015. Algaculture integration in conventional wastewater treatment plants: Anaerobic digestion comparison of primary and secondary sludge with microalgae biomass. Bioresource Technology. 184, 236-244.
59. Masojídek, J., Koblízek, M., Torzillo, G., 2004. Photosynthesis in Microalgae. In: Richmond A., Handbook of Microalgal Culture: Biotechnology and Applied Phycology. Oxford, Chapter 2, 178-213.
60. Méndez, R., Fernández, I., Campos, J.L., Mosquera-Corral, A., 2010. Aspectos energéticos de la tecnología Anammox. In: Mata, J and Fdez.-Polanco, F., Ecoeficiencia en la EDAR del Siglo XXI. Aspectos Ambientales y Energéticos. Chapter 7, 136-154.
61. Mendoza, J.L., Granados, M.R., De Godos, I., Acién, F.G., Molina, E., Banks, C., Heaven, S., 2013. Fluid-dynamic characterization of real scale raceway reactors for microalgae production, Biomass and Bioenergy. 54, 267–275.
62. Menger-Krug, E., Niederste-Hollenberg, J., Hillenbrand, T., Hiessl, H., 2012. Integration of Microalgae Systems at Municipal Wastewater Treatment Plants: Implications for Energy and Emission Balances. Environmental Science and Technology, 46(21), 11505-11514.
63. Metcalf and Eddy, 2003. Wastewater Engineering: Treatment and reuse. Edn. Fourth. Edited by: Mc Graw Hill.
64. Molina-Grima, E., 1999. Microalgae mass culture methods. In: Encyclopedia of Bioprocess Technology: Fermentation, Biocatalysis and Bioseparation. Edited by Flickinger, M.C., Drew, S.W., John Wiley and Sons.
65. Molina-Grima, E., Acién Fernández, F.G., García Camacho, F., Camacho Rubio, F., Chisti, Y., 2001. Scale-up of tubular photobioreactors. Journal of Applied Phycology. 12, 355–368.
66. Mulbry, W., Kebede-Westhead, E., Pizarro, C., and Sikora, L., 2005. Recycling of manure nutrients: use of algal biomass from dairy manure treatment as a slow release fertilizer. Bioresource Technology. 96, 451-458.
67. Muñoz, R., Köllner, C., Guieysse, B., Mattiasson, B., 2004. Photosynthetically oxygenated salicylate biodegradation in a continuous stirred tank photobioreactor. Biotechnology and Bioengineering. 87 (6), 797–803.
68. Muñoz, R., and Guieysse, B., 2006. Algal-bacterial processes for the treatment of hazardous contaminants: a review. Water Research. 40, 2799-2815.
69. Muñoz, R., Alvarez, T., Muñoz, A., Terrazas, E., Guieysse, B., and Mattiasson, B., 2006. Sequential removal of heavy metals ions and organic pollutants using an algal-bacterial consortium. Chemosphere. 63, 903-911.

70. Muñoz, R., Meier, L., Diaz, I., Jeison, D., 2015. A critical review on the state-of-the-art of physical/chemical and biological technologies for an integral biogas upgrading. Reviews in Environmental Science and Bio/Technology (In press).
71. Mussatto, S.I., Dragone, G., Guimarães, P.M., Silva, J.P., Carneiro, L.M., Roberto, I.C., Vicente, A., Domingues, L., Teixeira, J.A., 2010. Technological trends, global market, and challenges of bio-ethanol production. Biotechnology Advances. 28(6), 817-830.
72. Ndimba, B.K., Ndimba, R.J., Johnson, T.S., Waditee-Sirisattha, R., Baba. M., Sirisattha, S., Shiraiwa, Y., Agrawal, G.K., Rakwal, R., 2013. Biofuels as a sustainable energy source: an update of the applications of proteomics in bioenergy crops and algae. Journal of Proteomics. 93, 234-244.
73. Oliveira, M.R., Beserra, J.O., Macambira, S., 2012. Development of a methodology for net energy analysis in biorefineries, regarding microalgae cultivation to improve energy yields in industrial wastes, Revista Latinoamericana de Biotecnología Ambiental y Algal. 3, 59–79.
74. Oswald, W.J., Gotaas, H.B., Golueke, C.G., Kellen, W.R., 1957. Algae in waste treatment. Sewage Industrial Wastes 29, 437–455.
75. Oswald, W.J., 1988. Large-Scale Algal Culture Systems (Engineering Aspects). In: Micro-Algal Biotechnology, Borowitzka, M.A. and L.J. Borowitzka (Eds.). Cambridge University Press, Cambridge, 357-394.
76. Oswald, W.J., 2003. My sixty years in applied algology. Journal of Applied Phycology. 15, 99-106.
77. Park, J. B. K. and Craggs R. J. 2010. Wastewater treatment and algal production in high rate algal ponds with carbon dioxide addition. Water Science and Technology. 61(3), 633-639.
78. Park, J.B.K., Craggs, R., Shilton, A., 2011a. Recycling algae to improve species control and harvest efficiency from high rate algae pond. Water Research. 45, 6637-6649.
79. Park, J.B.K., Craggs, R., Shilton, A., 2011b. Wastewater treatment high rate algal ponds for biofuel production. Bioresource Technology 102, 35–42.
80. Passos, F., Uggetti, E., Carrère, H., Ferrer, I., 2014. Pretreatment of microalgae to improve biogas production: a review, Bioresource Technology. doi: http://dx.doi.org/10.1016/j.biortech.2014.08.114
81. Pereira, M., Bartolomé, M.C., Sánchez-Fortum, S.S., 2013. Bioadsorption and bioaccumulation of chromium trivalent in Cr (III)-tolerant microalgae: A mechanism for chromium resistance. Chemosphere. 93, 1057-1063.
82. Persson, M., Jönsson, O., Wellinger, A., 2006. Biogas upgrading to vehicle fuel standards and grid injection. IEA Bioenergy. http://www.iea-biogas.net/_download/publitask37/upgrading_report_final.pdf. Accessed 1 March 2015.
83. Posadas, E., Garcia-Encina, P.A., Soltau, A., Dominguez, A., Diaz, I., Muñoz, R., 2013. Carbon and nutrient removal from centrates and domestic wastewater using algal-bacterial biofilm bioreactors. Bioresource Technology. 139, 50-58.
84. Posadas, E., Muñoz, A., García-González, M. C., Muñoz, R., García-Encina, P. A. 2014. A case study of a pilot high rate algal pond for the treatment of fish farm and domestic wastewaters. Journal of Chemical Technology and Biotechnology. DOI: 10.1002/jctb.4417.
85. Posadas, E., Morales, M.M., Gomez, C., Acien-Fernandez, G., Muñoz, R., 2015. Influence of pH and CO_2 source on the performance of microalgae-based secondary domestic wastewater treatment in outdoors pilot raceways. Chemical Engineering Journal. 265, 239-248.
86. Powell, N., Shilton, A.N., Pratt, S., Chisti, Y., 2008. Factors Influencing Luxury Uptake of Phosphorus by Microalgae in Waste Stabilization Ponds. Environ Science and Technology. 42(16), 5958-5962.
87. Powell, N., Shilton, A., Chisti, Y., Pratt, S., 2009. Towards a luxury uptake process via microalgae - Defining the polyphosphate dynamics. Water Research. 43(17), 4207-4213.
88. Rahaman, M.S.A., Cheng, L.-H., Xu, X.-H., Zhang, L., Chen, H.-L., 2011. A review of carbon dioxide capture and utilization by membrane integrated microalgal cultivation processes. Renewable and Sustainable Energy Reviews. 15(8), 4002–4012.
89. Ramaraj, R and Dussadee, N., 2015. Biological purification processes for biogas using algae cultures: A review. International Journal of Sustainable and Green Energy. 4(1-1), 20-32.
90. Rawat, I., Ranjith Kumar, R., Mutanda, T., Bux, F., 2011. Dual role of microalgae: Phycoremediation of domestic wastewater and biomass production for sustainable biofuels production. Applied Energy 88, 3411–3424.
91. Rittmann, B.E., McCarty, P.L., 2001. Environmental biotechnology: principles and applications, McGraw-Hill Book Co, New York.
92. Royal Decree 661/2007 (https://www.boe.es/boe/dias/2007/05/26/pdfs/A22846-22886.pdf. Last visited: 24 March 2015).
93. Royal Decree 413/2014 (http://www.boe.es/boe/dias/2014/06/10/pdfs/BOE-A-2014-6123.pdf. Last visited: 24 March 2015).

94. Ruiz-Martínez, A., Martin García, N., Romero, I., Seco, A., Ferrer, J., 2012. Microalgae cultivation in wastewater: Nutrient removal from anaerobic membrane bioreactor effluent. Bioresource Technology 126, 247–253.
95. Ryckebosch, E., Drouillon, M., Vervaeren, H., 2011. Techniques for transformation of biogas to biomethane. Biomass and Bioenergy. 35, 1633-1645.
96. Selvaratnam, T., Pegallapati, A., Montelya, F., Rodriguez, G., Khandan, N., Lammers, P., Van Voorhies, W., 2014. Feasibility of Algal Systems for Sustainable Wastewater Treatment. ICREGA'14 - Renewable Energy: Generation and Applications. Springer Proceedings in Energy. Chapter 4, 37-48.
97. Serejo, M., Posadas, E., Boncz, M., Blanco, S., Garcia-Encina, P.A., Muñoz, R. (2015). Influence of biogas flow rate on biomass composition during the optimization of biogas upgrading in microalgal-bacterial processes. Environmental Science and Technology. 49(5), 3228–3236.
98. Shilton, A.N., Powell, N., Guieysse, B., 2012. Plant based phosphorus recovery from wastewater via algae and Macrophytes. Current Opinion in Biotechnology. 23, 884–889.
99. Show, K.Y. and Lee, D.J. 2013. Production of Biohydrogen from Microalgae. In: Biofuels from Algae, ed. by Pandey, A., India, T., Lee, D.J., Chisti, Y., Soccol, C.R., 189–204. ISBN: 978-0-444-59558-4.
100. Sialve, B., Bernet, N., Bernard, O., 2009. Anaerobic digestion of microalgae as a necessary step to make microalgal biodiesel sustainable, Biotechnology Advances. 27, 409–416.
101. Simionato, D., Block, M.A., La Rocca, N., Jouhet, J., Maréchal, E., Finazzi, G., Morosinotto, T., 2013. The response of Nannochloropsis gaditana to nitrogen starvation includes de novo biosynthesis of triacylglycerols, a decrease of chloroplast galactolipids, and reorganization of the photosynthetic apparatus. Eukaryotic Cell. 12, 665–676.
102. Singh, M., Reynolds, D.L., Das, K.C., 2011. Microalgal system for treatment of effluent from poultry litter anaerobic digestion. Bioresource Technology. 102, 10841–10848.
103. Sydney, E.B., Sturm, W., de Carvalho, J.C., Thomaz-Soccol, V., Larroche, C., Pandey, A., Soccol, C.R., 2010. Potential carbon dioxide fixation by industrially important microalgae. Bioresource Technology. 101(15), 5892–5896.
104. Tarlan, E., Dilek, F.B., Yetis, U., 2002. Effectiveness of algae in the treatment of a wood-based pulp and paper industry wastewater. Bioresource Technology. 84, 1-5.
105. Thompson, R.B. and Meisinger, J.J., 2002. Management factors affecting ammonia volatilization from land-applied cattle slurry in the Mid-Atlantic USA. Journal of Environmental Quality 31, 1329–1338.
106. Tredici, M., 2004. Mass production of microalgae: Photobioreactors. In: Richmond A., Handbook of Microalgal Culture: Biotechnology and Applied Phycology. Oxford, Chapter 9, 178-213.
107. Tredici, M.R., 2009. Photobiology of microalgae mass cultures: Understanding the tools for the next green revolution. Biofuels. 1, 143-162.
108. Van Lier, J.B., 2008. High-rate anaerobic wastewater treatment: diversifying from end-of-the-pipe treatment to resource-oriented conversion techniques. Water Science and Technology. 57, 1137-1148.
109. Wang, J., Peng, Y., Wang, S., Gao, Y., 2008. Nitrogen Removal by Simultaneous Nitrification and Denitrification via Nitrite in a Sequence Hybrid Biological Reactor. Chinese Journal of Chemical Engineering. 16, 778—784.
110. Wilbanks, T.J. and Fernández, S., 2014. Climate Change and Infrastructure, Urban Systems, and Vulnerabilities: Technical Report for the US Department of Energy in Support of the National Climate Assessment. Island Press.
111. Wildschut, L.R., 2010. El binomio agua-energía. Aspectos a mejorar. In: Mata, J and Fdez.-Polanco, F., Ecoeficiencia en la EDAR del Siglo XXI. Aspectos Ambientales y Energéticos.Chapter 4, 64-78.
112. WWF. Observatorio de la electricidad, Enero 2015 (http://awsassets.wwf.es/downloads/oe_ene_2015.pdf. Last visited: 04 March 2015).
113. Wunderlin, P., Mohn, J., Joss, A., Emmenegger, L., Siegrist, H., 2012. Mechanisms of N2O production in biological wastewater treatment under nitrifying and denitrifying conditions. Water Research. 46, 1027-1037.
114. Xu, X., Song, C., Wincek, R., Andresen, J.M., MilLer, B.G., Scaroni, A.W., 2003. Separation of CO_2 from power plant flue gas using a novel CO_2 molecular basket adsorbent. Fuel Chemistry Division. 18, 162–163.

Aims and scope of the thesis

Chapter 2

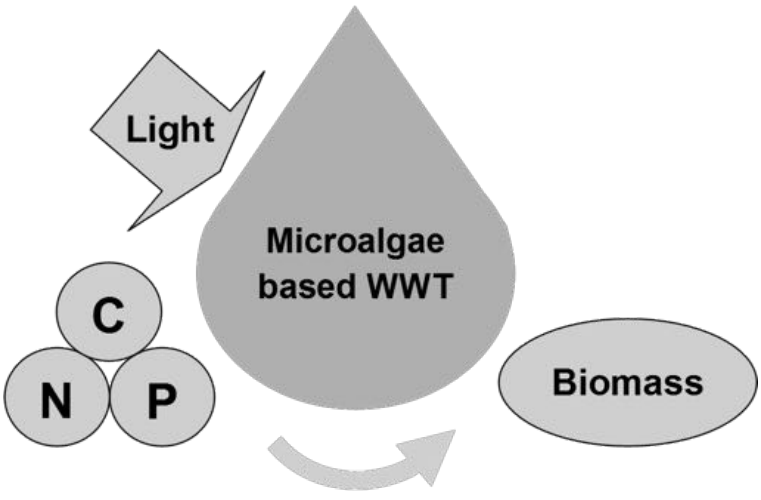

2.1. Justification of the thesis

The rapid and steady increase in human population over the past decades has entailed the generation of large amounts of wastewaters and greenhouse gases such as carbon dioxide (CO_2) or nitrous oxide (N_2O), which represent nowadays two of the major challenges to the environmental sustainability of our planet. In this context, algal-bacterial processes have emerged as a promising wastewater treatment (WWT) biotechnology based on the ability of microalgae to simultaneously remove carbon (C) (organic and inorganic), nitrogen (N) and phosphorus (P) via mixotrophic assimilation, and support via photosynthetic oxygenation the bacterial oxidation of the organic matter and ammonium present in the wastewater. This photosynthetic-based bioremediation provides a superior water management compared to conventional aerobic activated sludge or anaerobic digestion technologies in terms of cost-effective organic matter removal, nutrient recovery and CO_2 footprint. The synergistic relationships established between microalgae and bacteria can support consistent pollutant removal efficiencies and biomass productivities during the treatment of domestic, livestock and industrial wastewaters, at lower operating costs and environmental impacts than conventional WWT technologies. In addition, the high efficiency of microalgae to fix anthropogenic CO_2 via photosynthesis allows the mitigation of greenhouse emissions, which represents an additional advantage of microalgae-based WWT in comparison with other biotechnologies in terms of reduced carbon footprint. However, microalgae-based WWT still presents severe technical limitations that hinder its full-scale implementation owing to the lack of systematic empirical studies quantitatively evaluating the metabolism of microalgae and microalgae-bacteria consortia, the limited performance to completely remove all nutrients in wastewaters with a low C/N ratio, the poor sedimentation ability of some microalgae species (which results in effluent total suspended solid concentrations above the maximum EU discharge limits), the limited quantitative knowledge on the nutrient and energy recovery during the anaerobic digestion of the microalgae produced from WWT and on the ability of microalgal-bacterial cultures to synthesize N_2O (which could eventually jeopardize the environmental sustainability of these

processes). Therefore, more research on innovative microalgal processes and systematic quantitative studies on conventional microalgae-based technologies devoted to overcome the above mentioned limitations is necessary in order to consolidate algal-bacterial processes as a platform technology for a cost-effective and sustainable pollution control.

2.2. Main objectives

The overall objective of the present thesis was the development and systematic evaluation of the potential of both innovative and conventional WWT processes based on the synergistic relationship between microalgae and bacteria in terms of pollutant removal efficiency and environmental sustainability using a C, N and P mass balances approach in order to overcome the main limitations of microalgae-based WWT biotechnologies.

More specifically, the individual goals pursued to achieve this overall objective were:

a. Evaluation of the competitive advantage of symbiotic microalgae-bacteria consortia over axenic microalgae cultures during WWT in terms of culture robustness and C, N and P removal (**Chapter 3**).
b. Development of innovative operational strategies and photobioreactor configurations devoted to overcome the main technical limitations of conventional microalgal processes:

    b.1. Enhancing N removal and biomass harvesting during WWT in a novel anoxic-aerobic photobioreactor with continuous biomass recycling (**Chapter 4**).

    b.2. Coupling biogas upgrading and nutrient removal during the treatment of diluted centrates in a High Rate Algal Pond (HRAP) interconnected to an external CO_2 absorption column (**Chapter 5**).

    b.3. Evaluating nutrient and energy recovery in the integrated process of microalgae growth (under autotrophic and mixotrophic conditions) coupled with anaerobic digestion (**Chapter 6**).

c. Evaluating the environmental sustainability in terms of the N_2O emission potential of WWT in a novel anoxic-aerobic photobioreactor (**Chapter 4**) and in conventional HRAPs (**Chapter 7**).

2.3. Development of the thesis

In the present thesis, the performance of symbiotic algal-bacterial consortia in terms of C, N and P removal, energy recovery potential via anaerobic digestion and N_2O emissions during WWT was assessed using a C, N and P mass balance approach under different operational strategies and photobioreactor configurations in order to overcome the main technical limitations hindering the full scale implementation of microalgae-based processes.

In order to fulfill these objectives, the potential of the synergistic effects derived from the symbiosis between microalgae and bacteria during WWT under stress conditions was assessed in terms of their metabolic plasticity and robustness using a C, N and P mass balance approach (**Chapter 3**). The technical and environmental performance of innovative operational strategies and photobioreactor configurations devoted to enhance N removal and biomass harvesting was evaluated in a novel anoxic-aerobic photobioreactor (**Chapter 4**), in a biogas upgrading and nutrient removal HRAP interconnected to an external CO_2 absorption column (**Chapter 5**) and in the integrated process of microalgae growth coupled with anaerobic digestion (**Chapter 6**).

Finally, the environmental sustainability of the novel anoxic-aerobic photobioreactor developed (**Chapter 4**) and of conventional HRAPs (**Chapter 7**) was also assessed by quantifying and comparing the N_2O emissions and their associated CO_2 footprint with conventional biological WWT technologies.

Mixotrophic metabolism of *Chlorella sorokiniana* and algal-bacterial consortia under extended dark-light periods and nutrient starvation

Alcántara, C., Fernández, C., García-Encina, P., Muñoz, R., 2015. AMAB. 99(5), 2393-2404.

Chapter 3

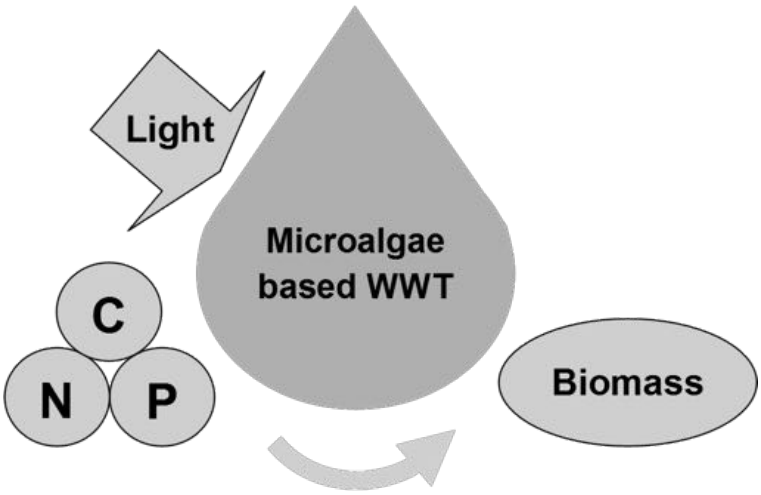

Appl Microbiol Biotechnol (2015) 99:2393–2404
DOI 10.1007/s00253-014-6125-5

ENVIRONMENTAL BIOTECHNOLOGY

Mixotrophic metabolism of *Chlorella sorokiniana* and algal-bacterial consortia under extended dark-light periods and nutrient starvation

Cynthia Alcántara · Carolina Fernández · Pedro A. García-Encina · Raúl Muñoz

Received: 8 July 2014 / Revised: 26 September 2014 / Accepted: 29 September 2014 / Published online: 24 October 2014

Abstract Microalgae harbor a not fully exploited industrial and environmental potential due to their high metabolic plasticity. In this context, a better understanding of the metabolism of microalgae and microalgal-bacterial consortia under stress conditions is essential to optimize any waste-to-value approach for their mass cultivation. This work constitutes a fundamental study of the mixotrophic metabolism under stress conditions of an axenic culture of *Chlorella sorokiniana* and a microalgal-bacterial consortium using carbon, nitrogen, and phosphorous mass balances. The hydrolysis of glucose into volatile fatty acids (VFA) during dark periods occurred only in microalgal-bacterial cultures and resulted in organic carbon removals in the subsequent illuminated periods higher than in *C. sorokiniana* cultures, which highlighted the symbiotic role of bacterial metabolism. Acetic acid was preferentially assimilated over glucose and inorganic carbon by *C. sorokiniana* and by the microalgal-bacterial consortium during light periods. $N\text{-}NH_4^+$ and $P\text{-}PO_4^{-3}$ removals in the light stages decreased at decreasing duration of the dark stages, which suggested that N and P assimilation in microalgal-bacterial cultures was proportional to the carbon available as VFA to produce new biomass. Unlike microalgal-bacterial cultures, *C. sorokiniana* released $P\text{-}PO_4^{-3}$ under anaerobic conditions, but this excretion was not related to polyhydroxybutyrate accumulation. Finally, while no changes were observed in the carbohydrate, lipid and protein content during repeated extended dark-light periods, nutrient deprivation boosted both C-acetate and C-glucose assimilation and resulted in significantly high biomass productivities and carbohydrate contents in both *C. sorokiniana* and the microalgal-bacterial cultures.

Keywords Algal-bacterial consortium · Bioremediation · *C. sorokiniana* · Extended dark-light periods · Mass balances · Nutrient deprivation

Introduction

Microalgae can play a key role in the treatment of water pollution and support a green bioeconomy in this XXI century due to their high metabolic versatility and productivity rates. Microalgae are able to grow simultaneously under photoautotrophic and heterotrophic conditions (Pérez-García et al. 2010), and even nitrifying activity has been detected in *Chlorella* in the presence of ammonium (Kessler and Oesterheld 1970). Guieysse et al. (2013) confirmed the presence of the enzyme nitrate reductase (an enzyme involved in the bacterial denitrification pathway) in axenic cultures of *Chlorella vulgaris*. In addition, luxury P uptake in microalgae can result into structural P contents of up to 3 %, which could support a microalgae-based enhanced biological P removal (EBPR) and allow for nutrient recycling via fertilization with microalgae biomass (Powell et al. 2008, 2009; Arbib et al. 2014). In this context, microalgae cultivation as a platform technology for secondary or tertiary wastewater treatment can support a simultaneous C, N, and P removal via mixotrophic fixation and the heterotrophic degradation of persistent organic pollutant (Muñoz and Guieysse 2006; Abreu et al. 2012). Microalgae-based wastewater treatment results in a large production of residual biomass from which high-added-value products such as lipids, carbohydrates, amino acids, and polyunsaturated fatty

Electronic supplementary material The online version of this article (doi:10.1007/s00253-014-6125-5) contains supplementary material, which is available to authorized users.

C. Alcántara · C. Fernández · P. A. García-Encina · R. Muñoz (✉)
Department of Chemical Engineering and Environmental Technology, Valladolid University, Dr. Mergelina, s/n, 47011 Valladolid, Spain
e-mail: mutora@iq.uva.es

acids or pigments could be extracted (Pérez-García et al. 2011a; Cea-Barcía et al. 2014).

The potential of microalgae to support a sustainable and economically profitable bioeconomy is based on the ability of microalgae to accumulate or biotransform biogenic and xenobiotic compounds when exposed to stress growth conditions using mechanisms similar to those found in bacterial metabolic routes (Prajapati et al. 2013; Markou and Nerantzis 2013). For instance, lipid accumulation occurs under nutrient deprivation conditions (Chu et al. 2013), salinity (Takagi et al. 2006), or heavy metal stress (Liu et al. 2008). Likewise, nutrient stress cultivation is used to enhance microalgal carbohydrate content (Kim et al. 2014). Recent studies have shown that certain cyanobacteria are capable of producing polyhydroxyalkanoates under extended dark-light periods or nutrient deprivation conditions similarly to polyphosphate accumulating bacteria (PAO) (Panda and Mallick 2007). In this context, Sharma and Mallick (2005) reported polyhydroxybutyrate (PHB) accumulation in *Nostoc muscorum* of 14, 20, and 35 % (*w*/*w*) when supplemented with 0.2 % acetate (585 g/m^3 C-acetate) and incubated under dark conditions for 3, 5, and 7 days, respectively. All these findings suggest that bacterial and algal metabolic pathways potentially involve similar precursors and enzymes (Subashchandrabose et al. 2011), which indicates that microalgal biotechnology harbors an industrial and environmental potential higher than that currently exploited. Thus, the elucidation of the influence of stress cultivation conditions on carbon and nutrient uptake, and biomass composition of microalgae and microalgae-bacteria consortia, is of key relevance in the optimization of any waste-to-value approach for microalgae mass cultivation and constitutes one of the most relevant knowledge gaps in this field. However, the lack of systematic empirical studies quantitatively evaluating the metabolism of microalgae and microalgae-bacteria consortia under stress conditions still hampers the exploitation of the full potential of these microorganisms. Therefore, the synergistic effects derived from the symbiosis between microalgae and bacteria in terms of metabolic plasticity and robustness represents a key niche for research in microalgal biotechnology.

This work constitutes a fundamental study using a carbon, nitrogen, and phosphorous mass balance approach of the mixotrophic metabolism under stress conditions of an axenic culture of *Chlorella sorokiniana* and a microalgal-bacterial consortium. Hence, the influence of repeated extended dark-light periods and nutrient deprivation on microbial growth, PHB and phosphorous accumulation, macroscopic biomass composition, and removal efficiencies of organic and inorganic carbon, nitrogen, and phosphorus was assessed.

Materials and methods

Microorganisms and inoculum cultivation conditions

The microalga *C. sorokiniana 211/8k* was obtained from the Culture Collection of Algae (SAG) of Göttingen University (Germany). The algal-bacterial consortium was obtained from a high-rate algal pond (HRAP) treating diluted centrates at the Department of Chemical Engineering and Environmental Technology of Valladolid University (Spain). This consortium was harvested from the HRAP broth by centrifugation for 10 min at 15,317×*g* (Sorvall, LEGEND RT+ centrifuge, Thermo Scientific) and resuspended in Sorokin-Krauss mineral salt medium (SK MSM). The microalgae/cyanobacteria population (from now on referred to as microalgae) was composed of (percentage of cells) *Limnothrix mirabilis (Böcher) Anagnostidis* (57.1 %), *Woronichinia sp.* (15.9 %), *Synechocystis aquatilis Sauvageau* (12.7 %), *Geitlerinema sp.* (11.4 %) and *Cyanosarcina sp.* (2.9 %). The composition of the bacterial population was not analyzed quantitatively by molecular tools but qualitatively assessed by microscopic observations, which confirmed the presence of bacteria in the algal-bacterial consortium used. *C. sorokiniana* and the microalgal-bacterial inocula were incubated in enriched SK MSM at 30 °C under magnetic agitation at 300 rpm and a photosynthetic active radiation (PAR) of 100±11 μE/m^2·s for 5 days. The SK medium was prepared according to Alcántara et al. (2013) and enriched with sterile solutions of glucose, CH_3COONa, peptone, and yeast extract to a final concentration of 1.25, 1.71, 0.0625, and 0.0625 g/dm^3, respectively.

Mixotrophic cultivation under extended dark-light periods

The first series of experiments consisted of cycles of extended dark stages (DS) under anaerobic conditions followed by illuminated stages (LS) at 100±11 μE/m^2·s. The duration of the dark stages in *C. sorokiniana* cultures was fixed at 7 days, while the illuminated stages lasted for 8, 14, and 30 days. On the other hand, the dark stages lasted for 7, 5, and 2.5 days in the tests conducted with the algal-bacterial consortium, while the duration of the subsequent illuminated stages was set at 14 days (Table S1 and Table S2 in "Supplementary Material"). The experiments were performed batchwise in 2.1 dm^3 glass bottles (five bottles for *C. sorokiniana* under sterile conditions and five bottles for the algal-bacterial consortium) containing 1.9 dm^3 of sterile modified BG-11 mineral salt medium (BG-11 MSM). This medium was composed of (per dm^3 of distilled water) the following: 0.1909 g NH_4Cl, 0.04 g K_2HPO_4, 0.075 g $MgSO_4 \cdot 7H_2O$, 0.036 g $CaCl_2 \cdot 2H_2O$, 0.006 g citric acid, 0.006 g ferric ammonium citrate, 0.001 g Na_2EDTA, 0.02 g Na_2CO_3, and 1 cm^3 of a trace element solution containing (per dm^3 of distilled water) 2.86 g H_3BO_3, 1.81 g $MnCl_2 \cdot 4H_2O$, 0.22 g $ZnSO_4 \cdot 7H_2O$, 0.08 g $CuSO_4 \cdot 5H_2O$,

0.39 g $Na_2MoO_4 \cdot 2H_2O$, and 0.0404 g $CoCl_2 \cdot 6H_2O$. The final pH of the medium was ≈7.2. The BG-11 MSM was supplemented with 0.375 g glucose/dm^3 and 0.513 g CH_3COONa/dm^3 as organic carbon source at the beginning of each dark period, which resulted in an initial total organic carbon (TOC) concentration of 300 g/m^3 (150 g/m^3 as C-CH_3COONa and 150 g/m^3 as C-glucose) (typical TOC concentrations in domestic wastewaters according to Asano et al. 2002). The initial nitrogen and phosphorus concentrations (50 g N-NH_4^+/m^3 and 7 g P-PO_4^{-3}/m^3, respectively) also mimicked the typical N and P concentrations in medium-strength domestic wastewater (Asano et al. 2002). In addition, *C. sorokiniana* and the algal-bacterial cultures were supplemented at the beginning of every dark stage with a sterile buffer solution of $NaHCO_3$ and $NaCO_3$ in order to increase the pH up to 9.0±0.3 to prevent acidification during the dark stage. The different buffer capacity observed in *C. sorokiniana* and the algal-bacterial broths resulted in average inorganic carbon (IC) concentrations of 105±2 and 147±17 g/m^3 at the beginning of each dark stage, respectively. These IC concentrations also corresponded to typical IC concentrations in domestic wastewater (≈100–150 g/m^3) (Asano et al. 2002). The term TIC represents here the total inorganic carbon in the system (gas C-CO_2 + dissolved IC). The bottles were always flushed with sterile nitrogen (N_2) for 15 min at the beginning of every cycle and allowed to equilibrate for 2 h prior to sampling (the renewal of the bottle's headspace was performed in a sterile bench by filtering the N_2 through 0.20-μm nylon filters previously autoclaved to maintain the sterility in *C. sorokiniana* cultures). The cultures were incubated at 30 °C under continuous magnetic agitation at 300 rpm.

Gas samples of 100 μL were drawn from the headspace of the bottles to measure the concentrations of CO_2, O_2, N_2, and CH_4 by GC-TCD. Liquid samples of 200 cm^3 were also drawn (under sterile conditions using sterile plastic syringes in an sterile bench in *C. sorokiniana* cultures) at the beginning and end of each dark and light stage in order to determine the concentrations of dissolved TOC, dissolved IC, dissolved N species (TN, N-NH_4^+, N-NO_2^-, N-NO_3^-, and $N_{organic}$), dissolved P (P-PO_4^{-3}), and biomass concentration as total (TSS) and volatile (VSS) suspended solid concentration. The concentration of acetic, propionic, isobutyric, butyric, isovaleric, valeric, isocaproic, hexanoic, and heptanoic acids were quantified by GC-FID. The term VFA* stands here for the total carbon concentration of volatile fatty acids (C-VFA) except acetic acid. The liquid volume extracted was replaced by fresh BG-11 MSM (previously autoclaved for 20 min at 120 °C in *C. sorokiniana* cultures) before the beginning of each DS, in order to maintain the initial cultivation volume (1.9 dm^3). Likewise, the pH and TOC, N, and P concentrations were also adjusted at the beginning of each DS at a pH of 9, 300 g/m^3 of TOC, 50 g/m^3 of N-NH_4^+, and 7 g/m^3 of P-PO_4^{-3}. The C, N, and P contents of the algal and algal-bacterial biomass formed were also experimentally determined along with the PHB and lipid content. The protein and carbohydrate contents in the biomass were also determined.

Mixotrophic growth under nutrient deprivation conditions

A second series of experiments using *C. sorokiniana* and the microalgal-bacterial consortium was conducted in the presence of continuous irradiation (PAR of 100±11 μE/$m^2 \cdot s$) and initial C-CH_3COONa and C-glucose concentrations of 150 g C/m^3 (initial TOC concentration of 300 g/m^3) under N and P deprivation, where K_2HPO_4 was replaced by an equimolar concentration of KCl in the BG-11 MSM. The bottles were also initially flushed with sterile N_2 for 15 min to remove the O_2 from the headspace and allowed to equilibrate for 2 h prior to sampling. The test was monitored for 12 days as above-described sampling every 3 days until the N and P contents in the biomass remained constant (Table S3 in "Supplementary Material").

Mass balance calculation

A mass balance calculation was conducted for C, N, and P considering all their chemical species at the beginning and end of each dark and light stage. The validity of the experimentation carried out was assessed by means of recovery factors defined as follows (Alcántara et al. 2013):

$$\text{C mass recovery (\%)} = \frac{[\text{C-CO}_2 + \text{TOC} + \text{IC} + \text{C}_{\text{biomass}}]_{\text{END POINT}}}{[\text{C-CO}_2 + \text{TOC} + \text{IC} + \text{C}_{\text{biomass}}]_{\text{START POINT}}} \times 100 \quad (1)$$

$$\text{N mass recovery (\%)} = \frac{[\text{N-NH}_4^+ + \text{N-NO}_2^- + \text{N-NO}_3^- + \text{N}_{\text{biomass}} + \text{N}_{\text{organic}}]_{\text{END POINT}}}{[\text{N-NH}_4^+ + \text{N-NO}_2^- + \text{N-NO}_3^- + \text{N}_{\text{biomass}} + \text{N}_{\text{organic}}]_{\text{START POINT}}} \times 100 \quad (2)$$

$$\text{P mass recovery (\%)} = \frac{[\text{P-PO}_4^{-3} + \text{P}_{\text{biomass}}]_{\text{END POINT}}}{[\text{P-PO}_4^{-3} + \text{P}_{\text{biomass}}]_{\text{START POINT}}} \times 100 \quad (3)$$

where C-CO_2 is the carbon concentration as gas CO_2 in the bottles' headspace, TOC is the total dissolved organic carbon concentration in the aqueous phase (C-CH_3COONa+

C-glucose+$C_{organic}$), IC is the dissolved inorganic carbon concentration in the aqueous phase in equilibrium with C-CO_2, $C_{biomass}$ is the particulate carbon concentration in the form of microalgal or microalgal-bacterial biomass, $C_{organic}$ is the dissolved organic carbon concentration from the particulate carbon hydrolyzed, and N-NH_4^+, N-NO_2^-, and N-NO_3^- represent the concentration of ammonium, nitrite, and nitrate, respectively, while $N_{biomass}$ and $N_{organic}$ account for the concentration of particulate organic nitrogen in the biomass and dissolved organic nitrogen from the particulate nitrogen hydrolyzed. P-PO_4^{-3} is the phosphorus concentration in the aqueous phase, and $P_{biomass}$ is the particulate phosphorus concentration in the form of biomass.

Analytical procedures

The irradiation was measured as PAR using a LI-250A light meter (LI-COR Biosciences, Germany). The pressure of the bottles' headspace was measured using a PN 5007 pressure sensor (IFM, Germany). The gas concentrations of CO_2, CH_4, O_2, and N_2 were determined using a CP-3800 gas chromatograph (Varian, USA) coupled with a thermal conductivity detector and equipped with a CP-Molsieve 5A (15 m×0.53 mm×15 μm) and a CP-Pora BOND Q (25 m×0.53 mm×15 μm) columns. The injector, detector, and oven temperatures were maintained at 150, 175, and 40 °C, respectively. Helium was used as the carrier gas at 13.7 cm^3/min. TOC, IC, and TN concentrations were determined using a TOC-V CSH analyzer equipped with a TNM-1 module (Shimadzu, Japan). N-NO_3^-, N-NO_2^-, and P-PO_4^{-3} were analyzed by HPLC-IC according to Alcántara et al. (2013). The soluble P concentration was also determined according to Eaton et al. (2005) using a spectrophotometer U-2000 (Hitachi, Japan). A Crison micropH 2002 (Crison instruments, Spain) was used for pH determination. Aliquots of 10 cm^3 of cultivation broth were filtered through 0.22 μm and acidified with H_2SO_4 to pH 2 prior to volatile fatty acid analysis in an Agilent 7820A GC-FID equipped with a G4513A autosampler and a Chromosorb WAW packed column (2 m×1/8″× 2.1 mm SS) (10 % SP 1000, 1 % H_3PO_4, WAW 100/120) (Teknokroma, Spain). The injector, oven, and detector temperatures were 375, 130, and 350 °C, respectively. N_2 was used as the carrier gas at 45 cm^3/min. The concentration of C-glucose was determined as the difference between the TOC and the sum of C-VFA and $C_{organic}$. The determination of the TSS and VSS concentrations of microalgal and microalgal-bacterial biomass was performed according to Eaton et al. (2005). The analysis of $C_{biomass}$ and $N_{biomass}$ was conducted using a LECO CHNS-932, while P biomass was measured using a 725-ICP Optical Emission Spectrophotometer (Agilent, USA) at 213.62 nm. The concentration of $C_{organic}$ and $N_{organic}$ released into the liquid phase was determined based on the percentage of structural C and N in the biomass and the decrease in TSS concentration in the dark stages. The identification, quantification, and biometry measurements of microalgae were carried out by microscopic examination (OLYMPUS IX70, USA) of microalgal samples (fixed with lugol acid at 5 % and stored at 4 °C prior to analysis) according to Sournia (1978). The determination of PHB was carried according to Zúñiga et al. (2011) using chloroform as extraction solvent in an Agilent 6890N GC-MS equipped with a DB-WAX column (30 m×0.250 mm× 0.25 μm) (J&W Scientific®, USA). The injector temperature was set at 250 °C. The oven temperature was initially maintained at 40 °C for 5 min, increased at 10 °C/min up to 200 °C and finally increased at 5 °C/min up to 240 °C (maintained for 2 min). Total lipid content in the biomass was quantified gravimetrically according to Gómez et al. (2013). Protein content in the biomass was estimated using a nitrogen to protein conversion factor of 4.44 (González et al. 2010). The carbohydrate content was estimated from the difference between the total biomass concentration and its content of lipids, proteins, and ashes.

Results

The results obtained, given as the average ± the error at 95 % confidence interval (n=5), were summarized in Tables S1, S2, and S3. The C, N, and P mass balances during dark cultivation showed recovery factors of 99.9± 1.7, 100.2±2.8, and 101.1±4.3 % in *C. sorokiniana* cultures, respectively, and 100.0±0.4, 99.8±0.4, and 99.8± 19.6 % in the algal-bacterial cultures (Tables S1 and S2). Similarly, the percentages of recovery obtained during illuminated cultivation were 105.7±12.5 % for C, 100.0 ±3.0 % for N, and 103.8±16.4 % for P in *C. sorokiniana* cultures and 100.3±0.5 % for C, 101.2±4.6 % for N, and 105.7±34.1 % for P in the algal-bacterial cultures (Tables S1 and S2). Finally, the C mass balance under nutrient deprivation conditions showed recovery factors of 99.8±5.3 and 99.6±1.7 % in *C. sorokiniana* and algal-bacterial cultures, respectively (Table S3).

Mixotrophic cultivation under extended dark-light periods

C. sorokiniana underwent a partial hydrolysis during the DS with a decrease in biomass concentration (as TSS) of 7.6±0.8, 15±6 and 17±9 % during DS I, DS II, and DS III, respectively. This hydrolysis entailed the built up of $C_{organic}$ and $N_{organic}$ in the liquid phase as a consequence of the solubilization of $C_{biomass}$ and $N_{biomass}$ (Fig. 1a and Table S1). However, biomass hydrolysis was negligible

in algal-bacterial consortium and acidogenesis from glucose occur in all DS, which resulted in increasing VFA concentrations and therefore in the acidification of the cultivation broth to neutral pH (Fig. 1b and Table S2). The fraction of glucose hydrolyzed to VFAs remained constant following 7 and 5 days of dark cultivation (63±2 % and a final pH of 7.2±0.2), while glucose biotransformation decreased to 39±6 % when the dark cultivation decreased to 2.5 days (final pH of 7.7±0.3). This acidogenesis from glucose in algal-bacterial cultures increased propionic acid concentrations at decreasing durations of the dark stage, with a maximum share of 60 % of the total VFA following 2.5 days of DS (Fig. 2). Neither isocaproic, hexanoic, nor heptanoic acid was detected at the end of the different DS evaluated (Fig. 2). On the other hand, an increase in the soluble $P\text{-}PO_4^{-3}$ concentration of 43 and 45 % was reported in *C. sorokiniana* cultures following DS I and DS II, respectively, while this value decreased to 20 % after DS III (Fig. 3a). Surprisingly, a negligible phosphorus release to the cultivation broth was recorded in the algal-bacterial consortium (Fig. 3b). The PHB (Fig. 3a), carbohydrate, protein, and lipid content in *C. sorokiniana* during dark cultivation remained constant at 0.1±0.0, 45±2, 43±2, and 0.7±0.1 %, along the three cycles tested. In the algal-bacterial cultures, an increase in the PHB concentration from 0.5±0.0 to 3.3±0.3 % occurred during the first 7 days of DS, but this value decreased during the first illuminated period and remained constant at 0.7±0.2 % along the entire experiment (Fig. 3b). The carbohydrate, protein, and lipid contents of the microalgal-bacterial biomass remained constant at 50±1, 32±1, and 2.5±0.1 %, respectively.

The biomass stoichiometric formulas experimentally determined following the LS I, II, and III for *C. sorokiniana*, and the algal-bacterial consortium were $CH_{1.73}O_{0.32}N_{0.17}S_{0.005}P_{0.007}$ and $CH_{1.74}O_{0.53}N_{0.15}S_{0.007}P_{0.009}$, respectively. *C. sorokiniana* presented biomass productivities of 70 g TSS/m^3·d, 19 g TSS/m^3·d, and 16 g TSS/m^3·d during the illuminated stages I, II, and III, respectively and a complete C-acetate assimilations (161±1, 150±3 and 160±5 g C-acetate/m^3, respectively) (Fig. 1a and Table S1). Surprisingly, *C. sorokiniana* only assimilated 26±5 % of the C-glucose during LS I (40±8 g C-glucose/m^3), while no glucose assimilation was recorded during LS II and III (Fig. 1a and Table S1). In the algal-bacterial cultures, both the initial C-acetate and the VFA formed from glucose biotransformation during DS were completely removed in LS I and LS II, with biomass productivities of 43 g TSS/m^3·d and 50 g TSS/m^3·d, respectively. These C eliminations corresponded with an assimilation of 191±17 g C-acetate/m^3 (136±25 g/m^3 from the initial C-acetate and 55±30 g/m^3 from glucose acidogenesis) and 46±5 g/m^3 corresponding to C-VFA* during LS I and 198±42 g C-acetate/m^3 (150±34 g/m^3 from the initial C-acetate and 48±55 g/m^3 from glucose acidogenesis) and 45±4 g/m^3 of C-VFA* during LS II (Fig. 1b and Table S2). Biomass productivity decreased to 24 g TSS/m^3·d in the illuminated stage III, which corresponded with an assimilation of 194±8 g C-acetate/m^3 and 17±9 g/m^3 of C-VFA*. C-glucose removal accounted for 0.2±0.0 % (3±10 g C-glucose/m^3 assimilated), 68±7 % (37±14 g C-glucose/m^3 assimilated), and 13±3 % (11±16 g C-glucose/m^3 assimilated) in LS I, LS II, and LS III, respectively (Fig. 1b and Table S2). TIC concentrations remained roughly constant during the illuminated stages, with an average TIC assimilation of 5.1±1.4 % in *C. sorokiniana* cultures and a TIC generation of 7.2±1.7 % (as a result of an intense respiratory release of CO_2) in the microalgal-bacterial broths (Fig. 1). *C. sorokiniana* supported $N\text{-}NH_4^+$ removals of 97±1, 59±12, and 67±13 % during the illuminated stages I, II, and III, respectively. Likewise, $N\text{-}NH_4^+$ removals of 97±7, 100±2, and 55±8 % were recorded in the algal-bacterial cultures during LS I, LS II, and LS III. Neither NO_2^- nor NO_3^- was produced by microalgae or by the algal-bacterial cultures (Tables S1 and S2). On the other hand, $P\text{-}PO_4^{-3}$ removal efficiencies of 81±21, 32±16, and 29±18 % were recorded in *C. sorokiniana* cultures in LS I, LS II, and LS III. Likewise, the algal-bacterial consortia supported $P\text{-}PO_4^{-3}$ removals of 84±18, 79±18, and 42±23 % in LS I, LS II, and LS III, respectively (Fig. 3).

Mixotrophic growth under nutrient deprivation conditions

Surprisingly, *C. sorokiniana* presented an average biomass productivity of 134 g TSS/m^3·d after 3 days of mixotrophic cultivation in the absence of N and P, while this productivity decreased sharply to 14 g TSS/m^3·d by day 6 and to 9 g TSS/m^3·d by day 12. Likewise, an average biomass productivity of 185 g TSS/m^3·d was recorded in the algal-bacterial cultures after 3 days of cultivation, which gradually decreased to 8 g TSS/m^3·d by day 12. A total C-acetate assimilation of 86±19 % (corresponding to 130±21 g C-acetate/m^3) was observed during *C. sorokiniana* cultivation, with removals of 43±15, 4.7±0.9, 19±8, and 20±8 % by day 3, 6, 9, and 12, respectively (Fig. 4a and Table S3). On the other hand, the algal-bacterial consortia presented a total C-acetate removal of 100 % (150±6 g C/m^3), with an assimilation of 91±7 % within the first 3 days (Fig. 4b and Table S3). Microalgae cultures assimilated 83±14 % of the C-glucose available (141±19 g C/m^3) within the first 3 days, and surprisingly glucose assimilation ceased afterwards (Fig. 4a and Table S3). Similarly, 93±8 % of the initial C-glucose (146±9 g C/m^3) was assimilated by the algal-bacterial cultures, with a removal of 70±9 % within the first 3 days of cultivation (Fig. 4b and Table S3). *C. sorokiniana* cultures underwent an increase in TIC from 7±1 to 11±1 % within the first 3 days likely associated with the aerobic biodegradation of C-

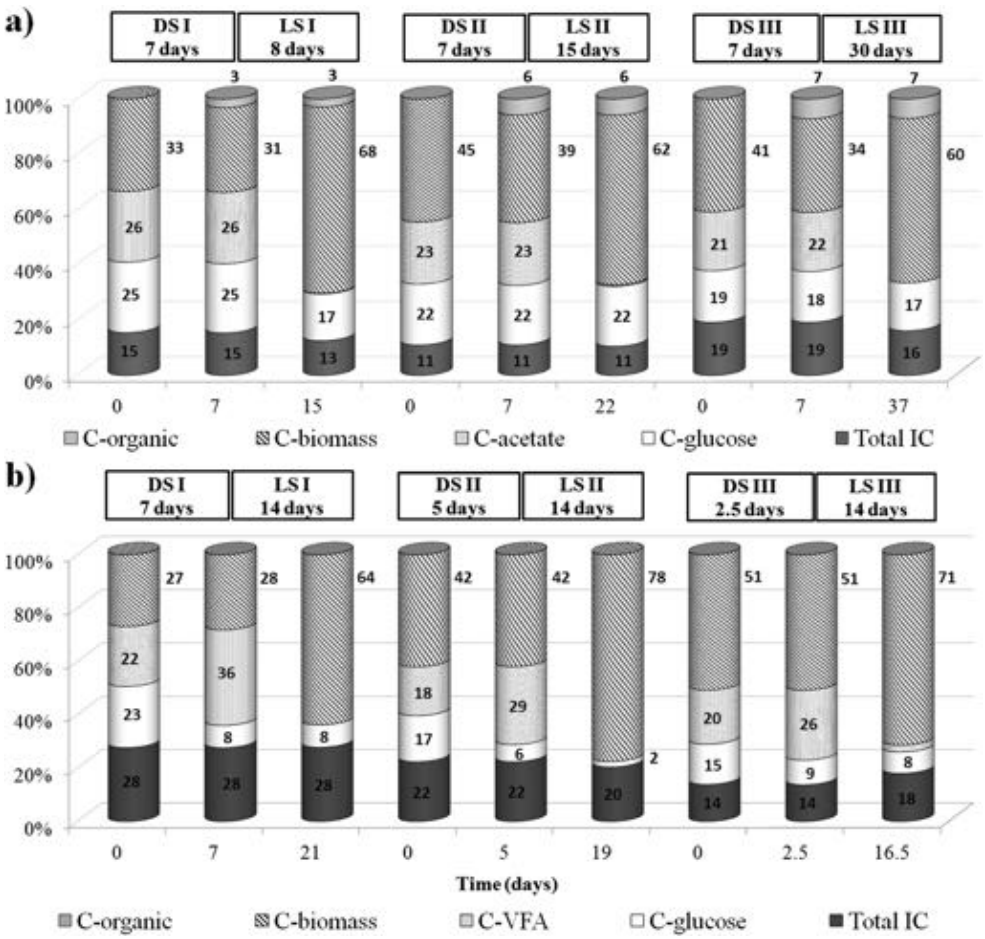

Fig. 1 Initial and final carbon distribution along the three sequential DS-LS cycles assessed in *C. sorokiniana* (**a**) and microalgal-bacterial (**b**) cultures

acetate and C-glucose. Afterwards, TIC concentration remained roughly constant during the entire cultivation (Fig. 4a and Table S3). In contrast, the algal-bacterial cultures showed a gradual TIC assimilation from 13±2 to 3±0 % (Fig. 4b and Table S3).

The carbohydrate content in *C. sorokiniana* increased from 48±1 to 72±1 %. This increase was concomitant with a decrease in the protein content from 40±1 to 16 ±1 %, while lipid and PHB contents remained constant at 0.8±0.1 and 0.4±0.0 %, respectively (Fig. 5a).

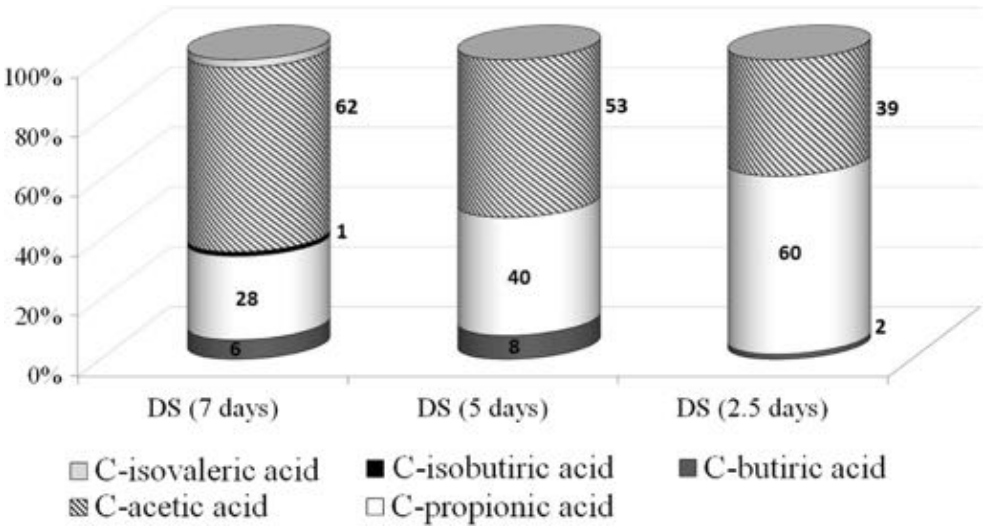

Fig. 2 VFA distribution at the end of the dark stages assessed in algal-bacterial cultures

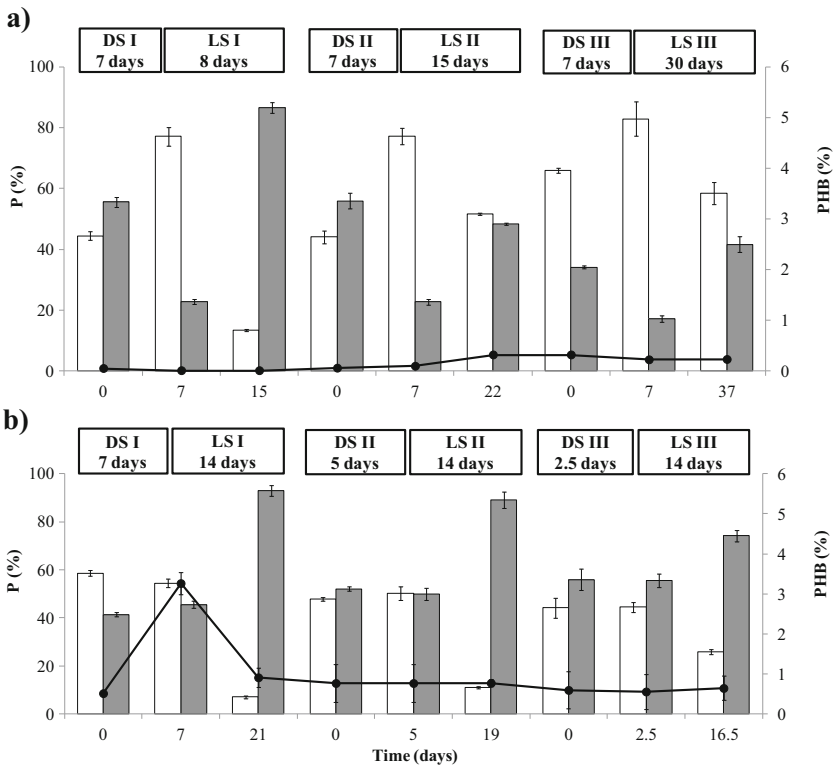

Fig. 3 Time course of the distribution of dissolved P-PO_4^{-3} (□) and $P_{biomass}$ (■) species and PHB content (–●–) in *C. sorokiniana* (**a**) and algal-bacterial (**b**) cultures

Similarly, the carbohydrate content in the algal-bacterial consortium increased from 49±3 to 65±2 %, along with a severe decrease in the protein content from 33±3 to 18±2 %. The lipid content remained constant at 2.3±0.3 %, while PHB concentration initially increased from 2.9±0.2 to 3.9±0.1 % within the first 3 days under nutrient limitation but gradually decreased to 1.1±0.2 % (Fig. 5b).

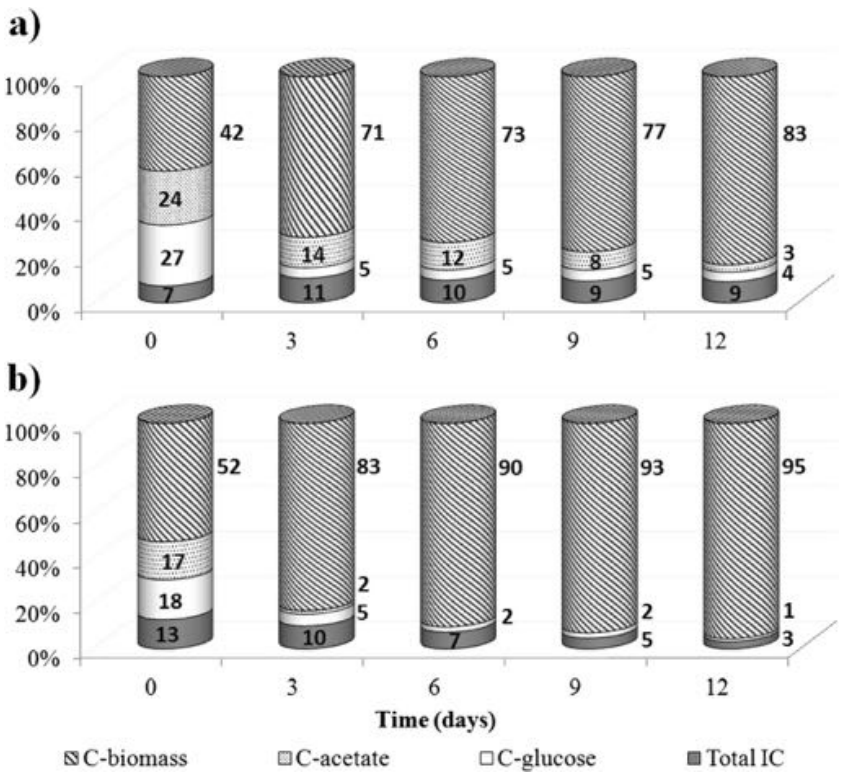

Fig. 4 Carbon distribution during *C. sorokiniana* (**a**) and algal-bacterial (**b**) mixotrophic cultivation under nutrient deprivation

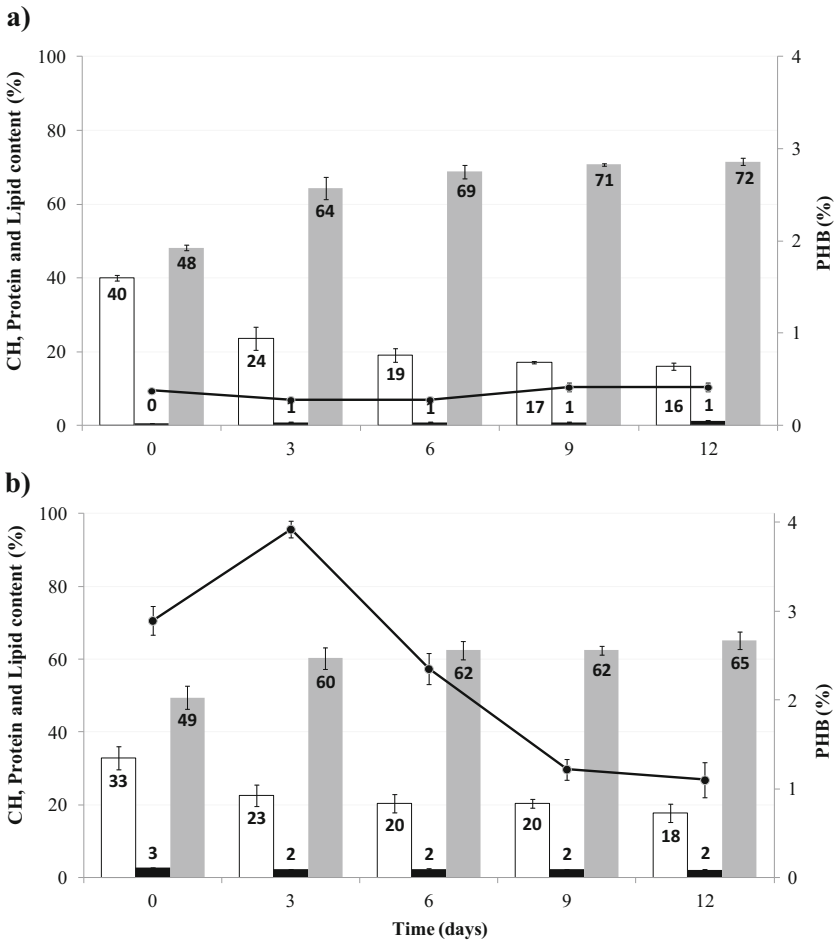

Fig. 5 Time course of carbohydrate (▩), protein (□), lipid (■), and PHB content (–●–) during the mixotrophic cultivation of *C. sorokiniana* (**a**) and the algal-bacterial consortium (**b**) under nutrient deprivation

Discussion

Carbon assimilation

The recovery factors of ≈100 % in all C mass balances validated both the analytical and instrumental methods used. *C. sorokiniana* clearly showed a higher affinity for acetate than for glucose or IC as a carbon source in both series of experiments, which suggest that C-acetate assimilation resulted more energetically favorable. It seems that as long as the level of acetate remains low (≤4000 g/m^3), some microalgae can use it as their preferential carbon source. This is important because acetate is a readily available and inexpensive substrate derived from many industrial applications and its use does not entail limitations during microalgae cultivation (Pérez-García et al. 2011a, b). In addition, the high pH recorded at the end of every LS (9.5±1.4 in *C. sorokiniana* and 10±0.7 in algal-bacterial cultures) as a result of photosynthetic activity, mediated an IC distribution mainly shifted towards bicarbonate and carbonate, which constitute IC species not readily available for *C. sorokiniana* growth (De Godos et al. 2010; Alcántara et al. 2013). Glucose assimilation by *C. sorokiniana* occurred only during LS I and resulted in a 26±5 % glucose removal, which was in agreement with the limited glucose assimilation (28±2 %) reported by Alcántara et al. (2013) during the mixotrophic cultivation of *C. sorokiniana* in a minimum MSM at initial N-NH_4^+ and P-PO_4^{-3} concentrations of 95±1 and 13±1 g/m^3, respectively. Although it is generally accepted that glucose can serve as a carbon source for the growth of certain microalgae, the effect of glucose on microalgae metabolism is species specific and influenced by the impinging irradiation (Kamiya and Kowallik 1987; Kamiya and Saitoh 2002). Interestingly, 83±14 % of C-glucose was assimilated by *C. sorokiniana* during the first 3 days of mixotrophic cultivation under nutrient starvation, which suggests that nutrient deprivation boosted both C-acetate and C-glucose assimilations. This additional TOC assimilation resulted in an increase of the dissolved IC within the first 3 days due to combined effect of an intensive respiratory release of CO_2 and a gradual increase in the pH of the cultivation broth (Fig. 4a and Table S3). These results confirm that microorganisms exhibiting a dual photoautotrophic and heterotrophic metabolism can shift their nutritional mode based on substrate and light availability (Abreu et al. 2012). Hence, when simple carbohydrates or organic acids are present in the medium, microalgae and cyanobacteria likely shift their

metabolism from an autotrophic to a mixotrophic nutrition mode to save energy (Venkata Mohan et al. 2014). The hydrolysis experienced by *C. sorokiniana* during the DS resulted in a decrease of TSS and consequently in increases in the concentration of dissolved $C_{organic}$ and $N_{organic}$ in the cultivation broth that were not further assimilated into biomass during the subsequent LS (Fig. 1a and Table S1). Based on the negligible hydrolysis of the algal-bacterial culture and its higher biomass productivity during LS II and III, the results suggest that *C. sorokiniana* was more sensitive to the absence of energy supply during the extended dark stages.

The results obtained in the cultivation of the algal-bacterial consortium suggested that the hydrolysis of glucose into VFAs was mediated by bacterial metabolism. The fact that the propionate to acetate ratio increased at decreasing duration of the dark stage indicated that glucose was firstly converted into propionic acid and finally into acetic acid. Thus, the ability of microalgal-bacterial consortia to hydrolyze and biotransform complex carbohydrates into simple organic molecules confirm the potential of these symbiotic consortia for wastewater treatment (He et al. 2013). The algal-bacterial biomass productivities and the negligible IC assimilation recorded also suggest that the extent of acidogenesis from glucose boosted TOC removal and consequently the superior algal-bacterial growth during the illuminated stages (Fig. 1b and Table S2). Nevertheless, the assimilation of the glucose not hydrolyzed was negligible. Similarly to *C. sorokiniana* cultures, nutrient starvation triggered C-glucose assimilation by the algal-bacterial consortium, which assimilated 93±8 % of the initial C-glucose (Fig. 4b and Table S3). Surprisingly, the 185 g TSS/m^3·d algal-bacterial productivity recorded during the first 3 days of cultivation in the absence of nutrients was higher than *C. sorokiniana* productivity (134 g TSS/m^3·d). This higher productivity was associated to the simultaneous occurrence of photoautotrophic microalgae growth, which entailed an assimilation of total IC of 78±7 % (165±14 mg of TIC consumed) during experiment II (Fig. 4b and Table S3).

Nitrogen and phosphorus removal

The recovery factors of ≈100 % in N and P mass balances also validated both the analytical and instrumental methods used during the evaluation of the fate of these nutrients. The absence of both N losses by stripping (closed bottles) and nitrification in both *C. sorokiniana* and algal-bacterial cultures confirm that the main mechanism for $N\text{-}NH_4^+$ removal was assimilation into biomass (as $N_{biomass}$) (Table S1 and Table S2). $N\text{-}NH_4^+$ removals of 97±1, 59±12, and 67±13 % and $P\text{-}PO_4^{-3}$ removals of 81±7, 32±4, and 29±6 % were recorded in *C. sorokiniana* cultures during the illuminated periods I, II, and III, respectively (Table S1). Based on the fact that the microalgal N content experimentally determined in *C. sorokiniana* remained constant at 9.7±0.3 %, the decrease in $N\text{-}NH_4^+$ removal during LS II and LS III points out to a deterioration in *C. sorokiniana* metabolism mediated by the prolonged absence of light during DS II and III (Table S1). On the other hand, the release of $P\text{-}PO_4^{-3}$ by *C. sorokiniana* during the dark stages together with the decrease in $P\text{-}PO_4^{-3}$ assimilation during LS II and III induced a progressive decline in microalgal $P_{biomass}$. Hence, the P content of *C. sorokiniana* decreased from 1.5±0.2 % in LS I to 0.9±0.0 and 0.6±0.2 % by the end of LS II and LS III, respectively. These results confirmed that microalgae, similarly to PAOs (De-Bashan and Bashan 2004; Bajekal and Dharmadhikari 2008; Mesquita et al. 2013), can release P under anaerobic conditions in the absence of light, but P assimilation in the subsequent illuminated stages did not occur in a similar extent (e.g., structural P decreased from 1.9 to 0.8 % during DS I and increased again to 1.5 % at the end of LS I). Luxury P uptake in microalgae is influenced by the dissolved phosphate concentration, light intensity, and temperature during microalgae cultivation (Cade-Menun and Paytan 2010; Fanta et al. 2010) and might explain the highly variable phosphorus removal often reported in microalgae-based wastewater treatment. Indeed, the amount of $P_{biomass}$ is the result of the combined effects of a luxury uptake and a growth-associated P uptake (Powell et al. 2008, 2009). In this regard, the deterioration in the activity of *C. sorokiniana* caused by the cultivation under prolonged dark periods likely promote the preferential uptake of $P\text{-}PO_4^{-3}$ for growth during LS periods.

$N\text{-}NH_4^+$ removals in the microalgal-bacterial cultures of 97±7, 100±2, and 55±8 % and $P\text{-}PO_4^{-3}$ removals of 84±7, 79±11, and 42±6 % were recorded in the illuminated stages I, II, and III, respectively (Table S2). Despite similar $N\text{-}NH_4^+$ concentrations were initially present at the beginning of each cycle in both cultures, the algal-bacterial biomass exhibited lower $N_{biomass}$ contents than microalgae (7.3±0.2 % regardless of the operational stage). The absence of phosphorus release to the cultivation medium during the dark period along with the steady $P\text{-}PO_4^{-3}$ removal rates during the illuminated stages can explain the constant $P_{biomass}$ content in the algal-bacterial biomass (1.1±0.1, 0.9±0.2, and 0.9±0.1 % at the end of LS I, LS II, and LS III, respectively). Finally, it must be stressed that both $N\text{-}NH_4^+$ and $P\text{-}PO_4^{-3}$ removals surprisingly decreased at decreasing duration of the dark stages, which suggested that N and P assimilation in algal-bacterial cultures was influenced by the availability of VFAs, which itself was influenced by the duration of the dark stages.

Macroscopic biomass composition

While no changes were observed in the carbohydrate, lipid, and protein contents in the test series performed using extended dark-light cycles, nutrient starvation resulted in a steady increase in carbohydrate content in both *C. sorokiniana* and microalgal-bacterial cultures. In this context, phosphorus-starved microalgae and cyanobacteria can experience an

increased intracellular storage of carbohydrates, the extent of this accumulation being strain specific (González-Fernández and Ballesteros 2012). In our particular case, the carbohydrate/protein ratio in *C. sorokiniana* under N and P starvation increased from 1.2 to 2.7 within the first 3 days and up to 4.5 by day 12, which corresponded with an initial and final carbohydrate content of 48±1 and 72±1 %, respectively (Fig. 5a). These results were in agreement with the increase from 0.15 to 3.7 reported by Dean et al. (2008) in the carbohydrate/protein ratio during *Chlamydomonas reinhardtii* cultivation under P deficient conditions, while a lower increase in the carbohydrate/protein ratio from 0.4 to 1.0 was observed by Sigee et al. (2007) in the cultivation of P-starved *Scenedesmus subspicatus*. A slightly lower carbohydrate accumulation from 49±3 to 65±2 % was obtained in the algal-bacterial cultures (Fig. 5b), where the carbohydrate/protein ratio increased from 1.5 to 2.7 during the first 3 days and up to 3.7 by day 12. A negligible lipid accumulation concomitant with a decrease in the protein content was observed in both *C. sorokiniana* and algal-bacterial cultures under N and P deprivation (Fig. 5). While the fact that nitrogen starvation induces an increase in the biomass lipid content has been consistently proven (Li et al. 2012; Simionato et al. 2013), the presence of P plays a key role on lipid productivity under nitrogen deficient conditions in both microalgae (Feng et al. 2012; Chu et al. 2013) and bacteria (Harold 1966; Kulaev et al. 1999). For instance, Chu et al. (2013) reported that the P assimilated under nitrogen deficiency was utilized by the algal cells to metabolically synthesize enzymes for the lipid synthesis. Thus, the absence of phosphorous under nitrogen starvation in our cultivation medium was likely a suppression factor for lipid accumulation and promoted instead carbohydrates accumulation (Chu et al. 2013).

Cultivation under extended dark-light periods did not boost PHB accumulation neither in *C. sorokiniana* nor in the algal-bacterial consortium. In our particular study, PHB accumulation in *C. sorokiniana* cultures was negligible despite the release of P during the dark stages (which was hypothesized to be associated with the supply of the microbial energy demand in the absence of light) (Fig. 3a). On the other hand, a maximum accumulation of PHB of 3.3±0.3 % was observed at the end of the first 7 days of dark stage in the algal-bacterial cultures, which in fact was not associated with a $P\text{-}PO_4^{-3}$ release to the cultivation medium (Fig. 3b). PHB content decreased to 0.9±0.2 % during the first illuminated stage and remained roughly constant afterwards.

In the absence of N and P, *C. sorokiniana* possessed a constant PHB content of 0.4±0.0 % along the 12 days of cultivation (Fig. 5a), which was in agreement with the 0.7 % PHB content reported by De Philippis et al. (1992) during photoautotrophic cultivation of *Spirulina maxima* under N starvation. On the other hand, the PHB concentration in the microalgal-bacterial biomass increased during the first 3 days from 2.9±0.2 to 3.9±0.1 % but gradually decreased to 1.1±0.2 % afterwards (Fig. 5b). The results here obtained suggest that despite the ability of some cyanobacteria to accumulate significant amounts of PHB during mixotrophic cultivation under extended dark periods or nutrient deprivation (Sharma and Mallick 2005; Panda and Mallick 2007), PHB accumulation in *C. sorokiniana* and the algal-bacterial consortium here tested was not induced under N and P limiting conditions.

In brief, the ability of microalgal-bacterial consortia to hydrolyze and biotransform glucose into simple organic molecules under extended dark periods confirmed the potential of these symbiotic consortia for wastewater treatment. N and P assimilation in algal-bacterial cultures during the illuminated periods was influenced by the carbon available as VFAs, which itself was a function of the duration of the dark stages. C-VFA (initial C-acetate + C-VFA from glucose acidogenesis in the algal-bacterial cultures) was the preferred carbon source in *C. sorokiniana* and in the algal-bacterial consortium based on the low-glucose and inorganic carbon assimilations recorded. Hence, in the presence of simple carbohydrates or organic acids, microalgae and cyanobacteria can shift their metabolism from an autotrophic to a mixotrophic nutrition mode to save energy. Neither PHB nor lipid accumulation was induced in *C. sorokiniana* or in the algal-bacterial consortium under extended dark-light periods or N and P deprivation. Surprisingly, nutrient deprivation boosted an efficient C-acetate and C-glucose assimilation and resulted in a steady increase in carbohydrate content concomitant with a decrease in protein concentration in *C. sorokiniana* and microalgal-bacterial cultures. This work provided new insights on the potential of indigenous microalgae-bacteria symbiotic consortia as a platform technology to avoid the high cost and technical limitations associated with the axenic cultivation of microalgae in order to consolidate an industrial scale microalgae-to-biofuel technology based on wastewater treatment.

Acknowledgments This research was supported by the regional government of Castilla y León and the European Social Fund (Contract N° E-47-2011-0053564 and Project Ref. GR76). The financial support of the Ministry of Economy and Competitiveness and the National Institute for Agricultural Research and Technology and Food is also gratefully acknowledged (Project Ref. RTA2013-00056-C03-02).

References

Abreu AP, Fernandes B, Vicente AA, Teixeira J, Dragone G (2012) Mixotrophic cultivation of *Chlorella vulgaris* using industrial dairy waste as organic carbon source. Bioresour Technol 118:61–66

Alcántara C, García-Encina PA, Muñoz R (2013) Evaluation of mass and energy balances in the integrated microalgae growth-anaerobic digestion process. Chem Eng J 221:238–246

Arbib Z, Ruiz J, Álvarez-Díaz P, Garrido-Pérez C, Perales JA (2014) Capability of different microalgae species for phytoremediation

processes: wastewater tertiary treatment, CO_2 bio-fixation and low cost biofuels production. Water Res 49:465–474

Asano T, Burton FL, Leverenz HL, Tsuchihashi R, Tchobanoglous G (2002) Metcalf and Eddy, wastewater engineering: treatment and reuse, 4th edn. McGraw-Hill, New York

Bajekal SS, Dharmadhikari NS (2008) Use of polyphosphate accumulating organisms (PAO) for treatment of phosphate sludge. The 12th World Lake Conference: 918–922

Cade-Menun BJ, Paytan A (2010) Nutrient temperature and light stress alter phosphorus and carbon forms in culture-grown algae. Mar Chem 121:27–36

Cea-Barcía G, Buitrón G, Moreno G, Kumar G (2014) A cost-effective strategy for the bio-prospecting of mixed microalgae with high carbohydrate content: diversity fluctuations in different growth media. Bioresour Technol 163:370–373

Chu FF, Chu PN, Cai PJ, Li WW, Lam PKS, Zeng RJ (2013) Phosphorus plays an important role in enhancing biodiesel productivity of *Chlorella vulgaris* under nitrogen deficiency. Bioresour Technol 134:341–346

De Godos I, Vargas VA, Blanco S, García-González MC, Soto R, García-Encina PA, Becares E, Muñoz R (2010) A comparative evaluation of microalgae for the degradation of piggery wastewater under photosynthetic oxygenation. Bioresour Technol 101:5150–5158

De Philippis R, Ena A, Guastiini M, Sili C, Vincenzini M (1992) Factors affecting poly-β-hydroxybutyrate accumulation in cyanobacteria and in purple non-sulfur bacteria. FEMS Microbiol Lett 103(2–4):187–194

Dean AP, Nicholson JM, Sigee DC (2008) Impact of phosphorus quota and growth phase on carbon allocation in *Chlamydomonas reinhardtii*: an FTIR microspectroscopy study. Eur J Phycol 43(4): 345–354

De-Bashan LE, Bashan Y (2004) Recent advances in removing phosphorus from wastewater and its future use as fertilizer (1997–2003). Water Res 38(19):4222–4246

Eaton AD, Clesceri LS, Greenberg AE (2005) Standard methods for the examination of water and wastewater, 21st edn. American Public Health Association/American Water Works Association/Water Environment Federation, Washington DC, USA

Fanta SE, Hill WR, Smith TB, Roberts BJ (2010) Applying the light: nutrient hypothesis to stream periphyton. Freshw Biol 55:931–940

Feng P, Deng Z, Fan L, Hu Z (2012) Lipid accumulation and growth characteristics of *Chlorella zofingiensis* under different nitrate and phosphate concentrations. J Biosci Bioeng 114(4):405–410

Gómez C, Escudero R, Morales MM, Figueroa FL, Fernández-Sevilla JM, Acién FG (2013) Use of secondary-treated wastewater for the production of *Muriellopsis sp*. Appl Microbiol Biotechnol 97(5): 2239–2249

González CV, Cerón Mdel C, Acien FG, Segovia CS, Chisti Y, Fernández JM (2010) Protein measurements of microalgal and cyanobacterial biomass. Bioresour Technol 101:7587–7591

González-Fernández C, Ballesteros M (2012) Linking microalgae and cyanobacteria culture conditions and key-enzymes for carbohydrate accumulation. Biotechnol Adv 30(6):1655–1661

Guieysse B, Plouviez M, Coilhac M, Cazali L (2013) Nitrous oxide (N_2O) production in axenic *Chlorella vulgaris* microalgae cultures: evidence, putative pathways, and potential environmental impacts. Biogeosciences 10(10):6737–6746

Harold FM (1966) Inorganic polyphosphates in biology: structure, metabolism, and function. Bacteriol Rev 30(4):772–794

He PJ, Mao B, Lü F, Shao LM, Lee DJ, Chang JS (2013) The combined effect of bacteria and *Chlorella vulgaris* on the treatment of municipal wastewaters. Bioresour Technol 146:562–568

Kamiya A, Kowallik W (1987) Photoinhibition of glucose uptake in *Chlorella*. Plant Cell Physiol 28:611–619

Kamiya A, Saitoh T (2002) Blue-light-control of the uptake of amino acids and of ammonia in *Chlorella* mutants. Physiol Plant 116:248–254

Kessler E, Oesterheld H (1970) Nitrification and induction of nitrate reductase in nitrogen deficient algae. Nature 228:287–288

Kim KH, Choi IS, Kim HM, Wi SG, Bae HJ (2014) Bioethanol production from the nutrient stress-induced microalga *Chlorella vulgaris* by enzymatic hydrolysis and immobilized yeast fermentation. Bioresour Technol 153:47–54

Kulaev I, Vagabov V, Kulakovskaya T (1999) New aspects of inorganic polyphosphate metabolism and function. J Biosci Bioeng 88(2): 111–129

Li Y, Fei X, Deng X (2012) Novel molecular insights into nitrogen starvation induced triacylglycerols accumulation revealed by differential gene expression analysis in green algae *Micractinium pusillum*. Biomass Bioenergy 42:199–211

Liu ZY, Wang GC, Zhou BC (2008) Effect of iron on growth and lipid accumulation in *Chlorella vulgaris*. Bioresour Technol 99(11): 4717–4722

Markou G, Nerantzis E (2013) Microalgae for high-value compounds and biofuels production: a review with focus on cultivation under stress conditions. Biotechnol Adv 31(8):1532–1542

Mesquita DP, Leal C, Cunha JR, Oehmen A, Amaral AL, Reis MA, Ferreira EC (2013) Prediction of intracellular storage polymers using quantitative image analysis in enhanced biological phosphorus removal systems. Anal Chim Acta 770:36–44

Muñoz R, Guieysse B (2006) Algal–bacterial processes for the treatment of hazardous contaminants: a review. Water Res 40(15):2799–2815

Panda B, Mallick N (2007) Enhanced poly-β-hydroxybutyrate accumulation in a unicellular cyanobacterium, *Synechocystis sp.* PCC 6803. Lett Appl Microbiol 44(2):194–198

Pérez-García O, de-Bashan LE, Hernández JP, Bashan Y (2010) Efficiency of growth and nutrient uptake from wastewater by heterotrophic, autotrophic, and mixotrophic cultivation of *Chlorella vulgaris* immobilized with *Azospirillum brasilense*. J Phycol 46(4):800–812

Pérez-García O, Escalante FME, de-Bashan LE, Bashan Y (2011a) Heterotrophic cultures of microalgae: metabolism and potential products. Water Res 45(1):11–36

Pérez-García RO, Bashan Y, Puente ME (2011b) Organic carbon supplementation of municipal wastewater is essential for heterotrophic growth and ammonium removing by the microalgae *Chlorella vulgaris*. J Phycol 47(1):190–199

Powell N, Shilton AN, Pratt S, Chisti Y (2008) Factors influencing luxury uptake of phosphorus by microalgae in waste stabilization ponds. Environ Sci Technol 42(16):5958–5962

Powell N, Shilton A, Chisti Y, Pratt S (2009) Towards a luxury uptake process via microalgae—defining the polyphosphate dynamics. Water Res 43(17):4207–4213

Prajapati SK, Kaushik P, Malik A, Vijay VK (2013) Phycoremediation coupled production of algal biomass, harvesting and anaerobic digestion: possibilities and challenges. Biotechnol Adv 31(8): 1408–1425

Sharma L, Mallick N (2005) Accumulation of poly-β-hydroxybutyrate in *Nostoc muscorum*: regulation by pH, light–dark cycles, N and P status and carbon sources. Bioresour Technol 96(11):1304–1310

Sigee DC, Bahrami F, Estrada B, Webster RE, Dean AP (2007) The influence of phosphorus availability on carbon allocation and P quota in *Scenedesmus subspicatus*: a synchrotron-based FTIR analysis. Phycology 46(5):583–592

Simionato D, Block MA, La Rocca N, Jouhet J, Maréchal E, Finazzi G, Morosinotto T (2013) The response of *Nannochloropsis gaditana* to nitrogen starvation includes de novo biosynthesis of triacylglycerols, a decrease of chloroplast galactolipids, and reorganization of the photosynthetic apparatus. Eukaryot Cell 12(5):665–676

Sournia A (1978) Phytoplanton Manual. Museum National d' Historie Naturelle, París. United Nations Educational. Scientific and Cultural Organization (Unesco)

Subashchandrabose SR, Ramakrishnan B, Megharaj M, Venkateswarlu K, Naidu R (2011) Consortia of cyanobacteria/microalgae and bacteria: biotechnological potential. Biotechnol Adv 29(6):896–907

Takagi M, Karseno, Yoshida T (2006) Effect of salt concentration on intracellular accumulation of lipids and triacylglyceride in marine microalgae *Dunaliella* cells. J Biosci Bioeng 101(3):223–226

Venkata Mohan S, Devi MP, Subhash GV, Chandra R (2014) Algae oils as fuels. Biofuels from Algae, Elsevier 8:155–187

Zúñiga C, Morales M, Le Borgne S, Revah S (2011) Production of polyhydroxybutyrate (PHB) by *Methylobacterium organophilum* isolated from a methanotrophic consortium in a two-phase partition bioreactor. J Hazard Mater 190(1–3):876–882

Supplementary material

Mixotrophic metabolism of *Chlorella sorokiniana* and algal-bacterial consortia under extended dark-light periods and nutrient starvation

Applied Microbiology and Biotechnology

Cynthia Alcántara, Carolina Fernández, Pedro A. García-Encina, Raúl Muñoz*

Department of Chemical Engineering and Environmental Technology, Valladolid University, Dr. Mergelina, s/n, 47011, Valladolid, Spain
* Corresponding author: mutora@iq.uva.es

Content:

Table S1: C, N and P mass balances in the dark (DS) and light stages (LS) during *C. sorokiniana* mixotrophic growth

Table S2. C, N and P mass balances in the dark (DS) and light stages (LS) during microalgal-bacterial consortium mixotrophic growth

Table S3. C mass balances during mixotrophic cultivation of *C. sorokiniana* and algal-bacterial consortia in the absence of nutrients

Table S1. C, N and P mass balances in the dark (DS) and light stages (LS) during *C. sorokiniana* mixotrophic growth

***C. sorokiniana* cultures**										
Carbon mass balance		**C-CO_2 (g/m^3)**	**IC (g/m^3)**	**TOC (g/m^3)**	**C-acetate (g/m^3)**	**C-VFA* (g/m^3)**	**C-glucose (g/m^3)**	**$C_{biomass}$ (g/m^3)**	**$C_{organic}$ (g/m^3)**	**Recovery (%)**
DS I (7 days)	DS initial[1]	0.2 ± 0.0	95 ± 1	319 ± 2	158 ± 6	0.0 ± 0.0	157 ± 3	207 ± 1	0.0 ± 0.0	99.1
	DS final = LS initial	19 ± 5	92 ± 18	335 ± 9	161 ± 1	0.0 ± 0.0	155 ± 6	191 ± 1	19 ± 8	
LS I (8 days)	LS final	0.0 ± 0.0	84 ± 2	135 ± 4	0.0 ± 0.0	1.2 ± 0.1	115 ± 5	456 ± 32	19 ± 8	108.9
DS II (7 days)	DS initial	0.1 ± 0.0	73 ± 1	298 ± 1	150 ± 2	0.4 ± 0.0	148 ± 2	298 ± 29	0.0 ± 0.0	100.3
	DS final = LS initial	0.3 ± 0.2	73 ± 3	335 ± 4	150 ± 3	2.4 ± 0.3	144 ± 2	261 ± 25	38 ± 5	
LS II (15 days)	LS final	0.3 ± 0.2	70 ± 3	186 ± 12	0.0 ± 0.0	3.6 ± 0.7	144 ± 18	410 ± 26	38 ± 5	99.9
DS III (7 days)	DS initial[1]	0.4 ± 0.2	145 ± 5	303 ± 43	160 ± 6	1.7 ± 0.0	141 ± 42	310 ± 19	0.0 ± 0.0	100.4
	DS final = LS initial	0.8 ± 0.4	145 ± 10	355 ± 43	160 ± 5	2.6 ± 0.3	139 ± 45	257 ± 25	53 ± 11	
LS III (30 days)	LS final	0.0 ± 0.0	130 ± 1	199 ± 43	0.0 ± 0.0	0.0 ± 0.0	139 ± 50	482 ± 30	54 ± 12	108.4
Nitrogen mass balance		**N-NH_4^+ (g/m^3)**		**N-NO_2^- (g/m^3)**		**N-NO_3^- (g/m^3)**		**$N_{biomass}$ (g/m^3)**	**$N_{organic}$ (g/m^3)**	**Recovery (%)**
DS I (7 days)	DS initial[1]	50 ± 2		0.0 ± 0.0		0.0 ± 0.0		42 ± 0	1.5 ± 0.1	101.5
	DS final = LS initial	50 ± 0		0.0 ± 0.0		0.0 ± 0.0		39 ± 0	5.2 ± 0.6	
LS I (8 days)	LS final	1.4 ± 0.3		0.0 ± 0.0		0.0 ± 0.0		87 ± 4	5.2 ± 0.2	99.0
DS II (7 days)	DS initial[1]	44 ± 4		0.0 ± 0.0		0.0 ± 0.0		57 ± 5	14 ± 3	99.4
	DS final = LS initial	49 ± 4		0.0 ± 0.0		0.0 ± 0.0		49 ± 3	17 ± 4	
LS II (15 days)	LS final	20 ± 3		0.0 ± 0.0		0.0 ± 0.0		82 ± 5	13 ± 3	99.5
DS III (7 days)	DS initial[1]	50 ± 8		0.0 ± 0.0		0.0 ± 0.0		62 ± 2	6.7 ± 0.5	99.8
	DS final = LS initial	57 ± 1		0.0 ± 0.0		0.0 ± 0.0		50 ± 6	11 ± 1	
LS III (30 days)	LS final	19 ± 8		0.0 ± 0.0		0.0 ± 0.0		89 ± 2	11 ± 0	101.4
Phosphorus mass balance		**P-PO_4^{-3} (g/m^3)**				**$P_{biomass}$ (g/m^3)**				**Recovery (%)**
DS I (7 days)	DS initial[1]	6.4 ± 0.4				8.0 ± 0.0				100.3
	DS final = LS initial	11 ± 1				3.3 ± 0.0				
LS I (8 days)	LS final	2.1 ± 0.1				14 ± 2				111.3
DS II (7 days)	DS initial[1]	6.7 ± 0.2				8.5 ± 1.8				103.1
	DS final = LS initial	12 ± 1				3.6 ± 0.2				
LS II (15 days)	LS final	8.2 ± 1.1				7.7 ± 0.5				101.6
DS III (7 days)	DS initial[1]	9.6 ± 1.2				5.0 ± 0.8				99.9
	DS final = LS initial	12 ± 2				2.5 ± 0.1				
LS III (30 days)	LS final	8.5 ± 0.7				5.9 ± 0.0				98.7

[1]Culture volume, pH and C, N and P concentrations were adjusted at the beginning of a new DS at 1.9 dm^3, pH of 9, 300 g/m^3 of TOC, 50 g/m^3 of N-NH_4^+ and 7 g/m^3 of P-PO_4^{-3}

Table S2. C, N and P mass balances in the dark (DS) and light stages (LS) during microalgal-bacterial consortium mixotrophic growth

Algal-bacterial consortium cultures										
Carbon mass balance		**C-CO_2 (g/m^3)**	**IC (g/m^3)**	**TOC (g/m^3)**	**C-acetate (g/m^3)**	**C-VFA* (g/m^3)**	**C-glucose (g/m^3)**	**$C_{biomass}$ (g/m^3)**	**$C_{organic}$ (g/m^3)**	**Recovery (%)**
DS I (7 days)	DS initial[1]	2.4 ± 0.1	183 ± 9	300 ± 23	136 ± 25	12 ± 2	153 ± 31	178 ± 57	0.0 ± 0.0	100.0
	DS final = LS initial	34 ± 8	177 ± 16	292 ± 23	191 ± 17	46 ± 5	56 ± 8	187 ± 30	0.0 ± 0.0	
LS I (14 days)	LS final	0.2 ± 0.0	183 ± 8	55 ± 4	0.0 ± 0.0	0.0 ± 0.0	55 ± 6	420 ± 19	0.0 ± 0.0	100.5
DS II (5 days)	DS initial	6.3 ± 0.9	186 ± 18	297 ± 38	150 ± 34	2.4 ± 0.1	144 ± 42	349 ± 14	0.0 ± 0.0	100.1
	DS final = LS initial	37 ± 18	179 ± 19	298 ± 32	198 ± 42	45 ± 4	54 ± 14	349 ± 31	0.0 ± 0.0	
LS II (14 days)	LS final	0.0 ± 0.0	170 ± 59	17 ± 3	0.0 ± 0.0	0.0 ± 0.0	17 ± 3	648 ± 21	0.0 ± 0.0	100.3
DS III (2.5 days)	DS initial[1]	1.2 ± 0.0	123 ± 38	315 ± 11	180 ± 18	0.8 ± 0.0	135 ± 21	451 ± 21	0.0 ± 0.0	99.8
	DS final = LS initial	2.4 ± 0.2	121 ± 33	316 ± 38	200 ± 8	33 ± 8	82 ± 13	450 ± 26	0.0 ± 0.0	
LS III (14 days)	LS final	0.1 ± 0.0	160 ± 30	94 ± 3	6.4 ± 2.2	16 ± 2	72 ± 9	634 ± 64	0.0 ± 0.0	100.1
Nitrogen mass balance		**N-NH_4^+ (g/m^3)**		**N-NO_2^- (g/m^3)**		**N-NO_3^- (g/m^3)**		**$N_{biomass}$ (g/m^3)**	**$N_{organic}$ (g/m^3)**	**Recovery (%)**
DS I (7 days)	DS initial[1]	50 ± 3		0.0 ± 0.0		0.0 ± 0.0		31 ± 9	0.0 ± 0.0	100.0
	DS final = LS initial	49 ± 3		0.0 ± 0.0		0.0 ± 0.0		31 ± 6	0.0 ± 0.0	
LS I (14 days)	LS final	1.5 ± 0.6		0.0 ± 0.0		0.0 ± 0.0		79 ± 2	0.0 ± 0.0	99.9
DS II (5 days)	DS initial[1]	51 ± 4		0.0 ± 0.0		0.0 ± 0.0		61 ± 3	0.1 ± 0.0	99.8
	DS final = LS initial	50 ± 1		0.0 ± 0.0		0.0 ± 0.0		62 ± 8	0.2 ± 0.0	
LS II (14 days)	LS final	0.1 ± 0.0		0.0 ± 0.0		0.0 ± 0.0		110 ± 14	0.0 ± 0.0	100.4
DS III (2.5 days)	DS initial[1]	50 ± 1		0.9 ± 0.0		0.0 ± 0.0		78 ± 4	0.0 ± 0.0	99.7
	DS final = LS initial	50 ± 1		1.0 ± 0.2		0.0 ± 0.0		77 ± 13	0.0 ± 0.0	
LS III (14 days)	LS final	23 ± 2		0.0 ± 0.0		0.0 ± 0.0		107 ± 17	0.4 ± 0.0	103.3
Phosphorus mass balance		**P-PO_4^{-3} (g/m^3)**				**$P_{biomass}$ (g/m^3)**				**Recovery (%)**
DS I (7 days)	DS initial[1]	5.6 ± 0.9				3.9 ± 0.2				107.9
	DS final = LS initial	5.6 ± 0.6				4.7 ± 1.1				
LS I (14 days)	LS final	0.9 ± 0.0				12 ± 1				121.4
DS II (5 days)	DS initial[1]	7.1 ± 0.3				7.8 ± 1.9				92.1
	DS final = LS initial	6.9 ± 0.7				6.8 ± 1.2				
LS II (14 days)	LS final	1.4 ± 0.0				12 ± 3				96.2
DS III (2.5 days)	DS initial[1]	6.2 ± 0.9				7.8 ± 1.9				99.4
	DS final = LS initial	6.2 ± 0.2				7.7 ± 2.0				
LS III (14 days)	LS final	3.6 ± 0.4				10 ± 3				99.4

[1]Culture volume, pH and C, N and P concentrations were adjusted at the beginning of a new DS at 1.9 dm^3, pH of 9, 300 g/m^3 of TOC, 50 g/m^3 of N-NH_4^+ and 7 g/m^3 of P-PO_4^{-3}

Table S3. C mass balances during mixotrophic cultivation of *C. sorokiniana* and algal-bacterial consortia in the absence of nutrients

C. sorokiniana cultures							
Carbon mass balance	**C-CO_2 (g/m^3)**	**IC (g/m^3)**	**TOC (g/m^3)**	**C-acetate (g/m^3)**	**C-glucose (g/m^3)**	**$C_{biomass}$ (g/m^3)**	**Recovery (%)**
Day 0	11 ± 1	45 ± 3	322 ± 10	151 ± 21	171 ± 18	264 ± 2	-
Day 3	0.7 ± 0.0	68 ± 3	116 ± 5	87 ± 4	29 ± 5	449 ± 15	100.1
Day 6	0.1 ± 0.0	64 ± 5	109 ± 4	81 ± 10	29 ± 9	476 ± 6	102.6
Day 9	0.0 ± 0.2	60 ± 2	83 ± 2	51 ± 5	29 ± 10	492 ± 0	97.5
Day 12	0.0 ± 0.2	55 ± 3	48 ± 4	21 ± 3	27 ± 9	525 ± 9	99.0
Algal-bacterial consortium cultures							
Carbon mass balance	**C-CO_2 (g/m^3)**	**IC (g/m^3)**	**TOC (g/m^3)**	**C-acetate (g/m^3)**	**C-glucose (g/m^3)**	**$C_{biomass}$ (g/m^3)**	**Recovery (%)**
Day 0	13 ± 2	113 ± 2	307 ± 11	150 ± 6	157 ± 9	465 ± 27	-
Day 3	0.2 ± 0.0	90 ± 2	61 ± 5	14 ± 0.8	47 ± 8	738 ± 15	100.1
Day 6	7.7 ± 0.2	64 ± 5	21 ± 1	0.0 ± 0.0	21 ± 4	801 ± 13	100.0
Day 9	0.1 ± 0.0	42 ± 8	21 ± 1	0.0 ± 0.0	21 ± 1	823 ± 14	99.8
Day 12	0.0 ± 0.0	32 ± 3	11 ± 1	0.0 ± 0.0	11 ± 1	833 ± 4	98.6

Evaluation of wastewater treatment in a novel anoxic-aerobic algal-bacterial photobioreactor with biomass recycling through carbon and nitrogen mass balances

Alcántara, C., Domínguez, J.M., García, D., Blanco, S., Pérez, R., García-Encina, P., Muñoz, R., 2015. BITE. 191, 173–186.

Chapter 4

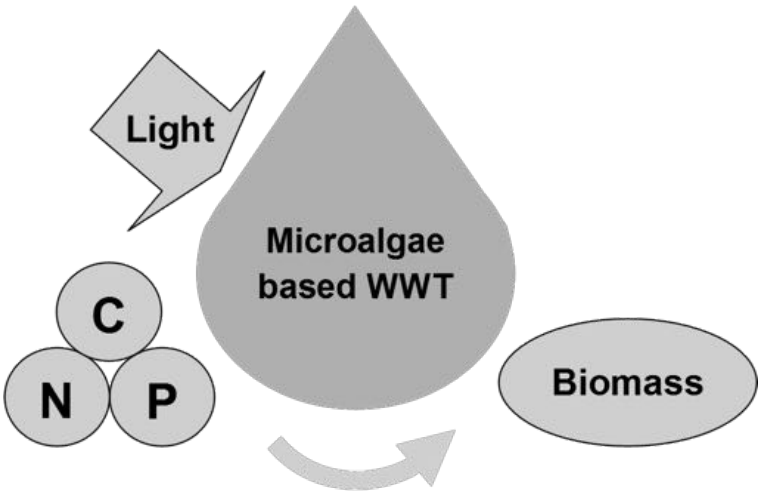

Bioresource Technology 191 (2015) 173–186

Contents lists available at ScienceDirect

Bioresource Technology

journal homepage: www.elsevier.com/locate/biortech

Evaluation of wastewater treatment in a novel anoxic–aerobic algal–bacterial photobioreactor with biomass recycling through carbon and nitrogen mass balances

Cynthia Alcántara [a], Jesús M. Domínguez [a], Dimas García [a], Saúl Blanco [b,1], Rebeca Pérez [a], Pedro A. García-Encina [a], Raúl Muñoz [a,*]

[a] Department of Chemical Engineering and Environmental Technology, Valladolid University, Dr. Mergelina, s/n, 47011 Valladolid, Spain
[b] Department of Biodiversity and Environmental Management, University of León, 24071 León, Spain

HIGHLIGHTS

- A HRT of 2 days enabled TOC, IC and TN removal efficiencies of ≈80%.
- Light intensity and DOC governed the extent of N removal mechanisms.
- Biomass recycling resulted in fast settling flocs and low effluent TSS.
- *Chlorella vulgaris* and Proteobacteria were the main microorganisms in the system.
- N_2O emissions were far below the reported IPCC emission factor for WWTPs.

GRAPHICAL ABSTRACT

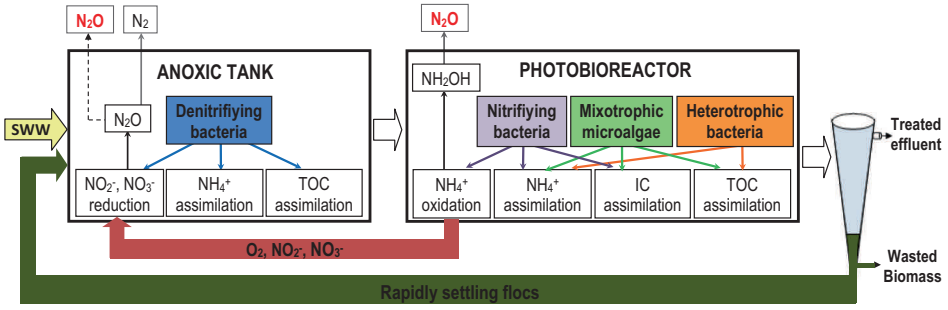

ARTICLE INFO

Article history:
Received 13 March 2015
Received in revised form 29 April 2015
Accepted 30 April 2015
Available online 7 May 2015

Keywords:
Algal–bacterial symbiosis
Dissimilatory nitrogen removal
Enhanced sedimentation
Inorganic carbon competition
Nitrous oxide emissions

ABSTRACT

Algal–bacterial symbiosis, implemented in an innovative anoxic–aerobic photobioreactor configuration with biomass recycling, supported an efficient removal of total organic carbon (86–90%), inorganic carbon (57–98%) and total nitrogen (68–79%) during synthetic wastewater treatment at a hydraulic and sludge retention times of 2 days and 20 days, respectively. The availability of inorganic carbon in the photobioreactor, determined by its supply in the wastewater and microalgae activity, governed the extent of nitrogen removal by assimilation or nitrification–denitrification. Unexpectedly, nitrate production was negligible despite the high dissolved oxygen concentrations, denitrification being only based on nitrite reduction. Biomass recycling resulted in the enrichment of rapidly settling algal flocs, which supported effluent total suspended solid concentrations below the European Union maximum discharge limits. Finally, the maximum nitrous oxide emissions recorded were far below the emission factors reported for wastewater treatment plants, confirming the environmental sustainability of this innovative photobioreactor in terms of global warming impact.

1. Introduction

The synergistic relationship between microalgae and bacteria play a key role during the secondary or tertiary treatment of domestic wastewater in photobioreactors (De Godos et al., 2009; Arbib et al., 2014). Photosynthetic oxygenation, together with microalgae heterotrophic metabolism, can boost the biodegradation of organic pollutants present in wastewater (Muñoz and Guieysse, 2006). This *in situ* photosynthetic oxygen (O_2) supply, apart from reducing carbon dioxide (CO_2) emissions from organic matter oxidation, can significantly decrease the costs associated with mechanical aeration in activated sludge systems, which

* Corresponding author.
E-mail address: mutora@iq.uva.es (R. Muñoz).
[1] Current address: The Institute of the Environment, La Serna, 58, 24007 León, Spain.

http://dx.doi.org/10.1016/j.biortech.2015.04.125
0960-8524/

represent 45–75% of the total operational costs in conventional wastewater treatment plants (WWTPs) (Chae and Kang, 2013). In addition, the capacity of microalgae to simultaneously remove carbon (C), nitrogen (N) and phosphorus (P) via mixotrophic assimilation represents an important advantage in comparison with aerobic activated sludge or anaerobic digestion technologies in terms of enhanced nutrient recovery (Arbib et al., 2014).

However, despite all these advantages, microalgal–bacterial wastewater treatment processes still present severe technical limitations that hinder their full-scale development. For instance, the poor sedimentation ability of most microalgae species often results in effluent suspended solid concentrations far above the maximum permissible discharge limits in natural water bodies. Likewise, the hydraulic retention times (HRT) applied in High Rate Algal Ponds (HRAP) (3–10 days) often limit the nitrification of ammonium (NH_4^+), which is a must in the implementation of N removal strategies via denitrification (Posadas et al., 2015). In this context, nitrite (NO_2^-) or nitrate (NO_3^-) reduction represents a key metabolic pathway to remove N in wastewaters with low C/N ratios when the supply of external C-CO_2 to support a complete nutrient removal via microalgal assimilation is not technical or economically feasible (Molina Grima et al., 2003). Therefore, the development of innovative operational strategies and photobioreactor configurations to simultaneously enhance both N removal and biomass harvesting is required to move towards a sustainable industrial-scale implementation of microalgae-based wastewater treatment systems. In addition, the environmental sustainability of microalgae-based wastewater treatment has been questioned due to the ability of microalgae or associated bacteria to synthesize nitrous oxide (N_2O), a greenhouse gas with a global warming potential 298 times higher than CO_2. N_2O emissions could jeopardize the benefits associated to photosynthetic CO_2 capture in a net greenhouse gas mass balance (Fagerstone et al., 2011; Alcántara et al., 2015). Unfortunately, the number of studies assessing N_2O emissions from algal–bacterial photobioreactors treating wastewater is scarce.

In this work, the operation of an innovative anoxic–aerobic algal–bacterial photobioreactor configuration with biomass recycling (De Godos et al., 2014) was optimized in order to promote N removal via denitrification and the development of a rapidly settling algal–bacterial population. The influence of the HRT, intensity and regime of light supply, and dissolved O_2 concentration (DOC) in the photobioreactor on the mechanisms underlying C and N removal in the anoxic and aerobic tanks was assessed using a mass balance approach. The sedimentation characteristics (Sludge Volume Index (SVI) and biomass settling rate) and N_2O emission potential of the biomass present in both reactors were also evaluated. Finally, a detailed characterization of the microalgal and bacterial population dynamics was conducted using morphological and molecular identification tools.

2. Methods

2.1. Microorganisms and culture conditions

The anoxic and aerobic tanks were initially filled with 3.2 g/L of total suspended solids (TSS) of a consortium composed of microalgae and cyanobacteria (from now on referred to as microalgae) from a HRAP treating diluted vinasse (Serejo et al., 2015), and aerobic activated sludge from Valladolid WWTP (Spain). The microalgal and bacterial cultures used as inocula were initially settled (centrifugation was discarded to avoid the disruption of the flocs) and the biomass resuspended in synthetic wastewater (SWW) prior to inoculation in both reactors. The SWW was initially composed of (per L of distilled water): 500 mg Glucose, 1750 mg $NaHCO_3$, 458 mg NH_4Cl, 62 mg KH_2PO_4, 7 mg NaCl, 4 mg $CaCl_2{\cdot}2H_2O$, 75 mg $MgSO_4{\cdot}7H_2O$, 2.5 mg $FeSO_4$, 20 mg EDTA, 0.00125 mg $ZnSO_4$, 0.0025 mg $MnSO_4$, 0.0125 mg H_3BO_3, 0.0125 mg $Co(NO_3)_2$, 0.0125 mg Na_2MoO_4, and 6.25×10^{-6} mg $CuSO_4$. This composition resulted in 200 mg/L of dissolved total organic carbon (TOC), 250 mg/L of dissolved inorganic carbon (IC) and 120 mg/L of N-NH_4^+. The use of real wastewater was discarded in this preliminary study in order to prevent the typical fluctuations in composition associated to real wastewater feeding. A buffer composed of 1.1 g KH_2PO_4/L_{SSW} and 2.3 g K_2HPO_4/L_{SSW} was additionally supplemented to maintain the photobioreactor pH at 7.8 ± 0.1 in order to promote bacterial nitrification and minimize N-losses by ammonia (NH_3) stripping. Despite buffer addition did not allow P mass balance evaluation, pH control by buffer addition was required to prevent the increase on pH as a result of the intense photosynthetic activity, which would inhibit both microalgal and bacterial metabolic pathways.

2.2. Experimental photobioreactor

The experimental set-up consisted of an anoxic tank interconnected to a photobioreactor (Fig. 1). The aerobic tank (photobioreactor) was an enclosed jacketed 3.5 L glass tank (AFORA, Spain) with a total working volume of 2.7 L. The photobioreactor was continuously illuminated by 4 × 5 meter strip LED lamps (F30W-12V, Spain) arranged in a circular configuration, which provided 400 ± 51 μE/m^2 s at the outer wall of the photobioreactor. The temperature and magnetic agitation of the photobioreactor were maintained constant at 24 ± 1 °C and 300 rpm, respectively, while the pH was maintained at 7.8 ± 0.1 by daily addition of 0.8 mL of chlorhydric acid (37%) during Stages I and II. The anoxic reactor consisted of a gas-tight 1 L polyvinyl chloride tank with a total working volume of 0.9 L maintained in the dark and magnetically stirred at 300 rpm. The SWW, previously sterilized at 121 °C for 20 min and maintained at 7 °C, was fed to the anoxic tank and continuously overflowed by gravity into the aerobic photobioreactor. The algal–bacterial broth was continuously recycled at 3 L/d from the photobioreactor to the anoxic tank in order to provide the NO_2^- and NO_3^- (generated in the photobioreactor via biological nitrification) required for denitrification. The temperature of the anoxic tank was maintained constant at 24 ± 1 °C. An Imhoff cone with a volume of 1 L and interconnected to the outlet of the photobioreactor was used as a settler. The algal–bacterial biomass settled was recycled from the bottom of the settler into the anoxic tank at 0.5 L/d and wasted 3 days a week in order to control the algal–bacterial sludge retention time (SRT). The experiment was run for 186 days (June 2014–November 2014).

2.3. Experimental design

The design of the experimentation was conducted based on the hypothesis that algal–bacterial photobioreactors for wastewater treatment can support the oxidation of NH_4^+ into NO_2^-/NO_3^-, which can then be easily removed through denitrification (using the organic matter present in SWW) under anoxic conditions via internal recycling of the photobioreactor broth (De Godos et al., 2014). During the first 47 days (Stage I), the process was operated at a HRT of 4 days (HRT_{anoxic} = 1 day, $HRT_{aerobic}$ = 3 days) and a SRT of 27 ± 5 days under continuous illumination (Table 1). In Stage II (35 days), the HRT was decreased to 2 days while maintaining a SRT of 20 ± 6 days. Based on the absence of nitrification in the aerobic tank, the DOC was decreased from 21 ± 4 mg/L to 10 ± 2 mg/L during Stage III (40 days) via continuous air bubbling at 10 mL/min through a ceramic sparger located at the bottom of the photobioreactor to rule out any potential inhibition of nitrifying bacteria by photooxidation. During Stage IV (32 days), the DOC and light intensity were decreased to 5.8 ± 0.9 mg O_2/L and 162 ± 40 μE/m^2 s,

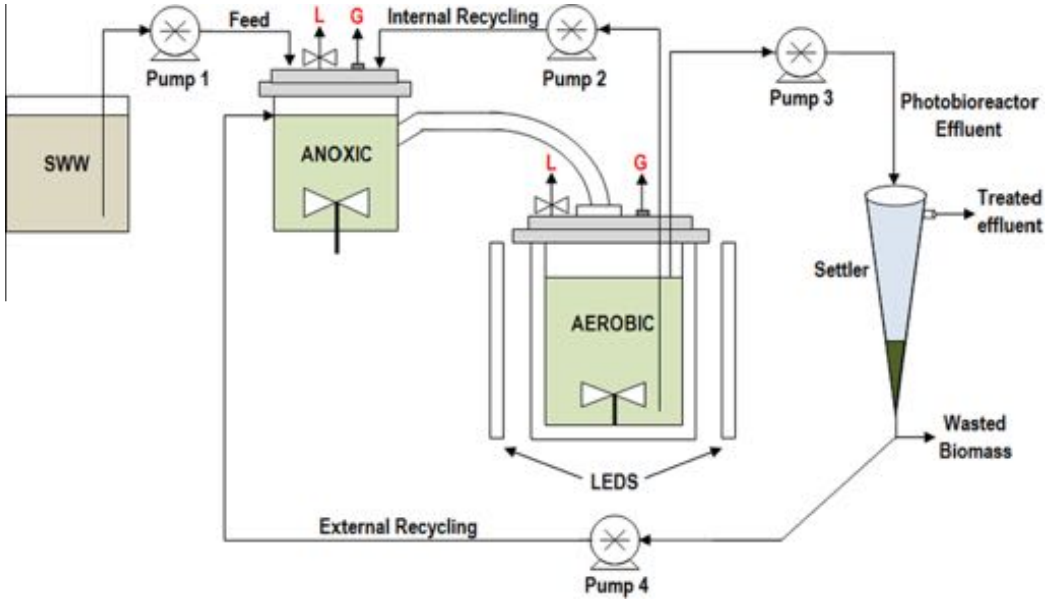

Fig. 1. Schematic of the anoxic–aerobic photobioreactor configuration. L and G represent the gas and liquid sampling points in the anoxic and aerobic reactors.

Table 1
Operational conditions and process parameters during the evaluation of the performance of the anoxic–aerobic photobioreactor. The concentrations shown correspond to the average values ± standard deviations at steady state during stages I-V.

Stage			I		II		III		IV		V	
Reactor		SWW	Anoxic	Aerobic	Anoxic	Aerobic	Anoxic	Aerobic	Anoxic	Aerobic	Anoxic	Aerobic
Experimental period (d)		N.A.[a]	47		35		40		32		32	
HRT (d)		N.A.[a]	4		2		2		2		2	
SRT (d)		N.A.[a]	27 ± 5		20 ± 6		21 ± 3		21 ± 2		21 ± 4	
Light intensity (μE/m^2 s)	Day (12 h)	N.A.[a]	0.0 ± 0.0	420 ± 21	0.0 ± 0.0	400 ± 51	0.0 ± 0.0	400 ± 51	0.0 ± 0.0	162 ± 40	0.0 ± 0.0	160 ± 43
	Night (12 h)											0.0 ± 0.0
Inlet SWW flow (L/d)		N.A.[a]	0.9 ± 0.1		1.7 ± 0.2		1.7 ± 0.2		1.7 ± 0.2		1.7 ± 0.1	
Internal recycling (L/d)		N.A.[a]	3		3		3		3		3	
External recycling (L/d)		N.A.[a]	0.5		0.5		0.5		0.5		0.5	
TOC (mg/L)		205 ± 6	31 ± 1	20 ± 1	45 ± 1	29 ± 2	39 ± 1	21 ± 1	38 ± 1	24 ± 1	38 ± 0	25 ± 1
IC (mg/L)		253 ± 7	57 ± 2	6.1 ± 1.5	160 ± 4	114 ± 3	98 ± 1	19 ± 5	103 ± 1	33 ± 2	123 ± 1	65 ± 3
N-NH_4^+ (mg/L)		121 ± 3	42 ± 1	28 ± 1	55 ± 1	33 ± 1	35 ± 1	5.5 ± 0.6	31 ± 1	3.1 ± 1.0	31 ± 1	3.8 ± 0.6
N-NO_2^- (mg/L)		0.0 ± 0.0	0.1 ± 0.0	0.9 ± 0.2	0.0 ± 0.0	4.8 ± 0.5	0.0 ± 0.0	13 ± 0	0.0 ± 0.0	20 ± 1	0.0 ± 0.0	20 ± 0
N-NO_3^- (mg/L)		0.0 ± 0.0	0.1 ± 0.0	0.6 ± 0.1	0.1 ± 0.0	0.5 ± 0.3	0.1 ± 0.0	0.6 ± 0.1	0.1 ± 0.0	0.4 ± 0.0	0.1 ± 0.0	0.6 ± 0.3
TN (mg/L)		123 ± 7	43 ± 1	30 ± 2	55 ± 1	39 ± 1	35 ± 1	20 ± 0	31 ± 1	24 ± 1	32 ± 1	25 ± 1
TOC recovery (%)		N.A.[a]	100		101		99		100		99	
IC recovery (%)		N.A.[a]	100		100		101		101		100	
N-NH_4^+ recovery (%)		N.A.[a]	102		102		98		98		100	
TN recovery (%)		N.A.[a]	100		100		98		99		100	
N_2O (ppm_v)		N.A.[a]	7.2 ± 2.5	24 ± 7	10 ± 1	129 ± 23	5.5 ± 1.7	1.9 ± 1.1	2.6 ± 1.6	3.7 ± 2.8	14 ± 8	70 ± 7[b]
Shannon–Wiener index (inoculum = 2.6)		N.A.[a]	3.2	3.0	3.2	3.0	3.5	3.2	3.5	3.3	3.4	3.3
pH		7.5 ± 0.1	7.6 ± 0.1	7.9 ± 0.2	7.5 ± 0.0	7.7 ± 0.1	7.5 ± 0.1	7.8 ± 0.1	7.6 ± 0.0	7.7 ± 0.0	7.5 ± 0.1	7.6 ± 0.1
Air flow (mL/min)		N.A.[a]	0	0	0	0	0	10	0	7	0	1[c]
DOC (mg/L)	Day (12 h)	N.A.[a]	0.8 ± 0.2	21 ± 3	1.1 ± 0.5	21 ± 4	1.6 ± 0.4	10 ± 2	2.2 ± 0.4	5.8 ± 0.9	2.2 ± 0.7	23 ± 3
	Night (12 h)											5.6 ± 0.7

[a] N.A. = Not applicable.
[b] N_2O concentration measured during light period.
[c] Air flow only injected in the photobioreactor during the night.

respectively, in order to discard a light-mediated nitrifying bacteria inhibition. Finally, cycles of 12 h of light (160 ± 43 μE/m^2 s) and 12 h of dark (1 mL/min of air flow) were set in the photobioreactor during Stage V (32 days) to provide a competitive advantage for nitrifying bacteria growth during the dark periods (Table 1).

Gas samples of 100 μL were taken from the headspace of the anoxic and aerobic tanks (after pressure measurement) three times a week to record the N_2O gas concentration by gas chromatography electron captor detector. Liquid samples of 100 mL were also drawn three times a week from the SWW storage tank (influent), anoxic tank, aerobic tank, wastage and clarified effluent to monitor the concentration of dissolved TOC, dissolved IC, dissolved N species (total nitrogen (TN), N-NH_4^+, N-NO_2^- and N-NO_3^-) and biomass concentration as TSS. The DOC, temperature and pH of the cultivation broth in both tanks were in situ recorded every day. The C and N content of the algal–bacterial biomass generated, along with the characterization of the populations of microalgae and bacteria, were also experimentally determined in both tanks under steady

state conditions at the end of each operational stage. In addition, the SVI and settling rates of the algal–bacterial consortia present in the anoxic and aerobic tanks were also measured.

A virtual composition of the influent wastewater to the anoxic tank was calculated considering the dilution effect mediated by the internal and external recirculations in order to evaluate the actual C and N removals in the denitrification reactor. Therefore, virtual concentrations (V_i) for dissolved IC, TOC, N-NH_4^+, N-NO_2^- and N-NO_3^- were calculated at the entrance of the anoxic tank according to Eq. (1):

$$V_i \left(\frac{mg}{L}\right) = \frac{(Ci_{feed} \times Q_{feed}) + (Ci_{photobio} \times Q_{RI}) + (Ci_{photobio} \times Q_{RE})}{Q_{feed} + Q_{RI} + Q_{RE}} \quad (1)$$

where Ci_{feed} and $Ci_{photobio}$ correspond to the dissolved concentrations of the parameter i = TOC, IC, N-NH_4^+, N-NO_2^-, N-NO_3^- and TN in the SWW and photobioreactor effluent, respectively, while Q_{feed} represents the SWW flow rate, Q_{RI} the internal recirculation flow rate and Q_{RE} the external recirculation flow rate.

A mass balance calculation was conducted for TOC, IC, N-NH_4^+ and TN in each operational stage under steady state conditions. The validity of the experimentation carried out was thus assessed by means of recovery factors according to Eq. (2):

$$M_i \text{ mass recovery } (\%) = \frac{\left((M_{i_{rem}})_{anox} + (M_{i_{rem}})_{photobio} + M_{i_{effluent}}\right)}{(M_i)_{SWW}} \times 100 \quad (2)$$

where $(M_{i_{rem}})_{anox}$ represents the mass flow rate (g/d) of the parameter i = TOC, IC, N-NH_4^+ and TN removed in the anoxic tank, $(M_{i_{rem}})_{photobio}$ the mass flow rate (g/d) of the parameter i removed in the photobioreactor, $M_{i_{effluent}}$ represents the mass flow rate (g/d) of the parameter i in the treated effluent and $(M_i)_{SWW}$ the mass flow rate (g/d) of the parameter i in the SWW.

Additional effluent biodegradability tests were performed in duplicate in 500 mL E-flasks containing 225 mL of treated effluent and 25 mL of aerobic activated sludge. The assays were closed with cotton plugs and incubated in the dark for 10 days at 25 ± 1 °C under continuous magnetic agitation at 200 rpm. Dissolved TOC, IC, TN, DOC and TSS concentrations were measured at day 0, 5 and 10.

2.4. Analytical procedures

The impinging irradiation was measured as photosynthetically active radiation (PAR) using a LI-250A light meter (LI-COR Biosciences, Germany) and expressed in μE/m^2 s. The pressure at the head-space of the anoxic and aerobic tanks was measured using a PN 5007 (IFM, Germany). The N_2O gas concentration was determined using a Bruker Scion 436 gas chromatograph (Palo Alto, USA) equipped with an Electron Capture Detector and a HS-Q packed column (1 m × 2 mm ID × 3.18 mm OD) (Bruker, USA). Injector, detector and oven temperatures were set at 100 °C, 300 °C and 40 °C, respectively. Nitrogen was used as the carrier gas at 20 mL/min. External standards prepared in volumetric bulbs (Sigma–Aldrich, USA) were used for N_2O quantification.

TN, TOC and IC concentrations were determined using a Shimadzu TOC-V CSH analyzer equipped with a TNM-1 module (Japan). N-NH_4^+ was measured using the Nessler analytical method in a spectrophotometer U-200 (Hitachi, Japan) at 425 nm. N-NO_2^- and N-NO_3^- were analyzed by high-performance liquid chromatography-ion chromatography (HPLC-IC) with a Waters 515 HPLC pump coupled with a Waters 432 ionic conductivity detector and equipped with an IC-Pak Anion HC (150 mm × 4.6 mm) Waters column. N-NO_2^- and N-NO_3^- were also determined by colorimetry according to Eaton et al. (2005). DOC and temperature were determined using an OXI 330i oximeter (WTW, Germany), while a Crison micropH 2002 (Crison instruments, Spain) was used for pH determination. The concentration of TSS, SVI and biomass settling rate were determined according to Eaton et al. (2005). The analysis of the C and N biomass content was conducted using a LECO CHNS-932 elemental analyzer. The identification, quantification and biometry measurements of microalgae were conducted by microscopic examination (OLYMPUS IX70, USA) of the algal–bacterial cultivation broths (fixed with lugol acid at 5% and stored at 4 °C prior to analysis) according to Sournia (1978).

Biomass samples from both the anoxic and aerobic reactors were collected at the end of every stage and immediately stored at -20 °C in order to evaluate the richness and composition of the bacterial communities. The V6–V8 regions of the bacterial 16S ribosomal ribonucleic acid (rRNA) genes were amplified by Polymerase Chain Reaction (PCR) analysis using the universal bacterial primers 968-F-GC and 1401-R (Sigma–Aldrich, St. Louis, MO, USA; Nübel et al., 1996). The PCR mixture (50 μL) contained 2 μl of each primer (10 ng μl^{-1} each primer), 25 μL of BIOMIX ready-to-use 2 × reaction mix (Bioline, Ecogen), PCR reaction buffer and deoxynucleotide triphosphates (dNTPs), 2 μL of the extracted deoxyribonucleic acid (DNA) and Milli-Q water up to a final volume of 50 μL. PCR was performed in a iCycler Thermal Cycler (Bio Rad Laboratories, Inc) with the following thermo-cycling program for bacterial amplification: 2 min of pre-denaturation at 95 °C, 35 cycles of denaturation at 95 °C for 30 s, annealing at 56 °C for 45 s, and elongation at 72 °C for 1 min, with a final 5-min elongation at 72 °C. Size and yield of PCR products were estimated using a 2000-bp DNA ladder, Hypperladder II (Bioline, USA Inc) in 1.8% agarose gel (w/v) electrophoresis and GelRed Nucleic Acid Gel staining (Biotium). The denaturing gradient gel electrophoresis (DGGE) analysis of the amplicons was performed on 8% (w/v) polyacrylamide gels with a urea/formamide denaturing gradient of 45–65% (Roest et al., 2005). Electrophoresis was performed with a D-Code Universal Mutation Detection System (Bio Rad Laboratories, Inc) in 0.5 × TAE buffer at 60 °C and 85 V for 16 h. The gels were stained with GelRed Nucleic Acid Gel (1:10,000 dilution; Biotium) for 1 h.

The sequencing and DNA sequence analysis were carried out as follows: Individual bands were excised from the DGGE gel with a sterile blade, resuspended in 50 μl of ultrapure water, and maintained at 60 °C for 1 h to allow DNA extraction from the gel. A volume of 5 μl of the supernatant was used for reamplification with the original primer sets. Before sequencing, PCR products were purified with the GenElute PCR DNA Purification Kit (Sigma-Aldrich, St. Louis, MO, USA). The taxonomic position of the sequenced DGGE bands was obtained according to Frutos et al. (2015). Sequences were deposited in GenBank Data Library under accession numbers KP797888–KP797908. Bacterial DGGE profiles were compared using the GelCompar IITM software (Applied Maths BVBA, Sint-Martens-Latem, Belgium). The gels were normalized by using internal standards. After image normalization, bands were defined for each sample using the bands search algorithm within the program. The software carries out a density profile analysis for each lane, detects the bands, and calculates the relative contribution of each band to the total band intensity in the lane. Similarity indices within the bacterial populations were calculated from the densitometric curves of the scanned DGGE profiles by using the Pearson product–moment correlation coefficient (Häne et al., 1993), and were subsequently used to depict a dendrogram by using UPGMA clustering with error resampling (500 resampling experiments). Peak heights in the densitometric curves were also used to determine the Shannon–Wiener diversity indices according to Eq. (3):

$$H = -\sum [P_i \ln(P_i)] \quad (3)$$

where P_i is the importance probability of the bands in a lane ($P_i = n_i/n$, n_i is the height of an individual peak and n is the sum of all peak heights in the densitometric curves).

3. Results and discussion

The TOC, IC and TN mass balances showed average recovery factors of 100 ± 0%, 100 ± 1% and 99 ± 1%, respectively, which validated both the analytical and instrumental methods used in this study (Table 1). The symbiosis between microalgae and bacteria in this anoxic–aerobic photobioreactor configuration supported a very efficient and robust organic C elimination, with TOC removals of 88 ± 2% regardless of the operational conditions (Fig. 2a). On the other hand, IC removal was correlated with microalgae activity in the photobioreactor and the HRT, with a maximum removal of 98 ± 6% during Stage I (Fig. 2b). NH_4^+ removal was significantly influenced by the extent of nitrification in the photobioreactor, with an average NH_4^+ removal of 77 ± 2% during Stages I and II and 95 ± 2% during Stages III, IV and V (Fig. 2c). However, TN removal remained roughly constant at 76 ± 5% during the entire experiment as a result of a TN removal shift from N-NH_4^+ assimilation into biomass in the photobioreactor towards NO_2^- denitrification in the anoxic tank. In this context, TN removal in the anoxic tank was directly linked with the N-NH_4^+ transformed into N-NO_2^- through nitrification in the photobioreactor. Thus, the lower the TN removal in the photobioreactor (high NO_2^- concentration in the effluent) the higher the TN removal in the anoxic tank (high NO_2^- concentration removed by denitrification) (Fig. 2d). In addition, high biomass productivities (106 ± 16 g/$m^3_{reactor}$ d) were recorded during the entire experiment. This macroscopic photobioreactor performance was comparable to that reported by De Godos et al. (2009) in an outdoors 464-L HRAP treating piggery wastewater at 10 days of HRT under a maximum irradiation of 1354 μE/m^2 s, where a maximum biomass productivity of 80 g/$m^3_{reactor}$ d with total carbon and nitrogen removals of 77% and 69%, respectively, were recorded. Similarly, Posadas et al. (2015) reported TOC removals of 84 ± 1% and TN removals of 66 ± 5%, corresponding with biomass productivities of 135 ± 1 g/$m^3_{reactor}$ d, during secondary domestic wastewater treatment in an outdoors 800-L HRAP at a HRT of 2.8 ± 0.2 d under a light irradiance of 2125 μE/m^2 s (9.3 ± 1.7 h/day). Finally, Arbib et al. (2013) reported a maximum biomass productivity of 63 g/m^3 d in an outdoors 533 L-HRAP sparged with flue gas (4–5% CO_2) at 20 mL/min treating domestic wastewater at 8 days of HRT under a maximum light intensity of 2000 μE/m^2 s. This biomass productivity corresponded with a TN removal of 93%, while TOC removal remained negligible likely due to the low biodegradability of the organic matter present in the wastewater. Therefore, the high and consistent C and N removal efficiencies and biomass productivities recorded at HRTs as low as 2 days under 12 h light/12 h dark cycles at moderately high light intensities demonstrated the potential of this innovative anoxic–aerobic photobioreactor for wastewater treatment.

3.1. Carbon and nitrogen removal in the anoxic tank

TOC removals of 65 ± 2% were recorded in the anoxic tank regardless of the type and concentration of electron acceptors supplied to the anoxic tank (Fig. 2a). Indeed, O_2 was the main electron acceptor during Stages I (21 ± 3 mg O_2/L) and II (21 ± 4 mg O_2/L), while NO_2^- accounted for 0.9 ± 1.2 mg N-NO_2^-/L (≈10% of the electron acceptor potential of the DOC) and 4.8 ± 0.5 N-NO_2^-/L (≈52% of the electron acceptor potential of the DOC) in Stages I and II, respectively. NO_2^- became the main electron acceptor with 13 ± 0 mg N-NO_2^-/L, 20 ± 1 mg N-NO_2^-/L and 20 ± 0 mg N-NO_2^-/L during Stages III, IV and V, respectively. This heterotrophic TOC removal resulted in average TOC concentrations in the anoxic tank of 38 ± 1 mg/L, which were associated with an average N-NH_4^+ elimination of 22 ± 2% (Figs. 2c and 3a). This corresponded with a ratio of 4.9 ± 0.2 g $TOC_{removed}$/g N-$NH_{4removed}^+$, which matched the 5.2 ± 0.4 g $C_{biomass}$/g $N_{biomass}$ ratio obtained from the elemental analysis of the algal–bacterial biomass generated in the anoxic tank and suggested that all N-NH_4^+ removed in the anoxic tank was assimilated as structural N by heterotrophic bacteria. The active denitrification occurring in the anoxic tank resulted in a complete depletion of N-NO_2^- and N-NO_3^- from stage I onward (Fig. 4a). IC removal in the anoxic tank was negligible during the entire experiment, which confirmed that autotrophic assimilation (biotic removal) and/or CO_2 stripping (abiotic removal) at a pH of 7.6 ± 0.1 did not occur under these operational conditions (Figs. 2b and 3a). The extent of TN removal under anoxic conditions was directly proportional with the N-NO_2^- and N-NO_3^- supplied from the photobioreactor to the anoxic tank via internal recycling. Hence, TN removal increased from 23 ± 2% in Stage I to 61 ± 3% in Stage V mediated by the stepwise increase in N-NO_2^- concentration in the photobioreactor (Fig. 2d), which resulted in TN concentrations in the anoxic tank decreasing from 43 ± 1 mg TN/L to 32 ± 1 mg TN/L, respectively (Table 1 and Fig. 4c).

3.2. Carbon and nitrogen removal in the photobioreactor

Mixotrophic microalgae and aerobic bacteria in the photobioreactor assimilated as structural carbon 24 ± 3% of the influent TOC supplied in the SWW (Fig. 2a), resulting in average effluent TOC concentrations of 24 ± 1 mg/L regardless of operational conditions (Fig. 3b). The additional effluent biodegradability tests conducted confirmed that this residual effluent TOC concentration corresponded with the non-biodegradable fraction of the organic matter present in the SWW, which indeed matched the concentration of the recalcitrant chelating agent EDTA. The occurrence of IC limitation in the photobioreactor during Stage I, as suggested by the low IC concentrations recorded (6.1 ± 1.5 mg/L), can explain the absence of a significant nitrification in this unit. Hence, the fact that autotrophic nitrifiers were outcompeted by microalgae during IC uptake likely cause that most IC and/or N-NH_4^+ were removed by assimilation into algal and heterotrophic bacterial biomass (Figs. 3b and 4b). At this point, the HRT was decreased to 2 days while maintaining the SRT at 20 ± 6 days in order to favor nitrifying activity (Stage II) (Table 1). Despite the increase in TOC loading rate, the system was able to maintain a stable DOC in the culture broth of 21 ± 4 mg O_2/L due to an intense photosynthetic activity during Stage II. This high DOC, coupled with the decrease in the HRT, entailed an accumulation of IC and N-NH_4^+ in the photobioreactor during Stage II, which decreased the algal–bacterial biomass concentration from 2531 ± 191 mg TSS/L to 2061 ± 37 mg TSS/L (Figs. 3b, 4b and 5a). This increase in IC and N-NH_4^+ availability resulted in a significantly higher nitrification activity, which resulted in N-NO_2^- concentrations of 4.8 ± 0.5 mg/L in the steady state corresponding to Stage II (Table 1 and Fig. 4b). Stage III was characterized by an active air diffusion in the photobioreactor at a flow rate of 10 mL/min, which supported an efficient O_2 stripping and the stabilization of the DOC at 10 ± 2 mg O_2/L (Table 1). This moderate DOC, together with the high irradiation (400 ± 51 μE/m^2 s) and neutral pH (7.8 ± 0.1) in the photobioreactor, entailed an enhanced utilization of the IC for biomass formation via photosynthesis and nitrification. This autotrophic IC removal (93 ± 10%, Fig. 2b) resulted in an increase in biomass concentration up to 2881 ± 160 mg TSS/L (Fig. 5a) and final IC, N-NH_4^+ and N-NO_2^- steady state concentrations in the effluent of 19 ± 5 mg IC/L, 5.5 ± 0.6 mg N-NH_4^+/L and 13 ± 0 mg N-NO_2^-/L, respectively (Figs. 3b and 4b). At this point it should be highlighted that O_2 is

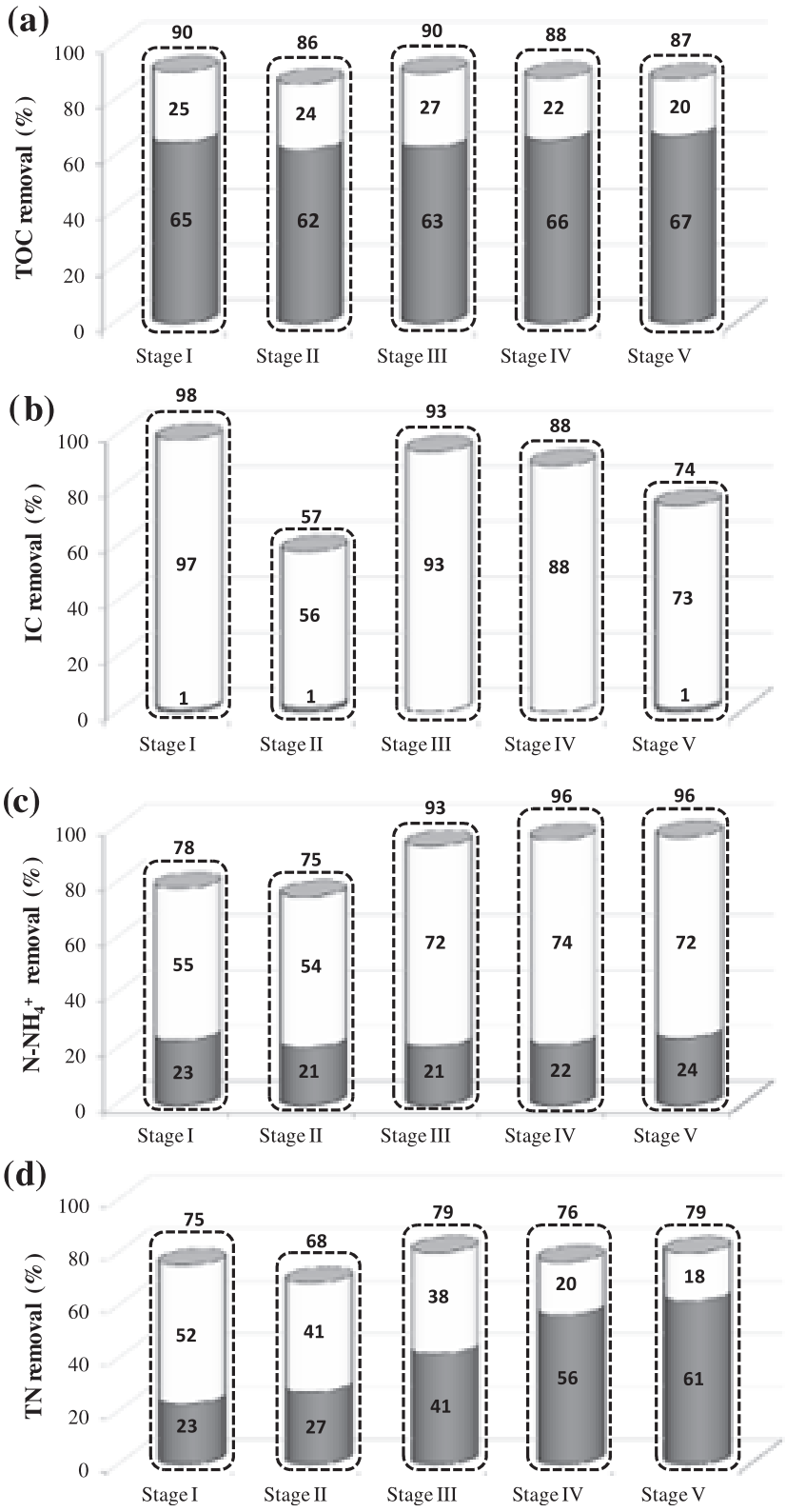

Fig. 2. TOC (a), IC (b), N-NH_4^+ (c) and TN (d) removals in the anoxic tank (grey) and photobioreactor (white), respectively, during the steady state of the 5 operational stages evaluated.

a product of photosynthesis, which competes with CO_2 as a substrate for the active sites of the enzyme ribulose bisphosphate carboxylase (RuBisCO) (a key catalyst of the Calvin cycle to transform CO_2 into organic compounds) (Madigan et al., 2009). Thus, a potential competition between O_2 and CO_2 for RuBisCO enzyme active sites likely occurred at the high DOC recorded during Stage II. Indeed, despite the extent of DO-mediated inhibition in microalgae is strain specific (Peng et al., 2013), a DOC higher than 20–25 mg O_2/L often results in decreased yields of biomass production, pigment content and promotes a photooxidative damage on

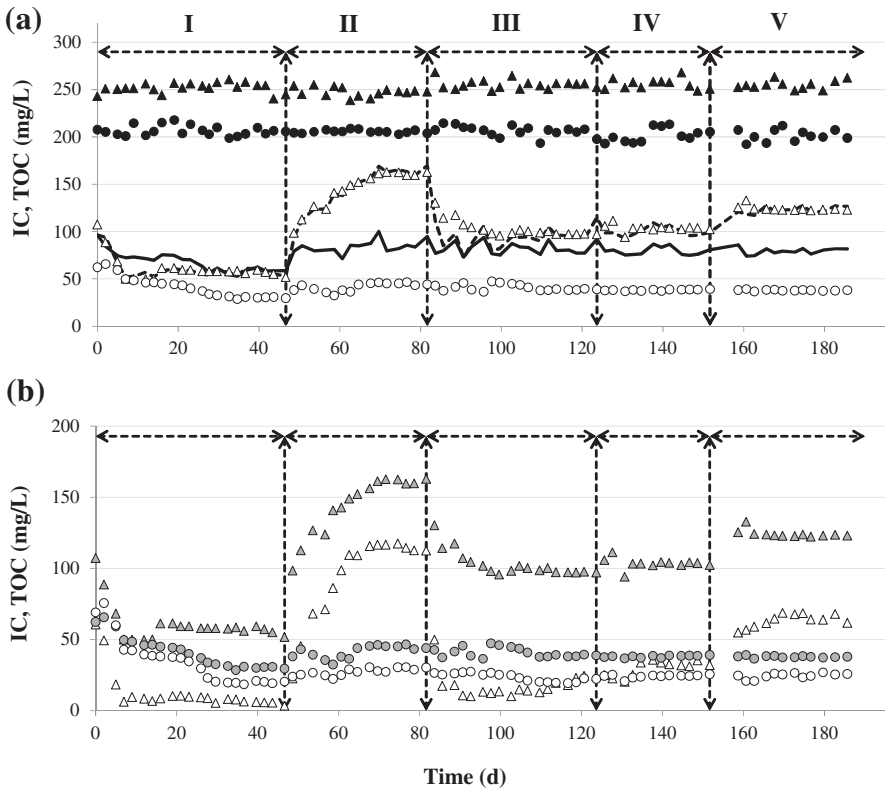

Fig. 3. Time course of (a) IC (–▲–) and TOC (–●–) concentration in the SWW, virtual inlet IC (- - -) and TOC (—) concentrations in the anoxic tank due to the dilution effect mediated by the internal and external recirculations, concentrations of IC (–Δ–) and TOC (–○–) in the anoxic tank, and of (b) the inlet IC (▲) and TOC (●), and outlet IC (–Δ–) and TOC (–○–) concentrations in the photobioreactor. Vertical dashed lines separate the different operational stages.

microalgae cells (Tredici, 1999). The decrease in both DOC (5.8 ± 0.9 mg O_2/L) and light intensity (162 ± 40 μE/m^2 s) imposed during Stage IV (Table 1) clearly boosted NH_4^+ nitritation, with an increase in N-NO_2^- concentration up to 20 ± 1 mg N-NO_2^-/L at a constant pH of 7.7 ± 0.0. Unexpectedly, N-NO_3^- production remained inhibited despite the availability of IC, NO_2^- and dissolved O_2 (Table 1 and Fig. 4b). Biomass concentration decreased to 2134 ± 224 mg TSS/L in the photobioreactor during Stage IV (Fig. 5a) as a result of the less active photosynthetic activity, which also induced a decrease in IC removal efficiencies to 88 ± 7% (Fig. 2b) and a slight increase in the effluent IC concentrations of 33 ± 2 mg IC/L (Fig. 3b). A detailed C balance in the system revealed that the decrease in $C_{biomass}$ concentration in the photobioreactor during Stage IV was higher than the corresponding increase in IC concentration, which suggests that part of the IC was removed by air stripping. The high light intensity (400 μE/m^2 s) supplied to the photobioreactor during previous stages might have partially inhibited bacterial nitrifiers in the photobioreactor since it has been consistently shown that high irradiations can inhibit nitrification via photooxidation of the bacterial cytochrome (Lavrentyev et al., 2000). For instance, Guerrero and Jones (1996) reported a 80% NH_4^+ oxidizing bacteria inhibition at a light intensity of 115 μE/m^2 s due to cytochrome photooxidation. Similarly, Yoshioka and Saijo (1984) observed light inhibition of both NH_4^+ and NO_2^- oxidizing bacteria at light intensities as low as 75 μE/m^2 s (12-h light:12-h dark). Finally, 12 h/12 h light-dark cycles combined with process aeration during dark periods were set during Stage V in order to provide a competitive advantage to nitrifying bacteria. Under these operational conditions, the removal efficiency of IC dropped to 73 ± 4% (Fig. 2b), corresponding to IC and TSS concentrations in the photobioreactor of 65 ± 3 mg/L and 1593 ± 83 mg/L, respectively (Figs. 3b and 5a). Nevertheless, no enhancement in nitrifying activity was recorded, the effluent N-NO_2^- concentration remaining constant at 20 ± 0 mg/L with a negligible N-NO_3^- production (Fig. 4b). Further research on light-mediated inhibition on nitrifying activity is therefore needed given the current interest in microalgae-based wastewater treatment in outdoors photobioreactors. Finally, the extent of TN removal in the photobioreactor (mainly due to assimilation at pH of 7.8 ± 0.1) gradually decreased with the increase in NH_4^+ nitrification despite the enhanced N-NH_4^+ removal by assimilation, which resulted in TN concentrations in the effluent above the maximum concentration of TN permissible for wastewater discharge into the environment according to European Directive 91/271/CEE on discharge of domestic waters (15 mg TN/L) during the entire experiment (Fig. 4c). In this context, the optimization of the internal recycling has the potential to further decrease the effluent TN concentrations.

3.3. Algal–bacterial population and sedimentation capacity

The high similarity found in the populations of microalgae (Fig. 6) and bacteria (Table 2) present in the aerobic and anoxic tanks during the entire experimentation was due to the high internal ($Q_{RI} = 1.8 \times Q_{feed}$) and external ($Q_{RE} = 0.3 \times Q_{feed}$) recycling rates used in this system.

The microalgae inoculum, which was mainly composed of (% of cells) *Pseudanabaena* sp. (42%), *Planktothrix isothrix* (32%), *Stigeoclonium setigerum* (11%), *Chlorella* sp. (3%), *Scenedesmus ecornis* (2%) and other minor species (10%), was rapidly overcome by *S. ecornis* (35%) and *Scenedesmus obtusus* (46%) during Stage I (Fig. 6). The abundance of the genus *Scenedesmus* decreased over time concomitantly with the appearance of *Chlorella* sp. (40%), *Acutodesmus obliquus* (37%) and *Pseudanabaena* sp. (22%) in Stage II. Stage III was characterized by a severe change in microalgae population, with new species such as *C. vulgaris* (48%), *Leptolyngbya benthonica*

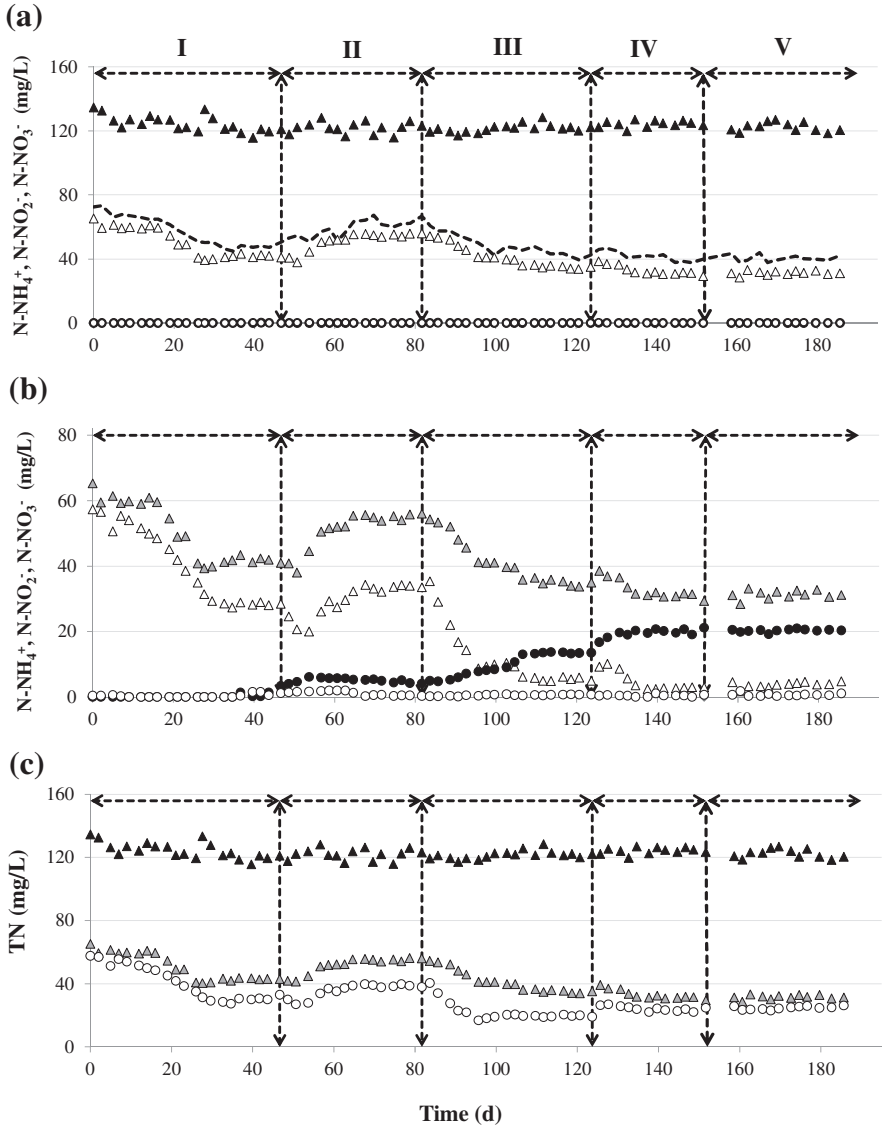

Fig. 4. Time course of (a) N-NH_4^+ (–▲–) concentration in the SWW, virtual influent N-NH_4^+ concentration in the anoxic tank after dilution (- - -), concentration of N-NH_4^+ (–Δ–), N-NO_2^- (–●–) and N-NO_3^- (–○–) in the anoxic tank), of (b) the concentrations of inlet N-NH_4^+ (▲) and outlet N-NH_4^+ (–Δ–), N-NO_2^- (–●–) and N-NO_3^- (–○–) in the photobioreactor, and of (c) TN concentration in the SWW (–▲–), anoxic tank (▲) and photobioreactor (–○–). Vertical dashed lines separate the different operational stages.

(16%) and *Geitlerinema* sp. (7%) becoming dominant along with *A. obliquus* (18%). Finally, *C. vulgaris* became the most important species during Stage IV and V (66%) (Fig. 6).

The effluent TSS concentration accounted for 56 ± 6 mg TSS/L during Stage I, II and III (Fig. 5b) (98 ± 1% of TSS removal), which remained under the maximum permissible discharge limit in EU legislation (60 mg TSS/L to 2000–100,000 Inhabitants Equivalent (European Directive 91/271/CEE on discharge of domestic waters). However, the dominance of *C. vulgaris* in Stage IV and V entailed an increase in the effluent TSS concentration up to 91 ± 19 mg TSS/L (96 ± 2% of TSS removal) and 145 ± 6 mg TSS/L (91 ± 2% of TSS removal), respectively (Fig. 5b).

The Shannon–Wiener diversity index takes into account both the sample richness (relative number of DGGE bands) and evenness (relative intensity of every band) of the species present in a microbial community, with low and high typical values of 1.5 and 3.5, respectively (McDonald, 2003). The activated sludge inoculum sample exhibited a relatively low bacterial diversity index (2.6), while bacterial diversity increased gradually in both reactors up to 3.5 (highlighting the high biodiversity of the communities established in the system during the entire experiment) (Table 1). The analysis of the Pearson similarity coefficients showed low similarities of 36% and 26% between the inoculum and the microbial communities present in the anoxic and aerobic reactors, respectively, from Stage I to V. On the other hand, the differences among microbial communities in the anoxic and aerobic tank during the entire experiment were negligible, with high similarities among bacterial populations of 87% and 79%, respectively. From the DGGE gel, 21 bands were sequenced and 4 different phyla were retrieved from the Ribosomal Database Project (RDP): Proteobacteria (15 bands), Actinobacteria (3 bands), Chlamydiae (1 band) and Firmicutes (1 band), while one band remained unclassified (Table 2). Proteobacteria was the main phylum in both reactors, while Actinobacteria, Chlamydiae and Firmicutes phyla, which are typically responsible of organic matter degradation in wastewater sludge treatment plants, were mostly present in the inoculum (bands 16–20). The denitrifiers *Simplicispira* (band 13) and *Thauera* (Band 14) (Hao et al., 2013) were the dominant genus in the anoxic and aerobic reactors. Bacteria from the genus *Rhizobiales* were found in bands 10 and 11 in both reactors from

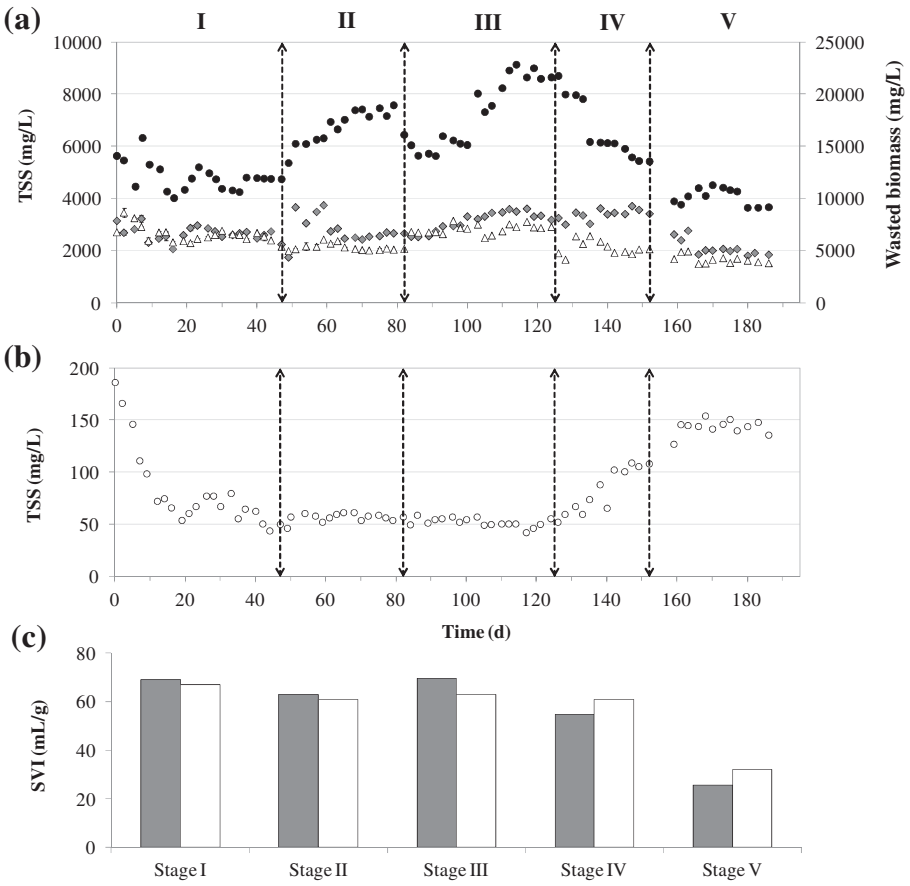

Fig. 5. Time course of TSS concentration in (a) the biomass wastage (–●–), anoxic tank (♦) and photobioreactor (–Δ–), and (b) the final effluent (–○–) during the entire experiment. Vertical dashed lines separate the different operational stages. SVI (c) in the anoxic (grey bars) and aerobic (white bars) reactor at the end of each operational stage.

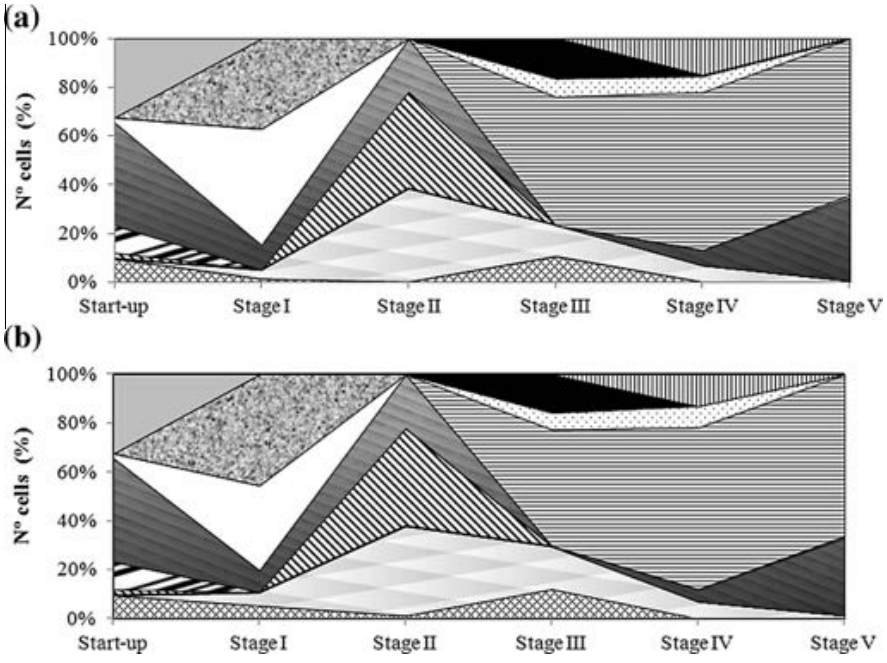

Fig. 6. Time course of the microalgae population structure in the anoxic (a) and aerobic (b) reactor during the entire operational period. *Scenedesmus ecornis*, *Pseudanabaena* sp., *Acutodesmus obliquus*, *Chlorella* sp., *Scenedesmus obtusus*, *Stigeoclonium setigerum*, *Planktothrix isothrix*, *Leptolyngbya benthonica*, *Chlorella vulgaris*, *Limnothrix planctonica*, *Geitlerinema* sp. and others.

Table 2
RDP classification of the bacterial DGGE bands sequenced with at least 50% of confidence level, and corresponding closest relatives in Genbank obtained by the BLAST search tool with their similarity percentages, and environments from which they were retrieved. Intensity < 20 = x, 20 ⩽ intensity ⩾ 80 = xx, intensity > 80 = xxx.

Taxonomic placement (50% confidence level)	Band n°	Aerobic					Start-up	Anoxic					Closest relatives in blast name (accession number)	Similarity (%)	Source of origin
		I	II	III	IV	V		I	II	III	IV	V			
Phylum Proteobacteria	1	xx		xx	xxx	xxx		xxx		xxx	xxx	xxx	Uncultured bacterium (JQ054610)	89	Soil
Class *Gammaproteobacteria*															
Order *Aeromonadales*															
Family *Aeromonadaceae*	2			xxx	xx	xx		xxx	xx	xxx			*Aeromonas* sp. (KJ576901)	99	Distillery waste water contaminated aquatic resource
Genus *Aeromonas*	3		xx	xxx	xxx	xxx		xxx	xxx	xxx	xxx	xxx	*Aeromonas aquariorum* (KC953873)	99	Hypereutrophic water
													Aeromonas sp. (JN697677)	96	Rice root endosphere
Order *Enterobacteriales*															
Family *Enterobacteriaceae*	4		x	x	x	x		xx	xx	xx	x	xx	*Klebsiella* sp. (JF701187)	92	Acclimated activated sludge under anaerobic/anoxic/aerobic reactor for dimethylaminobenzene removal
Genus *Citrobacter*	5	xx	xxx	xxx	xxx	xxx		xx	xx	xxx	xx	xxx	*Citrobacter freundii* (KF938666)	99	Membrane bioreactor activated sludge
													Citrobacter sp. (KF657722)	99	Coastal sediments
Order *Xanthomonadales*															
Family *Xanthomonadaceae*															
Genus *Pseudofulvimonas*	6	xx	xxx	xxx	xxx	xxx		xxx	xxx	xxx	xxx	xxx	Uncultured *Xanthomonadaceae* (EU305597)	100	Effect of organic matter on nitrite oxidation and heterotrophic bacteria in wastewater plant (WWTP)
	7	xx	xx	xx	xxx	xx		xxx	xx	xx			Uncultured *Xanthomonadaceae* (EU305594)	89	Effect of organic matter on nitrite oxidation and heterotrophic bacteria in wastewater plant (WWTP)
Order *Alteromonadales*															
Family *Shewanellaceae*															
Genus *Shewanella*	8			xxx	xxx	xxx		xxx	xxx	xxx	xxx	xxx	Uncultured *Shewanella* sp. (KC166842)	98	Sediment of an anaerobic aquifer
													Shewanella putrefaciens (NR_074817)	98	Culture Collection
Class *Alphaproteobacteria*	9	xxx	xxx	xx				xxx	xxx	xxx			Uncultured *Ancalomicrobium* sp. (JF817705)	99	Microbial fuel cell anode
													Uncultured bacterium (FR774629)	97	Wastewater treatment plant
													Uncultured bacterium (DQ35498)	97	Activated sludge
Order *Rhizobiales*	10	xx						xxx					Uncultured *Mesorhizobium* sp. (HM987196)	90	Bioreactor simulating a low temperature oil reservoir
	11	xx	xx	xx	xx			xx	xxx		xx		Uncultured bacterium (FJ971727)	95	Granular sludge
													Uncultured *Alphaproteobacteria* (CU918729)	95	Mesophilic anaerobic digester treating municipal wastewater sludge

Table 2 (*continued*)

Taxonomic placement (50% confidence level)	Band n°	Aerobic					Start-up	Anoxic					Closest relatives in blast name (accession number)	Similarity (%)	Source of origin
		I	II	III	IV	V		I	II	III	IV	V			
Order *Rhodobacterales* Family *Rhodobacteraceae*	12	xx	xx	xxx	xxx	xxx		xx	xxx	xxx	xxx	xxx	Uncultured *Rhodobacter* sp.(JF522357)	89	Microbial fuel cell
Class *Betaproteobacteria* Order *Burkholderiales* Family *Comamonadaceae* Genus *Simpliscipira*	13		xx						xx				Environmental 16S rDNA sequence (CU466846)	94	Wastewater treatment plant anoxic basin
													Simplicispira sp. (AM236310)	94	Commercial nitrifying inoculum
Order *Rhodocyclales* Family *Rhodocyclaceae* Genus *Thauera*	14	x			xx	xxx	xx	xx	xxx	xxx	xxx	xxx	Uncultured *Thauera* sp. (KC166840)	96	Sediment of an anaerobic aquifer
													Uncultured bacterium (AB563209)	96	Biofilm attached to perlite in an aerobic biological reactor treating dairy farm wastewater
													Thauera sp.(AM231040)	96	Activated sludge
Class *Deltaproteobacteria* Order *Desulfovibrionales* Family *Desulfovibrionaceae* Genus *Desulfovibrio*	15					xx	xx			xxx	xxx	xxx	Uncultured bacterium (KC179062)	97	Activated sludge taken from a microaerobic bioreactor treating for synthetic wastewater using glucose as the sole carbon source
													Uncultured bacterium (AB175371)	97	Mesophilic anaerobic BSA digester
Phylum *Actinobacteria* Class *Actinobacteria* Subclass *Actinobacteridae* Order *Actinomycetales*	16		x	x			x			x	xx		Uncultured bacterium (JQ038784)	99	Biotrickling filter (BTF) treating low concentrations of methyl mercaptan, toluene, alpha-pinene and hexane
													Uncultured *Actinobacteria* (CU926089)	98	Mesophilic anaerobic digester which treats municipal wastewater sludge
Suborder *Micrococcineae* Family *Intrasporangiaceae*	17		x	x	xx	xx	xx		xx	x	xx	x	*Arsenicicoccus bolidensis* (FM163604)	86	Soil
Subclass *Acidimicrobidae* Order *Acidimicrobiales* Suborder *Acidimicrobineae* Family *Lamiaceae* Genus *Lamia*	18		xx	xx	xx		xx	x	xx	xx			Uncultured bacterium (KF428019)	99	Sewage activated sludge

(*continued on next page*)

Table 2 (*continued*)

Taxonomic placement (50% confidence level)	Band n°	Aerobic					Start-up	Anoxic					Closest relatives in blast name (accession number)	Similarity (%)	Source of origin
		I	II	III	IV	V		I	II	III	IV	V			
													Candidatus Microthrix parvicella (JQ624332)	99	Wastewater treatment plant
													Candidatus Microthrix parvicella (X89560)	99	Culture collection
Phylum *Chlamydiae*															
Class *Chlamydiae*															
Order *Chlamydiales*															
Family *Parachlamydiaceae*															
Genus *Parachlamydia*	19						x						*Protochlamydia naegleriophila* (FJ532294)	94	Sludge from clarifier
Phylum Firmicutes															
Class *Clostridia*															
Order *Clostridiales*															
Family *Peptostreptococcaceae*															
Genus *Clostridium XI*	20	x					xx	x		xx	xx	xx	Uncultured bacterium (AM500813)	99	Composting sample
													Uncultured bacterium (KC551590)	99	Activated sludge
Unclassified Bacteria	21	xx		xx	xxx	xxx	x	xx			xxx	xxx	*Phormidium* sp. (EU078511)	94	

Stage I to IV ($20 \leqslant$ intensity $\geqslant 80$), which are typically associated with the oxidation of NO_2^- into NO_3^- during nitrification. Unexpectedly, NH_4^+ oxidizing bacteria were not detected during the entire experiment likely due to the low nitrifying bacteria concentration in the culture broth mediated by the competition with microalgae population for IC.

The SVIs of the algal–bacterial biomass from the anoxic tank and photobioreactor remained similar and constant from Stage I to IV, with average values of 64 ± 7 mL/g and 63 ± 3 mL/g, respectively (Fig. 5c). These SVIs values corresponded with average settling rates of 1.4 ± 0.3 m/h in the anoxic tank and 1.9 ± 0.2 m/h in the photobioreactor, which were significantly higher than the sedimentation rates of 0.42 m/h and 0.28 m/h reported in a similar photobioreactor configuration by De Godos et al. (2014) in the anoxic and aerobic reactors, respectively. During Stage V, the SVI decreased to 26 mL/g in the anoxic tank and 32 mL/g in the photobioreactor, along with an increase in the sedimentation rate of 2.8 m/h in both reactors (Fig. 5c). SVI values below 100 mL/g are indicative of good settling, while SVI values above 150 mL/g are typically associated with sludge bulking and a poor sedimentation performance (Parker et al., 2001). Therefore, the implementation of settled biomass recycling strategies resulted in the enrichment of algal–bacterial flocs with a good sedimentation capacity. In this context, Park et al. (2011, 2013) recently reported that algal–bacterial biomass recycling improved biomass settleability by up to 20% by increasing the cell residence time of readily settleable algal species. This operational strategy increased both the dominance and average size of their colonies and promoted the formation of larger algal/bacterial aggregates (>500 μm).

3.4. Environmental sustainability

Microalgae-based wastewater treatment in this innovative photobioreactor configuration only generated relevant N_2O emissions in the aerobic reactor, with maximum N_2O concentrations of 129 ± 23 ppm_v at Stage II (Table 1). During nitrification, NH_3 is first converted to hydroxylamine (NH_2OH) to be further transformed into NO_2^-. N_2O can be produced from NH_2OH by either chemical decomposition or chemical oxidation with NO_2^- as electron acceptor under O_2 limiting conditions (0.1–0.5 mg/L) (Kampschreur et al., 2009; Law et al., 2015). Wunderlin et al. (2012) also observed that N_2O might be produced via NH_2OH aerobic oxidation under NO_2^- limiting conditions in the excess of NH_3. This is consistent with the findings of Sutka et al. (2006), who recorded a decreased contribution of NO_2^- reduction to N_2O production compared to NH_2OH oxidation at increasing oxygen concentration in *Nitrosomonas europaea* cultures. In this particular study, the high DO and NH_4^+ (Table 1) concentrations during Stage II likely boosted N_2O production via NH_2OH oxidation. The injection of air during Stage III (1.9 ± 1.1 ppm_v of N_2O) and Stage IV (3.7 ± 2.8 ppm_v of N_2O) (Table 1) resulted in emission factors of $4.4 \cdot 10^{-6}$ g N-N_2O/g N-input and $5.9 \cdot 10^{-6}$ g N-N_2O/g N-input, respectively. These N_2O emission factors were ≈1000 times lower than the N_2O emission factor typically recorded in WWTPs ($5–6 \cdot 10^{-3}$ g N-N_2O/g N-input) (IPCC, 2006; Gustavsson and la Cour Jansen, 2011). In addition, the CO_2 footprint associated with the N_2O emissions monitored during Stage III and IV was 0.3 g CO_2/m^3 WW treated, which compared favorably against the indirect carbon footprint from electricity use for aeration and mixing in activated sludge processes (119–378 g CO_2/m^3 WW treated) and even for mixing in HRAPs (3–14 g CO_2/m^3 WW treated). These preliminary estimations suggest that N_2O emissions in this innovative algal–bacterial photobioreactor should not compromise the environmental sustainability of wastewater treatment in terms of global warming impact.

Thus, this novel anoxic–aerobic algal–bacterial photobioreactor with biomass recycling allowed maximizing N recovery via biomass assimilation due to the simultaneous utilization of organic and inorganic C while removing the excess of N via denitrification. This entails an important advantage in terms of nutrient recovery potential in comparison with conventional WWTPs where the absence of photosynthetic microorganisms prevents the use of IC as a fixation tool. Moreover, dissimilatory N removal through nitrification–denitrification pathway represents a key alternative route when the C/N ratio in the target wastewater is low. Likewise, photosynthetic oxygenation along with the high sedimentation capability of biomass resulted in an effluent with a high DOC and TSS concentration below the EU discharge limits. In this context, mechanical oxygenation represents one of the most costly steps in WWTPs (45–75% of the total operational costs, Chae and Kang, 2013) while microalgae harvesting can jeopardize the efficiency of conventional HRAPs during wastewater treatment (20–30% of the total cost of producing the biomass, Molina Grima et al., 2003), which highlights the potential of this novel photobioreactor configuration as a cost effective wastewater treatment platform. In addition, the system exhibited a consistent and efficient wastewater treatment performance at a HRT of 2 days, which suggested that the capital costs associated to the scale-up of this photobioreactor could be easily affordable. Finally, this innovative algal–bacterial photobioreactor should not compromise the environmental sustainability of wastewater treatment in terms of global warming impact since its associated C footprint was far below the typical C footprint associated with conventional WWTPs.

4. Conclusions

This innovative anoxic–aerobic algal–bacterial photobioreactor operated with biomass recycling supported efficient TOC, IC and TN removals. The intensity and regime of light supply along with the DOC governed the extent of the assimilatory and dissimilatory N removal mechanisms. Biomass recycling resulted in rapidly settling algal flocs and low effluent TSS concentrations. Microalgal taxonomic analyses revealed that *C. vulgaris* and *Pseudanabaena* sp. were the dominant microalgae species, while Proteobacteria was the main phylum according to bacterial phylogenetic analyses. Finally, N_2O emissions were far below the IPCC emission factor reported for WWTPs, which confirmed the environmental sustainability of this technology.

Acknowledgements

This research was supported by the regional government of Castilla y León and the European Social Fund (Belgium) (Contract N° E-47-2011-0053564 and Projects VA024U14 and GR76). The financial support of the Ministry of Economy and Competitiveness (Red Novedar) (Spain) and the National Institute for Agricultural Research and Technology and Food is also gratefully acknowledged (Project Ref. RTA2013-00056-C03-02).

References

Alcántara, C., Muñoz, R., Norvill, Z., Plouviez, M., Guieysse, B., 2015. Nitrous oxide emissions from high rate algal ponds treating domestic wastewater. Bioresour. Technol. 177, 110–117.

Arbib, Z., Ruiz, J., Álvarez-Díaz, P., Garrido-Pérez, C., Barragan, J., Perales, J.A., 2013. Effect of pH control by means of flue gas addition on three different photobioreactors treating urban wastewater in long-term Operation. Ecol. Eng. 57, 226–235.

Arbib, Z., Ruiz, J., Álvarez-Díaz, P., Garrido-Pérez, C., Perales, J.A., 2014. Capability of different microalgae species for phytoremediation processes: Wastewater tertiary treatment, CO_2 bio-fixation and low cost biofuels production. Water Res. 49, 465–474.

Chae, K.Y., Kang, J., 2013. Estimating the energy independence of a municipal wastewater treatment plant incorporating green energy resources. Energy Convers. Manage. 72, 664–672.

De Godos, I., Blanco, S., García-Encina, P.A., Becares, E., Muñoz, R., 2009. Long-term operation of high rate algal ponds for the bioremediation of piggery wastewaters at high loading rates. Bioresour. Technol. 100, 4332–4339.

De Godos, I., Vargas, V.A., Guzmán, H.O., Soto, R., García, B., García, P.A., Muñoz, R., 2014. Assessing carbon and nitrogen removal in a novel anoxic–aerobic cyanobacterial–bacterial photobioreactor configuration with enhanced biomass sedimentation. Water Res. 61, 77–85.

Eaton, A.D., Clesceri, L.S., Greenberg, A.E., 2005. Standard Methods for the Examination of Water and Wastewater, second ed. American Public Health Association/American Water Works Association/Water Environment Federation, Washington DC, USA.

European Directive 91/271/CEE, <http://eur-lex.europa.eu/legal-content/EN/TXT/PDF/?uri=CELEX:31991L0271&from=EN>, 1998 (accessed 10.02.15).

Fagerstone, K.D., Quinn, J.C., Bradley, T.H., De Long, S.K., Marchese, A.J., 2011. Quantitative measurement of direct nitrous oxide emissions from microalgae cultivation. Environ. Sci. Technol. 45, 9449–9456.

Frutos, O.D., Arvelo, I.A., Perez, R., Quijano, G., Muñoz, R., 2015. Continuous nitrous oxide abatement in a novel denitrifying off-gas bioscrubber. Appl. Microbiol. Biotechnol. 99, 3695–3706.

Guerrero, M.A., Jones, R.D., 1996. Photoinhibition of marine nitrifying bacteria. I. Wavelength-dependent response. Mar. Ecol. Prog. Ser. 141, 183–192.

Gustavsson, D.J.I., la Cour Jansen, J., 2011. Dynamics of nitrogen oxides emission from a full-scale sludge liquor treatment plant with nitritation. Water Sci. Technol. 63, 2838–2845.

Häne, B.G., Jäger, K., Drexler, H.G., 1993. The Pearson product-moment correlation coefficient is better suited for identification of DNA fingerprint profiles than band matching algorithms. Electrophoresis 14, 967–972.

Hao, R., Li, S., Li, J., Meng, C., 2013. Denitrification of simulated municipal wastewater treatment plant effluent using a three-dimensional biofilm-electrode reactor: Operating performance and bacterial community. Bioresour. Technol. 143, 178–186.

IPCC, 2006. 2006 IPCC Guidelines for National Greenhouse Gas Inventories. In: Eggleston, H.S., Buendia, L., Miwa, K., Ngara, T., Tanabe, K. (Eds.). IGES, Japan, pp. 6.24–26.26.

Kampschreur, M.J., Temmink, H., Kleerebezem, R., Jetten, M.S.M., van Loosdrecht, M.C.M., 2009. Nitrous oxide emission during wastewater treatment. Water Res. 43, 4093–4103.

Lavrentyev, P.J., Gardner, W.S., Yang, L., 2000. Effects of the zebra mussel on nitrogen dynamics and the microbial community at the sediment-water interface. Aquat. Microb. Ecol. 21, 187–194.

Law, Y., Ye, L., Pan, Y., Yuan, Z., 2015. Nitrous oxide emissions from wastewater treatment processes. Phil. Trans. R. Soc. B. 367, 1265–1277.

Madigan, M.T., Martinko, J.M., Dunlap, P.V., Clark, D.P., 2009. Brock Biology of Microorganisms, twelfth ed. Pearson International Edition, San Francisco.

McDonald, G., 2003. Biogeography: Space, Time and Life. Wiley, New York.

Molina Grima, G.E., Belarbi, E.H., Acien Fernandez, F.G., Medina, R.A., Chisti, Y., 2003. Recovery of microalgal biomass and metabolites: process options and economics. Biotechnol. Adv. 20, 491–515.

Muñoz, R., Guieysse, B., 2006. Algal–bacterial processes for the treatment of hazardous contaminants: a review. Water Res. 40, 2799–2815.

Nübel, U., Engelen, B., Felske, A., Snaidr, J., Wieshuber, A., Amann, R.I., Ludwig, W., Backhaus, H., 1996. Sequence heterogeneities of genes encoding 16S rRNAs in *Paenibacillus polymyxa* detected by temperature gradient gel electrophoresis. J. Bacteriol. 178, 5636–5643.

Park, J.B.K., Craggs, R., Shilton, A., 2011. Recycling algae to improve species control and harvest efficiency from high rate algae pond. Water Res. 45, 6637–6649.

Park, J.B.K., Craggs, R.J., Shilton, A.N., 2013. Investigating why recycling gravity harvested algae increases harvestability and productivity high rate algae ponds. Water Res. 47, 4904–4917.

Parker, D.S., Kinnear, D.J., Wahlberg, E.J., 2001. Review of folklore in design and operation of secondary clarifiers. J. Environ. Eng. 127, 476–484.

Peng, L., Lan, C.Q., Zhang, Z., 2013. Evolution, Detrimental Effects, and Removal of Oxygen in Microalga Cultures: A Review. AICHE. Environ. Prog. Sustain. Energy 32, 982–988.

Posadas, E., Morales, M.M., Gomez, C., Acien-Fernandez, G., Muñoz, R., 2015. Influence of pH and CO_2 source on the performance of microalgae-based secondary domestic wastewater treatment in outdoors pilot raceways. Chem. Eng. J. 265, 239–248.

Roest, K., Heilig, H.G., Smidt, H., de Vos, W.M., Stams, A.J.M., Akkermans, A.D.L., 2005. Community analysis of a full-scale anaerobic bioreactor treating paper mill wastewater. Syst. Appl. Micriobiol. 28, 175–185.

Serejo, M., Posadas, E., Boncz, M., Blanco, S., Garcia-Encina, P.A., Muñoz, R., 2015. Influence of biogas flow rate on biomass composition during the optimization of biogas upgrading in microalgal–bacterial processes. Environ. Sci. Technol. 49, 3228–3236.

Sournia, A., 1978. Phytoplanton Manual. Museum National d' Historie Naturelle, París. United Nations Educational. Scientific and Cultural Organization (Unesco).

Sutka, R.L., Ostrom, N.E., Ostrom, P.H., Breznak, J.A., Gandhi, H., Pitt, A.J., Li, F., 2006. Distinguishing nitrous oxide production from nitrification and denitrification on the basis of isotopomer abundances. Appl. Environ. Microbiol. 72, 638–644.

Tredici, M.R., 1999. Photobioreactors. In: Flickinger, M.C., Drew, S.W. (Eds.), Encyclopedia of Bioprocess Technology: Fermentation, Biocatalysis and Bioseparation. J. Wiley & Sons, New York, pp. 395–419.

Wunderlin, P., Mohn, J., Joss, A., Emmenegger, L., Siegrist, H., 2012. Mechanisms of N_2O production in biological wastewater treatment under nitrifying and denitrifying conditions. Water Res. 46, 1027–1037.

Yoshioka, T., Saijo, Y., 1984. Photoinhibition and recovery of NH_4-oxidizing bacteria and NO_2-oxidizing bacteria. J. Gen. Appl. Microbiol. 30, 151–166.

Evaluation of the simultaneous biogas upgrading and treatment of centrates in a HRAP through C, N and P mass balances

Alcántara, C., García-Encina, P., Muñoz, R., 2015. WST
(doi: 10.2166/wst.2015.198)

Chapter 5

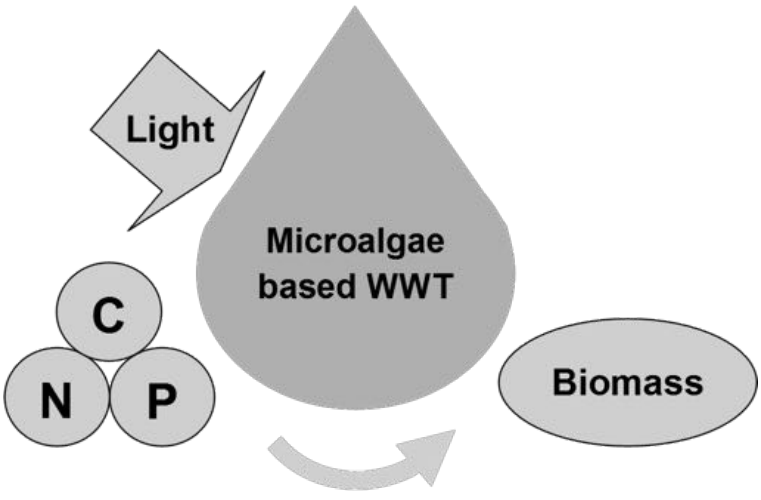

Evaluation of the simultaneous biogas upgrading and treatment of centrates in a HRAP through C, N and P mass balances

Cynthia Alcántara, Pedro A. García-Encina and Raúl Muñoz

ABSTRACT

The simultaneous capture of CO_2 from biogas and removal of carbon and nutrients from diluted centrates in a 180-L high rate algal pond (HRAP) interconnected to a 2.5 L absorption column were evaluated using a C, N and P mass balance approach. The experimental set-up was operated indoors at 75 $\mu E/m^2 \cdot s$ for 24 h/d at 20 days of hydraulic retention time for 2 months of steady state, and supported a C-CO_2 removal in the absorption column of 55 ± 6%. C fixation into biomass only accounted for 9 ± 2% of the total C input, which explains the low biomass productivity recorded in the HRAP. In this context, the low impinging light intensity along with the high turbulence in the culture broth entailed a C stripping as CO_2 of 49 ± 5% of the total carbon input. Nitrification was the main NH_4^+ removal mechanism and accounted for 47 ± 2% of the inlet N-NH_4^+, while N removal as biomass represented 14 ± 2% of the total nitrogen input. A luxury P uptake was recorded, which resulted in a P-PO_4^{-3} biomass content over structural requirements (2.5 ± 0.1%). P assimilation corresponded with a 77 ± 2% of the inlet dissolved P-PO_4^{-3} removed.

Key words | algal-bacterial consortium, biogas upgrading, bioremediation, luxury P uptake, mass balances, nitrification

Cynthia Alcántara
Pedro A. García-Encina
Raúl Muñoz (corresponding author)
Department of Chemical Engineering and Environmental Technology,
Valladolid University,
Dr. Mergelina, s/n, 47011,
Valladolid,
Spain
E-mail: *mutora@iq.uva.es*

INTRODUCTION

Microalgae are photoautotrophic micro-organisms highly efficient to fix CO_2 using solar energy, 1.8 kg of CO_2 being required per kg of microalgae produced (Chisti 2007; Lardon *et al.* 2009; Alcántara *et al.* 2013). Despite the inhibitory CO_2 concentration thresholds in microalgae are often low and strain specific, tolerances to CO_2 concentrations of up to 50% have been reported in *Scenedesmus Obliquus* strains (Lam *et al.* 2012; Arbib *et al.* 2014). Photoautotrophic microalgae growth can support both the mitigation of greenhouse emissions by capturing CO_2 from industrial gas emission and the removal of nutrients from wastewaters with low C/nutrients ratios such as anaerobic effluents (Arbib *et al.* 2012). In this context, microalgae-based wastewater treatment in high rate algal ponds (HRAPs) represents an opportunity to simultaneously remove the CO_2 present in biogas and the residual carbon and nutrients from digestates at low energy costs and environmental impacts (Park & Craggs 2010). Hence, the supply of biogas to HRAPs can provide the additional C source required to boost nutrient removal by assimilation and result in a significant production of biomass that could be further used as a substrate for the subsequent generation of biogas (De Godos *et al.* 2010; Alcántara *et al.* 2013). Likewise, microalgae-based CO_2 removal during biogas upgrading will result in lower transportation costs and a higher biogas energy content, as CO_2 accounts for 25 – 50% of the biogas on a volume basis (Sialve *et al.* 2009; Hernández *et al.* 2013). However, despite the above-mentioned advantages of photosynthetic biogas upgrading coupled with nutrient removal from diluted centrates, little information is available about the C, N and P removal mechanisms (biotic, abiotic and/or dissimilatory) of this process.

This work was devised to evaluate the mechanisms governing the simultaneous upgrading of biogas and diluted centrate treatment in a HRAP interconnected to an external CO_2 absorption column using a carbon, nitrogen and phosphorous mass balance approach. For this purpose, the C, N and P speciation in the influent and effluent streams in this two-stage experimental set-up, along with the removal efficiencies of organic and inorganic carbon, nitrogen and

doi: 10.2166/wst.2015.198

phosphorus, were assessed in order to elucidate the removal mechanisms in this combined wastewater treatment-CO_2 capture process.

MATERIALS AND METHODS

Experimental set-up

The indoors experimental set-up consisted of a 1.3 m^2 180-L HRAP (202 cm length × 63 cm width × 15 cm depth) interconnected to a 2.5 L external CO_2 bubble column (Ø = 4 cm; height = 195 cm) (Figure 1). The HRAP was continuously agitated using a 6-blade paddle wheel, which supported a liquid recirculation velocity of 0.2 m/s at the center of the pond channel. The HRAP was illuminated using a bench of 15 Gro-Lux fluorescent lamps (Sylvania, Germany) providing a cool white fluorescent light of 75 ± 5 μE/m^2·s of PAR at the culture surface for 24 h/d. The initial operational conditions of this experimentation corresponded to the last steady state of the study conducted by Bahr *et al.* (2014), which was maintained for 2 month under steady state to obtain enough experimental data to evaluate the C, N and P mass balances. At the starting point of the experiment, the microalgae/cyanobacteria population (from now on referred to as microalgae) was composed of (percentage of cells) *Phormidium* sp. (71%), *Oocystis* (20%) and *Microspora* sp. (9%). The composition of the bacterial population was not characterized by molecular tools but microscopic observations confirmed the presence of bacteria in the algal-bacterial consortium initially present in the HRAP. Centrate wastewater was obtained by centrifugation of the anaerobically digested mixed sludge of Valladolid WWTP (Spain), which was 8-fold diluted with tap water due to the potential inhibition of microalgae growth by their high NH_4^+ concentrations (González *et al.* 2008). Typically, the vertical light attenuation is associated with different waterborne materials (Xu *et al.* 2005). In this context, total suspended solids (TSS) concentration represents the most important factor controlling the light attenuation coefficient (Kd) (Gallegos 2001; Devlin *et al.* 2008). In our particular case, Kd associated with TSS in diluted centrates (0.17 m^{-1}) was significantly lower than those values associated to light-limiting conditions (above 5 m^{-1}) (Devlin *et al.* 2008). Therefore, a potential light limitation in the culture broth associated to turbidity in the 8-fold diluted centrate cultivation medium was ruled out. The HRAP was continuously fed (Watson Marlow 102 UR pump) with the diluted centrates in order to maintain a hydraulic retention time (HRT) of 20 days. The average TOC, IC, TN and P-PO_4^{-3} concentrations in the diluted centrates during the entire experiment were 11 ± 2 g/m^3, 95 ± 3 g/m^3, 92 ± 3 g/m^3 and 8.9 ± 0.4 g/m^3, respectively. Simulated biogas (Abello Linde, Spain) containing CO_2 (30%) and N_2 (70%) instead of CH_4 due to its potential explosion hazards was supplied to the bubble column at 22 mL/min through a ceramic sparger located at the bottom of the column (HRT_{column} = 1.9 h) co-currently with a recycling microalgal broth stream drawn at 20 mL/min (1 m/h) from the HRAP (Figure 1). The HRAP cultivation broth was daily supplemented with 50 cm^3 of NaOH (20 g/dm^3) to maintain the pH at 8.1 ± 0.1 in order

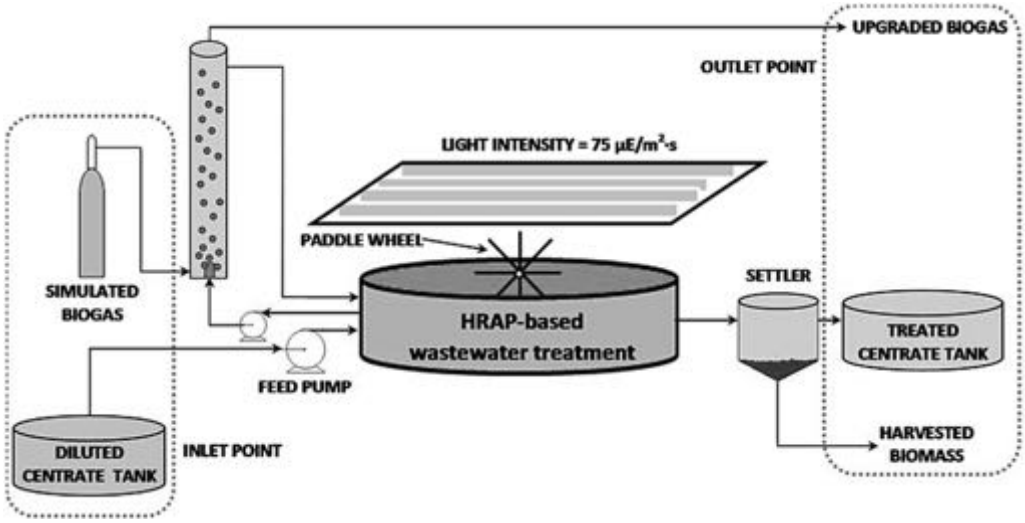

Figure 1 | Schematic of the experimental set-up devoted to the simultaneous biogas upgrading and diluted centrate treatment.

to promote bacterial nitrification and minimize N-losses by NH_3 stripping. The sedimentation of the HRAP cultivation broth was carried out in a 8 L settler located at the outlet of the HRAP (Figure 1) from which biomass harvesting was carried out once a week. The areal biomass productivity was determined according to Posadas *et al.* (2014).

Gas samples of 100 μL were periodically drawn at the inlet and outlet of the absorption bubble column to monitor the CO_2, N_2 and O_2 concentrations by GC-TCD. Liquid samples were also drawn twice a week from the diluted centrate (influent) and HRAP effluent to monitor the concentration of dissolved TOC, dissolved IC, dissolved N species (TN, N-NH_4^+, N-NO_2^-, N-NO_3^- and $N_{organic}$), dissolved P (P-PO_4^{-3}) and biomass concentration as TSS. The temperature, dissolved oxygen (DO) concentration and pH in the HRAP were also recorded. Prior to analysis (except for TSS determination), liquid samples were centrifuged for 10 min at 10,000 rpm and 23 °C (Sorvall, LEGEND RT + centrifuge, Thermo Scientific, USA), and filtered through 0.20 μm nylon filters. The C, N and P content of the algal-bacterial biomass formed was also experimentally determined.

Mass balance calculation

A mass balance calculation was conducted for C, N and P based on the average concentrations of all their chemical species at the inlet ('IN' = diluted centrate feed + inlet biogas) and outlet ('OUT' = treated effluent + settled algal-bacterial biomass waste + upgraded biogas) of the experimental system under steady state (Figure 1). The validity of the experimentation carried out was assessed by means of recovery factors defined as follows:

$$\text{C mass recovery}\,(\%) = \frac{[\text{C-}CO_2 + \text{TOC} + \text{IC} + C_{biomass}]_{OUT}}{[\text{C-}CO_2 + \text{TOC} + \text{IC} + C_{biomass}]_{IN}} \times 100 \quad (1)$$

$$\text{N mass recovery}\,(\%) = \frac{[\text{N-}NH_4^+ + \text{N-}NO_2^- + \text{N-}NO_3^- + N_{biomass} + N_{organic}]_{OUT}}{[\text{N-}NH_4^+ + \text{N-}NO_2^- + \text{N-}NO_3^- + N_{biomass} + N_{organic}]_{IN}} \times 100 \quad (2)$$

$$\text{P mass recovoery}\,(\%) = \frac{[\text{P-}PO_4^{-3} + P_{biomass}]_{OUT}}{[\text{P-}PO_4^{-3} + P_{biomass}]_{IN}} \times 100 \quad (3)$$

where C-CO_2 is the carbon input in the simulated biogas, TOC is the total dissolved organic carbon in the aqueous phase, IC is the dissolved inorganic carbon in the aqueous phase, $C_{biomass}$ is the particulate carbon in the form of microalgal-bacterial biomass, N-NH_4^+, N-NO_2^- and N-NO_3^- represent the dissolved ammonium, nitrite and nitrate, respectively, while $N_{biomass}$ and $N_{organic}$ account for the particulate organic nitrogen in the form of biomass and the dissolved organic nitrogen accumulated in the HRAP culture broth, respectively. P-PO_4^{-3} stands for the phosphorus in the aqueous phase and $P_{biomass}$ for the particulate phosphorus in the form of biomass. All parameters were estimated as the total mass of the target compound over the 2 months of experimentation.

Analytical procedures

The impinging irradiation at the surface of the HRAP was measured as PAR using a LI-250A light meter (LI-COR Biosciences, Germany). The pressure at the bottom and top of the bubble column was measured using a PN 5,007 pressure sensor (IFM, Germany). The gas concentrations of CO_2, O_2 and N_2 were determined using a CP-3800 gas chromatograph (Varian, USA) coupled with a thermal conductivity detector and equipped with a CP-Molsieve 5A (15 m × 0.53 mm × 15 μm) and a CP-Pora BOND Q (25 m × 0.53 mm × 15 μm) columns. The injector, detector and oven temperatures were maintained at 150 °C, 175 °C and 40 °C, respectively. Helium was used as the carrier gas at 13.7 cm^3/min. TOC, IC and TN concentrations were determined using a TOC-V CSH analyzer equipped with a TNM-1 module (Shimadzu, Japan). N-NH_4^+ concentration was measured using the Nessler analytical method in a U-2000 spectrophotometer (Hitachi, Japan) at 425 nm. N-NO_2^-, N-NO_2^- and P-PO_4^{-3} were analyzed by HPLC-IC according to Alcántara *et al.* (2013). The soluble P concentration was also determined according to Eaton *et al.* (2005) using a U-2000 spectrophotometer (Hitachi, Japan). A Crison micropH 2002 (Crison instruments, Spain) was used for pH determination. DO concentration and temperature were recorded using an OXI 330i oximeter (WTW, Germany). The determination of the TSS concentration of microalgal-bacterial biomass was performed according to Eaton *et al.* (2005). The analysis of $C_{biomass}$ and $N_{biomass}$ was conducted using a LECO CHNS-932, while P biomass was measured using a 725-ICP Optical Emission Spectrophotometer (Agilent, USA) at 213.62 nm. The identification, quantification and biometry measurements of microalgae were carried out by microscopic examination (OLYMPUS IX70, USA) of microalgal samples (fixed with lugol acid at 5% and stored at 4 °C prior to analysis)

according to Sournia (1978). The relative error associated to the counting procedure was ±10% in number of cells (Lund *et al.* 1958). The concentration of the $N_{organic}$ released into the liquid phase was determined as the difference between the TN concentration and the sum of $N\text{-}NH_4^+$, $N\text{-}NO_2^-$ and $N\text{-}NO_3^-$.

RESULTS AND DISCUSSION

Algal-bacterial symbiosis can support a cost-effective wastewater treatment in this combined process as a result of the in-situ photosynthetic oxygenation of the culture broth (capable of oxidizing both organic matter and $N\text{-}NH_4^+$) and the high nutrient assimilation potential mediated by the high microalgae productivities (Muñoz & Guieysse 2006). In this combined system, microalgae population use both centrate IC and the CO_2 contained in the biogas as a C source to assimilate N and P in the form of new biomass (biotic nutrient removal) (Posadas *et al.* 2015). Moreover, $N\text{-}NH_4^+$ can be transformed into $N\text{-}NO_3^-$ by nitrifying bacteria under aerobic conditions, which entails a reduction in the total Kjeldahl nitrogen concentration in the effluent (De Godos *et al.* 2010). NH_4^+ nitrification contributes also to IC biotic removal as nitrifying bacteria are autotrophic micro-organisms. In addition, the high pH induced by microalgal photosynthesis can also enhance both N and P abiotic removal by $N\text{-}NH_4^+$ stripping as NH_3 gas or $P\text{-}PO_4^{-3}$ precipitation in the form of $Ca_5(OH)(PO_4)_3$ (De Godos *et al.* 2009; Posadas *et al.* 2015).

The C, N and P mass balances in the system under steady-state conditions showed recovery factors of 99.8%, 101.7% and 99.0%, respectively, which validated both the experimental protocol followed and the analytical and instrumental methods used in this study. The results obtained were given as the average ± the error at 95% confidence interval ($n = 21$). The specific growth rate of the microalgal-bacterial community accounted for 0.05 d^{-1}, which resulted in an average biomass concentration in the cultivation broth of 1.4 ± 0.0 g TSS/L during the 66 days of steady-state operation. The TSS removal efficiency in the settler of 98 ± 35% entailed effluent suspended solid concentrations of 22 ± 9 mg TSS/L, which were below the maximum permissible TSS discharge limit in EU legislation (35 mg TSS/L) (European Directive 91/271/CEE). The average biomass productivity in the HRAP was 2.2 ± 0.0 g/m^2·d, which agrees with the 2.1 ± 0.6 g TSS/m^2·d obtained by Posadas *et al.* (2014) in a 180-L HRAP treating domestic wastewater under similar indoor cultivation conditions. This biomass productivity was however significantly lower than the 10–30 g TSS/m^2·d range typically observed in outdoors full-scale HRAPs treating domestic wastewater and could be attributed to the low impinging irradiation used in this indoor study (Oswald 1988; Tredici 2004; Park & Craggs 2010). The moderate culture broth temperature (25 ± 1°C), together with the high turbulence in the pilot HRAP, mediated evaporation losses of 4.5 ± 0.4 L/m^2·d. This high turbulence associated to pilot-scale HRAPs is often promoted by the use of a high power engine and the absence of guide vanes devoted to soften the change in direction of the cultivation broth (Mendoza *et al.* 2013; Posadas *et al.* 2014).

C speciation

The structural carbon content (on a dry weight basis) of the harvested algal-bacterial biomass remained constant and accounted for 41 ± 0%, which was slightly lower than the 43–56% carbon content typically reported for microalgal biomass (Sydney *et al.* 2010; Arbib *et al.* 2014). This carbon was fixed by the algal-bacterial biomass under fully photoautotrophic conditions (as TOC concentration in the influent wastewater only represented 1 ± 0% (11 ± 2 g TOC/m^3) of the total carbon input) and corresponded with 9 ± 2% of the total C input (Figure 2). This assimilation corresponded to a biotic C removal of 0.9 ± 0.4 g $C_{biomass}$/m^2·d, which entailed a CO_2 sequestration of 1.6 g CO_2/g of biomass formed. This poor C fixation was likely due to the low impinging irradiation (75 ± 5 μE/m^2·s) at the cultivation broth surface, which limited microalgae growth throughout the entire process.

Approximately 89 ± 1% of the total IC input (gas $C\text{-}CO_2$ + dissolved IC) was provided by bubbling through the absorption column a simulated biogas containing a

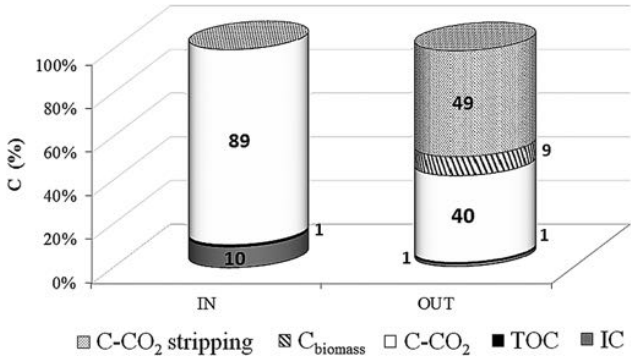

Figure 2 | Carbon distribution in the influent (IN) and effluent (OUT) streams in the experimental set-up.

CO_2 concentration of 171 ± 1 g C-CO_2/m^3. The remaining 10 ± 1% was supplied as dissolved IC in the diluted centrates (95 ± 3 g IC/m^3 of wastewater) (Figure 2). The low liquid recirculation rate from the HRAP through the absorption column resulted in a low C-CO_2 absorption from the biogas into the liquid phase, which supported a C-CO_2 biogas removal of 55 ± 6%. However, additional experiments increasing this recirculation rate from 1 to 10 m/h, which entailed an increase in the liquid/gas (L/G) recirculation ratio from 0.9 to 9.4, boosted CO_2 removal from 55 ± 6 to 100 ±0%. C-CO_2 stripping was the main mechanism of carbon removal in the system, representing 49 ± 5% of the C output (Figure 2) and corresponding to an abiotic C elimination of 4.7 ± 0.8 g/m^2·d. In this context, the estimated average dissolved C-CO_2 concentration at pH = 8.1 ± 0.1 in the cultivation broth during the 66 operational days was 2.4 ± 0.3 g/m^3, which was significantly higher than the aqueous CO_2 concentration in equilibrium with the atmospheric CO_2 (0.4 g/m^3) and supported the occurrence of an abiotic C removal. In this regard, De Godos *et al.* (2009) reported a 59% loss of inorganic carbon by stripping in a 464-L HRAP treating 10-fold diluted swine manure. Similarly, up to 50% of the influent carbon was removed by stripping in a 180-L HRAP treating fish farm wastewater (Posadas *et al.* 2014). In our particular study, the high turbulence associated to pilot-scale HRAPs and the low light intensity at the culture broth surface (which hindered CO_2 assimilation into biomass) can explain the high abiotic carbon removal recorded. The C-CO_2 that was not lost by stripping or assimilated into biomass left the system in the outlet biogas stream (40 ± 5%) (Figure 2). In a hypothetical scenario with biogas composed by CH_4 instead N_2 (initial composition of 30% (v/v) of CO_2 and 70% (v/v) of CH_4) the 55 ± 6% of C-CO_2 removal in the column would result in an enrichment in the biogas CH_4 content up to 87% (v/v). This increase in bio-methane content would correspond with a gain of 19% in the biogas energy content (from 25,067 to 31,040 KJ/Nm^3, assuming a heating value for CH_4 of 50 kJ/g (Alcántara *et al.* 2013)). In this context, biomethane regulations of some European countries require a CH_4 content over 95% and O_2 below 0.5% due to its associated explosion hazards (Mandeno *et al.* 2005; Huguen & Le Saux 2010). However, preliminary assays in our lab at a liquid to biogas ratio of ≈1 have shown CH_4 removals <1% by absorption but contamination of the upgraded biogas with O_2 and N_2 of up to 3%, which suggests that despite photosynthetic CO_2 removal during biogas upgrading can significantly reduce the transportation costs and burning efficiency per cubic meter of biogas, O_2 and N_2 content in the biogas upgraded currently entails a technical limitation to the full-scale implementation of this biotechnology.

N and P speciation

The biomass harvested in the settler presented a structural nitrogen content of 6.6 ± 0.1%, which remained constant during the entire experiment as previously observed with the structural carbon and entailed a biotic N removal of 0.15 ± 0.1 g N/m^2·d. This N content was in accordance to the typical content reported for microalgae, which ranges from 6.6 to 9.3% (Oswald 1988; Grobelaar 2004). Nitrification was the main NH_4^+ removal mechanism and was supported by the high DO concentration (7.0 ± 0.1 g/m^3) and constant IC supply to the cultivation over the 2 months experimentation. In this context, the inlet N-NH_4^+ (which represented 100 ± 0% of the N input, Figure 3(a)) was totally transformed (99 ± 19%) into N-NO_3^-, $N_{biomass}$ and $N_{organic}$ at average shares of 47 ± 2%, 14 ± 2% and 38 ± 2%, respectively, (Figure 3(a)). In our particular study, the limited microalgal photosynthetic nitrogen fixation likely boosted the high nitrifying activity herein observed, which itself prevented ammonia stripping. The 38 ± 2% of $N_{organic}$ present in the N output (Figure 3(a)) was the result of a $N_{organic}$ accumulation in the culture broth

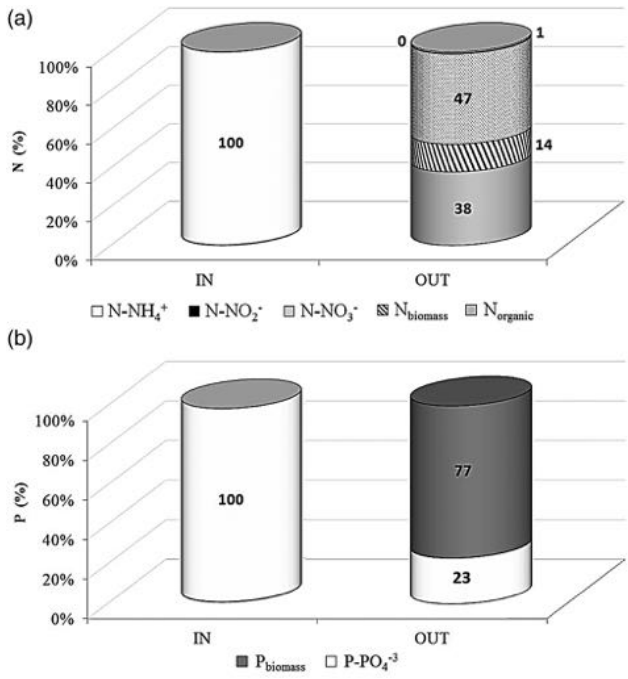

Figure 3 | Nitrogen and phosphorus distribution in the influent (IN) and effluent (OUT) streams in the experimental set-up.

during the 66 days of steady-state operation from 13 to 40 g/m^3 likely associated to microalgal-bacterial metabolite excretion during their photoautotrophic growth and cell lysis.

The phosphorus content in the harvested biomass accounted for 2.5 ± 0.1%, which agrees with P range (0.2–3.9) reported by Powell *et al.* (2009). The large variability in P content often reported in microalgae is due to the potential occurrence of a luxury phosphorus uptake in some microalgae species, where phosphorus is accumulated over structural requirements in order to store energy in the form of polyphosphate (Powell *et al.* 2008, 2009). Thus, the high $P_{biomass}$ herein recorded (2.5 ± 0.1%) was likely the result of the combination of a luxury uptake and a growth-associated P uptake (Powell *et al.* 2008, 2009) since a typical P content of 1% is observed when the uptake of P-PO_4^{-3} occurs preferentially for microalgal biomass formation (Alcántara *et al.* 2013). A possible explanation for this is that the high growth rate induced by the exposure to a high light intensity results in this form of polyphosphate being utilized by the cells for synthesis of cellular constituents at a rate that exceeds replenishment (Powell *et al.* 2008). In this regard, Hessen *et al.* (2002) reported a 3-fold increase in the biomass polyphosphate content when decreasing the light intensity from 70 to 10 μE/m^2·s, while a 8-fold increase was observed by Powell *et al.* (2008) when irradiation was decreased from 150 to 60 μE/m^2·s. Therefore, the low light intensity in our particular case likely restricted microalgal P assimilation to form new biomass and therefore promote P-PO_4^{-3} accumulation over structural requirements. Despite the limited microalgae growth recorded, the removal of dissolved P-PO_4^{-3} by assimilation accounted for 77 ± 2% (0.06 ± 0.0 g P/m^2·d), while the P-PO_4^{-3} that was not incorporated into biomass left the system in the effluent (23 ± 2%) (Figure 3(b)). In addition, algal populations gross changes seem to suggest that *Microspora* sp. could have replaced *Phormidium* sp. along the process but enough experimental evidence is lacking to fully support this observed change.

Energy and environmental considerations

Despite the low biomass productivity obtained in our particular study as a result of the technical difficulties to supply high irradiances in indoors pilot-scale systems, the upgrading of biogas mediated by CO_2 capture combined with wastewater treatment harbors a valuable potential from an environmental and energy viewpoint. Thus, a conservative biomass productivity of 20 g/m^2·d in full-scale HRAPs would result in a potential bio-methane production of 4.2 g CH_4/m^2·d (assuming a 50.6% of structural C and a CH_4 yield of 0.21 g CH_4/g microalgae (Alcántara *et al.* 2013)). The combustion of this bio-methane would entail an energy production of 88 KJ/m^2_{HRAP}·d (≈1 W/m^2) (assuming a CH_4 to electricity conversion efficiency of 41.7% (Lucas 2000)). In this context, Chisti (2013) reported a value of 34 KJ/m^2_{HRAP} ·d (0.4 W/m^2) as the minimum power requirement for mixing a 360-m^3 outdoors HRAP (300 m of total loop length × 4 m wide × 0.3 m deep) at a paddle wheel efficiency of 0.17 using a Manning coefficient of 0.012 (polymer-membrane lined smooth raceway channel) with 0.3 m/s of liquid velocity. The energy for mixing the cultivation broth represents the main power consumption during the operation of this combined HRAP-absorption column system, where the energy for external liquid recirculation between both units and for biogas sparging in the absorption column are negligible compared to the energy consumption associated to the mixing the culture broth. This energy represents 40% of the energy obtained from CH_4 combustion, which suggests that the photosynthetic CO_2 removal from biogas (which also reduces the transportation costs of biogas) and further combustion of the bio-methane obtained through anaerobic digestion of the biomass generated in the upgrading process would significantly improve the global energy balance of outdoors HRAPs during this combined wastewater treatment-CO_2 capture process.

Moreover, based on the nitrogen mass balance, this system released to aquatic ecosystems (purge+ clarified) 0.8 g N/g N_{input}, which compared with the typical gas N-N_2O emission factor in HRAPs of 0.00005 g N-N_2O/g N_{input} (Alcántara *et al.* 2015), clearly represented the main contribution regarding total nitrogen emissions from this system. Considering a N_2O emission factor of 0.00005 g N-N_2O/g N_{input} and a global warming potential of 298 g CO_2/g N_2O, this combined system would produce 7.2·10^{-3} g N_2O/m^3 of wastewater treated (WW treated), equivalent to 2.2 g CO_2/m^3 WW treated. On the other hand, the amount of CO_2 fixed by photosynthetic microalgae growth accounts for 521 g CO_2/m^3 WW treated, which confirmed the environmental sustainability of this process in terms of greenhouse gas emission mitigation. Despite a direct comparison with N_2O emissions from activated sludge processes is difficult given the large variation of the rates reported (Ahn *et al.* 2010), wastewater treatment plants with primary and activated sludge treatment present average N_2O emissions of 33·10^{-3} g N_2O/m^3 WW treated (Czepiel *et al.* 1995). In addition, the carbon footprint associated to N_2O emissions in this technology (2.2 g CO_2/m^3) compared

favorably against the indirect carbon footprint from electricity use for aeration and mixing of activated sludge tanks (119–378 g CO_2/m^3) and for mixing HRAPs (3–14 g CO_2/m^3 WW treated). This preliminary analysis suggests that N_2O generation by the microalgal-bacterial biomass present in the HRAP should not challenge the environmental performance of wastewater treatment in HRAPs in terms of global warming mitigation.

CONCLUSIONS

The C, N and P mass balances used to evaluate the removal mechanisms in this combined biogas upgrading-wastewater treatment process showed recovery factors close to 100%, which validated both analytical and instrumental methods used in this study. $C_{biomass}$ only accounted for 9% of the C input to the system, which explains the low biomass productivity recorded in the HRAP. The low light intensity used in this experimentation together with the high turbulence associated to pilot-scale HRAPs supported C-CO_2 stripping as the main mechanism of C removal in the system (≈ 49%). The C-CO_2 removal from biogas in the column (≈ 55%) entailed an increase of 19% in the biogas energy content, which highlighted the potential of this combined wastewater treatment-biogas upgrading process. Nitrification was the main NH_4^+ removal mechanism with a 47 ± 2% of the N-NH_4^+ input transformed into N-NO_3^-, while only 14 ± 2% of the nitrogen input was converted to $N_{biomass}$. A luxury uptake of P was hypothesized based on the high P biomass content (2.5 ± 0.1%) and the fact that light limitation often promotes polyphosphate accumulation. P-PO_4^{-3} assimilation into biomass accounted for 77 ± 2% of the phosphate removed in the process. Finally, a successful suspended solid removal was achieved in the settler (≈ 98%), which entailed effluent suspended solid concentrations below the maximum permissible EU discharge limit.

ACKNOWLEDGEMENTS

This research was supported by the regional government of Castilla y León and the European Social Fund (Contract N° E-47-2011-0053564 and Project Ref. GR76). The financial support of the Spanish Ministry of Economy and Competitiveness, and the National Institute for Research and Technology in Agriculture and Food is also gratefully acknowledged (Project Ref. RTA2013-00056-C03-02).

REFERENCES

Ahn, J. H., Kim, S., Park, H., Rham, B., Pagilla, K. & Chandran, K. 2010 N_2o emissions from activated sludge processes, 2008–2009: monitoring results of a national monitoring survey in the United States. *Environ. Sci. Technol.* **44**, 4505–4511.

Alcántara, C., García-Encina, P. A. & Muñoz, R. 2013 Evaluation of mass and energy balances in the integrated microalgae growth-anaerobic digestion process. *Chem. Eng. J.* **221**, 238–246.

Alcántara, C., Muñoz, R., Norvill, Z., Plouviez, M. & Guieysse, B. 2015 Nitrous oxide emissions from high rate algal ponds treating domestic wastewater. *Bioresour. Technol.* **177**, 110–117.

Arbib, Z., Ruiz, J., Álvarez, P., Garrido, C., Barragan, J. & Perales, J. A. 2012 *Chlorella stigmatophora* for urban wastewater nutrient removal and CO_2 abatement. *Int. J. Phytoremediation.* **14** (7), 714–725.

Arbib, Z., Ruiz, J., Álvarez, P., Garrido, C. & Perales, J. A. 2014 Capability of different microalgae species for phytoremediation processes: wastewater tertiary treatment, CO_2 bio-fixation and low cost biofuels production. *Water Res.* **49**, 465–474.

Bahr, M., Díaz, I., Domínguez, A., Sánchez-González, A. & Muñoz, R. 2014 Microalgal-biotechnology as a platform for an integral biogas upgrading and nutrient removal from anaerobic effluents. *Environ. Sci. Technol.* **48** (1), 573–581.

Czepiel, P., Crill, P. & Harris, R. 1995 Nitrous oxide emission from municipal wastewater treatment. *Environ. Sci. Technol.* **29**, 2352–2356.

Chisti, Y. 2007 Biodiesel from microalgae. *Biotechnol. Adv.* **25** (3), 294–306.

Chisti, Y. 2013 Microalgal Biotechnology: Potential and Production. In: *De Gruyter bookshelf* (C. Posten & C. Walter, eds.). Berlin, Boston, pp. 97–115. ISBN: 9783110225013. Q1

De Godos, I., Blanco, S., García-Encina, P. A., Becares, E. & Muñoz, R. 2009 Long-term operation of high rate algal ponds for the bioremediation of piggery wastewaters at high loading rates. *Bioresour. Technol.* **100** (19), 4332–4339.

De Godos, I., Blanco, S., García-Encina, P. A., Becares, E. & Muñoz, R. 2010 Influence of flue gas sparging on the performance of high rate algae ponds treating agro-industrial wastewaters. *J. Hazard. Mater.* **179** (1–3), 1049–1054.

Devlin, M. J., Barry, J., Mills, D. K., Gowen, R. J., Foden, J., Sivyer, D. & Tett, P. 2008 Relationships between suspended particulate material, light attenuation and Secchi depth in UK marine waters. *Estuar. Coast. Shelf S.* **79**, 429–439.

Eaton, A. D., Clesceri, L. S. & Greenberg, A. E. 2005 *Standard Methods for the Examination of Water and Wastewater.* 2st edn. American Public Health Association/American Water Works Association/Water Environment Federation, Washington DC, USA.

European Directive 91/271/CEE on discharge of domestic wastewaters.

Gallegos, C. 2001 Calculating optical water quality targets to restore and protect submersed aquatic vegetation: overcoming problems in portioning the diffuse attenuation

co-efficient for photosynthetically active radiation. *Estuaries* **24** (3), 381–397.

González, C., Marciniak, J., Villaverde, S., García-Encina, P. A. & Muñoz, R. 2008 Microalgae-based processes for the biodegradation of pretreated piggery wastewaters. *Appl. Microbiol. Biotechnol.* **80**, 891–898.

Grobelaar, J. U. 2004 Algal nutrition. In: *Handbook of Microalgal Culture: Biotechnology of Applied Phycology* (A. Richmond, ed.). Blackwell, Oxford, pp. 97–115. ISBN: 9780632059539.

Hernández, D., Riaño, B., Coca, M. & García-González, M. C. 2013 Treatment of agroindustrial wastewater using microalgae–bacteria consortium combined with anaerobic digestion of the produced biomass. *Bioresour. Technol.* **135**, 598–603.

Hessen, D. O., Faerovig, P. J. & Andersen, T. 2002 Light, nutrients, & P:C ratios in algae: Grazer performance related to food quality and quantity. *Ecology* **83** (7), 1886–1898.

Huguen, P. & Le Saux, G. 2010 Perspectives for a European standard on biomethane: a biogasmax proposal. European Biogasmax project. http://www.biogasmax.eu/media/d3_8_new_lmcu_bgx _eu_standard_14dec10_vf__077238500_0948_26012011.pdf. (accessed 10 October 2014).

Lam, M. K., Lee, K. T. & Mohamed, A. R. 2012 Current status and challenges on microalgae-based carbon capture. *Int. J. Greenh. Gas Con.* **10**, 456–469.

Lardon, L., Hélias, A., Sialve, B., Steyer, J. P. & Bernard, O. 2009 Life-cycle assessment of biodiesel production from microalgae. *Environ. Sci. Technol.* **43** (17), 6475–6481.

Lucas, K. 2000 On the thermodynamics of cogeneration. *Int. J. Therm. Sci.* **39** (9–11), 1039–1046.

Lund, J. W. G., Kipling, C. & Le Cren, E. D. 1958 The inverted microscope method of estimating algal numbers and the statistical basis of estimations by counting. *Hydrobiologia* **11** (2), 143–170.

Mandeno, G., Craggs, R., Tanner, C., Sukias, J. & Webster-Brown, J. 2005 Potential biogas scrubbing using a high rate pond. *Water Sci. Technol.* **51**, 253–256.

Mendoza, J. L., Granados, M. R., De Godos, I., Acién, F. G., Molina, E., Banks, C. & Heaven, S. 2013 Fluid-dynamic characterization of real scale raceway reactors for microalgae production. *Biomass Bioenerg.* **54**, 267–275.

Muñoz, R. & Guieysse, B. 2006 Algal-bacterial processes for the treatment of hazardous contaminants: a review. *Water Res.* **40**, 2799–2815.

Oswald, W. J. 1988 Large-Scale Algal Culture Systems (engineering aspects). In: *Micro-algal Biotechnology* (L. J. Borowitzka, ed.). Cambridge University Press, Cambridge, pp. 357–394.

Park, J. B. K. & Craggs, R. J. 2010 Wastewater treatment and algal production in high rate algal ponds with carbon dioxide addition. *Water Sci. Technol.* **61** (3), 633–639.

Posadas, E., Muñoz, A., García-González, M. C., Muñoz, R. & García-Encina, P. A. 2014 A case study of a pilot high rate algal pond for the treatment of fish farm and domestic wastewaters. *J. Chem. Technol. Biot.* DOI:10.1002/jctb.4417

Posadas, E., Morales, M. M., Gomez, C., Acien-Fernandez, G. & Muñoz, R. 2015 Influence of pH and CO_2 source on the performance of microalgae-based secondary domestic wastewater treatment in outdoors pilot raceways. *Chem. Eng. J.* **265**, 239–248.

Powell, N., Shilton, A. N., Pratt, S. & Chisti, Y. 2008 Factors influencing luxury uptake of phosphorus by microalgae in waste stabilization ponds. *Environ. Sci. Technol.* **42** (16), 5958–5962.

Powell, N., Shilton, A., Chisti, Y. & Pratt, S. 2009 Towards a luxury uptake process via microalgae-defining the polyphosphate dynamics. *Water Res.* **43** (17), 4207–4213.

Sialve, B., Bernet, N. & Bernard, O. 2009 Anaerobic digestion of microalgae as a necessary step to make microalgal biodiesel sustainable. Biotechnol. Adv. **27** (4), 409–416.

Sournia, A. 1978 Phytoplanton Manual. Museum National d' Historie Naturelle, París. United Nations Educational. Scientific and Cultural Organization (Unesco).

Sydney, E. B., Sturm, W., de Carvalho, J. C., Thomaz-Soccol, V., Larroche, C., Pandey, A. & Soccol, C. R. 2010 Potential carbon dioxide fixation by industrially important microalgae. *Bioresour. Technol.* **101** (15), 5892–5896.

Tredici, M. R. 2004 Mass production of microalgae: photobioreactors. In: *Handbook of Microalgal Culture: Biotechnology of Applied Phycology* (A. Richmond, ed.). Blackwell, Oxford, pp. 178–214. ISBN: 9780632059539.

Xu, J., Hood, R. R. & Chao, S. Y. 2005 A simple empirical optical model for simulating light attenuation variability in a partially mixed estuary. *Estuaries* **28** (4), 572–580.

First received 6 September 2014; accepted in revised form 15 April 2015. Available online 30 April 2015

Evaluation of mass and energy balances in the integrated microalgae growth-anaerobic digestion process

Alcántara, C., García-Encina, P., Muñoz, R., 2013. CEJ. 221, 238–246.

Chapter 6

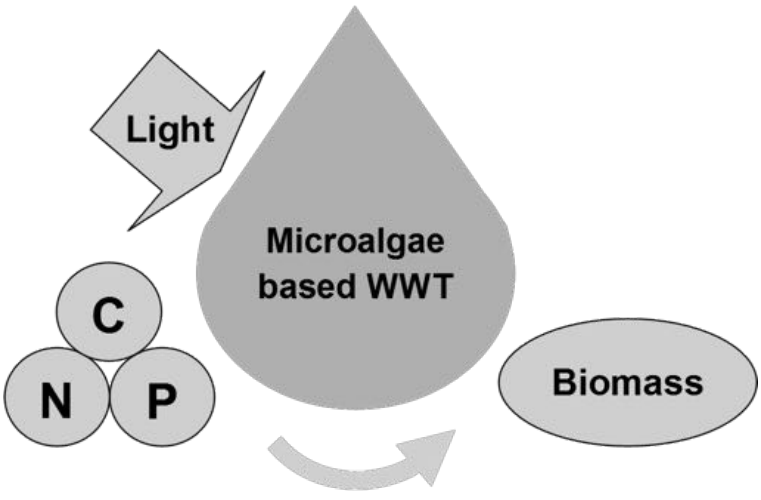

Chemical Engineering Journal 221 (2013) 238–246

Contents lists available at SciVerse ScienceDirect

Chemical Engineering Journal

journal homepage: www.elsevier.com/locate/cej

Evaluation of mass and energy balances in the integrated microalgae growth-anaerobic digestion process

Cynthia Alcántara, Pedro A. García-Encina, Raúl Muñoz *

Department of Chemical Engineering and Environmental Technology, Valladolid University, Paseo del Prado de la Magdalena, s/n, Valladolid, Spain

HIGHLIGHTS

- The C source did not significantly modify the *Chlorella sorokiniana* composition.
- During anaerobic digestion ≈50% of the initial C in the biomass was hydrolyzed.
- CO_2 and CH_4 accounted for 14% and 35% of the initial microalgae C, respectively.
- The recoveries of $N\text{-}NH_4^+$ and $P\text{-}PO_4^{-3}$ from anaerobic digestion were 65% and 83%.
- The total energy recovered as CH_4 in the growth-digestion process was ≈3.6%.

GRAPHICAL ABSTRACT

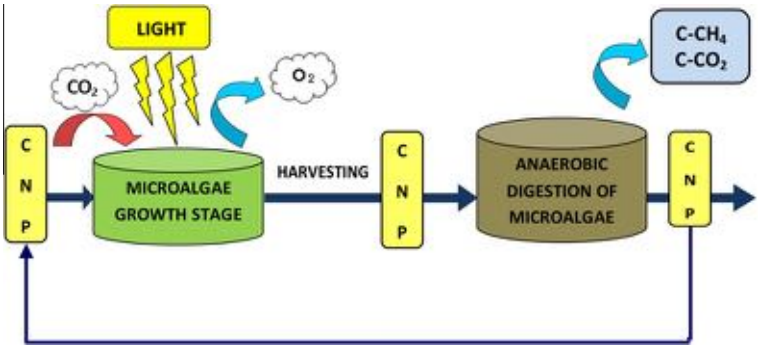

ARTICLE INFO

Article history:
Received 13 November 2012
Received in revised form 28 January 2013
Accepted 30 January 2013
Available online 9 February 2013

Keywords:
Biomethanization
Mass and energy balances
Microalgae anaerobic digestion
Nutrient recovery
Photosynthetic efficiency

ABSTRACT

The production of biofuels based on microalgae as feedstock is associated with a high demand of nutrients, mostly nitrogen and phosphorus. The integration of microalgae growth with anaerobic digestion can significantly improve the economic and energy balance of such a promising platform technology. However, the lack of information about the fundamental mass and energy balances of this integrated process restricts its full scale implementation. This study quantified both the mass (carbon, nitrogen and phosphorus) and energy balances in the integrated process of *Chlorella sorokiniana* cultivation (under photoautotrophic and mixotrophic conditions) coupled with anaerobic digestion in batch mode in order to properly design the microalgae growth-anaerobic digestion process and minimize the overall microalgae cultivation costs. Under fully photoautotrophic growth, the productivity during the microalgae exponential growth phase was 147 g/m^3 d, with an overall photosynthetic efficiency of 7.4%. The productivity of the mixotrophically-grown microalgae was 165 g/m^3 d. However, the photosynthetic activity of *C. sorokiniana* decreased at increasing glucose concentrations in the tested range (180–440 g/m^3). During the anaerobic digestion of photoautotrophically-grown microalgae 55 ± 1% of the initial carbon present in the biomass was hydrolyzed (15 ± 1% to $C\text{-}CO_2$ and 33 ± 1% to $C\text{-}CH_4$). The potential recovery of the N and P present in the biomass accounted for 59 ± 2% as $N\text{-}NH_4^+$ and 89 ± 2% as $P\text{-}PO_4^{-3}$, respectively. During the anaerobic digestion of mixotrophically-grown microalgae, 46 ± 1% of the initial carbon as biomass was hydrolyzed (14 ± 1% to $C\text{-}CO_2$ and 36 ± 1% to $C\text{-}CH_4$) with a nutrient recovery of 70 ± 3% as $N\text{-}NH_4^+$ and 77 ± 2% as $P\text{-}PO_4^{-3}$. The energy recovery from the chemical energy fixed as biomass under photoautotrophic and mixotrophic conditions was 48% and 61%, respectively, and decreased to ≈3.5% when referred to the total energy available during the growth stage.

* Corresponding author. Tel.: +34 983186424.
E-mail address: mutora@iq.uva.es (R. Muñoz).

1385-8947/$ - see front matter © 2013 Elsevier B.V. All rights reserved.
http://dx.doi.org/10.1016/j.cej.2013.01.100

Fig. 1. Experimental set-up of microalgae cultivation under autotrophic and mixotrophic conditions.

1. Introduction

The current scenario of exhaustion of fossil fuel resources, increasing oil prices and global warming as a result of the accumulation of greenhouse gases in the atmosphere are strongly motivating research on biofuel production from renewable biomass [1,2]. Nowadays, conventional biodiesel is mainly produced from plant oils (palm, canola and soybean), and despite its lower CO_2 footprint compared to fossil fuels the production of biodiesel from crops entails severe negative environmental impacts [3]. Hence, land overexploitation due the uncontrolled use of pesticides and fertilizers, and competition for cropland (which might result in a global food crisis if expected to satisfy the current world's fuel demand) rank among the main drawbacks of conventional biodiesel [4].

In this context, microalgae have emerged as a promising feedstock for biofuel production based on their high photosynthetic yields, year-round production and ability to grow in both marine, fresh and wastewaters. Besides the above mentioned advantages, microalgae have the ability to mitigate greenhouse emissions by photosynthetically fixing the CO_2 released in industrial processes and do not compete with cropland [5,6]. Despite most research carried out in the past 5 years has mainly focused on microalgal biodiesel, the high cost (4–20 €/kg) and technical limitations of axenic microalgae biomass cultivation nowadays have limited its industrial application [7–11].

Anaerobic digestion appears as a promising alternative for biofuel production based on the possibility of using residual algal biomass as a substrate for biomethane production and its potential for recovering an important part of the nutrients (N and P) provided in the growth stage, which can offset a significant fraction of the process operating costs [12]. In this regard, recent sustainability studies have shown that the indirect energy input associated to nutrients supply constitutes a major energy cost and environmental burden during microalgae cultivation [13–15]. However, despite the potential of microalgae anaerobic digestion, there are still significant technical–economic limitations in the cultivation and biomethanization of microalgae that restrict its full-scale implementation [16]. Of them, the lack of empirical studies evaluating the fundamental mass and energy balances of the integrated microalgae growth-anaerobic digestion process [17,18]. This information is crucial to quantify the potential for nutrient and energy recovery in the overall biofuel production process [19,20].

The main objective of this work was the quantification of the C, N, P and energy balances in the integrated process of microalgae growth (under autotrophic and mixotrophic conditions) coupled with anaerobic digestion. On the one hand, the photosynthetic efficiency, nutrient and carbon requirements, and biomass productivities of *Chlorella sorokiniana* were determined under photoautotrophic and mixotrophic conditions. On the other hand, the biomethane production yield and the potential for nutrient and energy recovery during the anaerobic digestion of the microalgae produced were also quantified.

2. Materials and methods

2.1. Microorganisms and inoculum growth conditions

The microalgae *C. sorokiniana 211/8k* was obtained from the Culture Collection of Algae and Protozoa of the SAMS Research Services (Argyl, Scotland) and was cultivated in SK MSM (Sorokin–Krauss mineral salt medium). This medium was composed of (per cubic decimeter of distilled water): 1.25 g KNO_3, 0.625 g $MgSO_4{\cdot}7H_2O$, 0.1105 g $CaCl_2{\cdot}2H_2O$, 0.1142 g H_3BO_3, 0.0498 g $FeSO_4{\cdot}7H_2O$, 0.0882 g $ZnSO_4{\cdot}7H_2O$, 0.0144 g $MnCl_2{\cdot}4H_2O$, 0.0071 g MoO_3, 0.0157 g $CuSO_4{\cdot}5H_2O$, 0.0049 g $Co(NO_3)_2{\cdot}6H_2O$, 0.5 g EDTA, 0.6247 g KH_2PO_4, 1.3251 g K_2HPO_4. pH was adjusted at 6.8 with KOH and the medium was autoclaved before use ($MgSO_4{\cdot}7H_2O$ was autoclaved separately and added to complete the culture medium afterwards to avoid salt precipitation). Prior to inoculation, the MSM was enriched with a sterile solution of glucose, peptone and yeast extract to give 3.125, 0.0625 and 0.0625 g/dm^3, respectively. The inoculum was incubated at 30 °C under continuous magnetic agitation at 300 rpm and continuously illuminated for 4 days. The alga was subcultivated every 4 weeks on agar plates (enriched MSM plus 1% w/v agar) at room temperature (23 °C) under light for 10 days and stored at 4 °C afterwards.

2.2. Microalgae growth under photoautotrophic and mixotrophic conditions

The cultivations of microalgae under photoautotrophic and mixotrophic conditions were carried out separately but in the same experimental set-up (see Fig. 1). Once the first cultivation test was finished all the glass bottles were rigorously cleaned and sterilize to start the second cultivation test.

2.2.1. Test 1: Microalgae grown photoautotrophically

Photoautotrophically-grown microalgae were cultivated for 9.5 days in ten 1.25 dm^3 sterile glass bottles containing 0.5 dm^3 of a sterile minimum mineral salt medium (MSM) composed of (per cubic meter of distilled water): 6805 g $NaHCO_3$, 2015 g Na_2CO_3, 78.6 g K_2HPO_4, 355.7 g NH_4Cl, 500 g K_2SO_4, 500 g NaCl, 100 g $MgSO_4{\cdot}7H_2O$, 20 g $CaCl_2{\cdot}2H_2O$, 6.8 g $FeSO_4{\cdot}7H_2O$, 42 g EDTA (Ethylenediaminetetraacetic acid), 0.00025 g $ZnSO_4{\cdot}7H_2O$, 0.0005 g $MnSO_4{\cdot}H_2O$, 0.0025 g H_3BO_3, 0.00025 g $Co(NO_3)_2{\cdot}6H_2O$, 0.00025 g $Na_2MoO_4{\cdot}2H_2O$, 1.25×10^{-6} g $CuSO_4{\cdot}5H_2O$. The concentrations of carbonate and bicarbonate in the MSM corresponded with an initial equilibrium concentration (at pH of 7.6) of CO_2 at the flask's head-space of 18 ± 0.7% (82.7 ± 3.4 g/m^3) (Table 1), which represents a typical concentration of combustion process off-gases [21–23]. Prior to sterilization, the bottles were flushed with Helium in order to establish an O_2 free atmosphere, closed with butyl septa and sealed with plastic caps. Following sterilization, the pH of the cultivation medium was decreased to 7.6 by injecting 1.6 ml of HCl (37%) and the systems were allowed to equilibrate under magnetic agitation for 2 h at 25 °C prior to inoculation.

2.2.2. Test 2: Microalgae grown mixotrophically

Mixotrophically-grown microalgae were cultivated for 11.5 days in twelve 1.25 dm^3 glass bottles containing 0.5 dm^3 of

Table 1
C, N and P mass balances during microalgae growth under autotrophic (AG) and mixotrophic (MG) conditions.

Mass balances in the cultivation stage								
Initial				Final				
Carbon mass balance								
C-CO_2 (g/m^3)	IC (g/m^3)	TOC (g/m^3)	$C_{biomass}$ (g/m^3)	C-CO_2 (g/m^3)	IC (g/m^3)	TOC (g/m^3)	$C_{biomass}$ (g/m^3)	Recovery (%)
AG								
82.7 ± 3.4	1020.9 ± 12.8	17.3 ± 0.1	5.3 ± 0.0	3.6 ± 0.2	931.7 ± 8.3	51.6 ± 2.7	215.8 ± 5.8	103.4 ± 0.5
MG								
8.9 ± 0.5	130.8 ± 1.2	220.1 ± 3.3	4.0 ± 0.0	0.1 ± 0.0	53.8 ± 5.1	146.4 ± 3.9	167.0 ± 7.0	100.1 ± 1.9
Nitrogen mass balance								
N-NH_4^+ (g/m^3)	N-NO_2^- (g/m^3)	N-NO_3^- (g/m^3)	$N_{biomass}$ (g/m^3)	N-NH_4^+ (g/m^3)	N-NO_2^- (g/m^3)	N-NO_3^- (g/m^3)	$N_{biomass}$ (g/m^3)	Recovery (%)
AG								
94.8 ± 0.7	3.0 ± 0.2	0.0 ± 0.0	0.9 ± 0.0	60.1 ± 0.4	3.5 ± 0.3	0.0 ± 0.0	34.5 ± 0.9	99.0 ± 0.1
MG								
94.5 ± 0.5	0.0 ± 0.0	0.0 ± 0.0	0.7 ± 0.0	63.8 ± 0.5	0.0 ± 0.0	0.0 ± 0.0	30.3 ± 1.3	98.7 ± 1.3
Phosphorus mass balance								
P-PO_4^{-3} (g/m^3)		$P_{biomass}$ (g/m^3)		P-PO_4^{-3} (g/m^3)		$P_{biomass}$ (g/m^3)		Recovery (%)
AG								
13.7 ± 0.3		0.1 ± 0.0		10.6 ± 0.4		3.3 ± 0.1		99.6 ± 3.7
MG								
13.1 ± 0.2		0.1 ± 0.0		10.7 ± 0.4		2.6 ± 0.1		100.6 ± 3.9

sterile minimum MSM supplemented with 1 ml of a 301.4 g/dm^3 glucose stock solution as the organic carbon source, which resulted in an initial C-glucose concentration of 200 g/m^3 to mimic the organic matter present in domestic wastewater [24]. The dissolved total organic carbon concentration range used (80–290 g/m^3) corresponded to the typical TOC concentrations in domestic wastewaters according to Asano et al. [25]. The concentrations of carbonate and bicarbonate in this glucose-enriched MSM were modified to represent also the typical inorganic carbon concentrations in domestic wastewater (inorganic carbon concentrations ranging from 100 to 150 g/m^3) [25]. Hence, the MSM for mixotrophic growth was composed of (per cubic meter of distilled water): 1700 g $NaHCO_3$, 500 g Na_2CO_3, 500 g $C_6H_{12}O_6$, 78.6 g K_2HPO_4, 355.7 g NH_4Cl, 500 g K_2SO_4, 500 g NaCl, 100 g $MgSO_4{\cdot}7H_2O$, 20 g $CaCl_2{\cdot}2H_2O$, 6.8 g $FeSO_4{\cdot}7H_2O$, 42 g EDTA, 0.00025 g $ZnSO_4{\cdot}7H_2O$, 0.0005 g $MnSO_4{\cdot}H_2O$, 0.0025 g H_3BO_3, 0.00025 g $Co(NO_3)_2{\cdot}6H_2O$, 0.00025 g $Na_2MoO_4{\cdot}2H_2O$, 1.25×10^{-6} g $CuSO_4{\cdot}5H_2O$. Prior to sterilization, the bottles were flushed with Helium, closed with butyl septa and sealed with plastic caps. Following sterilization, the pH of the cultivation medium was decreased to 7.6 by injecting 0.2 ml of HCl (37%) and the systems were allowed to equilibrate as above described for 2 h at 25 °C prior to inoculation. The initial CO_2 headspace concentration in the bottles was 1.9 ± 0.1% (8.9 ± 0.5 g/m^3) (Table 1).

The bottles were inoculated in both tests with fresh *C. sorokiniana* at an initial concentration of 11 g/m^3, incubated at 30 °C under continuous magnetic agitation at 300 rpm and continuously illuminated at an average intensity of 82 ± 7 ($\mu E/m^2$ s). Gas samples of 100 μL were taken under sterile conditions to record the CO_2 and O_2 headspace concentrations by GC-TCD. In addition, liquid samples of 100 ml were also drawn at the beginning and end of the growth phase to quantify the dissolved total organic carbon (TOC), dissolved inorganic carbon (IC), dissolved total nitrogen (TN, N-NH_4^+, N-NO_2^- and N-NO_3^-), dissolved phosphorus (P-PO_4^{-3}) and microalgae biomass concentrations. The C, N and P content of the algal biomass formed was also experimentally determined. At the end of the growth phase, the microalgae were harvested from the cultivation broths by centrifugation for 10 min at 10,000 rpm (Sorvall, LEGEND RT + centrifuge, Thermo Scientific), resuspended in tap water to avoid cell lysis and further used as the raw material in the anaerobic digestion tests.

The influence of glucose concentration on *C. sorokiniana* metabolism under mixotrophic conditions was evaluated in an additional set of experiments conducted in duplicate as above described at C-glucose concentrations of 180, 200, 310 and 440 g/m^3 in the MSM used for mixotrophic growth and also at 310 g/m^3 in SK.

2.3. Microalgae anaerobic digestion

The anaerobic digestion of microalgae was performed batchwise in triplicate in 120 ml serum bottles filled with 80 ml of culture broth (microalgae + anaerobic inoculum), under strictly anaerobic conditions (Helium atmosphere) in an orbital shaker at 35 °C (initial pH of 7.9 and 7.6 for microalgae cultivated under autotrophic and mixotrophic conditions, respectively). The substrate to inoculum ratio was 0.5 (VS:VS). The inoculum used to digest the microalgae was an anaerobic bacterial sludge from Valladolid wastewater treatment plant previously adapted to microalgae for 2 months. In the digestion of autotrophically-grown microalgae, the anaerobic sludge contained 9.8 g/dm^3 of total suspended solids (TSS) and the concentration of microalgae was 13.3 g TSS/dm^3. On the other hand, the concentration of anaerobic inoculum and microalgae in the digestion of mixotrophically grown microalgae was 5.4 and 9.3 g TSS/dm^3, respectively. Anaerobic tests prepared in triplicate as above described containing only anaerobic inoculum were used as control. The anaerobic digestion tests (74 days for biomass cultivated autotrophically and 89 days for biomass cultivated mixotrophically) were monitored by periodic measurements of the headspace pressure and biogas composition. Gas samples of 100 μL were periodically taken to record the concentration of CO_2 and CH_4 in the biogas produced. Furthermore, liquid samples were also drawn at the beginning and end of the anaerobic digestion tests to determine the concentration of TOC, IC, TN, N-NH_4^+, N-NO_2^-, N-NO_3^-, P-PO_4^{-3} and TSS. The C, N and P content of the raw algal biomass, the anaerobic inoculum and the final digested biomass was also experimentally determined.

2.4. Mass and energy balances

A mass balance calculation was conducted for C, N and P considering all their chemical forms at the beginning and end of both the

growth and anaerobic digestion stages. The validity of the experimentation carried out was assessed by means of the recovery factor. In the particular case of the microalgae growth stage under both photoautotrophic and mixotrophic conditions, the recovery factor was defined as follows:

$$\text{C recovery } (\%) = \frac{[\text{C-CO}_2 + \text{TOC} + \text{IC} + \text{C}_{\text{biomass}}]_{\text{END POINT}}}{[\text{C-CO}_2 + \text{TOC} + \text{IC} + \text{C}_{\text{biomass}}]_{\text{START POINT}}} \times 100 \quad (1)$$

$$\text{N recovery } (\%) = \frac{[\text{N-NH}_4^+ + \text{N-NO}_2^- + \text{N-NO}_3^- + \text{N}_{\text{biomass}}]_{\text{END POINT}}}{[\text{N-NH}_4^+ + \text{N-NO}_2^- + \text{N-NO}_3^- + \text{N}_{\text{biomass}}]_{\text{START POINT}}} \times 100 \quad (2)$$

$$\text{P recovery } (\%) = \frac{[\text{P-PO}_4^{-3} + \text{P}_{\text{biomass}}]_{\text{END POINT}}}{[\text{P-PO}_4^{-3} + \text{P}_{\text{biomass}}]_{\text{START POINT}}} \times 100 \quad (3)$$

where C-CO_2 is the carbon as gaseous CO_2 at the flask's headspace, TOC is the total dissolved organic carbon in the aqueous phase, IC is the dissolved inorganic carbon at the aqueous phase in equilibrium with the gaseous C-CO_2($CO_2(g) \leftrightarrow CO_2(l) + H_2O \leftrightarrow HCO_3^- + H^+ \leftrightarrow CO_3^{-2} + 2H^+$), $C_{biomass}$ is the particulate carbon in the form of microalgal biomass, N-NH_4^+ is the nitrogen as ammonium, N-NO_2^- is the nitrogen as nitrite and N-NO_3^- is the nitrogen as nitrate at the aqueous phase, $N_{biomass}$ is the particulate organic nitrogen in the biomass, P-PO_4^{-3} is the phosphorus at the aqueous phase and $P_{biomass}$ is the particulate phosphorus in the form of biomass.

The N and P mass balances in the anaerobic digestion stage were similar to those defined in Eqs. (2) and (3). In the C balance of the anaerobic digestion stage, C as methane (C-CH_4) must be included:

$$\text{C recovery } (\%) = \frac{[\text{C-CO}_2\text{C-CH}_4 + \text{TOC} + \text{IC} + \text{C}_{\text{biomass}}]_{\text{END POINT}}}{[\text{C-CO}_2 + \text{C-CH}_4 + \text{TOC} + \text{IC} + \text{C}_{\text{biomass}}]_{\text{START POINT}}} \times 100 \quad (4)$$

These mass balances were also used to estimate the potential for bioenergy production and nutrient recovery from the anaerobic digestion of the algal biomass, in order to recycle the nutrients hydrolyzed back to the cultivation stage.

The photosynthetic efficiency (PE) during the exponential microalgae growth phase under photoautotrophic conditions was calculated as follows [2]:

$$\text{PE } (\%) = \frac{\text{TCEF}}{\text{TEA}} \times 100 = \frac{M \cdot H}{E \cdot T} \times 100 \quad (5)$$

where TCEF is the total chemical energy fixed in the form of biomass during the exponential growth phase (kJ), TEA is the total energy available from the light energy for microalgae growth during the exponential phase (kJ), M is the microalgae mass production (g) for a time period T (d), H is the specific chemical energy content of the algal biomass as heat (kJ/g) and E is the energy flow available as light energy for microalgae during the exponential growth stage (kJ/d). The value of H considered in the PE calculation was 21 kJ/g of microalgae [26,27].

In order to calculate E, the fraction of light energy absorbed by the glass bottle walls (G) was taken into account:

$$E = E' \times (1 - G) \quad (6)$$

where G was experimentally estimated by measuring the light intensity at both sides of the glass bottle wall ($G = 8.7 \pm 0.12\%$) and E' was calculated by multiplying the measured light intensity ($\mu E/m^2$ s) at the top and side of the bottles by their corresponding areas. The overall energy recovery from the biomass growing in the exponential growth phase under photoautotrophic and mixotrophic conditions was calculated based on TCEF (ER_{TCEF}) and TEA (ER_{TEA}) as follows:

$$(\text{ER})_{\text{TCEF}} \ (\%) = \frac{\text{ME}}{\text{TCEF}} \times 100 \quad (7)$$

$$(\text{ER})_{\text{TEA}} \ (\%) = \frac{\text{ME}}{\text{TEA}} \times 100 \quad (8)$$

where ME is the energy provided by the combustion of the methane obtained during the anaerobic digestion of the microalgal biomass produced during the exponential growth phase (kJ). The heating value here used for the CH_4 was 50 kJ/g [28]. Under photoautotrophic conditions TEA comprised only the impinging light energy, while for the mixotrophically grown microalgae, the energy supplied as light and the chemical energy provided by the glucose were considered to calculate TEA, respectively. The specific heating value of the glucose considered in $(ER)_{TEA}$ calculation was 15.6 kJ/g glucose [29].

2.5. Analytical procedures

TOC, IC and TN concentrations were determined using a Shimadzu TOC-V CSH analyzer equipped with a TNM-1 module (Japan). N-NO_3^-, N-NO_2^- and P-PO_4^{-3} were analyzed by HPLC-IC with a Waters 515 HPLC pump (Waters, Milford, USA) coupled with an ion conductivity detector (Waters 432, Milford, USA) using an IC-Pak Anion Guard-Pak column (Waters, Milford, USA), an IC-Pak Anion HC (150 mm × 4.6 mm) column (Waters, Milford, USA) and a Waters 717 plus autosampler (Waters, Milford, USA). A mobile phase consisting of acetonitrile (12%), n-Butanol (2%) and a buffer solution (2%) (16 g/dm^3 of $NaC_6H_{11}O_7$, 25 g/dm^3 of $Na_2B_4O_7{\cdot}10H_2O$, 18 g/dm^3 of H_3BO_3 and 0.25 dm^3/dm^3 of glycerol) was used as eluent at 2 ml/min. The dissolved and total phosphorus concentrations (total phosphorus previously digested after acidification with 18.6% HNO_3 in a microwave oven Mars Xpress, CEM, USA) were determined using a spectrophotometer U-2000 (Hitachi, Japan). All these analysis were carried out according to Eaton et al. [30]. A Crison micropH 2002 (Crison instruments, Barcelona, Spain) was used for pH determination.

The gaseous concentrations of CO_2, CH_4, O_2 and N_2 were analyzed using a gas chromatograph (Varian CP-3800, Palo Alto, CA, USA) coupled with a thermal conductivity detector and equipped with a CP-Molsieve 5A (15 m × 0.53 mm × 15 μm) and a CP-Pora BOND Q (25 m × 0.53 mm × 15 μm) columns. The injector and detector temperatures were 150 °C and 175 °C, respectively. Helium was the carrier gas at 13.7 ml/min. The pressure of the head-space of the anaerobic digestion assays was measured using a PN 5007 (IFM, Germany).

The light intensity was measured using a Li-250 A light meter (Li-COR Biosciences, Germany) and expressed in $\mu E/m^2$ s. The photosynthetically active radiation (PAR) was assumed to have a wavelength close to 550 nm, where 1 W/m^2 of PAR was equivalent to 4.6 μE/ms [31].

The biomass concentration was estimated from culture absorbance measurements at 550 nm (OD_{550}) using a HITACHI U2000 UV/visible spectrophotometer (Hitachi Ltd., Tokyo, Japan). In addition, the determination of the total suspended solid and volatile solid concentration was performed according to Eaton et al. [30]. The analysis of the $C_{biomass}$, $N_{biomass}$ and $S_{biomass}$ was conducted using a LECO CHNS-932.

3. Results and discussion

The results obtained were summarized in Tables 1 and 2 and given as the average ± the error at 95% confidence interval ($n = 10$ for autotrophic growth (AG), $n = 12$ for mixotrophic growth (MG) and $n = 3$ for the anaerobic digestion tests).

Table 2
C, N and P mass balances for the anaerobic digestion of microalgae cultivated under autotrophic (AG) and mixotrophic (MG) conditions.

Mass balances to the anaerobic digestion stage									
Initial					Final				
Carbon mass balance									
$C\text{-}CO_2$ (g/m^3)	$C\text{-}CH_4$ (g/m^3)	IC (g/m^3)	TOC (g/m^3)	$C_{biomass}$ (g/m^3)	$C\text{-}CO_2$ (g/m^3)	$C\text{-}CH_4$ (g/m^3)	IC (g/m^3)	TOC (g/m^3)	$C_{biomass}$ (g/m^3)	Recovery (%)
AG										
0.0 ± 0.0	0.0 ± 0.0	17.9 ± 0.0	1.2 ± 0.0	6720.6 ± 0.0	227.4 ± 11.9	520.5 ± 4.4	505.9 ± 4.9	116.7 ± 5.0	3052.1 ± 39.7	104.2 ± 1.9
MG										
0.0 ± 0.0	0.0 ± 0.0	22.1 ± 0.0	0.8 ± 0.0	4459.4 ± 0.0	162.6 ± 11.1	428.5 ± 6.5	448.6 ± 20.3	214.1 ± 17.7	2430.9 ± 27.9	135.9 ± 0.5
Nitrogen mass balance										
$N\text{-}NH_4^+$ (g/m^3)	$N\text{-}NO_2^-$ (g/m^3)	$N\text{-}NO_3^-$ (g/m^3)	$N_{biomass}$ (g/m^3)		$N\text{-}NH_4^+$ (g/m^3)	$N\text{-}NO_2^-$ (g/m^3)	$N\text{-}NO_3^-$ (g/m^3)	$N_{biomass}$ (g/m^3)		Recovery (%)
AG										
1.3 ± 0.0	0.0 ± 0.0	0.0 ± 0.0	1075.6 ± 0.0		637.5 ± 20.0	0.0 ± 0.0	0.0 ± 0.0	603.6 ± 17.7		108.7 ± 1.1
MG										
1.4 ± 0.0	0.0 ± 0.0	0.0 ± 0.0	809.1 ± 0.0		567.1 ± 23.8	0.0 ± 0.0	0.0 ± 0,0	429.9 ± 20.5		123.0 ± 2.3
Phosphorus mass balance										
$P\text{-}PO_4^{-3}$ (g/m^3)		$P_{biomass}$ (g/m^3)			$P\text{-}PO_4^{-3}$ (g/m^3)		$P_{biomass}$ (g/m^3)			Recovery (%)
AG										
0.03 ± 0.0		101.7 ± 0.0			90.3 ± 2.3		11.4 ± 2.3			99.3 ± 1.2
MG										
0.03 ± 0.0		69.1 ± 0.0			53.4 ± 1.3		15.7 ± 1.3			100.4 ± 1.0

3.1. Microalgae growth under photoautotrophic and mixotrophic conditions

The C, N and P mass balances in the photoautotrophic microalgae cultivation showed recovery factors of 103.4 ± 0.5%, 99.0 ± 0.1% and 99.6 ± 3.7%, respectively, and 100.1 ± 1.9%, 98.7 ± 1.3% and 100.6 ± 3.9% in the mixotrophic cultivation (Table 1). These results validated both the analytical and instrumental methods used in this study and the experimental protocols followed. The biomass stoichiometric formula experimentally determined for the microalgae cultivated under autotrophic and mixotrophic conditions were $CH_{1.63}N_{0.14}O_{0.43}P_{0.006}S_{0.005}$ and $CH_{1.68}N_{0.16}O_{0.48}P_{0.006}S_{0.008}$, respectively, which agree well with typical compositions reported for microalgae in literature. For instance, Chisti [1], Boelee et al. [32], Duboc et al. [33] and Oswald [34], reported microalgae stoichiometric formula of $CH_{1.83}N_{0.11}O_{0.48}P_{0.01}$, $CH_{1.78}N_{0.12}O_{0.36}$ $P_{0.01}$, $CH_{1.78}N_{0.12}O_{0.36}$, and $CH_{1.7}N_{0.15}O_{0.4}P_{0.0094}$, respectively. In our particular case, the composition of microalgae did not depend significantly on the nature of the carbon source ($C\text{-}CO_2$ and C-glucose).

3.1.1. C mass balances

Under fully photoautotrophic growth, *C. sorokiniana* assimilated 1.8 ± 0.1 g of CO_2 per g of microalgae formed, which agrees with the CO_2 consumed per g of TSS of microalgae reported by Lardon et al. [35] (1.8 g CO_2 per g of microalgae), and also released 1.0 ± 0.0 g of O_2 per g of CO_2 consumed, which agrees with the theoretical oxygen production estimated by Bahr et al. [36] (1.1 g O_2 per g of CO_2). This carbon was obtained from the $C\text{-}CO_2$ present in the flask's headspace (95.7 ± 0.3% of the initial $C\text{-}CO_2$ (82.7 ± 3.4 g/m^3)) and the dissolved inorganic carbon present initially in the MSM (8.7% ± 1.1 of the initial dissolved IC (1020.9 ± 12.8 g/m^3)) (Table 1). The total concentration of $C_{biomass}$ formed accounted for 210.5 ± 5.8 g/m^3, with an empirical C content in the biomass of 50.6%. The TOC present in the initial autotrophic cultivation medium (17.3 ± 0.1 g/m^3) (corresponding to the recalcitrant chelating agent EDTA) increased up to 51.6 ± 2.7 g/m^3 due to metabolite excretion by microalgae during their photoautotrophic growth. Based on the continuous light supply and presence of sufficient concentrations of dissolved IC (931.7 ± 8.3 g/m^3), $N\text{-}NH_4^+$ (60.1 ± 0.4 g/m^3) and $P\text{-}PO_4^{-3}$ (10.6 ± 0.4 g/m^3) at the end of the cultivation stage (Table 1), microalgae growth under photoautotrophic conditions was likely limited by either the high pH values or the high O_2 concentrations present at the end of the cultivation process (Figs. 2 and 3). On the one hand, the inorganic carbon distribution at the pH of 9.1 ± 0.2 recorded at the final point of the growth stage was mainly shifted towards carbonate, which constitutes an inorganic carbon species non-available for *C. sorokiniana* growth [37,38]. On the other hand, high NH_3 concentrations resulting from the combination of high NH_4^+ concentrations and high pH values can uncouple the electron transport in the photosystem II of microalgae and compete with H_2O in the oxidation reactions leading to O_2 production, which results in a partial inhibition of the photosynthetic process [39]. However, a hypothetical inhibition of *C. sorokiniana* growth by NH_3 at the conditions prevailing at the end of the photoautotrophic cultivation (60.1 ± 0.4 g/m^3 of $N\text{-}NH_4^+$ and pH of 9.1, corresponding to 24.9 ± 0.4 g/m^{3}of $N\text{-}NH_3$) was ruled since no significant effect on the growth of *C. sorokiniana* was observed by de Godos et al. [38] at 311 g/m^3 $N\text{-}NH_4^+$ and pH of 9.5 ± 0.1 (≈241 g/m^3 $N\text{-}NH_3$). The accumulation of photosynthetic O_2 at the flask's headspace as a result of the enclosed nature of the tests could have also inhibited the photosynthetic CO_2 fixation due to a potential photooxidative damage on the microalgal cells (24.5 ± 1.1 g O_2/m^3 in the aqueous phase) [40,41]. In addition, a potential competition between O_2 and CO_2 for the enzyme ribulose bisphosphate carboxylase (RubisCO) (a key catalyst of the Calvin

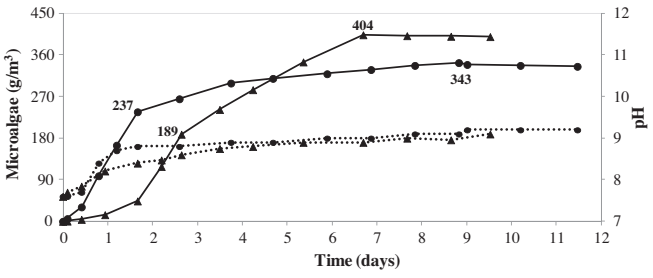

Fig. 2. Time course of microalgae concentration (—) and pH (••••) under autotrophic (▲) and mixotrophic conditions (●).

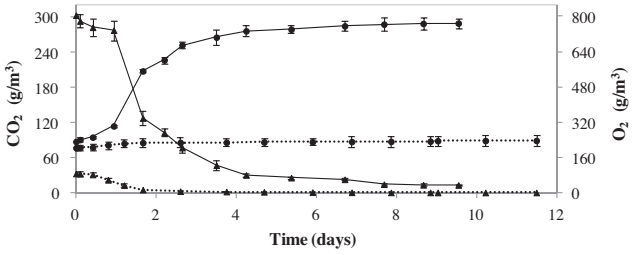

Fig. 3. Time course of CO_2 (▲) and O_2 (●) concentration during microalgae growth under autotrophic (—) and mixotrophic (••••) conditions. Vertical bars represent standard deviations from $n = 10$ for autotrophic growth and $n = 12$ for mixotrophic growth.

cycle to transform CO_2 to organic compounds) likely occurred at the high oxygen concentrations recorded [42–45].

Under mixotrophic conditions, the microalgae assimilated 58.9 ± 3.5% of the dissolved IC initially present in the MSM and 99.3 ± 0.4% of the initial C-CO_2 at the flask's headspace (Initial $(IC)_{TOTAL}$ = 8.9 ± 0.5 g/m^3 as C-CO_2 + 130.8 ± 1.2 g/m^3 as dissolved IC), with a pH of 9.2 at the end of the growth stage. Despite *C. sorokiniana* reached higher final biomass concentrations under photoautotrophic growth (Fig. 2), the overall productivity recorded during the exponential growth phase under mixotrophic conditions (165 g/m^3 d) was comparable to that achieved under fully photosynthetic growth (147 g/m^3 d). Likewise, the specific growth rate at the exponential growth phase (μ) under autotrophic conditions (1.5 d^{-1}) was similar to that recorded under mixotrophic growth conditions (1.6 d^{-1}) (Fig. 2). However, a longer lag phase was recorded under photoautotrophic cultivation conditions likely due to its higher initial concentrations of CO_2 in the flask headspace (303 g/m^3 CO_2 ≈18%) compared to those recorded under mixotrophic conditions (33 g/m^3 CO_2 ≈1.9%) (Fig. 3). In this regard, a longer acclimatization period of *C. sorokiniana* represented by an extended lag phase growth was observed by Mattos et al. [46] at 10% of CO_2. Thus, microalgae can possibly tolerate high concentration of CO_2 by adjusting their structural anatomy and redistribution of certain cellular organelles, which requires a longer adaptation period at the beginning of the growth stage [47]. Although most of the inorganic carbon present in the system was assimilated, only 73.7 g/m^3 of dissolved organic carbon was consumed in the presence of 500 g/m^3 of glucose (203 ± 3.3 g C-glucose/m^3) in the minimum MSM (Fig. 4). This represented only an uptake of 27.8 ± 2.3% of the initial C-glucose, with an assimilation of 0.17 g of C-glucose per g of microalgae produced. The total $C_{biomass}$ produced was 167 ± 7 g/m^3 with an empirical C content of 48%, very similar to that obtained under photoautotrophic growth (50.6%). In this context, an additional set of experiments was carried out at different initial concentrations of C-glucose (180, 200, 310 and 440 g/m^3) in order to assess the role of glucose on the metabolism of *C. sorokiniana*. The results obtained showed a similar organic and inorganic carbon assimilation, and biomass production at 180 g C-glucose/m^3 and 200 g/m^3. However, the photosynthetic inorganic carbon assimilation decreased at increasing glucose concentrations above 200 g/m^3 of C-glucose. In fact, negative inorganic carbon (C-CO_2 + IC) assimilations were recorded due to the intensive respiratory release of CO_2 at 310 and 440 g/m^3 of C-glucose (see Fig. 4). An additional experiment at 310 g/m^3 of C-glucose was carried out in SK MSM to assess the influence of the mineral salt medium on microalgae growth (Fig. 4). The results here obtained clearly show a higher glucose-mediated inhibition in the minimum MSM compared to the SK MSM, which supported a *C. sorokiniana* uptake of 58 g/m^3 of IC and 390 g/m^3 of TOC, compared to −28 g/m^3 and 209 g/m^3, respectively in the minimum MSM. Despite the ability of glucose to suppress the activity of the enzyme carbonic anhydrase (CA) in *C. sorokiniana* has been reported at concentrations as low as 90 g/m^3 (36 g C-Glucose/m^3) [48], the role of the salts present in the mineral salt medium on this inhibition remains unknown and deserves further investigation based on the recent interest on microalgae heterotrophic and mixotrophic growth processes [49–51].

3.1.2. N and P mass balances

During microalgae growth under autotrophic conditions TN (initially in the form of N-NH_4^+), decreased from 94.8 ± 0.7 g/m^3 to 60.1 ± 0.4 g/m^3 (Table 1), concomitantly with an assimilation of 33.6 ± 0.9 g/m^3 in the form of $N_{biomass}$. In this regard, the empirical N content of the biomass was 8.1%, which is in agreement with previously reported data. Neither NO_2^- nor NO_3^- were produced by microalgae in significant amounts. In addition, during photoautotrophic growth, 3.1 ± 0.6 g/m^3 of P-PO_4^{-3} were consumed (difference between the initial and final phosphate concentration) (Table 1). The P-PO_4^{-3} removed from the MSM correlated with the concentration of $P_{biomass}$ produced (3.2 ± 0.1 g/m^3), which implied an empirical microalgae P content of 0.8%. In this context, despite the nitrogen content is widely accepted to vary within a limited range of values (6.6–9.3%, [1,32–34]) the phosphorus content of algal cells can vary from 0.2% to 3.9% under different cultivation conditions [52]. This wide range is due to the occurrence of a luxury uptake of phosphorus by some microalgae species, where phosphorus is stored in the form of polyphosphate over structural phosphorus requirements [53].

During microalgae growth under mixotrophic conditions the concentration of N-NH_4^+ decreased from 94.5 ± 0.5 g/m^3 to 63.8 ± 0.5 g/m^3 (Table 1), with an assimilation of 29.6 ± 1.3 g/m^3 in the form of $N_{biomass}$ and an empirical N content of 8.7%. Neither NO_2^- nor NO_3^- were produced by microalgae. The P-PO_4^{-3} concentration consumed during mixotrophic growth (2.4 ± 0.3 g/m^3) correlated with the concentration of $P_{biomass}$ produced (2.5 ± 0.1 g/m^3), yielding an empirical microalgae P content of 0.7%.

3.2. Anaerobic digestion mass balances

The C, N and P mass balances in the anaerobic digestion of microalgae cultivated under photoautotrophic conditions showed recovery factors of 104.2 ± 1.9%, 108.7% ± 1.1% and 99.3 ± 1.2%, respectively, while in the anaerobic digestion of microalgae cultivated mixotrophically these recovery factors accounted for 135.9 ± 0.5% for C, 123.0 ± 2.3% for N and 100.4 ± 1.0% for P (Table 2). An explanation for the high C and N recovery factors here recorded might be the low initial activity of the anaerobic sludge inoculum used in this particular experiment. Hence, the amount of

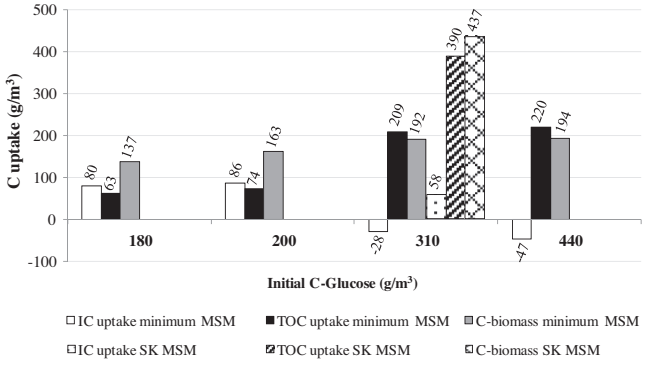

Fig. 4. Influence of C-glucose concentration on the carbon uptake (IC and TOC) and C-biomass production in minimum MSM. The carbon uptake and biomass production in Sorokin and Krauss MSM was also evaluated in the presence of 310 g/m^3 of C-glucose.

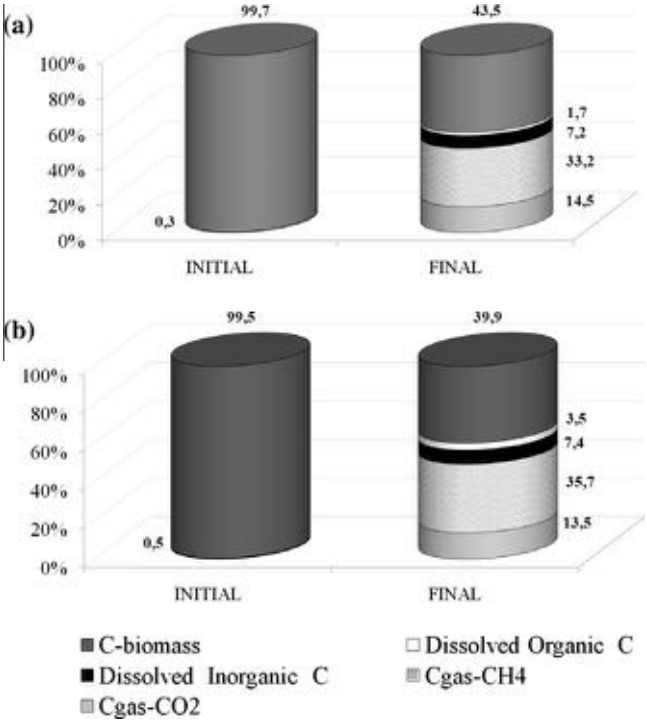

Fig. 5. Carbon distribution at the beginning and end of the anaerobic digestion of microalgae cultivated (a) under autotrophic conditions and (b) under mixotrophic conditions.

microalgae hydrolyzed, and consequently, the quantity of biogas produced and N released to the aqueous phase might have been overestimated since all these parameters were calculated as the difference between the algal tests and the control test. Therefore, a low activity in the control tests mediated by the lack of external carbon and energy source, together with the potential activation of the anaerobic inoculum in the presence of microalgae, might have contributed to the high recovery factors here recorded. As above explained, the release of P was not directly proportional to the hydrolysis of biomass due to the potential accumulation of non-structural phosphorus as discussed in Section 3.1.2.

3.2.1. C mass balances

The biomass particulate carbon represented 99.7% of the initial carbon in the system at the beginning of the anaerobic digestion of autotrophically grown microalgae (Fig. 5a), while the dissolved inorganic carbon accounted for the remaining 0.3%. $C_{biomass}$ concentration decreased from 6721 g/m^3 to 3052 ± 40 g/m^3, which represents a hydrolysis of 54.6 ± 0.6% of the initial particulate carbon after 74 days (=final biodegradability). During anaerobic digestion, 227.4 ± 11.9 g/m^3 of C-CO_2 and 520.5 ± 4.4 g/m^3 of C-CH_4 were produced (Table 2 and Fig. 6), which entails that 87.3 ± 1.8% of the hydrolyzed $C_{biomass}$ was converted to biogas (47.7 ± 0.5% of the initial carbon shared in 14.5 ± 0.7% as C-CO_2 and 33.2 ± 0.5% as C-CH_4) (Fig. 5a). This share corresponds to a biogas composition of 30.4 ± 0.7 % (v/v) of CO_2 and 69.6 ± 0.5 % (v/v) of CH_4, which agrees with typical biogas composition from microalgae anaerobic digestion reported in literature [12,54,55]. The remaining hydrolyzed carbon was not transformed into biogas but present in the system as dissolved inorganic carbon (7.2 ± 0.1%). The amount of dissolved organic carbon at the end of the anaerobic degradation was however negligible (1.7 ± 0.1%) (Fig. 5a).

At the beginning of the anaerobic digestion of the microalgae cultivated under mixotrophic conditions, the microalgal particulate carbon represented 99.5% of the initial carbon in the system, and decreased from 4459 g/m^3 to 2431 ± 28 g/m^3, which

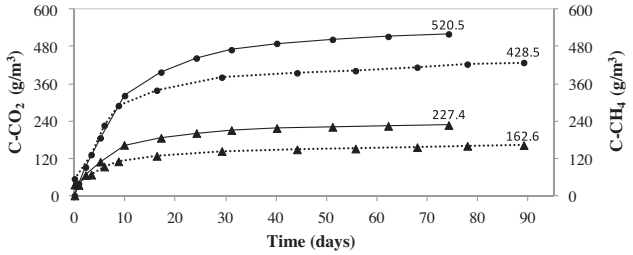

Fig. 6. Time course of C-CO_2 (▲) and C-CH_4 (●) concentration during the anaerobic digestion of the autotrophically (—) and mixotrophically (••••) grown microalgae. Vertical bars represent standard deviations from triplicates.

represents a hydrolysis of 45.5 ± 0.6% (Fig. 5b). During anaerobic digestion, 162.6 ± 11.1 g/m^3 of C-CO_2 and 428.5 ± 6.5 g/m^3 of C-CH_4 were released as biogas (Table 2 and Fig. 6), which represents 49.2 ± 0.5% of the total final carbon (13.5 ± 0.9% as C-CO_2 and 35.7 ± 0.5% as C-CH_4). The biogas composition from the anaerobic digestion of the microalgae cultivated mixotrophically was 27.5 ± 0.9 % (v/v) of CO_2 and 72.5 ± 0.5 % (v/v) of CH_4, similar to the shares obtained for the biogas produced from the autotrophically grown biomass. The hydrolyzed carbon not transformed into biogas remained in the system as dissolved inorganic carbon (7.4 ± 0.3%) and dissolved organic carbon (3.5 ± 0.3%) (Fig. 5b).

3.2.2. N and P mass balances

The N-NH_4^+ concentration at the end of the anaerobic digestion of microalgae cultivated under photoautotrophic conditions was 637.5 ± 20.0 g/m^3 (at a final pH of 8.3), which entails that 59.2 ± 1.9% of the initial particulate organic nitrogen ($N_{biomass}$) was released to the aqueous phase as N-NH_4^+ and therefore available for recycling to the microalgae cultivation stage. In this context, a potential inhibition of methane production mediated by a high pH and NH_4^+ concentration in the final digestion stages was ruled out based on the typical ammonium inhibitory range (1500–3000 mg/L and pH above 7.6) reported by McCarty [56] and the latest results published by Alzate et al. [57] for the anaerobic digestion of three microalgal consortia under comparable digestion conditions. The potential recovery of the particulate phosphorous ($P_{biomass}$) based on the PO_4^{3-} released was 88.8 ± 2.3%. A possible explanation for this high recovery of P-PO_4^{-3} (higher than the corresponding structural P) might be the release of polyphosphates accumulated in microalgal cells at the previous growth stage. Hence, microalgae, like phosphate accumulating bacteria (PAO) in activated sludge processes [58] might accumulate phosphorus above their structural P requirements during aerobic growth, which could be further released under anaerobic conditions. In this context, Powell et al. [52,53] observed that the accumulation and subsequent utilization of two types of polyphosphate present in microalgae (acid-soluble polyphosphate (ASP) and acid-insoluble polyphosphate (AISP)) is a function of the phosphate concentration in the culture medium. AISP is believed to be a form of phosphorus storage that is not utilized when microalgae are not phosphate-starved while ASP is involved in microalgae metabolism and can act as a short term form for phosphorus storage.

During the anaerobic digestion of mixotrophically grown microalgae, 69.9 ± 2.9% of the initial particulate nitrogen ($N_{biomass}$) was released as N-NH_4^+ to the aqueous phase (567.1 ± 23.8 g/m^3 of N-NH_4^+ at a final pH of 8.2). The potential for particulate phosphorous ($P_{biomass}$) recovery was also high (77.3 ± 1.9% of the initial particulate P). In this context, the recovery of nutrients from microalgae anaerobic digestion has been so far poorly addressed in literature despite playing a key role in the sustainability of microalgae-based biofuels [20,59]. As a matter of fact, the energy

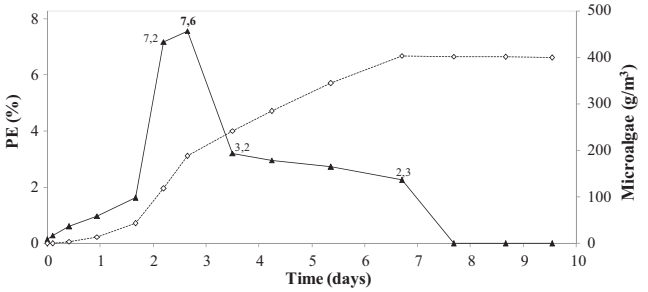

Fig. 7. Time course of the photosynthetic efficiency (▲) and microalgae concentration (◇) under autotrophic growth conditions.

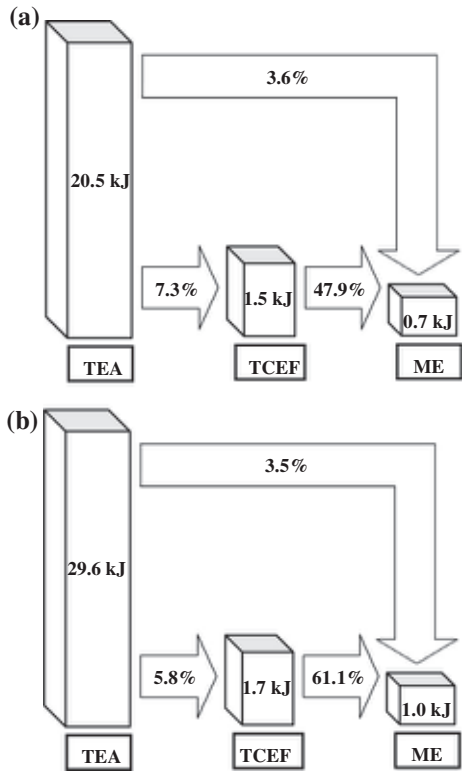

Fig. 8. Global energy conversion in the integrated microalgae cultivation-anaerobic digestion process for (a) autotrophically-grown microalgae and (b) mixotrophically grown microalgae during the exponential phase.

footprint associated to nutrient supply (N and P) can account for up to 45% of the total energy required for microalgae cultivation to produce biodiesel according to recent sustainability studies [15]. The recycling rates here obtained for N and P agree with those reported by Rösch et al. [18] in a modeling study (30–90% for N and 48–93% for P).

3.3. Energy balances

The overall PE recorded during the exponential growth phase of *C. sorokiniana* (40–64 h) under photoautotrophic conditions was 7.4% (Fig. 7), which agrees well with the typical PEs reported in outdoors photobioreactors, which range from 3.6% to 10% [9,31,60]. In this context, a global energy balance considering both microalgae growth and anaerobic digestion was conducted. Thus, the amount of energy fixed during microalgae exponential growth under autotrophic (Fig. 8a) and mixotrophic (Fig. 8b) conditions was compared with the potential energy obtained from the CH_4 produced during its further anaerobic digestion. The TCEF and ME were directly proportional to the amount of biomass produced during the exponential microalgae growth phase. Due to the higher productivity of biomass during the exponential growth phase under mixotrophic conditions, the TCEF and ME were slightly higher than under photoautotrophic growth. Likewise, the TEA during mixotrophic growth was higher than during autotrophic growth since the energy available as glucose was also taken into account in the energy balance. As a result, the energy recovery from the TCEF under photoautotrophic conditions was lower than under mixotrophic conditions, with 48% and 61% energy recoveries, respectively. However, the global energy recovery based on the TEA showed energy recoveries under phototrophic and mixotrophic conditions of 3.6% and 3.5%, respectively, which were higher than the 2% global energy recovery reported by Golueke and Oswald [61] for the anaerobic digestion of microalgae consortium (75% of *Chlorella* spp., 23% of *Scenedesmus* spp. and 1.5% of *Euglena* spp.) grown under autotrophic conditions.

4. Conclusions

The recovery factors obtained in the C, N and P mass balances (≈100%) validated the analytical and instrumental methods used in this study and the experimental protocols followed. The composition of microalgae did not change significantly with the nature of the carbon source (C-CO_2 and C-glucose). Despite the different growth conditions, *C. sorokiniana* showed a similar specific growth rate during the exponential growth phase, and therefore similar productivities, under autotrophic and mixotrophic conditions. However, a partial inhibition of *C. sorokiniana* inorganic carbon uptake by glucose was recorded above 200 g C-glucose/m^3. The results obtained during the anaerobic digestion of microalgae showed that approx. 50% of the initial $C_{biomass}$ was hydrolyzed and mainly found as biogas at the end of the test (14% as C-CO_2 and 35% as C-CH_4) regardless of the cultivation mode. The potential recoveries of $N_{biomass}$ and $P_{biomass}$ under autotrophic and mixotrophic conditions were ≈65% as N-NH_4^+ and ≈83% as P-PO_4^{-3}, respectively, which would result in a significant reduction in the operating costs of the microalgae cultivation process. The energy recovery as methane from the total chemical energy fixed by biomass under photoautotrophic and mixotrophic conditions during anaerobic digestion was 48% and 61%, respectively, while these values decreased to ≈3.6% when referred to the total energy available in the cultivation systems.

Acknowledgments

This research was supported by the regional government of Castilla y Leon and the European Social Fund (Contract No. E-47-2011-0053564 and project Ref. GR76). The Spanish Ministry of Economy and Competitiveness is also gratefully acknowledged for its financial support (CONSOLIDER-CSD 2007-00055 and RYC-2007-01667).

References

[1] Y. Chisti, Biodiesel from microalgae, Biotechnol. Adv. 25 (2007) 294–306.
[2] A. Garibay Hernández, R. Vázquez-Duhalt, M.P. Sánchez Saavedra, L. Serrano Carreón, A. Martínez Jiménez, Biodiesel a Partir de Microalgas. Revista de la Sociedad Mexicana de Biotecnologia y Bioingenieria A.C, Mexico, 2009, pp. 38–61.
[3] M. Balat, Potential alternatives to edible oils for biodiesel production – a review of current work, Energy Conv. Manage. 52 (2011) 1479–1492.
[4] M.M. Gui, K.T. Lee, S. Bhatia, Feasibility of edible oil vs. non-edible oil vs. waste edible oil as biodiesel feedstock, Energy 33 (2008) 1646–1653.
[5] A.L. Ahmad, N.H. Mat Yasin, C.J.C. Derek, J.K. Lim, Microalgae as a sustainable energy source for biodiesel production: a review, Renew. Sustain. Energy Rev. 15 (2011) 584–593.

[6] L. Brennan, P. Owende, Biofuels from microalgae—a review of technologies for production, processing, and extractions of biofuels and co-products, Renew. Sustain. Energy Rev. 14 (2010) 557–577.
[7] Y. Sumi, Microalgae pioneering the future, application and utilization, Life Sci. Res. Unit. 34 (2009) 9–21.
[8] N.H. Norsker, M.J. Barbosa, M.H. Vermuë, R.H. Wijffels, Microalgal production: a close look at the economics, Biotechnol. Adv. 29 (2011) 24–27.
[9] F.G. Acién, J.M. Fernández, J.J. Magán, E. Molina, Production cost of a real microalgae production plant and strategies to reduce it, Biotechnol. Adv. 30 (2012) 1344–1353.
[10] R. Harun, M. Davidson, M. Doyle, R. Gopiraj, M. Danquah, G. Forde, Technoeconomic analysis of an integrated microalgae photobioreactor, biodiesel and biogas production facility, Biomass Bioenergy 35 (2011) 741–747.
[11] I. Rawat, R. Ranjith Kumar, T. Mutanda, F. Bux, Biodiesel from microalgae: a critical evaluation from laboratory to large scale production, Appl. Energy 103 (2013) 444–467.
[12] B. Sialve, N. Bernet, O. Bernard, Anaerobic digestion of microalgae as a necessary step to make microalgal biodiesel sustainable, Biotechnol. Adv. 27 (2009) 409–416.
[13] Y. Chisti, Response to Reijnders: do biofuels from microalgae beat biofuels from terrestrial plants?, Trends Biotechnol 26 (2008) 351–352.
[14] E.A. Ehimen, Energy balance of microalgal-derived biodiesel, Energy Sour. 32 (2010) 1111–1120.
[15] M.R. Oliveira, J.O. Beserra, S. Macambira, Development of a methodology for net energy analysis in biorefineries, regarding microalgae cultivation to improve energy yields in industrial wastes, Rev. Latinoam. Biotecnol. Amb. Algal 3 (2012) 59–79.
[16] M. Ras, L. Lardon, S. Bruno, N. Bernet, J.P. Steyer, Experimental study on a coupled process of production and anaerobic digestion of *Chlorella vulgaris*, Bioresour. Technol. 102 (2011) 200–206.
[17] J. Yang, M. Xu, X. Zhang, Q. Hu, M. Sommerfeld, Y. Chen, Life-cycle analysis on biodiesel production from microalgae: water footprint and nutrients balance, Bioresour. Technol. 102 (2011) 159–165.
[18] C. Rösch, J. Skarka, N. Wegerer, Materials flow modeling of nutrient recycling in biodiesel production from microalgae, Bioresour. Technol. 107 (2012) 191–199.
[19] F. Paul, Potential biofuels influence on nutrient use and removal in the US, Better Crops 91 (2) (2007) 12–14.
[20] R. Pate, G. Klise, B. Wub, Resource demand implications for US algae biofuels production scale-up, Appl. Energy 88 (2011) 3377–3388.
[21] A. Kumar, S. Ergas, X. Yuan, A. Sahu, Q. Zhang, J. Dewulf, F.X. Malcata, H. van Langenhove, Enhanced CO_2 fixation and biofuel production via microalgae: recent developments and future directions, Trends Biotechnol. 28 (2010) 371–380.
[22] L. He, V.R. Subramanian, Y.J. Tang, Experimental analysis and model-based optimization of microalgae growth in photo-bioreactors using flue gas, Biomass Bioenergy 41 (2012) 131–138.
[23] F.M. Salih, Microalgae tolerance to high concentrations of carbon dioxide: a review, J. Environ. Protect. 2 (2011) 648–654.
[24] OECD. Guideline for testing of chemicals. Simulation test – aerobic sewage treatment, Technical report, Organisation for economic co-operation and development, Paris, 1996.
[25] T. Asano, F.L. Burton, H.L. Leverenz, R. Tsuchihashi, G. Tchobanoglous, Metcalf and Eddy, Wastewater Engineering: Treatment and Reuse, fourth ed., McGraw-Hill, New York, 2002.
[26] A.M. Illman, A.H. Scragg, S.W. Shales, Increase in *Chlorella* strains calorific values when grown in low nitrogen medium, Enzyme Microb. Technol. 27 (2000) 631–635.
[27] J.B.K. Park, R.J. Craggs, A.N. Shilton, Wastewater treatment high rate algal ponds for biofuel production, Bioresour. Technol. 102 (2011) 35–42.
[28] R.H. Perry, D.W. Green, Perry's Chemical Engineers' Handbook, seventh ed., McGraw-Hill, New York, 1999.
[29] A. Saterbak, K.Y. San, L.V. McIntire, Fundamentals of Bioengineering (BIOE252). Conservation Principles in Bioengineering, Pearson Prentice Hall Bioengineering, 2004 (Chapter 4).
[30] A.D. Eaton, L.S. Clesceri, A.E. Greenberg, Standard Methods for the Examination of Water and Wastewater, 21st ed., American Public Health Association/ American Water Works Association/Water Environment Federation, Washington DC, 2005.
[31] Q. Béchet, R. Muñoz, A. Shilton, B. Guieysse, Outdoor cultivation of temperature-tolerant *Chlorella sorokiniana* in a column photobioreactor, Biotechnol. Bioeng. 110 (1) (2013) 118–126.
[32] N.C. Boelee, H. Temmink, M. Janssen, C.J.N. Buisman, R.H. Wijffels, Scenario analysis of nutrient removal from municipal wastewater by microalgal biofilms, Water 2012 (4) (2012) 460–473.
[33] P. Duboc, I. Marison, U. von Stockar, Quantitative calorimetry and biochemical engineering, in: R.B. Kemp (Ed.), Handbook of Thermal Analysis and Calorimetry, Elsevier Sci, London, 1999, pp. 267–365.
[34] W.J. Oswald, Micro-algae and waste-water treatment, in: M.A. Borowitzka, L.J. Borowitzka (Eds.), Micro-algal Biotechnol, Cambridge University Press, Cambridge, 1988, pp. 305–328.
[35] L. Lardon, A. Hélias, B. Sialve, J.P. Steyer, O. Bernard, Life-cycle assessment of biodiesel production from microalgae, Environ. Sci. Technol. 43 (2009) 6475–6481.
[36] M. Bahr, A.J.M. Stams, F. de la Rosa, P.A. García-Encina, R. Muñoz, Assessing the influence of the carbon oxidation–reduction state on organic pollutant biodegradation in algal–bacterial photobioreactors, Appl. Microbiol. Biotechnol. 90 (2011) 1527–1536.
[37] S. Liehr, J. Eheart, M. Suidan, A modeling study of the effect of pH on carbon limited algal biofilms, Water Res. 22 (1988) 1033–1041.
[38] I. de Godos, V.A. Vargas, S. Blanco, M.C. García-González, R. Soto, P.A. García-Encina, E. Becares, R. Muñoz, A comparative evaluation of microalgae for the degradation of piggery wastewater under photosynthetic oxygenation, Bioresour. Technol. 101 (2010) 5150–5158.
[39] Y. Azov, J.C. Goldman, Free ammonia inhibition of algal photosynthesis in intensive cultures, Appl. Environ. Microbiol. 43 (1982) 735–739.
[40] E. Molina, J. Fernández, F.G. Acién, Y. Chisti, Tubular photobioreactor design for algal cultures, J. Biotechnol. 92 (2001) 113–131.
[41] I. Fernández, F.G. Acién, J.M. Fernández, J.L. Guzmán, J.J. Magán, M. Berenguel, Dynamic model of microalgal production in tubular photobioreactors, Bioresour. Technol. 126 (2012) 172–181.
[42] P.D. Tortell, Evolutionary and ecological perspectives on carbon acquisition in phytoplankton, Limnol. Oceanogr. 45 (2000) 744–750.
[43] J. Galmés, J. Flexas, A.J. Keys, J. Cifre, R.A.C. Mitchell, P.J. Madwick, R.P. Haslam, H. Medrano, M.A.J. Parry, Rubisco specificity factor tends to be larger in plant species from drier habitats and in species with persistent leaves, Plant Cell Environ. 28 (2005) 571–579.
[44] M.T. Madigan, J.M. Martinko, P.V. Dunlap, D.P. Clark, Brock Biology of Microorganisms, twelfth ed., Pearson International Edition, San Francisco, 2009.
[45] S. Raso, B. van Genugten, M. Vermuë, R.H. Wijffels, Effect of oxygen concentration on the growth of *Nannochloropsis* sp. at low light intensity, J. Appl. Phycol. 24 (2012) 863–871.
[46] E.R. Mattos, M. Singh, M.L. Cabrera, K.C. Das, Effects of inoculum physiological stage on the growth characteristics of *Chlorella sorokiniana* cultivated under different CO_2 concentrations, Appl. Biochem. Biotechnol. (2012), http://dx.doi.org/10.1007/s12010-012-9793-6.
[47] A. Papazia, P. Makridisb, P. Divanachb, K. Kotza-basisa, Bioenergetic changes in the microalgal photosynthetic apparatus by extremely high CO_2 concentrations induce an intense biomass production, Physiol. Plantarum 132 (3) (2008) 338–349.
[48] Y. Umino, Y. Shiraiwa, Effect of metabolites on carbonic anhydrase induction in *Chlorella regularis*, J. Plant Physiol. 139 (1991) 41–44.
[49] A.P. Abreu, B. Fernandes, A.A. Vicente, J. Teixeira, G. Dragone, Mixotrophic cultivation of *Chlorella vulgaris* using industrial dairy waste as organic carbon source, Bioresour. Technol. 118 (2012) 61–66.
[50] O. Perez-Garcia, F.M.E. Escalante, L.E. de-Bashan, Y. Bashan, Heterotrophic cultures of microalgae: metabolism and potential products, Water Res. 45 (2011) 11–36.
[51] T. Heredia-Arroyo, W. Wei, R. Ruan, B. Hu, Mixotrophic of *Chlorella vulgaris* and its potential application for the oil accumulation from non-sugar materials, Biomass Bioenergy 35 (2011) 2245–2253.
[52] N. Powell, A.N. Shilton, Y. Chisti, S. Pratt, Towards a luxury uptake process via microalgae – defining the polyphosphate dynamics, Water Res. 43 (2009) 4207–4213.
[53] N. Powell, A.N. Shilton, S. Pratt, Y. Chisti, Factors influencing luxury uptake of phosphorus by microalgae in waste stabilization ponds, Environ. Sci. Technol. 42 (2008) 5958–5962.
[54] D. Hernández, B. Riaño, M. Coca, M.C. García-González, Treatment of agro-industrial wastewater using microalgae–bacteria consortium combined with anaerobic digestion of the produced biomass. Bioresour. Technol., in press.
[55] E.A. Ehimen, Z.F. Sun, C.G. Carrington, E.J. Birch, J.J. Eaton-Rye, Anaerobic digestion of microalgae residues resulting from the biodiesel production process, Appl. Energy 88 (2011) 3454–3463.
[56] P. McCarty, Anaerobic waste treatment fundamentals – part two, Public Works 95 (10) (1964) 123–126.
[57] M.E. Alzate, R. Muñoz, F. Rogalla, F. Fdz-Polanco, S.I. Pérez-Elvira, Biochemical methane potential of microalgae: Influence of substrate to inoculum ratio, biomass concentration and pretreatment, Bioresour. Technol. 123 (2012) 488–494.
[58] S.S. Bajekal, N.S. Dharmadhikari, Use of poliphosphate accumulating organisms (PAOs) for treatment of phosphate sludge, twelfth World Lake Conference, India, 2008, pp. 918–922.
[59] T. Cai, S.Y. Park, Y. Li, Nutrient recovery from wastewater streams by microalgae: status and prospects, Renew. Sustain. Energy Rev. 19 (2013) 360–369.
[60] M.E. Huntley, D.G. Redalje, CO_2 mitigation and renewable oil from photosynthetic microbes: a new appraisal, Mitig Adapt Strat Global Clim 12 (2007) 573–608.
[61] C.G. Golueke, W.J. Oswald, Biological conversion of light energy to the chemical energy of methane, Appl. Microbiol. 7 (4) (1959) 219–227.

Nitrous oxide emissions from high rate algal ponds treating domestic wastewater

Alcántara, C., Muñoz, R., Norvill, Z., Plouviez, M., Guieysse, B. 2015. BITE. 177, 110–117.

Chapter 7

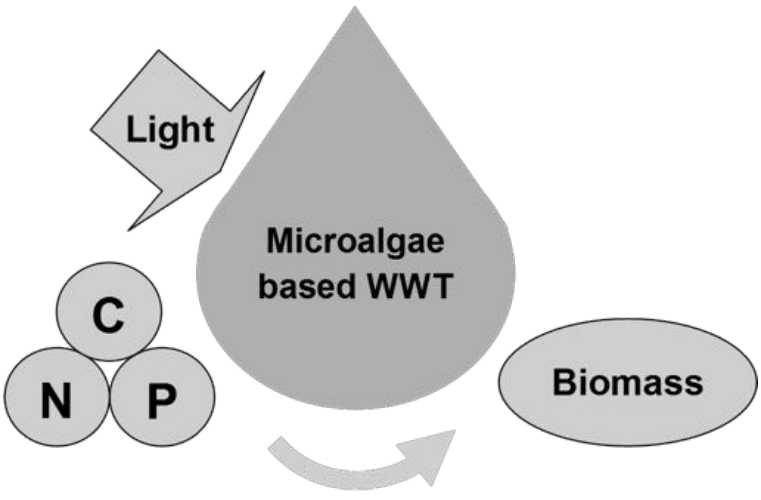

Bioresource Technology 177 (2015) 110–117

Contents lists available at ScienceDirect

Bioresource Technology

journal homepage: www.elsevier.com/locate/biortech

Nitrous oxide emissions from high rate algal ponds treating domestic wastewater

Cynthia Alcántara [a,b], Raúl Muñoz [b], Zane Norvill [a], Maxence Plouviez [a], Benoit Guieysse [a,*]

[a] School of Engineering and Advanced Technology, Massey University, Private Bag 11222, Palmerston North, New Zealand
[b] Department of Chemical Engineering and Environmental Technology, Valladolid University, Dr. Mergelina, s/n, 47011 Valladolid, Spain

HIGHLIGHTS

- Under normal operation, HRAP treating wastewater released <2 nmol N_2O/g TSS h.
- These N_2O emissions (⩽0.0047% N input) generated a low carbon footprint.
- External supply of nitrite significantly boosted N_2O production in darkness.
- Ammonium overloading was associated with N_2O emissions up to 11 nmol/g TSS h.
- *C. vulgaris* was the most likely significant N_2O producer in the HRAP microcosms.

GRAPHICAL ABSTRACT

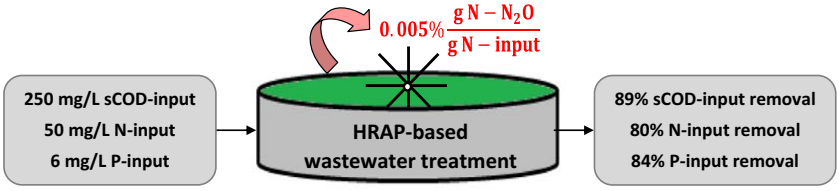

ARTICLE INFO

Article history:
Received 30 July 2014
Received in revised form 24 October 2014
Accepted 27 October 2014
Available online 18 November 2014

Keywords:
Algal pond
Chlorella vulgaris
Climate change
Nitrous oxide
Wastewater treatment performance

ABSTRACT

This study investigated the generation of N_2O by microcosms withdrawn from 7-L high rate algal ponds (HRAPs) inoculated with *Chlorella vulgaris* and treating synthetic wastewater. Although HRAPs microcosms demonstrated the ability to generate algal-mediated N_2O when nitrite was externally supplied under darkness in batch assays, negligible N_2O emissions rates were consistently recorded in the absence of nitrite during 3.5-month monitoring under 'normal' operation. Thereafter, HRAP A and HRAP B were overloaded with nitrate and ammonium, respectively, in an attempt to stimulate N_2O emissions via nitrite *in situ* accumulation. Significant N_2O production (up to 5685 ± 363 nmol N_2O/g TSS h) was only recorded from HRAP B microcosms externally supplied with nitrite in darkness. Although confirmation under full-scale outdoors conditions is needed, this study provides the first evidence that the ability of microalgae to synthesize N_2O does not affect the environmental performance of wastewater treatment in HRAPs.

1. Introduction

The treatment of wastewater in high rate algal ponds (HRAPs) arguably provides one of the most cost and resource efficient means to mass produce microalgae biomass for biofuel generation. In addition, these photobioreactors allow for a simultaneous nitrogen (N) and phosphorus (P) elimination through biomass assimilation at relatively short hydraulic retention time (HRT), which represents an important advantage in comparison with conventional wastewater treatment systems (De Godos et al., 2010). However, the benefits brought about by the use of wastewater as a source of nutrients and water might be compromised by the ability of microalgae and associated bacteria to synthesize N_2O (Weathers, 1984; Fagerstone et al., 2011; Albert et al., 2013; Guieysse et al.,

* Corresponding author.
E-mail address: mutora@iq.uva.es (R. Muñoz).

http://dx.doi.org/10.1016/j.biortech.2014.10.134
0960-8524/

2013), a critical greenhouse gas and ozone-depleting atmospheric pollutant (Ravishankara et al., 2009). For example, Florez-Leiva et al. (2010) detected N_2O emissions of 1–500 μmol of N_2O/m^2 d during *Nannochloris* cultivation in a 48 m^3 full-scale HRAP and Fagerstone et al. (2011) reported a N_2O emission factor of 0.0024% N-N_2O/N-input during *Nannochoropsis salina* cultivation in a bench-scale HRAP. While associated bacteria were suspected to cause N_2O emission in these past studies, recent findings have confirmed direct N_2O synthesis by axenic *Chlorella vulgaris* (Guieysse et al., 2013).

Despite the potential significance of N_2O emissions during algae cultivation, little is known about the mechanisms of N_2O synthesis by algae and/or associated microorganisms. Identifying key 'factors' and putative N_2O production routes is especially difficult during algae-based wastewater treatment because the bacterial, archaeal and algal pathways potentially involve similar precursors and enzymes (Hatzenpichler, 2012; Guieysse et al., 2013; Fig. 1). Hence, in view of the current lack of knowledge on the populations, mechanisms, and culture conditions involved in N_2O production from HRAPs, a better understanding of the role of microalgae in N_2O emissions during algae-based wastewater treatment in HRAPs is required before this cultivation platform can be scaled-up for biofuel production.

This work constitutes a study to assess the potential significance of N_2O emissions from two identical HRAPs inoculated with *C. vulgaris* and semi-continuously supplied with synthetic sewage. For this purpose, HRAP microcosms were periodically withdrawn and tested for N_2O production under various conditions using batch assays. Emphasis was given to the determination of the role of microalgae in N_2O emissions. The impact of the N-source and its loading on N_2O production was also assessed.

2. Methods

2.1. Microorganisms

The microalgae *C. vulgaris* was obtained as described by Novis et al. (2009) and cultivated in 250 mL E-flasks containing 125 mL of buffered BG-11 medium (pH ≈ 7.2; Guieysse et al., 2013) under a CO_2-enriched air atmosphere at 2% CO_2. E-flasks were incubated for 5 days at 25 ± 1.0 °C under continuous illumination (PAR = 92 μE/m^2 s) and shaking (160 rpm) using an orbital shaker (INFORS-HT Minitron incubation shaker, Switzerland).

A heterotrophic microbial inoculum was obtained by aerobically incubating a sample of soil (Palmerston North, New Zealand) in synthetic sewage water (SSW) composed of (per liter of deionized water): 160 mg peptone, 110 mg meat extract, 30 mg urea, 28 mg K_2HPO_4, 7 mg NaCl, 4 mg $CaCl_2{\cdot}2H_2O$ and 2 mg $MgSO_4{\cdot}7H_2O$ (OECD 303A, 1996). This SSW contained 250 ± 2 mg/L of chemical oxygen demand (COD), 50 ± 1 mg/L of total nitrogen (TN) and 5.7 ± 0.1 mg P-PO_4^{3-}/L. This culture was incubated for 7 days at 25 ± 1 °C under continuous darkness and magnetic agitation at 200 rpm.

A nitrifying culture was obtained by aerobically incubating a soil sample (Palmerston North, New Zealand) in Winogradsky Medium composed of (per liter of deionized water): 2 g $(NH_4)_2SO_4$, 1 g K_2HPO_4, 0.5 g $MgSO_4{\cdot}7H_2O$, 2 g NaCl, 0.4 $FeSO_4{\cdot}7H_2O$, 0.01 g $CaCO_3$. This culture was incubated for 7 days at 25 ± 1 °C under continuous darkness and magnetic agitation at 200 rpm. The presence of nitrite and nitrate in the medium after 7 days was confirmed by Ionic Chromatography analysis, which verified the nitrifying activity of the inoculum. The culture was centrifuged and the pellet was resuspended in SSW prior to inoculation in HRAPs.

2.2. High rate algal ponds: set-up and operating conditions

The experimental set-up consisted of two identical stainless steel HRAPs (A and B) with an individual working culture volume of 7 L (0.5 m long × 0.3 m wide × 0.06 m deep) and an illuminated area of 0.1 m^2. The reactors were illuminated using nine 36 W cool daylight fluorescent tubes (TLD 36 W/865, Philips) providing a PAR of 280 μE/m^2 s at the culture surface (measured with a 383274 data logger multimeter from EXTECH instruments, USA, equipped with a 401020 light adapter from the same manufacturer) applied using a 12:12 h light–dark cycle. In each reactor, the culture was mixed with a five-bladed paddle wheel operated at 28 rpm, which supported a liquid recirculation velocity of 0.1 m/s at the center of the pond channel. The HRAPs were initially filled with 7 L of BG-11 medium and inoculated with fresh *C. vulgaris* culture at an initial concentration of 81 ± 1 mg TSS/L. The heterotrophic microbial inoculum was resuspended in SSW and added to the HRAPs when the microalgae concentrations reached 414 ± 13 mg TSS/L. Following this, semi-continuous operation was started by daily replacing 1 L of HRAP culture with freshly prepared SSW in order to maintain a HRT of 7 days, which represents a conservative HRT for domestic wastewater treatment in HRAPs (García et al., 2006). Water evaporation losses were daily recorded and compensated with distilled water to avoid salt accumulation. The HRAPs were thus fed with SSW containing 50 ± 1 mg TN/L during the first 60 days of operation (Period I) before being inoculated with the nitrifying culture and further fed with the same SSW for an additional 45 days period (Period II). Hence, HRAP A and B were identically operated during Periods I and II. Thereafter, the influents semi-continuously fed to HRAP A and HRAP B were further supplemented with 100 mg N-NO_3^-/L_{SSW} and 100 mg N-NH_4^+/L_{SSW}, respectively, over the last 45 days of operation (Period III). Nitrate and ammonium addition at high concentration during Period III was performed to stimulate

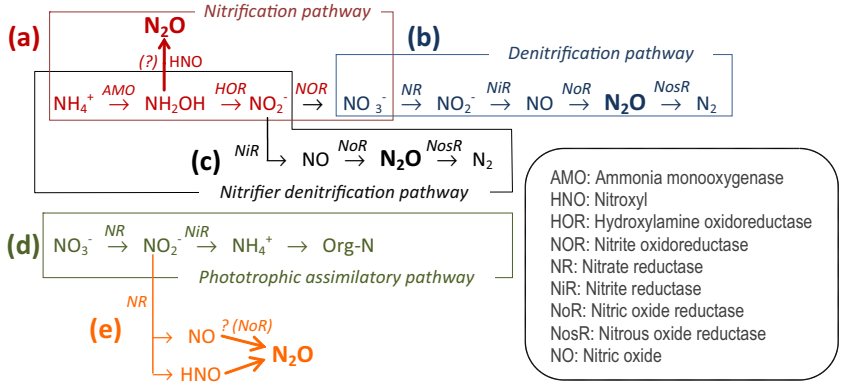

Fig. 1. Potential N_2O production metabolic pathways occurring in HRAPs ((?) = unclear pathway and/or putative enzyme type).

conditions potentially favorable to N_2O emissions in these systems based on past studies linking N_2O emissions in HRAPs with nitrification (Florez-Leiva et al., 2010) or denitrification (Fagerstone et al., 2011). This operational period should therefore not be considered as representative to real domestic wastewater treatment. An additional buffer of 1.52 g KH_2PO_4/L_{SSW} and 3.1 g K_2HPO_4/L_{SSW} was also supplemented to HRAP B during Period III to maintain the cultivation pH around 7 and therefore promote bacterial nitrification and minimize N-losses by NH_3 stripping. The HRAPs were operated indoors at room temperature (22 ± 1 °C).

Process monitoring involved the daily measurement (immediately before feeding) of the algal–bacterial biomass concentration (total suspended solids, TSS), optical density (OD), dissolved oxygen (DO) concentration, temperature (T) and pH in the HRAPs. The concentrations of dissolved and total COD, N-NH_4^+, N-NO_3^-, N-NO_2^- and P-PO_4^{3-} in the influent and effluent of the HRAPs were measured twice per week. The settleable solids, carbon (C), N, P content and the specific heat value of the algal–bacterial biomass produced were also experimentally determined every two months. The photosynthetic efficiency (PE) (in percentage of PAR reaching the pond surface photochemically converted into biomass) and concentration of *C. vulgaris* in the reactors were determined using a dynamic simulation of microbial growth based on De Godos et al. (2012). These results were confirmed by OD and measure of Chlorophyll content.

2.3. N_2O assays

N_2O production assays were performed in duplicate in 120 ml serum bottles filled with 50 ml of fresh HRAP cultures broth and air as gas headspace. The flasks were immediately sealed with butyl septa and aluminum caps and incubated at 25 ± 1 °C at 160 rpm (INFORS-HT Minitron incubation shaker, Switzerland) in darkness or under continuous illumination (92 μE/m^2 s of PAR) for 4–5 h. This incubation period was selected based on analytical constrains (sensitivity) and the previous work published by Guieysse et al. (2013), who reported that the kinetics of N_2O production by axenic *C. vulgaris* in batch assays were characterized by a rapid initial production for 4 h followed by a period of "linear" evolution lasting more than 24 h. Gas samples of 5 ml were taken at the end of the incubation to measure the N_2O headspace concentrations by Gas Chromatography Electron Captor Detector (GC-ECD). The results presented account for the total amount of N_2O produced in the flasks assuming that the aqueous N_2O concentration was at equilibrium with the gas phase (Henry constant of 0.025 mol/atm L, National Institute of Standards and Technology, USA). The initial and final headspace pressures were recorded using a SPER SCIENTIFIC pressure meter. Unless otherwise specified, the terms A and B are henceforth used to designate to origin of the HRAP (A or B) culture tested. Batch assays using HRAPs cultures supplied with 12 mM of N-NO_2^- (intermediate concentration as those tested by Guieysse et al., 2013) and incubated in darkness were repeatedly conducted given the frequent occurrence of nitrite at night during wastewater treatment HRAPs operated at high loading rates (García et al., 2006; De Godos et al., 2010) and past studies linking phototrophic N_2O synthesis to nitrite reduction under conditions repressing Photosystem II (Weathers, 1984; Albert et al., 2013; Guieysse et al., 2013). Additional batch assays supplied with 100 mg penicillin/L (purity > 99%; Penicillin G-K-Salt 1 580 IU/mg $C_{16}H_{17}N_2O_4SK$, SERVA, Germany) and 25 mg streptomycin/L (purity > 99%; Streptomycinsulfat, MERCK, USA) were regularly conducted to determine the significance of bacterial activity on N_2O generation, as reported by Fagerstone et al. (2011). These assays were supplied with 12 mM of N-NO_2^- and incubated under darkness. The first set of batch assays performed (Period I) also tested the influence of illumination on N_2O emission from HRAP cultures supplemented with 12 mM of N-NO_2^- or N-NH_4^+. Modeling of heterotrophic activity (based on remaining COD aerobic consumption and endogenous respiration) in the flasks showed there was enough oxygen in the gas headspace to ensure fully oxic conditions during the entire duration of the assays (data not shown).

2.4. Analytical procedures

The concentrations of TSS, dissolved and total COD, and settleable solids were determined according to Standard Methods (Eaton et al., 2005). OD was measured by spectrophotometer Helios-Alpha (Thermo Scientific, USA) at 683 nm. A CHEMets Kit Ammonia K-1510 (CHEMetrics, USA) was used to measure N-NH_4^+ concentration. N-NO_3^-, N-NO_2^- and P-PO_4^{3-} concentrations were analyzed using a Dionex ICS-2000 Ion Chromatograph (Dionex Corporation, Sunnyvale, USA) equipped with a Dionex IonPac AS11-HC column (250 mm × 4 mm) eluted at 1 mL/min with a 13 mM KOH aqueous solution. The DO concentration, T and pH were measured *in situ* with a Eutech WP PCD650 multiprobe analyser (Thermo Fisher Scientific Inc, USA). N_2O gas concentration was analyzed using a Shimadzu GC-2010 plus GC-ECD (Shimadzu, Japan) equipped with an Alltech Porapack QS 80/100 (12′ × 1/8″ × 0.85″ SS) column (Sigma–Aldrich, USA). The injector and detector temperatures were maintained at 380 °C and 315 °C, respectively, while nitrogen was used as the carrier gas at 30 mL/min. The biomass C and N content and specific heat were determined using an Elemental analyzer cube Vario Macro (Elementar, Germany) coupled with a LECO AC350 bomb calorimeter (LECO, Germany), while P content was measured using an Inductively Coupled Plasma Optical Emission Spectrophotometer (ICP-OES).

Polymerase Chain Reaction (PCR) analysis was carried out as follows: Aliquots were daily withdrawn from each HRAP and stored at −40 °C prior to analysis. After thawing, 1 mL of sample was transferred into an Eppendorf tube and spun at 13,000 g in a bench top microcentrifuge for 5 min to pellet the biomass. The supernatant was removed and Deoxyribonucleic Acid (DNA) samples were extracted using the Bioline isolate Genomic DNA kit according to the manufacturer's protocol (Bioline). After extraction, DNA extracts were quantified using a ND-1000 NanoDrop sampler (Thermo Scientific). PCR was carried out on the extracted genomic DNA using the primers and amplification conditions shown in Table 1. Each PCR reaction contained 1× Buffer with 1.5 mM $MgCl_2$ (Roche Diagnostics), 250 μM each dNTP, 10 pmol of each primer, 2 μl of template DNA and 1U Taq polymerase (Roche Diagnostics), in a final volume of 20 μl. Following PCR, 8 μl of reaction mix was analyzed on an agarose gel (2% (w/v) agarose in 1× Tris–acetate–EDTA buffer) and visualized using SYBR-SAFE (Invitrogen) on a gel documentation system (BIORAD). The norB, cnorB and qnorB primer pairs amplify fragments of genes encoding for bacterial NoR (nitric oxide reductase). The amoA 1F and 2R primer pair specifically amplifies a fragment of gene encoding for ammonia monooxygenase in bacteria whereas the amoA F and R amplifies a fragment gene encoding for ammonia monooxygenase in archaea. The 16S primer pairs 340F/1000R amplify a region of the 16S rDNA in archaea and are considered as 'universal' primer pairs for archaea. A negative control was included for each primer pairs; this reaction contains all components except the template DNA.

3. Results and discussion

3.1. HRAP performance

Although the full-scale implementation of HRAPs for wastewater remains limited, high performance was consistently reported during pilot-scale studies: Buelna et al. (1990) thus reported a

Table 1
Primers and conditions used during PCR analysis.

Gene	Primers	Sequence (5′–3′)	Exp. size (bp)	PCR conditions
Bacteria				
norB	norB1F	CGNGARTTYCTSGARCARCC	670	95 °C–5 min [95 °C–30 s, 54 °C–45 s, 68 °C–45 s] × 35 cycles 68 °C–7 min, 10 °C hold (Fagerstone et al., 2011)
	norB8R	CRTADGCVCCRWAGAAVGC		
cnorB	cnorBF	GACAAGNNNTACTGGTGGT	389	
	cnorBR	GAANCCCCANACNCCNGC		
qnorB	qnorBF	GGNCAYCARGGNTAYGA	262	94 °C–5 min [94 °C–20 s, 55 °C–1 min, 72 °C–1 min] × 30 cycles, 72 °C–10 min, 10 °C hold (Rotthauwe et al., 1997)
	qnorBR	ACCCANAGRTGNACNACCCACCA		
amoA	amoA1F	GGGGTTTCTACTGGTGGT	491	
	amoA2R	CCCCTCKGSAAAGCCTTCTTC		
Archaea				
amoA	amoAF	STAATGGTCTGGCTTAGACG	635	95 °C–5 min [94 °C–45 s, 53 °C–60 s, 72 °C–60 s] × 30 cycles 72 °C–15 min, 10 °C hold (Francis et al., 2005)
	amoAR	GCGGCCATCCATCTGTATGT		
16S	340F	CCCTAYGGGGYGCASCAG	660	98 °C–2 min [95 °C–30 s, 57 °C–30 s, 72 °C–90 s] × 30 cycles 72 °C–7 min, 10 °C hold (Gantner et al., 2011)
	1000R	GGCCATGCACYWCYTCTC		

88% COD removal efficiency in a 369 m^3 *Chlorella*-based HRAP operated at 10 d HRT; Arbib et al. (2013) reported a productivity of 5 g TSS/m^2 d in a 530 L of HRAP operated at 10 d HRT with *Scenedesmus obliquus*; De Godos et al. (2010) reported a 98 ± 1% ammonium removal efficiency in a 465 L HRAP; and Asmare et al. (2013) reported a 77% P-PO_4^{3-} removal efficiency in a 470 L open pond. As can be seen in Table 2, both HRAPs supported high and consistent sCOD, N, and P removal efficiencies during the periods representative to 'normal' operation with domestic wastewater (Periods I and II). This substrate removal was associated with total biomass productivities of 4.7 ± 0.1 and 5.1 ± 0.2 g TSS/m^2 d during Periods I and II, respectively (Table 2). The C, N and P content of the algal–bacterial biomass remained around 47 ± 2%, 8.1 ± 0.4% and 1.0 ± 0.1% in both reactors, regardless of the N and P loads (Table 2). Mass-balance analysis showed 78–82% and 83–84% of the influent TN and P-PO_4^{3-} were assimilated into biomass, respectively (Table 2). An additional TN removal of 20 ± 4% in both reactors during Periods I and II was likely caused by ammonia volatilization since pH was often high (Table 2). The specific heat of the algal–bacterial biomass was around 22 ± 5 kJ/g in both HRAPs (Table 2), in agreement with the calorific values of *C. vulgaris* cultures reported by Illman et al. (2000). Based on this data and the modeling of heterotrophic growth, the photosynthetic efficiency of *C. vulgaris* was similar in both reactors and estimated to 3.2–3.3% and 3.4–3.6% during Periods I and II, respectively (Table 2), in agreement with PEs reported in outdoors photobioreactors (Béchet et al., 2013). DO concentration remained high at all times during operation, even immediately after feeding and at night time (a consequence of the high turbulence and shallow geometry of the laboratory-scale reactors). Overall, the performance of the reactors agrees with heterotrophic and phototrophic growth theories and past data, suggesting the activity of microorganisms in the reactors can be considered as 'normal'. Results from N_2O emission monitoring can therefore be regarded as representative of domestic wastewater treatment in HRAPs, with consideration of the limitations associated with the use of indoor conditions and synthetic sewage.

3.2. Potential sources of N_2O from HRAPs

N_2O can be biologically generated by nitrifying bacteria, denitrifying bacteria, nitrifying–denitrifying bacteria, ammonium oxidizing archaea and microalgae (Fig. 1). The potential occurrence and significance of these pathways in wastewater treatment HRAPs is discussed below. With regards to N_2O synthesis via nitrification, and despite the inoculation with a nitrifying culture at the start of Period II, PCR analysis showed archaeal amoA and16s rRNA genes were never detected during the entire experiment while bacterial amoA genes were clearly detected at the start of Period I in HRAP A and at the beginning and end of Period III in HRAP B. Approximately 80% of the nitrogen supplied to the HRAPs was assimilated into biomass during Periods I and II. This high assimilation rate and the high pH conditions (favorable to ammonia volatilization) evidencing CO_2 transfer limitation, suggest slow-growing nitrifiers were outcompeted for N and/or C supply in the HRAPs. The light reaching the HRAPs (280 μE/m^2 s at the top of the culture) may have also inhibited bacterial and archaeal nitrifiers as Guerrero and Jones (1996) reported a bacterial nitrification inhibition of 80% at a light intensity of 115 μE/m^2 s, whereas Merbt et al. (2012) and French et al. (2012) reported archaeal growth inhibition at 15 μE/m^2 s and 30 μE/m^2 s, respectively, with no recovery of nitrifying activity following light deprivation.

With regards to N_2O synthesis by bacterial denitrifiers, PCR analysis evidenced the presence of norB, cnorB and qnorB genes in all samples withdrawn during Periods I and II. This detection is expected during wastewater treatment (since bacterial denitrifiers are facultative anaerobic heterotrophs involved in biodegradable COD (bCOD) removal) and does not inform on the quantitative significance of N_2O emissions via denitrification considering that DO concentration remained high at all times. Both Fagerstone et al. (2011) and Harter et al. (2013) hypothesized that bacterial denitrification in low-oxygen micro-environments caused N_2O emissions during algae cultivation. However, Guieysse et al. (2013) challenged the significance of this mechanism in well-mixed photobioreactors and demonstrated axenic *C. vulgaris* could indeed synthesize N_2O, possibly via nitrate reductase (NR)-mediated nitrite reduction into either nitrous oxide (NO) or nitroxyl (HNO) (Fig. 1e). It must finally be noted that with regards to the efficient bCOD removal reported and the low nitrate/dissolved oxygen concentration ratio (Table 2), heterotrophic denitrification was likely outcompeted for bCOD availability.

As seen in Fig. 2, the impacts of light and nitrite on N_2O emissions and the lack of repression of these emissions by bacterial antibiotics (Fig. 3) confirmed *C. vulgaris* was the most likely quantitatively significant N_2O producer found in the HRAP microbial communities. The reported repressing impact of light on N_2O emissions from algae cultures (Weathers, 1984; Fagerstone et al., 2011; Guieysse et al., 2013) is possibly explained by the light-dependent competitive reduction of nitrite into ammonium by nitrite-reductase (Fig. 1d).

3.3. Significance of N_2O emissions from HRAPs

As shown in Fig. 4, N_2O emissions consistently lower than 2 nmol N_2O/g TSS h were recorded from HRAP cultures sampled

Table 2
Summary of process parameters and their corresponding removal efficiencies during Periods I–III; the concentrations shown correspond to the values just before daily HRAPs feeding with fresh SSW.

	Periods I & II	Period I		Period II		Period III			
	HRAP A & B	HRAP A	HRAP B	HRAP A	HRAP B	HRAP A		HRAP B	
	Input	Output				Input	Output	Input	Output
Biomass productivity (g TSS/m^2 d)	N.A.[a]	4.6 ± 0.1	4.7 ± 0.1	5.2 ± 0.2	4.9 ± 0.2	N.A.[a]	4.4 ± 0.2	N.A.[a]	4.1 ± 0.2
TSS (mg/L)		466 ± 14	475 ± 14	534 ± 18	504 ± 17		461 ± 15		417 ± 17
Algae (mg/L)		409	419	476	448		403		361
PE (%)		3.2	3.3	3.6	3.4		3.2		2.9
Heat value (kJ/g)		22 ± 4	22 ± 4	21 ± 5	21 ± 4		21 ± 5		22 ± 6
OD		1.9 ± 0.0	1.9 ± 0.0	1.8 ± 0.1	1.4 ± 0.1		1.4 ± 0.1		1.4 ± 0.2
COD_{TOT} (mg/L)		617 ± 6	620 ± 8	629 ± 7	611 ± 13		549 ± 19		513 ± 37
COD_{SOL} (mg/L)	250 ± 2	35 ± 4	37 ± 4	23 ± 3	19 ± 3	229 ± 11	36 ± 5	259 ± 14	21 ± 5
COD_{SOL} removal (%)	N.A.[a]	86 ± 3	86 ± 2	91 ± 1	93 ± 1	85 ± 7		84 ± 7	
N-NH_4^+ (mg/L)	48 ± 1	0.1 ± 0.0	0.1 ± 0.0	0.1 ± 0.0	0.1 ± 0.0	48 ± 1	0.1 ± 0.0	148 ± 1	38 ± 4
N-NO_3^- (mg/L)	1.6 ± 0.0	0.3 ± 0.0	0.3 ± 0.1	0.3 ± 0.0	0.1 ± 0.0	102 ± 0	60 ± 19	1.6 ± 0.0	0.2 ± 0.2
N-NO_2^- (mg/L)	0.0 ± 0.0	0.0 ± 0.0	0.0 ± 0.0	0.0 ± 0.0	0.0 ± 0.0	0.0 ± 0.0	4.4 ± 1.0	0.0 ± 0.0	0.9 ± 0.5
TN (mg/L)	50 ± 1	0.4 ± 0.0	0.4 ± 0.1	0.4 ± 0.0	0.2 ± 0.0	150 ± 1	65 ± 19	150 ± 1	39 ± 3
N biomass (mg/L)	N.A.[a]	39 ± 2	41 ± 2	41 ± 1	40 ± 3	N.A.[a]	37 ± 3	N.A.[a]	34 ± 2
Inlet TN removed in biomass (%)		78 ± 5	80 ± 4	82 ± 3	78 ± 5		25 ± 2		23 ± 1
Inlet TN lost by stripping (%)		22 ± 5	20 ± 4	18 ± 3	22 ± 5	–		–	
TN removal (%)		99 ± 3	99 ± 3	99 ± 3	100 ± 3	–		–	
P-PO_4^{3-} (mg/L)	5.7 ± 0.1	1.0 ± 0.2	1.0 ± 0.1	0.9 ± 0.2	0.9 ± 0.1	5.7 ± 0.3	0.8 ± 0.4	902 ± 3	898 ± 5
P biomass (mg/L)	N.A.[a]	4.7 ± 0.1	4.7 ± 0.2	4.8 ± 0.6	4.8 ± 0.9	N.A.[a]	4.8 ± 0.5	N.A.[a]	3.9 ± 0.4
Inlet P-PO_4^{3-} removed in biomass (%)		83 ± 3	83 ± 4	84 ± 11	84 ± 16		85 ± 10		–
P-PO_4^{3-} removal (%)		83 ± 3	83 ± 3	84 ± 3	84 ± 3	85 ± 9		–	
C (%)		47 ± 2	46 ± 9	47 ± 1	47 ± 0	N.A.[a]	47 ± 1	N.A.[a]	46 ± 1
N (%)		8.5 ± 0.4	8.5 ± 0.3	7.7 ± 0.1	7.8 ± 0.4		8.1 ± 0.5		8.2 ± 0.4
P (%)		1.0 ± 0.0	1.0 ± 0.0	0.9 ± 0.1	0.9 ± 0.2		1.1 ± 0.1		0.9 ± 0.1
Settleable solids (mg/L)		233 ± 28	295 ± 38	229 ± 20	305 ± 23		245 ± 21		300 ± 33
pH	6.7 ± 0.1	8.3 ± 0.3	8.3 ± 0.2	9.3 ± 0.2	9.2 ± 0.2	7.0 ± 0.2	9.0 ± 0.2	7.1 ± 0.2	7.2 ± 0.1
T	25 ± 1	21 ± 1	21 ± 1	23 ± 1	23 ± 1	25 ± 0	22 ± 0	25 ± 0	22 ± 0
DO (mg O_2/L)	9.2 ± 0.2	10 ± 0	10 ± 0	10 ± 0	9.8 ± 0.8	9.2 ± 0.2	10 ± 0	9.2 ± 0.2	9.0 ± 0.9
Evaporation (L/m^2 d)	N.A.[a]	6.5 ± 0.4		7.0 ± 0.2		6.8 ± 0.2			

[a]N.A. = Not applicable as input parameter. The grey shade was used just to differentiate Period III from Period I and II. Period III operation coditions should not be considered as representative to real domestic wastewater treatment.

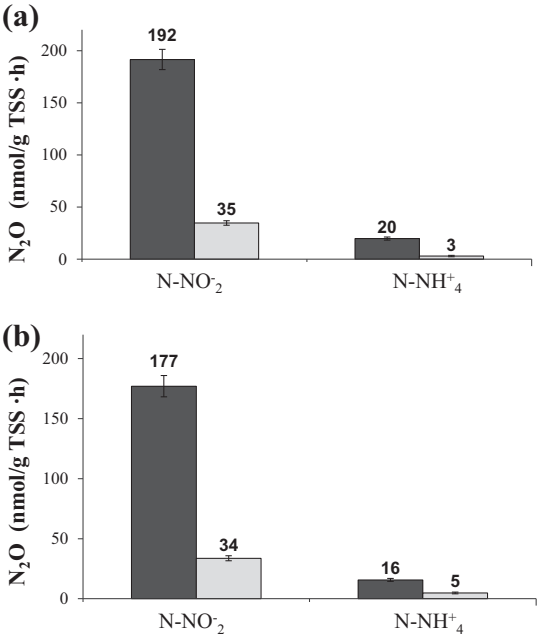

Fig. 2. N_2O production rates by microcosms withdrawn at 8:00 am from HRAP A (a) and HRAP B (b) during Period I, supplemented with 12 mM of $N\text{-}NO_2^-$ or $N\text{-}NH_4^+$, and incubated under continuous illumination (light columns) or under darkness (dark columns). Vertical bars show variations between duplicates.

under 'normal' N-loading of 7.1 g $N/m^3_{reactor}$ d, with no significant variation observed when samples were withdrawn at various times during a day cycle (ANOVA test at 95% of confidence interval). A 24-h average emission rate of 1 nmol N_2O/g TSS h would thus result in an emission factor of 0.0047% g $N\text{-}N_2O$/g N-input in a typical HRAP. Based on the analysis of Alcántara et al. (2014), N_2O emissions from domestic wastewater treatment in 0.3 m deep HRAPs operated at 6 d HRT could reach 0.3 g N_2O/capita-yr, which is 10-fold lower than the emission factor of 3.2 g N_2O/capita-yr (corresponding emission factor of 0.035%) recommended by the IPCC for quantifying N_2O emissions during wastewater treatment (IPCC, 2006). The secondary treatment of the sewage generated by 1 billion humans using HRAPs would therefore generate minor emissions (0.19 Gg $N\text{-}N_2O$/yr) in comparison to global emissions from domestic wastewater (0.22 Tg $N\text{-}N_2O$/yr; Mosier et al., 1999) and total anthropogenic N_2O emissions (6.9 Tg $N\text{-}N_2O$/yr; IPCC, 2001). While direct comparison with N_2O emissions from activated sludge processes is difficult given the large variation of the rates reported (Ahn et al., 2010), the carbon footprint of N_2O emissions from HRAPs (1.1 g of CO_2/m^3 wastewater treated) compares favorably against the carbon footprints from electricity use for aerating and mixing activated sludge tanks (119–378 g CO_2/m^3) and for mixing HRAP (3–14 g CO_2/m^3 treated). If more refined impact assessment also considering ozone depletion should be undertaken, this analysis suggests that under typical operation, N_2O generation by microalgae should not threat the performance of wastewater treatment in HRAPs with regards to climate change (Periods I and II in Fig. 4).

However, as seen in Figs. 2 and 3, the external supply of nitrite significantly boosted N_2O production during Periods I and II, in agreement with the observations linking nitrite availability and N_2O synthesis in microalgae (Weathers, 1984; Albert et al., 2013; Guieysse et al., 2013) and explained by the likely reduction of nitrite into N_2O as explained above (Fig. 1e). This effect deserves consideration given nitrite concentrations up to 35 ± 8 mg $N\text{-}NO_2^-$/L were reported by De Godos et al. (2010) as a result of partial ammonium nitrification during the treatment of diluted swine manure in outdoors HRAPs supplied with flue gas. This concentration of nitrite could cause N_2O emissions near 100 nmol/g TSS h based on the data reported by Guieysse et al. (2013) for axenic *C. vulgaris*. Therefore, the fact that inhibition of bacterial nitrification via CO_2 limitation during Periods I and II may have prevented nitrite accumulation in the experimental HRAPs herein studied must be considered before broadly extrapolating the environmental impact of HRAP-mediated N_2O.

To verify if nitrite accumulation or culture stress caused by N-overloading could trigger high N_2O emissions, the influents fed to HRAP A and B were further supplied with 100 mg $N\text{-}NO_3^-$/Lssw and 100 mg $N\text{-}NH_4^+$/Lssw, respectively (Period III). Although these changes did not dramatically impact photosynthetic efficiency and COD removal in the two reactors (Table 2), N-overload was associated with nitrite accumulation in HRAP A and, albeit weak, in HRAP B (Fig. 4). Interestingly, the abilities of the HRAPs' microbial communities to synthesize N_2O began to diverge thereafter:

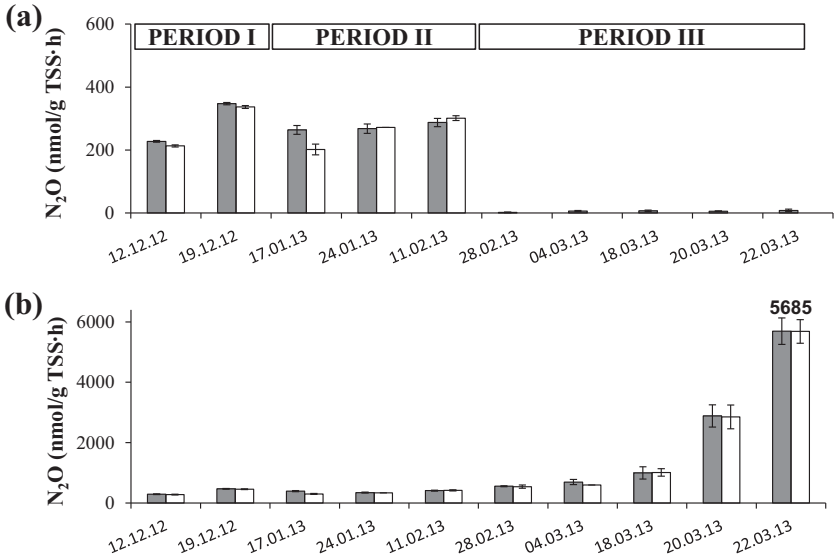

Fig. 3. N_2O production rates from microcosms withdrawn at 8:00 am from HRAP A (a) and HRAP B (b), incubated under darkness and supplied with 12 mM of $N\text{-}NO_2^-$ with (grey columns) or without (white columns) antibiotics. Vertical bars show variations between duplicates.

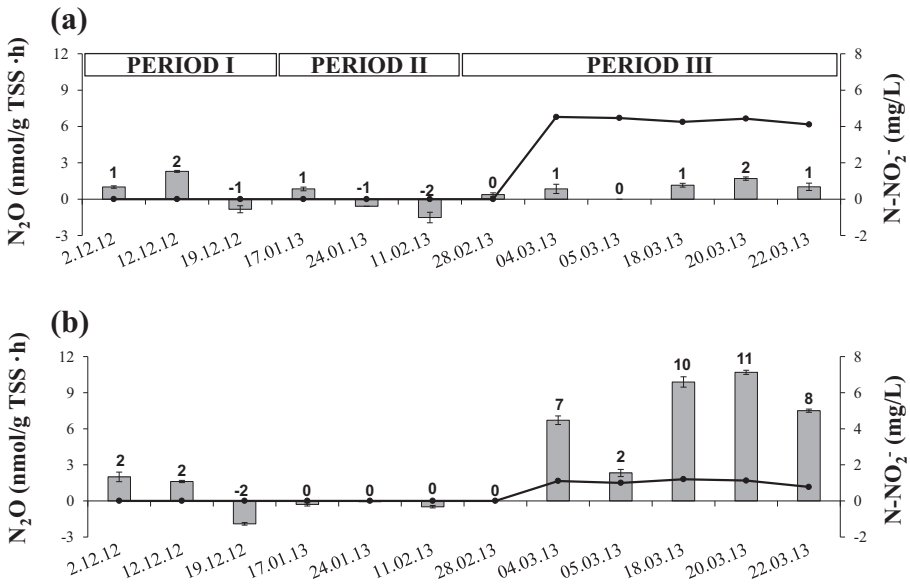

Fig. 4. Effluent N-NO_2^- concentrations (–●–) and N_2O production rates (columns) from microcosms withdrawn at 8:00 am from HRAP A (a) and HRAP B (b) and incubated under darkness. Vertical bars show variations between duplicates.

While N_2O production was negligible despite the presence of 4.4 ± 1.0 mg N-NO_2^-/L in HRAP A culture broth (Fig. 4a), N_2O emission increased up to 11 ± 0.2 nmol N_2O/g TSS h in HRAP B during Period III (Fig. 4b). In addition, when nitrite was externally supplied in batch assays, N_2O emissions from HRAP A microcosms drastically dropped (Fig. 3a), in contrast to HRAP B aliquots, in which this putative substrate triggered N_2O emissions up to 5685 ± 363 nmol N_2O/g TSS h (Fig. 3b). Despite the fact that norB genes were detected in HRAP A, bacterial nitrate denitrification (Fig. 1b) was unlikely in this system because DO concentration remained above 7 mg O_2/L (even at night) during the entire experiment whereas active denitrification occurs at O_2 concentrations of 0.5 mg/L (Wang et al., 2008). Under the hypothesis that N_2O emissions in these tests originated from nitrite reduction by *C. vulgaris* NR, a more plausible explanation for the drop of N_2O production seen in the positive controls assayed during Period III could have been the competitive substrate inhibition of nitrate (the 'natural' preferred substrate) and nitrite for NR (Fig. 1d and e) (Howard and Solomonson, 1981; Pessarakli, 2005). Additional 'competitive' batch assays however revealed nitrate addition did not impact N_2O production by axenic *C. vulgaris* in the presence of nitrite (data not shown), which could indicate another pathway is involved in N_2O synthesis (Tischner et al., 2004; Kamp et al., 2013). These results do not however provide unequivocal evidence for this because nitrate is also known to remove NR repression and its impact on NR activity depends on many factors (Pistorius et al., 1976; Berges, 1997), as further discussed below. Regardless the mechanisms involved, the influence of nitrate concentration on N_2O emissions is unclear and deserves further investigation.

Ammonium overloading was conducted at neutral pH in HRAP B (Phase III) (Table 2) and associated with a clear detection of bacterial amoA genes at the beginning and end of Period III, suggesting nitrification (Fig. 1a) could have caused the weak increase (1.0 ± 0.1 mg N-NO_2^-/L) in nitrite concentration in this reactor (Fig. 4b). However, bacterial nitrification unlikely caused the increase in N_2O production because the addition of antibiotics did not repress N_2O emissions during the entire experiment (Fig. 3b). Instead, bacterial nitrification followed by rapid algal uptake of nitrite in HRAP B culture broth may have improved the ability of *C. vulgaris* to synthesis N_2O prior to the addition of nitrite and antibiotics during batch assays. Interestingly, the positive influence of ammonium loading on N_2O emissions during Phase III opposes the common observation that ammonium represses NR activity (Berges, 1997). As in the case of the HRAP A microcosms during Phase III, it is important to consider the NR-mediated pathway for N_2O synthesis, albeit supported by considerable evidence in both plants and algae cells (Guieysse et al., 2013), remains an hypothesis and that alternative pathways have been proposed for NO and N_2O (Tischner et al., 2004; Kamp et al., 2013). However, the results herein presented do not unequivocally invalidate the NR-pathway hypothesis because *in vitro* NR activity depends on numerous factors (e.g. pH, intracellular concentrations of reductants and N substrates) and because NR regulation involves the constant turnover of precursors which expression and activities are themselves regulated by numerous factors (e.g. environmental changes, C and N fluctuations; Pistorius et al., 1976; Berges 1997). So the apparent 'booster' effect of ammonium seen in Fig. 4b could be linked to indirect effects causing weaker repression of the NO-synthase activity of NR prior to nitrite exposure during Phase III. Phosphate and neutral pH are also known to enhance NR activity (Howard and Solomonson, 1981; Kay and Barber, 1986). While further mechanistic investigation was beyond the scope of this study, the dramatic changes in N_2O-production abilities reported during Period III evidence the very high sensitivity of N_2O emissions to process operation. Based on these results, it is unfortunately premature to discuss possible mitigation strategies although minimizing nitrite accumulation seems to be of upmost importance. Further research is therefore recommended given the current lack of knowledge in this area.

4. Conclusions

N_2O emissions from HRAP cultures remained consistently low, even under high N-supply operation. However, HRAPs microcosms demonstrated the potential to generate N_2O when nitrite was externally supplied under darkness in batch assays. Further experiments confirmed these emissions were algal-mediated, likely through intracellularly nitrite reduction into N_2O by the enzyme nitrate reductase. Although thorough impact assessment and monitoring under full-scale conditions are needed, these results provide the first confirmation of the low N_2O-footprint of

wastewater treatment under "normal" conditions (Periods I and II) in lab-scale HRAPs.

Acknowledgements

This research was supported by the regional government of Castilla y Leon and the European Social Fund (Contract No. E-47-2011-0053564 and project Ref. GR76), the Spanish Ministry of Economy and Competitiveness (project CTQ2012-34949), Massey University, and the Marsden Fund Council from the New Zealand Government administrated by the Royal Society of New Zealand. Trish McLenachan, Quentin Béchet, Anne-Marie Jackson, John Edwards, Julia Stevenson, Chris Pratt and John Sykes are gratefully acknowledged for practical assistance.

Appendix A. Supplementary data

Supplementary data associated with this article can be found, in the online version, at http://dx.doi.org/10.1016/j.biortech.2014.10.134.

References

Ahn, J.H., Kim, S., Park, H., Rham, B., Pagilla, K., Chandran, K., 2010. N_2O emissions from activated sludge processes, 2008–2009: monitoring results of a national monitoring survey in the United States. Environ. Sci. Technol. 44, 4505–4511.

Albert, R.K., Bruhn, A., Ambus, P., 2013. Nitrous oxide emission from *Ulva lactuca* incubated in batch cultures is stimulated by nitrite, nitrate and light. J. Exp. Mar. Biol. Ecol. 448, 37–45.

Alcántara, C., Posadas, E., Guieysse, B., Muñoz, R., 2014. Microalgae-based waste water treatment. In: Se-Kwon, K. (Ed.), Handbook of Microalgae: Biotechnology Advances. Elsevier (In press).

Arbib, Z., Ruiz, J., Álvarez-Díaz, P., Garrido-Pérez, C., Barragán, J., Perales, J.A., 2013. Long term outdoor operation of a tubular airlift pilot photobioreactor and a high rate algal pond as tertiary treatment of urban wastewater. Ecol. Eng. 52, 143–153.

Asmare, A.M., Demessie, B.A., Murthy, G.S., 2013. Baseline study on the dairy wastewater treatment performance and microalgae biomass productivity of an open pond pilot plant: Ethiopian case. J. Algal Biomass Utln. 4, 88–109.

Béchet, Q., Muñoz, R., Shilton, A., Guieysse, B., 2013. Outdoor cultivation of temperature-tolerant *Chlorella sorokiniana* in a column photobioreactor under low power-input. Biotechnol. Bioeng. 110, 118–126.

Berges, J., 1997. Miniview: algal nitrate reductases. Eur. J. Phycol. 32, 3–8.

Buelna, G., Bhattarai, K.K., de la Noüe, J., Taiganides, E.P., 1990. Evaluation of various flocculants for the recovery of algal biomass grown on pig-waste. Biol. Waste 31, 211–222.

De Godos, I., Blanco, S., García-Encina, P.A., Becares, E., Muñoz, R., 2010. Influence of flue gas sparging on the performance of high rate algae ponds treating agro-industrial wastewaters. J. Hazard. Mater. 179, 1049–1054.

De Godos, I., Muñoz, R., Guieysse, B., 2012. Tetracycline removal during wastewater treatment in high-rate algal ponds. J. Hazard. Mater. 229–230, 446–449.

Eaton, A.D., Clesceri, L.S., Greenberg, A.E., 2005. Standard Methods for the Examination of Water and Wastewater, 21st ed. American Public Health Association/American Water Works Association/Water Environment Federation, Washington DC.

Fagerstone, K.D., Quinn, J.C., Bradley, T.H., De Long, S.K., Marchese, A.J., 2011. Quantitative measurement of direct nitrous oxide emissions from microalgae cultivation. Environ. Sci. Technol. 45, 9449–9456.

Florez-Leiva, L., Tarifeno, E., Cornejo, M., Kiene, R., Farías, L., 2010. High production of nitrous oxide (N_2O), methane (CH_4) and dimethylsulphoniopropionate (DMSP) in a massive marine phytoplankton culture. Biogeosci. Discuss. 7, 6705–6723..

Francis, C.A., Roberts, K.J., Beman, J.M., Santoro, A.E., Oakley, B.B., 2005. Ubiquity and diversity of ammonia-oxidizing archaea in water columns and sediments of the ocean. Proc. Natl. Acad. Sci. U.S.A. 102, 14683–14688.

French, E., Kozlowski, J.A., Mukherjee, M., Bullerjahn, G., Bollmann, A., 2012. Ecophysiological characterization of ammonia-oxidizing archaea and bacteria from freshwater. Appl. Environ. Microbiol. 78, 5773–5780.

Gantner, S., Andersson, A.F., Alonso-Sáez, L., Bertislon, S., 2001. Novel primers for 16S rRNA-based archaeal community analysis in environmental samples. J. Microbiol. Meth. 84, 12–18.

García, J., Green, B.F., Lundquist, T., Mujeriego, R., Hernández-Mariné, M., Oswald, W.J., 2006. Long term diurnal variations in contaminant removal in high rate ponds treating urban wastewater. Bioresour. Technol. 97, 1709–1715.

Guerrero, M.A., Jones, R.D., 1996. Photoinhibition of marine nitrifying bacteria. I. Wavelength-dependent response. Mar. Ecol. Prog. Ser. 141, 183–192.

Guieysse, B., Plouviez, M., Coilhac, M., Cazali, L., 2013. Nitrous oxide (N_2O) production in axenic *Chlorella vulgaris* microalgae cultures: evidence, putative pathways, and potential environmental impacts. Biogeosciences 10, 6737–6746.

Harter, T., Bossier, P., Verreth, J., Bodé, S., Van der Ha, D., Debeer, A.E., Boon, N., Boeckx, P., Vyverman, W., Nevejan, N., 2013. Carbon and nitrogen mass balance during flue gas treatment with *Dunaliella salina* cultures. J. Appl. Phycol. 25, 359–368.

Hatzenpichler, R., 2012. Diversity, physiology and niche differentiation of ammonia-oxidizing archaea. Appl. Environ. Microbiol. 78, 7501–7510.

Howard, W.D., Solomonson, L.P., 1981. Kinetic mechanism of assimilatory NADH: nitrate reductase from *Chlorella*. J. Biol. Chem. 256, 12725–12730.

Illman, A.M., Scragg, A.H., Shales, S.W., 2000. Increase in *Chlorella* strains calorific values when grown in low nitrogen medium. Enzyme Microbiol. Technol. 27, 631–635.

IPCC, 2001. Climate Change 2001: The Scientific Basis. University Press, Cambridge.

IPCC, 2006. 2006 IPCC Guidelines for National Greenhouse Gas Inventories. In: Eggleston, H.S., Buendia, L., Miwa, K., Ngara, T., Tanabe, K. (Eds.). IGES, Japan, pp. 6.24–26.26.

Kamp, A., Stief, P., Knappe, J., De Beer, D., 2013. Response of the ubiquitous pelagic diatom *Thalassiosira weissflogii* to darkness and anoxia. PLoS ONE 8, 1–11.

Kay, C.J., Barber, M.J., 1986. Assimilatory nitrate reductase from Chlorella. Effect of ionic strength and pH on catalytic activity. J. Biol. Chem. 261, 14125–14129.

Merbt, S.N., Stahl, D.A., Casamayor, E.O., Marti, E., Nicol, G.W., Prosser, J.I., 2012. Differential photoinhibition of bacterial and archaeal ammonia oxidation. FEMS Microbiol. Lett. 327, 41–46.

Mosier, A., Kroeze, C., Nevison, C., Oenema, O., Seitzinger, S., van Cleemput, O., 1999. An overview of the revised 1996 IPCC guidelines for national greenhouse gas inventory methodology for nitrous oxide from agriculture. Environ. Sci. Policy 2, 325–333.

Novis, P.M., Halle, C., Wilson, B., Tremblay, L.A., 2009. Identification and characterization of freshwater algae from a pollution gradient using rbcL sequencing and toxicity testing. Arch. Environ. Contam. Toxicol. 57, 504–514.

OECD. Guideline for testing of chemicals. Simulation test – aerobic sewage treatment 303 A, Technical report, Organisation for economic co-operation and development, Paris, 1996.

Pessarakli, M., 2005. Handbook of Photosynthesis, second ed. CRC Press, Boca Raton.

Pistorius, E.K., Gewitz, H.S., Voss, H., Vennesland, B., 1976. Reversible inactivation of nitrate reductase in *Chlorella vulgaris in vivo*. 128, 73–80.

Ravishankara, A.R., Daniel, J.S., Portmann, R.W., 2009. Nitrous oxide (N_2O): the dominant ozone-depleting substance emitted in the 21st century. Science 326, 123–125..

Rotthauwe, J.H., Witzel, K.P., Liesack, W., 1997. The ammonia monooxygenase structural gene amoA as a functional marker: molecular fine-scale analysis of natural ammonia-oxidizing populations. Appl. Environ. Microbiol. 63, 4704–4712.

Tischner, R., Planchet, E., Kaiser, W.M., 2004. Mitochondrial electron transport as a source for nitric oxide in the unicellular green alga *Chlorella sorokiniana*. FEBS Lett. 576, 151–155.

Wang, J., Peng, Y., Wang, S., Gao, Y., 2008. Nitrogen removal by simultaneous nitrification and denitrification via nitrite in a sequence hybrid biological reactor. Chin. J. Chem. Eng. 16, 778–784.

Weathers, P.J., 1984. N_2O evolution by green algae. Appl. Environ. Microbiol. 48, 1251–1253.

Supplementary Data

Title: Nitrous oxide emissions from high rate algal ponds treating domestic wastewater

Authors: Cynthia Alcántara, Raúl Muñoz, Zane Norvill, Maxence Plouviez and Benoit Guieysse

S1 – Dynamic modeling of reactor performance

S2 - PCR analysis

S3 – Daily variation in N_2O emissions (Period I)

S4 – Significance of N_2O emissions during wastewater treatment in HRAPs

3 Figures

4 Tables

11 Pages

S1 – Determination of photosynthetic efficiency (PE) and algal biomass productivity

The photosynthetic efficiency (PE) and concentration of *C. vulgaris* were determined using a dynamic simulation of microbial growth as described in De Godos et al. (2012). For this purpose it was assumed that i) heterotrophic growth was limited by the concentration of biodegradable COD (bCOD); ii) the volumetric rate of heterotrophic growth ($\frac{dX}{dt}$, g VSS m^{-3} d^{-1}) was described by the Monod kinetic model with endogenous decay (Equation 1): iii) algae productivity was described as a linear function of the light intensity reaching the aqueous surface because light intensity was low (no light saturation or inhibition, Equation 4); and 2) the pond broth was well mixed. Under these assumptions, the volumetric rate of heterotrophic growth can be described as:

$$\frac{dX}{dt} = \mu_{max} \cdot \frac{S \cdot X}{K_S + S} - k_d \cdot X \qquad (1)$$

where X (g VSS m^{-3}) is the concentration of active bCOD-consuming heterotrophs in the pond, S (g bCOD m^{-3}) is the concentration of bCOD in the pond, μ_{max} (d^{-1}) is the maximum specific growth rate, K_S (g bCOD m^{-3}) is the substrate saturation constant and k_d (d^{-1}) is the rate of microbial decay.

The volumetric rate of substrate consumption was calculated as:

$$\frac{dS}{dt} = -\frac{1}{Y} \cdot \frac{\mu_{max} S \cdot X}{K_S + S} \qquad (2)$$

where Y (g VSS g $bCOD_{used}^{-1}$) is the true heterotrophic yield.

The volumetric rate of debris production was calculated as:

$$\frac{dX_i}{dt} = f_d \cdot k_d \cdot X \qquad (3)$$

where X_i (g VSS m^{-3}) is the concentration of debris in the pond and f_d (-) is the cell debris coefficient.

Photosynthetic growth was described as:

$$V \cdot \frac{dA}{dt} = \frac{PE}{100} \cdot I \cdot a \cdot \frac{1}{HV} \cdot 86{,}400 \cdot f \quad (4)$$

Where V is the HRAP volume (m^3), A (g TSS m^{-3}) is the concentration of algae biomass photosynthesized, PE (%) is the photosynthetic efficiency, I (W m^{-2}) is the light irradiance reaching the pond surface, a (m^2) is the illuminated area, HV (J g TSS^{-1}) is the specific heat value of the algal biomass, and f is a function set to 1 when illumination is provided (12 hr each day) and 0 when lights are off.

Table S1-1 lists the input data used in the simulations, the value of the kinetics parameters were adjusted at the average pond temperature of 22°C. For each reactor and operational period considered, the PE and phototrophic biomass concentration were fitted by iteration based on a 6-days simulation (dt = 0.005 d, t= 0 correspond to the start of a new feeding cycle with f = 0 from 11 to 23 hours after each feeding, the active biomass concentration X was found to be equal to 41 g VSS m^{-3} at the start of each cycle) to fit the final predicted TSS concentration with the corresponding experimental TSS value (<1% error). The PE was thus estimated to be 2.9-3.6% of the PAR with photosynthesis contributing to more than 80% of the total TSS productivity. The algae concentrations thus reported (334-427 g TSS m^{-3}) were in agreement with the high OD of the culture broth (Table 2) caused by the high chlorophyll content of the biomass (e.g. 1.5-2.7% on February 24; the OD_{683}/DW ratio is highly variable and was found to fluctuate from 2-6 in axenic cultures). The amounts of N and P assimilated into biomass were calculated by mass balance based on the results from the C/N/P analysis (Table 2). Table S1-2 summarizes the operating conditions during Period I, Period II and Period III. Figure S1-1 represents the time course of $N\text{-}NO_3^-$ and $N\text{-}NH_4^+$ concentrations in the synthetic sewage water and in the effluent in HRAPs during the entire experiment.

Table S1-1: Parameters used in dynamic simulations

Parameter	Unit	Value	Origin
V	m^3	7	HRAP design
a	m^2	0.1	HRAP design
I	W m^{-2}	60.88	Experimental[a]
T	°C	22	Experimental
HV	J g TSS^{-1}	21000	Experimental[b]
VSS/TSS[c]	0.85	0.85	
μ_{max}	d^{-1}	6	
K_s	g bCOD m^{-3}	20	
Y	g VSS g $bCOD_{used}^{-1}$	0.4	Tchobanoglous et al. (2003)[d]
k_d	d^{-1}	0.12	
f_d	unitless	0.15	
Ω values for adjusting of parameter Φ at temperature T as: $\Phi_T = \Phi_{20} \cdot \Omega^{(T-20)}$			
μ_m	unitless	1.07	Tchobanoglous et al. (2003)[d]
k_d	unitless	1.04	
K_s	unitless	1	

[a] 280 μE m^{-2} s^{-1} at 550nm.

[b] Heat value for *Chlorella vulgaris* monoculture photosynthetically grown over a broad range of conditions (unpublished data); this value was preferred to the TSS heat value reported in our study (Table 2) for being more specific to algal biomass in the computation of algae productivities.

[c] Use for bCOD-degrading heterotrophs as algae concentration was directly computed as TSS.

[d] Typical values for the "activated-sludge process for the removal of organic matter from domestic wastewater".

Table S1-2: Operating conditions during Period I, Period II and Period III

	PERIOD I	PERIOD II	PERIOD III	
	60 days	45 days	45 days	
	HRAP A & B		HRAP A	HRAP B
	INPUT		INPUT	INPUT
$N\text{-}NO_3^-$ (mg/L)	1.6 ± 0.0		102 ± 0[a]	1.6 ± 0.0
$N\text{-}NH_4^+$ (mg/L)	48 ± 1		48 ± 1	148 ± 1[b]
TN (mg/L)	50 ± 1		150 ± 1	150 ± 1
$P\text{-}PO_4^{3-}$ (mg/L)	5.7 ± 0.1		5.7 ± 0.3	902 ± 3[c]

[a]HRAP A was supplemented with 100 mg $N\text{-}NO_3^-/L_{SSW}$.

[b]HRAP B was supplemented with 100 mg $N\text{-}NH_4^+/L_{SSW}$.

[c]HRAP B was supplemented with a buffer solution (1.52 g KH_2PO_4/L_{SSW} and 3.1 g K_2HPO_4/L_{SSW}).

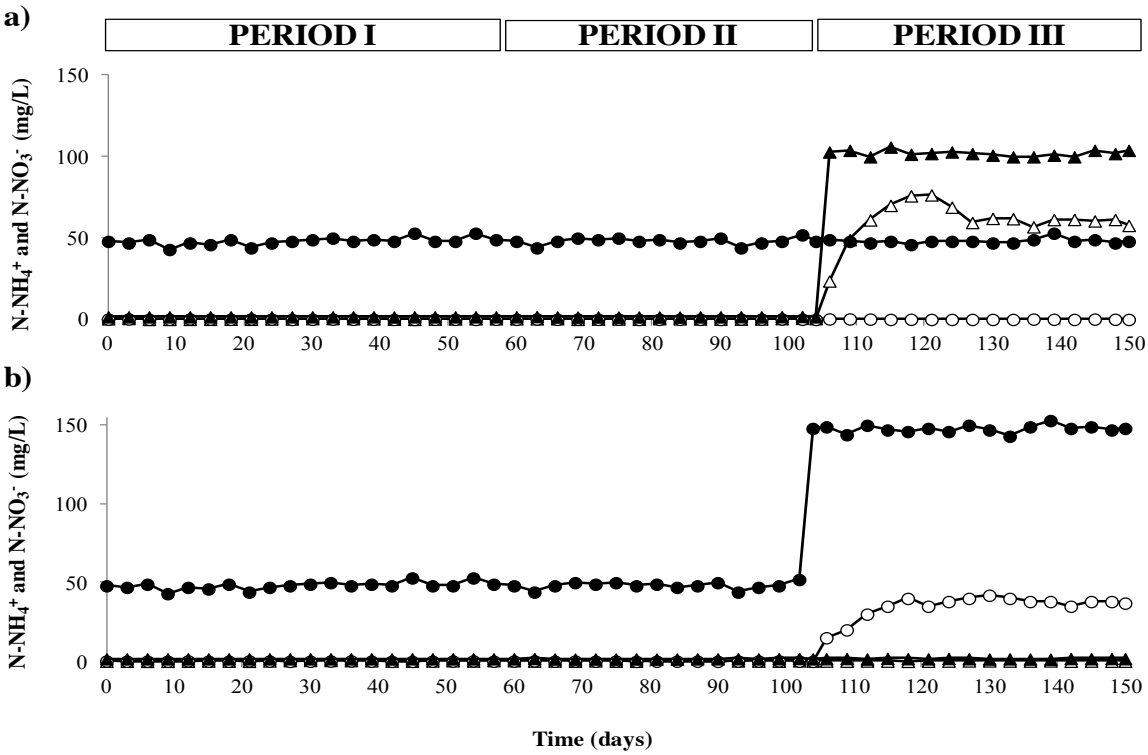

Figure S1-1: Time course of $N\text{-}NO_3^-$ concentration in the synthetic sewage water (–▲–) and in the effluent (–Δ–), and $N\text{-}NH_4^+$ concentration in the synthetic sewage water (–●–) and in the effluent (–○–) in HRAP A (a) and in HRAP B (b) during the entire experiment.

S2 - PCR analysis

The protocols and conditions used for PCR analysis are detailed in the main manuscript (Table 1): The norB, cnorB and qnorB primer pairs amplify fragments of genes encoding for bacterial NOR (NO-reductase). The amoA 1F and 2R primer pair specifically amplifies a fragment of gene encoding for ammonia monooxygenase in bacteria whereas the amoA F and R amplifies a fragment for ammonia monooxygenase in archaea. The 16S primer pairs 340F / 1000R amplify a region of the 16S rDNA in archaea. The 16S primers are considered a 'universal' primer pairs for bacteria and archaea. A negative control was included for each primer pairs; this reaction contains all components except the template DNA.

Results are shown in Figure S2-1 and summarized in Tables S2-1 and S2-2. A PCR product of the expected size was seen for the denitrification primer pair cnorB and qnorB in all samples. In contrast, norB as well as amoA (bacterial) products were not detected in all samples. No PCR products were obtained for any of the samples using the archaea-specific primers (Arch-amoAF/R and 16S 340F/1000R).

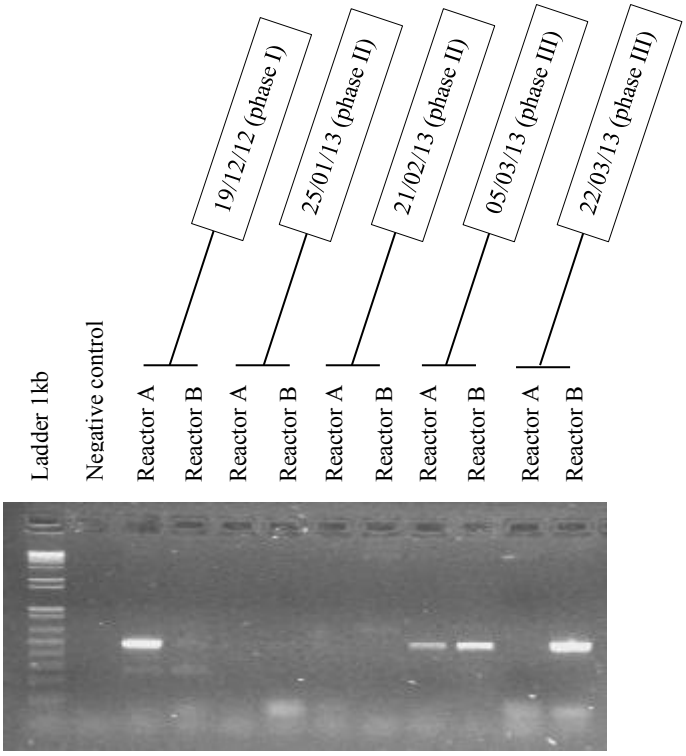

1 : amoA (bacteria) on 2% (w/v) agarose, in 1XTA

2: norB on 2% (w/v) agarose, in 1XTA

3: cnorB on 2% (w/v) agarose, in 1XTA

4: qnorB on 2% (w/v) agarose, in 1XTA

Figure S2-1: Results of PCR analysis viewed under UV on agarose gels.

Table S2-1: Results from genomic analysis for reactor A (Y indicates there was a band of the expected size; N means no band of the expected size).

Period	Date	amoA (*bacteria*)	norB	cnorB	qnorB	amoA (*archaea*)	16S (*archaea*)
I	19/12/12	Y	N	Y*	Y	N	N
II	25/01/13	N	Y	Y	Y	N	N
II	21/02/13	N	Y*	Y	Y*	N	N
III	05/03/13	Y	Y	Y*	Y*	N	N
III	22/03/13	N	Y	Y*	Y*	N	N

* an asterisk indicates the presence of other bands which are PCR artifacts or primer dimers.

Table S2-2: Results from genomic analysis for reactor B (Y indicates there was a band of the expected size; N means no band of the expected size).

Period	Date	amoA (*bacteria*)	norB	cnorB	qnorB	amoA (*archaea*)	16S (*archaea*)
I	19/12/12	N	Y*	Y*	Y	N	N
II	25/01/13	N	Y	Y	Y	N	N
II	21/02/13	N	Y*	Y*	Y*	N	N
III	05/03/13	Y	N	Y*	Y*	N	N
III	22/03/13	Y	Y	Y*	Y	N	N

* an asterisk indicates the presence of other bands which are PCR artifacts or primer dimers.

S3. Daily variation in N_2O emissions (Period I)

Figure S3-1 shows changes in N_2O emissions rates from HRAP cultures withdrawn at different times during the fed-batch cycle (12/12/2012). As can be seen, the generation rates remained low and showed no significant temporal variations (ANOVA test at 95% of confidence interval).

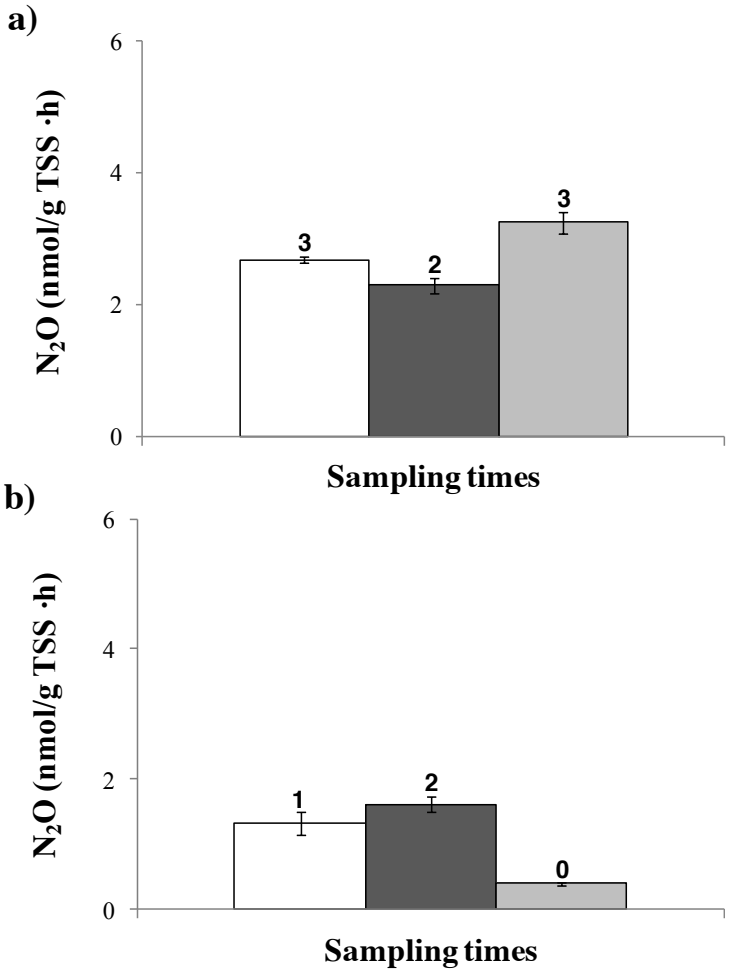

Figure S3-1: N_2O production by microcosms withdrawn from HRAP A (a) and HRAP B (b) sampled i) immediately before turning off the lights and 13h after SSW feeding (21:00 p.m) (□); ii) 2 hours before turning on the lights and 1 hour before SSW feeding (7:00 a.m) (■); immediately before turning on the lights and 1 h after SSW feeding (9:00 a.m) (□). Vertical bars represent max and min values from duplicates.

S4 – Significance of N_2O emissions during wastewater treatment in HRAPs

These simple calculations provide a 'conservative' estimation of the carbon footprint associated with N_2O emissions from HRAPs treating wastewater. Based on the results shown in Figure 4 of the main manuscript, it was assumed N_2O emissions averaged 2 nmol N_2O/g TSS-hr during 12 hr each day (night) and were negligible during the remaining 12 hr (daytime). Under 'normal' operation, the two HRAPs monitored in this study were loaded with 50 mg N/d and emitted 83.2 nmol N_2O/d (2.3 μg N-N_2O/d)[1]. This resulted in an emission factor of 0.0047% (N-N_2O/N-input)[2]. Based on the analysis of Alcántara et al., (2014)[3], N_2O emissions from domestic wastewater treatment in 0.3 m deep HRAPs operated at 6 d HRT were estimated to 0.3 g N_2O/capita-yr, which is 10 fold lower than the direct emission factor of 3.2 g N_2O/capita-yr (corresponding emission factor of 0.035%; Czepiel et al., 1995) recommended by the IPCC for quantifying N_2O emissions during biological wastewater treatment (IPCC, 2006). The secondary treatment of the sewage generated by 1 billion humans using HRAPs would therefore generate minor emissions (0.19 Gg N-N_2O/yr) in comparison to global emissions from domestic wastewater (0.22 Tg N-N_2O/yr; Mosier et al., 1999) and total anthropogenic N_2O emissions (6.9 Tg N- N_2O/yr; IPCC, 2001). While direct comparison with N_2O emissions from activated sludge processes is difficult given the large variation of the rates reported (Kampschreur et al., 2009; Ahn et al., 2010), the carbon footprint of N_2O emissions from HRAPs herein calculated (1.1 g CO_2/m^3 wastewater treated assuming N_2O has a 100-year global warming potential of 298 g CO_2/g N_2O) compares favorably against the carbon footprints from electricity use for aerating and mixing activated sludge tanks[4] (119-378 g CO_2/m^3) and for mixing HRAPs[5] (3-14 g CO_2/m^3 wastewater treated). Photosynthesis also fixes 22.6 g CO_2/m^2-d or 528 g CO_2/m^3 wastewater[4].

---

[1] Based on the total biomass of 3.465 g TSS recorded in the two HRAPs during Periods I and II (495 g TSS/L).

[2] Initial N concentration of 50 g N- NH_4^+/m^3.

[3] The average flow rate of 0.325 m^3/capita-d and primary-settled influent loading factors of 68 g bCOD/capita-d, 13.3 g N/capita-d and 3.28 g P/capita-d were based on the typical values for US individual residences (Tchobanoglous et al., 2003), assuming 50% bCOD removal efficiency during primary treatment and a bCOD/BOD5 ratio of 1.6. Algal productivity was estimated to 20 g/m^2-d based on simulations. The N and P contents of the heterotrophic and phototrophic biomasses were estimated to 9 and 1%, respectively. The area required for treatment, 6.5 m^2/capita-d, supported a total algae biomass of 780 g TSS/capita in the HRAP (130 g TSS/capita-d).

[4] Energy requirement for aeration of 0.33-0.62 kWh/m^3 (Plappally et al., 2012); electricity generation carbon footprint of 362 (EU) - 610 (USA) g CO_2/kWh (IPCC, https://www.ipcc.ch/pdf/special-reports/sroc/Tables/t0305.pdf).

[5] The energy requirement for mixing of 0.023 kWh/m^{-3} wastewater for a 0.3 deep HRAP operated at 6 d HRT was calculated based on Borowitzka (2005) assuming a pond channel width of 6 m, a mean fluid velocity of 0.15 m^{-1}, a paddle wheel efficiency of 0.17, and a Manning coefficient of 0.012 (smooth plastic on granular earth).

[6] Based on an average PAR of 100 W/m^2, an algal biomass heat value of 21 KJ/g TSS, a biomass carbon content of 50% (TSS), and a PE of 3%.

References

1. Ahn, J.H., Kim, S., Park, H., Rham, B., Pagilla, K., Chandran, K., 2010. N_2O emissions from activated sludge processes, 2008-2009: monitoring results of a national monitoring survey in the United States. Environ. Sci. Technol. 44, 4505-4511.
2. Alcántara, C., Posadas, E., Guieysse, B., Muñoz, R., 2014. Microalgae-based waste water treatment. In: Handbook of Microalgae: Biotechnology Advances. Edited by Se-Kwon K, Elsevier. (In press).
3. Borowitzka, M.A., 2005. Culturing microalgae in outdoor ponds. In: Andersen, I.R.A. (Ed.), Algal Culturing Techniques. Elsevier, Academic Press, New York, pp. 205–218.
4. Czepiel, P., Crill, P., Harris, R., 1995. Nitrous oxide emission from municipal wastewater treatment. Environ. Sci. Technol. 29, 2352-2356.
5. De Godos, I., Muñoz, R., Guieysse, B., 2012. Tetracycline removal during wastewater treatment in high-rate algal ponds. J. Hazard. Mater. 229– 230, 446– 449.
6. Fagerstone, K.D., Quinn, J.C., Bradley, T.H., De Long, S.K., Marchese, A.J., 2011. Quantitative measurement of direct nitrous oxide emissions from microalgae cultivation. Environ. Sci. Technol. 45, 9449–9456.
7. Francis, C.A., Roberts, K.J., Beman, J.M., Santoro, A.E., Oakley, B.B., 2005. Ubiquity and diversity of ammonia-oxidizing archaea in water columns and sediments of the ocean. Proceedings of the Natl. Acad. Sci. U.S.A. 102, 14683–14688.
8. Gantner, S., Andersson, A.F., Alonso-Sáez, L., Bertislon, S., 2001. Novel primers for 16S rRNA-based archaeal community analysis in environmental samples. J. Microbiol. Meth. 84, 12-18.
9. IPCC, 2001. Climate Change 2001: the Scientific Basis. Cambridge, University Press.
10. IPCC, 2006. 2006 IPCC Guidelines for National Greenhouse Gas Inventories. In: Eggleston, H.S., Buendia, L., Miwa, K., Ngara, T., Tanabe, K. (Eds.). IGES, Japan, pp. 6.24–26.26.
11. Kampschreur, M., Temmink, H., Kleerebezem, R., Jetten, M.S.M., van Loosdrecht M.C.M., 2009. Nitrous oxide emission during wastewater treatment. Wat. Res. 43, 4093-4103.
12. Mosier, A., Kroeze, C., Nevison, C., Oenema, O., Seitzinger, S., van Cleemput, O., 1999. An overview of the revised 1996 IPCC guidelines for national greenhouse gas inventory methodology for nitrous oxide from agriculture. Environ. Sci. Policy 2, 325–333.
13. Plappally, A.K., Lienhard, J.H., 2012. Energy requirements for water production, treatment, end use, reclamation, and disposal, Renew. Sustain. Energy Rev. 16, 4818–4848.
14. Rotthauwe, J. H., Witzel, K. P., Liesack, W., 1997. The ammonia monooxygenase structural gene amoA as a functional marker: molecular fine-scale analysis of natural ammonia-oxidizing populations. Appl. Environ. Microbiol. 63, 4704 – 4712.
15. Tchobanoglous, G., Burton, F.L., Stensel, H.D., 2003. Wastewater engineering: treatment and reuse, fourth ed. (Metcalf & Eddy) McGraw-Hill.

Conclusions and future work

Chapter 8

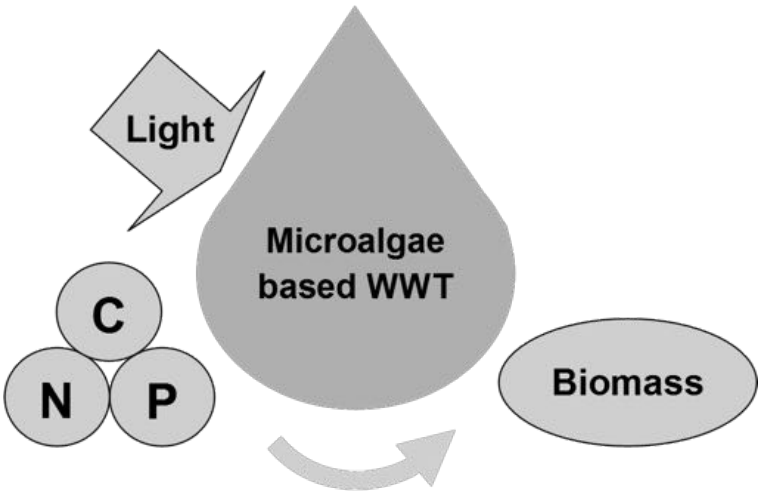

The results obtained in the present thesis confirmed the potential of algal-bacterial processes for water pollution control in terms of treatment efficiency, energy consumption and environmental sustainability when compared to conventional WWT technologies. The systematic comparison of the mixotrophic metabolism of an axenic culture of *Chlorella sorokiniana* and a microalgal-bacterial consortium demonstrated the superior performance and robustness of symbiotic consortia under stress conditions, which confirmed their potential as a platform technology to consolidate an industrial scale microalgae-to-bioenergy technology based on WWT (**Chapter 3**).

The synergistic relationship between microalgae and bacteria harbors an industrial and environmental potential higher than that currently exploited. In this context, different operational strategies and photobioreactor configurations were investigated in order to overcome the main limitations that nowadays still limit the full-scale implementation of algal-bacterial-based WWT. An evaluation of WWT performance in a novel anoxic-aerobic algal-bacterial photobioreactor with biomass recycling was conducted to overcome both the limited capacity of conventional HRAPs to completely remove all nutrients in wastewaters with a low C/N ratio and the low sedimentation capability of the microalgae established in the process (**Chapter 4**). **Chapter 4** demonstrated that algal-bacterial symbiosis in this photobioreactor configuration supported efficient TOC, IC and TN removals. Interestingly, the intensity and regime of light supply along with the DOC governed the extent of $N\text{-}NH_4^+$ removal by microalgae assimilation or nitrification-denitrification as a result of a competition between microalgae and nitrifying bacteria for IC. On the other hand, the implementation of a settled biomass recycling strategy resulted in the enrichment of algal-bacterial flocs with a good sedimentation capacity, which supported effluent TSS concentrations below the EU maximum discharge limits. In addition, this sedimentation enhancement strategy can increase the sustainability of microalgae-based WWT by supporting a cost-effective harvesting and valorization of the algal-bacterial biomass generated during WWT, which can be further used as a feedstock for bioenergy production.

Another strategy to enhance nutrient removal in wastewaters with a low C/N ratio is based on the additional supply of CO_2 to the process. In this context, the CO_2 contained

in the biogas obtained through AD can provide the additional C source required to boost nutrient removal by photosynthetic microalgal assimilation. In addition, this CO_2 sequestration simultaneously supports biogas upgrading towards biomethane, which would allow its injection into natural gas grids or its use as vehicle fuel. **Chapter 5** was focused on the evaluation of the performance and the removal mechanisms involved in the simultaneous capture of CO_2 from a simulated biogas and treatment of diluted centrates in an indoor 180-L HRAP interconnected to an absorption column. Despite the low impinging irradiation used in the HRAP and the low liquid recirculation rate from the HRAP to the absorption column resulted in a low biomass productivity of 2.2 $g/m^2 \cdot d$ and a 55% of C-CO_2 biogas removal, the implementation of this technology outdoors is expected to boost nutrient removal and biogas upgrading. In our particular study, this 55% C-CO_2 removal from biogas entailed an increase of 19% in the biogas energy content, which confirmed the potential of this combined wastewater treatment-biogas upgrading process. Similarly to the results described in **Chapter 4**, IC availability in the culture broth directly controlled the extent of nutrient removal via assimilation. In this context, the low irradiation provided a competitive advantage to nitrifying bacteria over microalgae (only 14% of the nitrogen input was converted to $N_{biomass}$), nitrification being the main NH_4^+ removal mechanism with a 47% of the N-NH_4^+ input transformed into N-NO_3^-. A luxury uptake of P mediated by a light limitation was hypothesized based on the high P biomass content (2.5%), which resulted in a P-PO_4^{-3} removal as biomass of 77%. Therefore, the light intensity in the HRAP and the biogas residence time in the absorption column were identified as key parameters during simultaneous microalgae-based biogas upgrading and WWT. The fact that the CO_2 present in the biogas could be used as a C source to boost the removal of residual N and P in AD effluents via biomass assimilation entails an added environmental benefit to the process in term of biomitigation of the eutrophication potential of these high-strength wastewaters. In addition, unlike conventional physical/chemical biogas upgrading technologies, photosynthetic biogas upgrading allows the valorization of this CO_2 in the form of a valuable algal biomass, which could be further used as a feedstock for the subsequent energy production as biogas or as biofertilizer.

In this context, an evaluation of the mass and energy balances in the integrated microalgae growth-anaerobic digestion process was conducted in **Chapter 6** in order to quantify the potential energy recovery via anaerobic digestion of the biomass harvested during WWT. The results obtained in **Chapter 6** suggested that the extent of biomass hydrolysis and biogas composition were not influenced by the previous microalgae cultivation mode (photoautotrophic or mixotrophic). The CH_4 contained in the biogas represented an energy recovery of up to 50% of the chemical energy fixed as biomass during microalgae cultivation, which demonstrated the potential of anaerobic digestion as a cost-effective route for valorization of microalgae in terms of energy production.

Finally, the quantification of N_2O emissions in two different algal-bacterial WWT systems, a HRAP (**Chapter 7**) and an anoxic-aerobic photobioreactor (**Chapter 4**), was conducted in order to assess the impact of algal-bacterial N_2O emissions on a net greenhouse gas mass balance. A 24-hr average emission factor of 4.7×10^{-5} g N-N_2O/g N-input was recorded from HRAP cultures sampled under a typical N-loading of 7.1 g N/$m^3_{reactor}$·d. Likewise, the quantification of N_2O emissions from the algal-bacterial nitrification-denitrification photobioreactor showed an average N_2O emission factor of 5.2×10^{-6} g N-N_2O/g N-input at a N-loading of 50 g N/$m^3_{reactor}$·d. The N_2O emission factors obtained in both studies were significantly lower than the IPCC emission factors reported for conventional activated sludge WWTPs, which suggested that N_2O emissions during microalgae-based WWT should not compromise the environmental sustainability of WWT in terms of global warming impact.

Despite the advances carried out in this thesis towards the widespread implementation of algal-bacterial processes for WWT, the scale up and outdoors evaluation of the processes developed constitute niches for future research. In addition, the quantification of N_2O emissions during the full-scale implementation of the photobioreactor configurations tested will be mandatory in order to confirm the environmental sustainability of algal-bacterial WWT processes in a real scenario. Based on the results here obtained, future lines of research in the field of microalgae-based WWT should focus on:

- The elucidation of the role of the regime and intensity of solar radiation on the inhibition of nitrifying activity can bring new insights on their influence on the performance and robustness of NH_4^+ nitrification, which is especially relevant in the treatment of wastewaters with a low C/N ratio. Likewise, further research on the influence of light intensity and IC supply on the extent of N-NH_4^+ removal by microalgae assimilation or nitrification-denitrification is needed in order to find the best operational conditions to maintain an equilibrium between microalgae and nitrifying bacteria activity. This is especially critical when the supply of external C-CO_2 to support a complete nutrient removal via microalgal assimilation is not technical or economically feasible given the current interest in outdoors algal-bacterial WWT photobioreactors.
- The study of the impact of CO_2 sparging on the performance of the anoxic-aerobic photobioreactor configuration based on the results obtained in **Chapter 4**.
- The elucidation of the role of environmental factors such as light intensity and temperature on microalgae P luxury uptake should be further assessed in order to exploit this promising metabolic route to improve biological P removal in outdoors algal-bacterial WWT photobioreactors.
- A continuous sustainability evaluation of N_2O emissions from outdoors algal-bacterial WWT technologies should be conducted to collect consistent N_2O emissions data from pilot-scale facilities under different WWT scenarios in order to identify the main metabolic pathways responsible of N_2O emissions in algal-bacterial WWT technologies. For instance, innovative operational strategies designed to avoid NH_4^+ or NO_2^- accumulation in the cultivation broth are required to develop a sustainable industrial-scale microalgae-based WWT technology.
- The integration of algal-bacterial processes in conventional WWTPs in order to enhance the sustainability of the WWT in this XXI century in terms of energy consumption and CO_2 and nutrient management based on the promising results obtained in **Chapter 6**.

About the author

Chapter 9

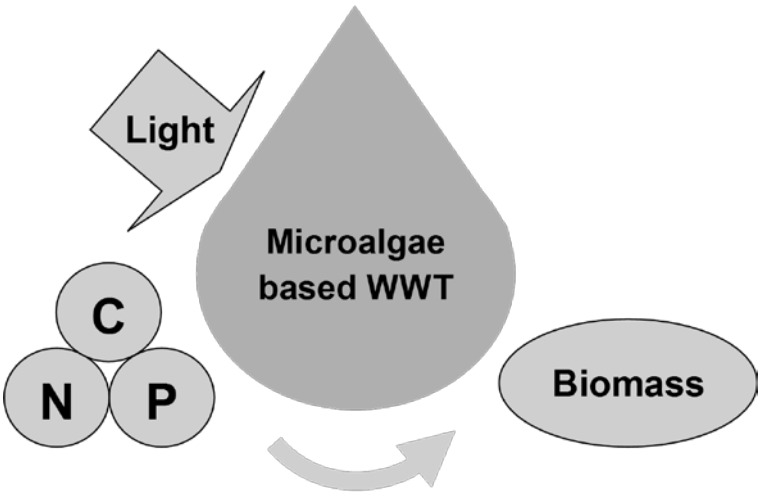

Biography

Cynthia Alcántara Pollo (Madrid, 1985) performed her Chemical Engineering studies at Valladolid University (2003-2010) and her Final Year Project on "*Sludge digestion coupled with microaerobic H_2S removal from biogas*". She worked as a chemical engineer in charge of the laboratory of process analysis in the company British Sugar from 2009 to 2011. In May 2011, Cynthia joined the Biological Gas Treatment and Microalgae Research Group headed by the Associate Professor Raúl Muñoz within the Environmental Technology Group (Department of Chemical Engineering and Environmental Technology, Valladolid University), where she performed a Research Master in Process and Systems Engineering (September 2011-September 2012). Cynthia was awarded with a research contract by the regional government of Castilla y León and the European Social Fund. Her PhD studies focused on the development of new operational strategies and photobioreactor configurations to overcome some of the current limitations of microalgae-based wastewater treatment. The candidate carried out within her PhD studies a 6-month research stay at Massey University (2012-2013, Palmerston North, New Zealand) under the supervision of the Associate Professor Benoit Guieysse, and an additional 3-month research stay at Universidad Nacional Autónoma de México (II-UNAM) (D.F, México) under the supervision of the Associate Professor Armando González Sánchez.

Publications in international journals

- **Alcántara, C.**, Domínguez, J.M., García, D., Blanco, S., Pérez, R., García-Encina, P.A., Muñoz, R., 2015. Evaluation of wastewater treatment in a novel anoxic-aerobic algal-bacterial photobioreactor with biomass recycling through carbon and nitrogen mass balances. Bioresource Technology. 191, 173-186.

- **Alcántara, C.**, García-Encina, P.A., Muñoz, R., 2015. Evaluation of the simultaneous biogas upgrading and treatment of centrates in a HRAP through C, N and P mass balances. Water Science and Technology (doi: 10.2166/wst.2015.198).

- **Alcántara, C.**, Muñoz, R., Norvill, Z., Plouviez, M., Guieysse, B., 2015. Nitrous oxide emissions from high rate algal ponds treating domestic wastewater. Bioresource Technology. 177, 110-117.

- **Alcántara, C.**, Fernández, C., García-Encina, P.A., Muñoz, R., 2015. Mixotrophic metabolism of *Chlorella sorokiniana* and algal-bacteria consortia under extended dark-light periods and nutrient starvation. Applied Microbiology and Biotechnology. 99(5), 2393-2404.

- **Alcántara, C.**, García-Encina, P.A., Muñoz, R., 2013. Evaluation of mass and energy balances in the integrated microalgae growth-anaerobic digestion process. Chemical Engineering Journal, 221, 238-246.

International book chapters

Alcántara, C., Posadas, E., Guieysse, B., Muñoz, R., 2015. Microalgae-based wastewater treatment. In: Handbook of Microalgae: Biotechnology Advances. Edited by Se-Kwon K, Elsevier, Chapter 29, 439-455.

National book chapters

Alcántara, C., Posadas, E., García-Encina, P.A., Muñoz, R., 2015. Eliminación de Carbono, Nitrógeno, Fósforo y Patógenos con Microalgas. In: Tecnologías Avanzadas para el tratamiento de Aguas residuales. 3rd Edition. Edited by: Mosquera A. Lápices 4. ISBN-13: 978-84-692-5028-0.

Contributions to conferences

- **Alcántara, C.**, García-Encina, P.A., Muñoz, R. Integrated microalgae growth-anaerobic digestion process as a biofuels technology production: mass and energy balances. 10th International Conference on Renewable Resources and Biorefineries. June 4-6th, 2014. Valladolid (Spain) (**Oral Presentation**).

- **Alcántara, C.,** García-Encina, P.A., Muñoz, R. Microalge Digestion: Quantification of mass balances (C, N, P, S) in the combined growth-digestion process. 9th European Workshop Biotechnology of Microalgae. June 4-5th, 2012. Nuthetal (Germany) (**Poster**).

Other merits

Research stays in International Research Centers

- Institute of Engineering of the Universidad Nacional Autónoma de México (II-UNAM). Mexico D.F., Mexico. October 2014-December 2014. **Armando González**. Project: Microalgae based biogas upgrading.

- School of Engineering and Advanced Technology, Massey University. Palmerston North, New Zealand. September 2012-March 2013. Professor **Benoit Guieysse**. Project: N_2O emissions from high rate algal ponds treating domestic wastewater.

Supervision

- **Master Thesis**. Jesús María Domínguez Niño (April 2014-September 2014). Quantification of N_2O and Carbon/Nitrogen removal in an anoxic-aerobic algal-bacterial photobioreactor. University of Valladolid (Spain).

- **Research Project.** Carolina Fernández Fernández (August 2013-October 2013). Study of mixotrophic metabolism of *Chlorella sorokiniana* and algal-bacterial cultures under extended light-dark periods. University of Valladolid (Spain).

Teaching

- **Environmental and Process Technology** (2013-2014). Assistant Lecturer. Industrial Engineering Degrees. 1st Course. University of Valladolid (Spain) Cord Subject. 2 ECTS credits.

- **Environmental and Process Technology** (2012-2013). Assistant Lecturer. Industrial Engineering Degrees. 1st Course. University of Valladolid (Spain) Cord Subject. 2 ECTS credits.

Workshops

- Strategies for bioenergy and biofuel production. Life cycles, assessment and evaluation. BIOCEN Summer School 2012, Tampere University. August, 2012. Tampere (Finland).

- Environmental Biotechnology Workshop, Valladolid University. July, 2012. Valladolid (Spain).

- Some Recent Developments for Modeling Environmental System. Environmental Course, Summer school 2009, Catania University. July, 2009. Catania (Italy).

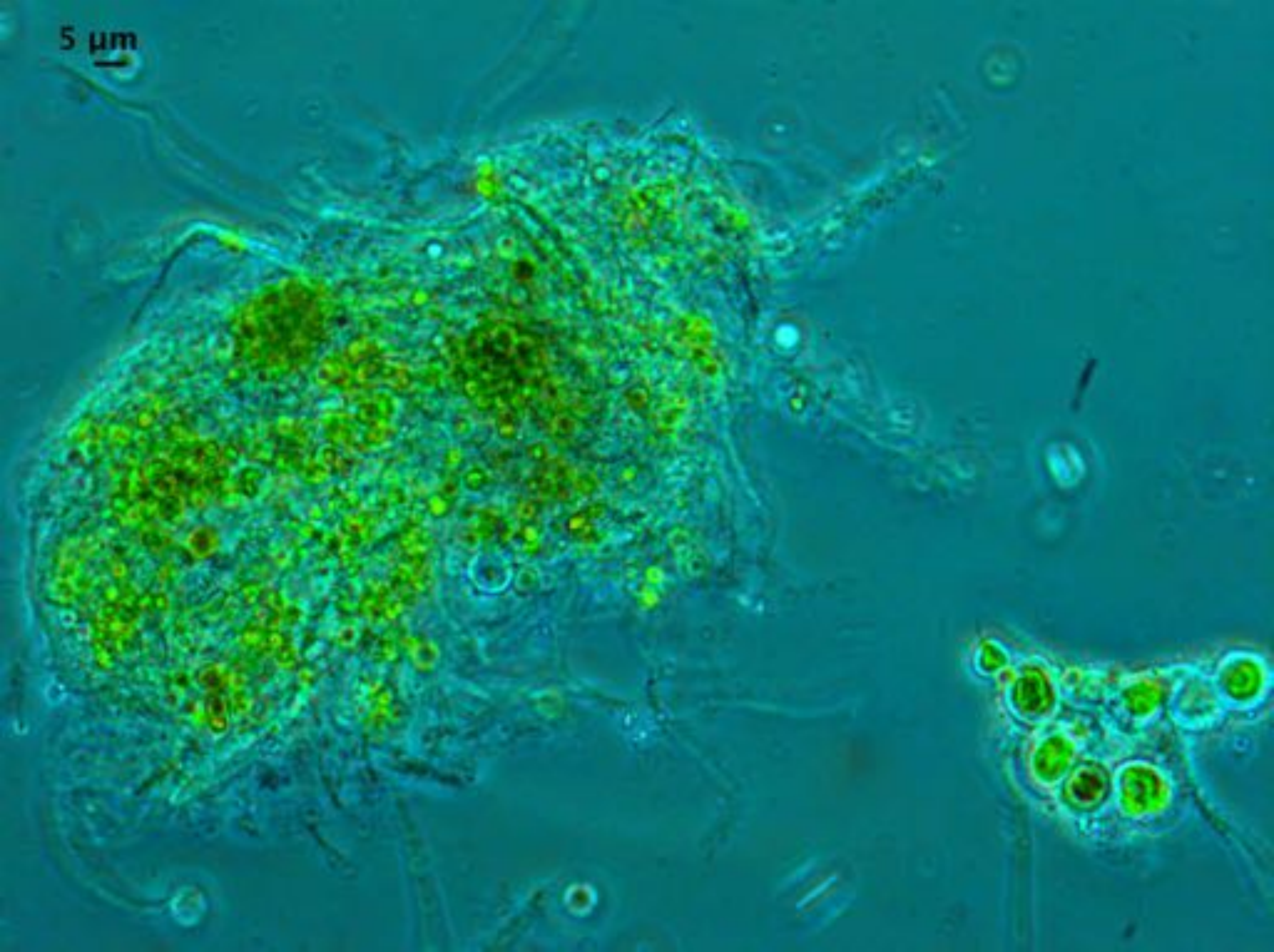
5 µm